

Tesi doctoral presentada per En/Na

**Adelina GEYER TRAYER**

amb el títol

**"Dynamics and structural evolution of collapse calderas: A comparison between field evidence, analogue and mathematical models"**

per a l'obtenció del títol de Doctor/a en

GEOLOGIA

Barcelona, 28 de marc del 2007.

Facultat de Geologia  
Departament de Geodinàmica i Geofísica



UNIVERSITAT DE BARCELONA



**PART II:**  
**FIELD STUDIES**

## PART II: FIELD STUDIES

### II. 1 INTRODUCTION

#### **II.1.1 The role of field studies in volcanology**

Field studies constitute the most important way to investigate and understand volcanic processes, from magma generation to the volcanic eruption, passing through the magma transport and storage. Consequently, field data is crucial in the study of caldera processes. The reconstruction of past collapse calderas and their comparison with present ones observed examples (e.g. Miyakejima – *Japan* , Geshi et al., 2002; Nakada et al., 2005) is a powerful tool to understand caldera mechanisms. However, direct observation of caldera-forming events is complex because their low frequency and its dangerousness. Only a very few examples have been directly observed in historical times.

Volcanic products are incorporated into the geological record and constitute a basis for reconstructing previous eruptions. Evidently, field studies of volcanic products are focused on characterizing their stratigraphy, lithology and sedimentology, and on reconstructing the corresponding eruptive sequence.

Moreover, fieldwork studies in volcanology are also based on the elaboration of detailed geological maps, combined with aerial and satellite images, which are useful to reconstruct the distribution of volcanic units.

Additionally, a detailed field and petrological study are able to provide enough information to determine pre-eruptive conditions of magma and the most probable causes that triggered the eruption. Lastly, field data is useful to adjust and test experimental and mathematical models.

However, the main problem of field data is that with time, the understanding of an eruptive sequence becomes more difficult. Post-eruptive processes may turn over or transform the original deposits and also incorporate into the stratigraphic record deposits from other eruptions. Consequently, our observations and results will be strongly conditioned and influenced by these post-eruptive processes as erosion, deformation,

---

alteration, etc. This has to be taken into account in the next section when analysing and interpreting field data results.

### **II.1.2 Objectives**

The objectives of this section are diverse. First, we present a summary of the different field observations that provide information about the different factors controlling volcanic processes (see section I.1.2) and specifically, collapse caldera processes.

The second objective, and possibly the most laborious part of this chapter is the elaboration of a worldwide collapse caldera database. For this, we have performed a comprehensive compilation of published field studies on calderas. More than 170 references have been revised, and their information has been summarized in a database linked to a Geographical Information System (GIS) application. Thus, it is possible to visualize the selected calderas in a world map and to filter them according to different attributes such as their age, structure, etc. On the one hand, the final aim of this database is to update the current knowledge on calderas based on field studies. In fact, worldwide caldera compilations are scarce. The IAVCEI (International Association of Volcanology and Chemistry) offers a summary of the largest calderas, Newhall and Dzurisin (1988) performed a laborious work compiling worldwide unrested large calderas. Also the Smithsonian National Museum of Natural History (<http://www.volcano.si.edu>) offers a database of those volcanoes active during the last 100.000 years. However, none of these previous compilations is complete enough. Therefore, our intention is to merge together these three databases and to complement them with new examples found in the bibliography. Evidently, this database does not include all the calderas of the world but tries to be representative enough for further studies and analyses.

Furthermore, once all available field data are introduced into the database, we are able to find out if there exists any correlation between the different characteristics of collapse calderas (e.g. morphology, age, dimensions, etc). This allows us to establish similarities and differences among the different calderas recorded in the database and to define certain types or groups to classify them. The final aim is to determine a common physical scenario for each caldera group. Finally, we will combine the results obtained

with subsequent analogue and mathematical models, in order to establish a genetic classification of calderas.

Moreover, we will compare our results with those obtained in other works (e.g. Walker, 1984; Spera and Crisp, 1981; Cole et al., 2004) also related to collapse calderas field data analysis and caldera classification. Therefore, in this section, we present also a short summary of most of these relevant works.

## **II.2 FIELD DATA AND CALDERAS**

### **II.2.1 General aspects**

Field studies on collapse calderas are specially focused on the study of the structural aspects, and on the volcanic deposits (Fig. 2.1). Certainly, a rigorous field study of the products and structures generated during a caldera-forming event may provide enough information to determine pre-caldera volcanic activity and may help to understand the most probable causes that triggered caldera collapse and how this occurred.

On the one hand, structural aspects include caldera size and morphology as well as the tectonic features (local and regional) related to the caldera. Basically, the principal ways to study the structural aspects are topography and image analysis (e.g. Deception – *Antarctica*, Martí et al., 1996; Rotorua – *New Zealand*, Milner et al., 2002), structural geophysics (e.g. Phlegrean Fields – *Italy*, Troise et al., 2003; Masaya – *Nicaragua*, Rymer et al., 1989; Miyakejima – *Japan*, Furuya et al., 2002), and fieldwork campaigns (e.g. Cerro Galán – *Argentina*, Francis et al., 2003; Turkey Creek – *U.S.A.*, Du Bray and Pallister, 1991). In most cases the combination of these methods provide a reliable description of the caldera structure (e.g. Miyakejima – *Japan*, Nakada et al., 2005) and the surrounding structural framework.

Volcanic deposits are studied principally through fieldwork (incl. sedimentology, stratigraphy and lithology analysis) (e.g. Crater Lake – *U.S.A.*, Suzuki-Kamata and Kamata, 1993; Las Cañadas – *Tenerife*, Edgar et al., 2002), and laboratory work (incl. lithology and petrology and geochemistry analysis) (e.g. Rotorua – *New Zealand*, Milner et al., 2002; Vesuvius - *Italy*, Cioni et al., 1999a) (Fig. 2.1). Additionally, the analysis

and detailed mapping of hydrothermalism, geothermalism and ore deposits may provide information about both the structural features of the caldera and the volcanic deposits (Fig. 2.1) particularly, on the post-caldera transformation they have suffered (McKee, 1979; Guillou-Frottier et al., 2000).

Once determined the most relevant factors controlling eruptive processes, we want to specify which type of data obtained in the field may inform us about them. First it is necessary to say that, field data around the collapse caldera and its surroundings provide information only in a local or regional scale. Information about plate scale factors and processes, such as the tectonic context, are available from other techniques like geophysics or from the geographical location of the volcano (i.e. caldera) combined with known information about plate tectonics.

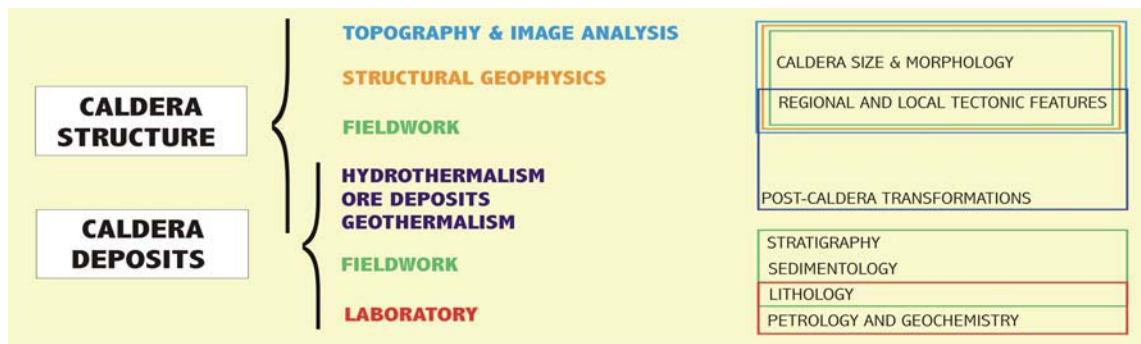


**Fig. 2.1:** Summary of the different techniques applied in the study of collapse calderas.

## II.2.2 Study of the caldera structure

The information concerning the caldera structure may be divided in two different groups (Fig. 2.2):

- **Regional and local tectonic features**
- **Caldera size and morphology**
- ❖ **REGIONAL AND LOCAL TECTONIC FEATURES**

Structural features that may provide information about caldera collapse processes cover from the regional to the local scale (Fig. 2.2).

On the one hand, in a regional scale, we find two important structural features: regional doming and the regional tectonic system. Regional doming may be caused by the accumulation of magma at deep crustal levels, i.e. by underplating. This regional-size accumulation of magma may lead to a bulging of the overlying crust (Bott, 1981). By contrast, regional doming may have also a pure structural origin due to the presence of a compressive regional stress field and the associated structures (e.g. Martínez-Martínez et al., 2002; Thiede et al., 2006). Additionally, the study of the regional tectonic fault system may explain, in some cases, caldera or eruption origin (e.g. Montefiascone – *Italy*, Nappi et al., 1991) (Fig. 2.3 A), as well as the caldera morphology (e.g. Silali – *Kenya*, Bosworth et al., 2003; Valles – *U.S.A.*, Self et al., 1986) (Fig. 2.3 B and C) In some cases, volcanism is partly tectonically controlled, by the intersection of regional fault and local structures (e.g. Taal – *Philippines*, Yokoyama et al., 1975).

In a local scale, the structural features are diverse. During the pre- and post-collapse stage it is possible to observe a local doming. It can have a pure structural origin due to the local tectonic system (Smith and Bailey, 1968) or it can be generated by the inflation of the magma chamber (i.e. injection of new magma inside the chamber) (e.g. Bonafede et al., 1986, Bonafede, 1990; De Natale and Pingue, 1993). After the collapse it is also feasible to observe local doming caused by the intrusion of magma bodies in the intracaldera deposits (e.g. Smith and Bailey, 1968; Fridrich and Mahood, 1984). Additionally, if the caldera roof has been fragmented during collapse, magma chamber inflation or magma intrusion bodies may produce also a differential uplift of the internal blocks through the reactivation of faults (e.g. Smith and Bailey, 1968; Elston, 1984). Both the post-collapse differential uplift and the local doming may have also a structural origin (e.g. Toquima – *U.S.A.*, Boden, 1986).

Furthermore, the observation of radial fractures may indicate local doming. Independent on the origin to the dome, during the doming process extensive surface fractures generate at the central part of the dome structure (Christiansen et al., 1977; Martí et al., 1994; Acocella et al., 2000; Lipman et al., 2000; Walter and Troll, 2001). Evidently, this observation is. These radial structures may appear prior to the collapse due to magma intrusion or inflation of the magma reservoir (e.g. Fernandina – *Galapagos*, Chadwick and Howard, 1991) (Fig. 2.3 D) or during the post-collapse stage in episodes of multicycling collapse process as indicated by some analogue models (see section III.2.1) (e.g. Martí et al., 1994; Walter and Troll, 2001). Also a possible

observable on the field are ring fractures. These may develop prior to the caldera collapse process during advanced stages of local doming. These structures have been also reproduced with analogue models on collapse calderas. If these ring fractures are related to the collapse process itself, they may provide information about the collapse mechanism. On the one hand, the inclination of ring fractures specifies if the caldera collapse took place through outward or inward dipping faults (e.g. Masaya – *Nicaragua*, Rymer et al., 1998). On the other hand, the total number of these structures reveals also some important aspects of the collapse process. A single circular fault may indicate a simple plate collapse whereas two ring faults point out nested calderas (see section III.2.1) (Phlegrean Fields – *Italy*, Orsi et al., 1991) (Fig. 2.3.E) or a combination of subsidence through vertical and reverse faults similar to analogue models results (see section III.2.1) (Batur – *Indonesia*, Williams and McBirney, 1979) (Fig. 2.3 F). In some cases it is also possible to observe a zone of multiple concentric fractures in agreement with analogue modelling (see section III.2.1) (e.g. Biblis Patera – *Mars*, Hodges and Moore, 1994) (Fig. 2.3 G). The presence of a tilted arc is also characteristic of collapse caldera structures. This may be originated by the sliding of material from the caldera walls during or after the collapse (e.g. Job Canyon – *U.S.A.*, John, 1995; Miyakejima – *Japan*, Nakada et al., 2005) or it is an effect of the collapse geometry due to the interaction between the vertical and the reverse “bell-shaped” faults (see section III.2.1) (Miyakejima – *Japan*, Nakada et al., 2005). Additionally, corresponding to the first stages of the caldera collapse it is possible to observe a downsagged zone (Branney, 1995). Analogue models justify this initial deformation as in collapse caldera cycles as the first response of the overlying material to the deflation of the magma chamber (see section III.2.1 and III.3.4.3.1) (Branney, 1995).

Another important structural feature that may provide information about the collapse process and the caldera morphology are the pre-existing fractures (e.g. Acocella et al., 2004; Holohan et al., 2005). In many cases, similar to regional tectonic systems, local structures, e.g. existing ring faults or extensional structures may control the development of posterior calderas (e.g. Deception – *Antarctica*, Martí et al., 1996; Rotorua – *New Zealand*, Milner et al., 2002).

Some of the structural features commented in this section are also observable with other techniques like geophysics, analogue models or mathematical models.

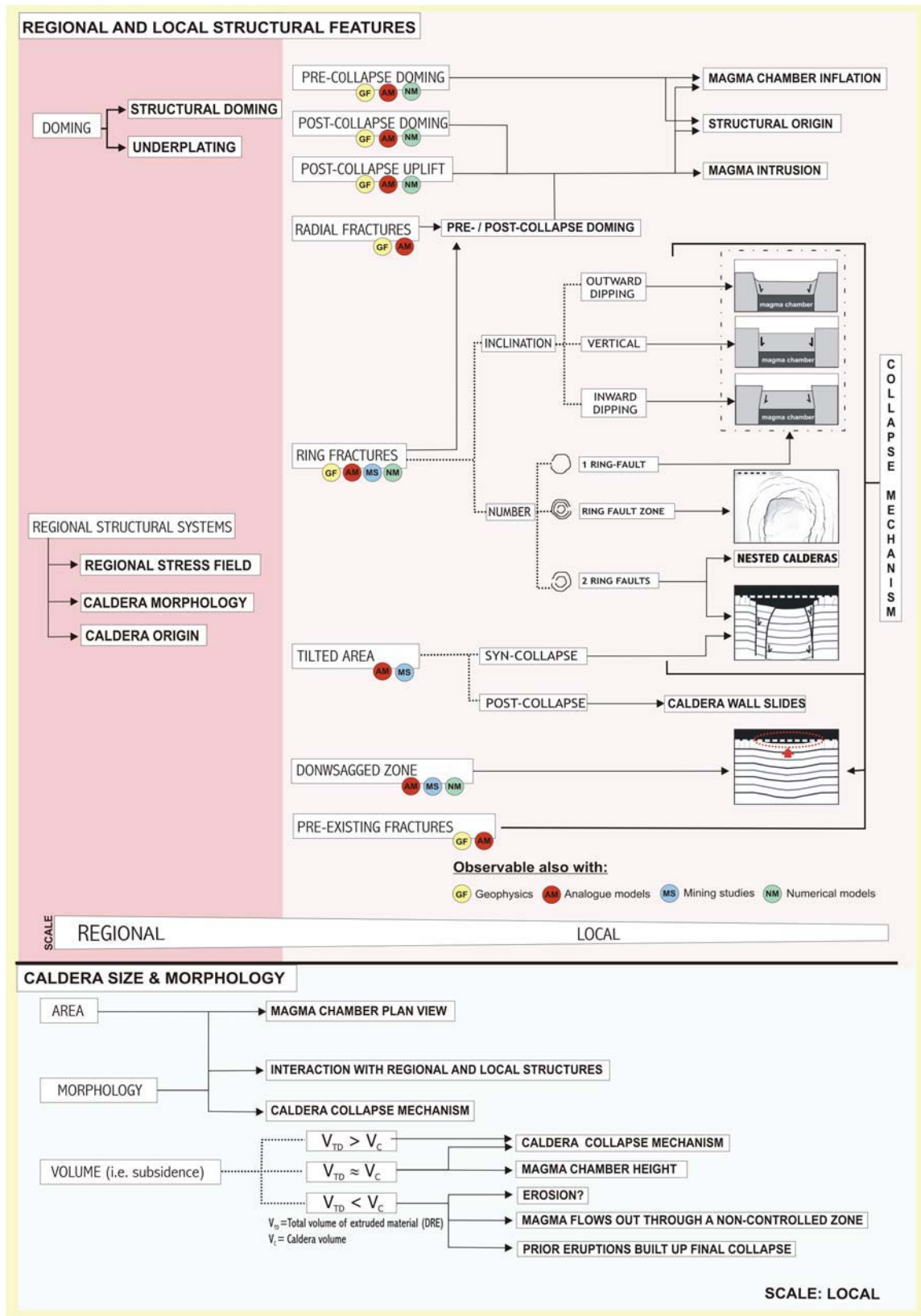
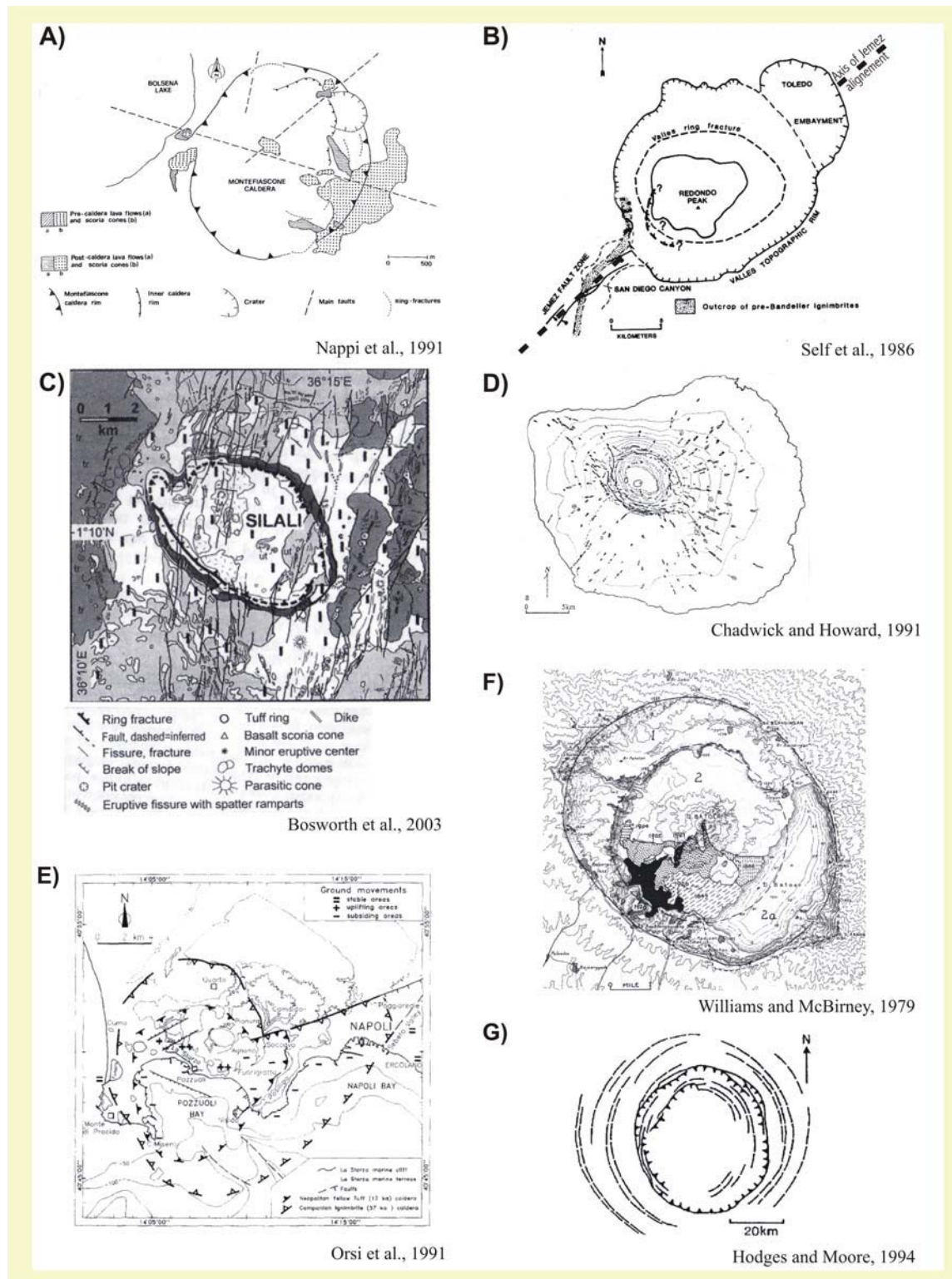


Fig. 2.2: Summary of the structural aspects observable on the field in a regional and local scales



**Fig. 2.3:** Examples of calderas on which different structural features are recognizable. **(A)** Montefiascone caldera is located at the intersection of regional structures. **(B)** Valles caldera, its elliptical morphology is possibly related to the regional field stress. The elongation of the caldera is parallel to the regional structures. **(C)** Silali caldera, the elongation of the caldera is perpendicular to the regional extensional structures, possibly due to pre-existing regional structures. **(D)** Fernandina a summit caldera with a great number of radial dike intrusions from the magma reservoir. **(E)** Phlegrean Fields, an example of nested caldera It has two ring faults structures clearly associated with two different caldera-forming events. **(F)** Batur caldera, the two rims are apparently of the same age. Collapse mechanism similar to analogue models results **(G)** Multiple concentric fractures at Biblis Patera, Mars extend outside the caldera wall.

## ❖ CALDERA SIZE AND MORPHOLOGY

Obviously, field observations of caldera size and morphology are restricted to a more local scale. On the one hand, the area of the caldera  $A_c$  and its plan view morphology may provide approximate information about the magma chamber plan view. Some authors proposed that assuming a caldera collapse controlled by near-vertical ring faults, the morphology and dimensions of the caldera structure at surface are an expression of the underlying magma chamber (Lipman, 1984; 1997; Roche and Druitt, 2001). This is obviously an approximation, since faults controlling subsidence are not necessarily vertical (e.g. Rabaul – *New Guinea*, Mori and McKee, 1987). Consequently, if these are outward- or inward-dipping the caldera diameter is larger or smaller than the magma chamber diameter, respectively. Additionally, the study of the depression morphology may give us information about the interaction of the caldera structure with regional or local tectonic structures, such as faults, graben structures, etc (e.g. Fantale – *Ethiopia*, Acocella et al., 2002; Toba – *Sumatra*, Bellier and Sébrier, 1994;).

Furthermore, the amount of subsidence and caldera volume combined with the volume of extruded deposits (in DRE) provide general information about the collapse mechanism, the size of the magma chamber, and post-caldera evolution. The study of different caldera samples and their associated deposits reveals that the total volume of extruded material  $V_{TD}$  can be greater, similar or smaller than the caldera volume  $V_C$ . In most cases,  $V_{TD} \approx V_C$ , i.e. the volume of extruded material is approximately equivalent to the caldera volume (e.g. Aira – *Japan*, Aramaki, 1984). Assuming that the area of the caldera depression at surface is approximately equivalent to that of the underlying magma chamber (i.e. subsidence of the roof took place as a rigid block along near-vertical ring faults), the amount of subsidence at surface  $S_s$  should correspond to the height of material withdrawn from the reservoir  $H_m$  (Fig. 2.4). Consequently, we obtain a minimum estimate of the magma chamber height.

However, there exist some caldera samples for which  $V_{TD} \gg V_C$ . In these cases, the amount of subsidence at surface  $S_s$  and the corresponding caldera volume  $V_C$  is insufficient to explain the volume of extruded magma from the reservoir (e.g. Latera – *Italy*, Nappi et al., 1991), i.e. apparently  $H_m \gg S_s$ . A possible explanation is that the collapse mechanism in these caldera samples differs from the rigid block subsiding along near-vertical ring faults. Maybe, structures controlling the subsidence

accommodate the displacement of the subsiding block at depth (Fig. 2.4) (Roche et al., 2000). A further explanation for  $V_{TD} \gg V_C$  may be an intensive break of the subsiding block during the collapse, which leads to a substantial dilatation of the subsided column filling the caldera depression. This phenomenon would disguise the real caldera volume (e.g. Miyakejima – *Japan*, Geshi et al., 2002). We have to consider also the possibility that the caldera depression could have been replenished by post-caldera volcanic activity deposits or by material slid from the caldera walls due to gravitational collapse (e.g. Tavua – *Fiji*, Setterfield et al., 1991). We can find in the literature also some caldera samples for which  $V_{TD} \ll V_C$  (Kumano – *Japan*, Miura, 1999; Fernandina – *Galapagos*, Munro and Rowland, 1996). The most probable reason for this observation is the possible existence of post-caldera erosion processes that may avoid the observation of the whole geologic record (Miura, 1999). However, there exist also a further explanation. This is the case of the caldera-forming eruption of Fernandina volcano in 1968. In that eruptive event magma flew out through a non-controlled zone permitting a major subsidence of the collapsing block but without a large material emission. Consequently, the small volume erupted was large enough to trigger what had been a potential collapse built up by numerous previous eruptions (Munro and Rowland, 1996).

Evidently, similar to the tectonic features, all these observations are strongly dependent on the erosion rate, the post collapse evolution and the geomorphological evolution. Therefore, we have to be aware when interpreting the available information.

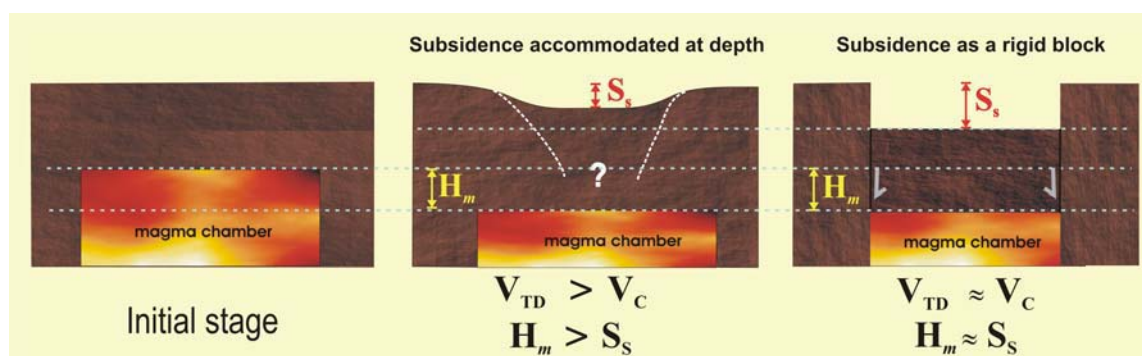


**Fig. 2.4:** Possible types of collapse mechanism inferred from the amount of extruded deposits associated with the caldera-forming eruption.  $S_p$  Subsidence at depth;  $S_s$  Subsidence at surface;  $V_c$  Volume of material in Dense Rock Equivalent (DRE);  $V_m$  Caldera volume.

### II.2.3 Study of the volcanic deposits

In order to understand caldera collapses it is also necessary to study the deposits formed during the caldera-cycle. The identification of transport and deposition mechanisms of the erupted material is crucial to know the eruptive mechanism and dynamics of the eruption. The disciplines that study the deposits erupted during a caldera-forming eruption are (Fig. 2.5):

- **Stratigraphy:** Identification, description and correlation of the different depositional units. Study of the vertical and horizontal spatial and temporal relationships.
- **Sedimentology:** Description and study of sedimentary structures and the relations between sediments, their genesis and diagenesis, the sedimentary environment and processes, etc.
- **Lithology:** Study of the composition and properties of the rocks visible on the field.
- **Petrology and geochemistry:** Description and systematic classification of rocks and study of the whole rock and mineral chemistry, respectively.

The stratigraphical, sedimentological and lithological studies are carried out on the field, whereas petrographical and geochemical analyses, as well as, some aspects of the lithological studies are performed in the laboratory. All disciplines act in a local scale according to the magma chamber size. However, they analyse from the whole eruptive unit associated with the caldera-forming event (stratigraphy, lithology), to the single mineral components of the volcanic rocks (petrology), passing through an analysis of both the sediments constituting the volcanic unit and the rocks discernable on the field (sedimentology, lithology).

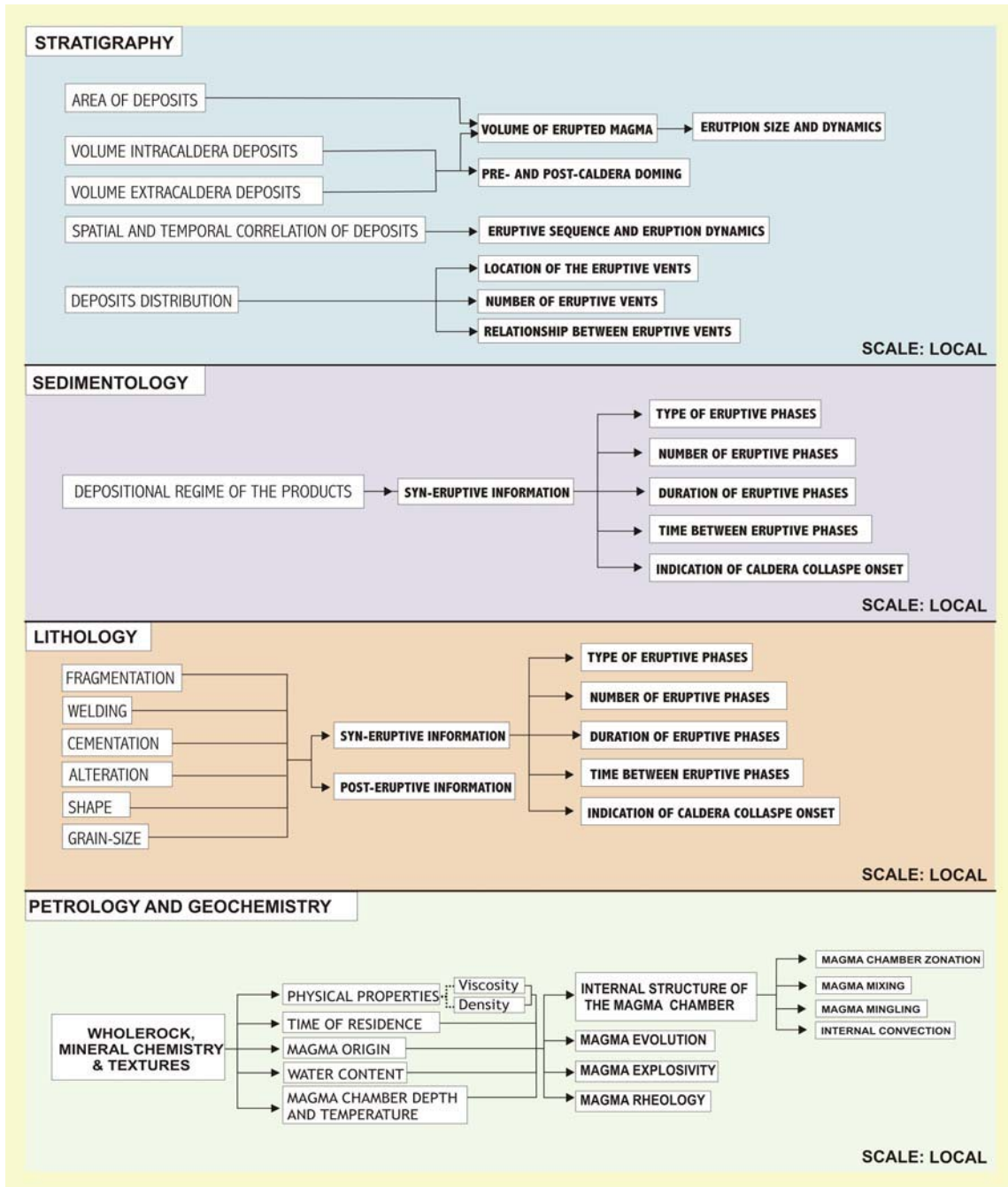


**Fig.2.5:** Summary of the type of information provided by the study of the volcanic deposits applying different disciplines.

## ❖ STRATIGRAPHY

Stratigraphical studies related to caldera-forming deposits are aimed to study different aspects concerning eruptive units (Fig. 2.5). They mainly focus on the investigation of the areal distribution of deposits formed during the caldera-forming event and their spatial and temporal correlation that may provide information about the eruptive sequence and dynamics, especially about the changes in the eruption size (e.g. Vesuvius – *Italy*, Cioni et al., 2003; Rotorua – *New Zealand*, Milner et al., 2002).

The area and the thickness of the deposits inside (intracaldera deposits) and outside (extracaldera deposits) the caldera depression may give an estimate of the erupted volume and consequently, an approximation of the eruption size (e.g. Lindsay et al., 2001). In some cases, studying the variations in the thickness of the deposits and the contact geometry between pre-, syn- and post-collapse eruptive or depositional units it is possible to infer processes of pre- and post-collapse doming (e.g. Bursum – *U.S.A.*, Ratté et al., 1984).

Furthermore, the distribution of deposits around the volcanic area and the type and distribution of vent- and conduit-derived lithic clasts permits the location of the eruptive vents (e.g. Atitlán – *Guatemala*, Rose et al., 1987), the estimation of the number of possible vent (Allen, 2001 and references therein) and spatial and temporal relationship between them (e.g. Vesuvius – *Italy*, Cioni et al., 2003). A good example, is the study of the isopach (contour lines of equal deposit thickness) and isopleths (contour lines of equal lithic sizes) maps of the tephra layers (e.g. Miyakejima – *Japan*, Nakada et al., 2005)(Fig. 2.6) that may provide information about the location of the eruptive vents (e.g. Kos Plateau – *Greece*, Allen et al., 1999; Allen, 2001), the height (e.g. Ceboruco – *Mexico*, Gardner and Tait, 2000) and the energy of the eruption column (e.g. Las Cañadas – *Tenerife*, Edgar et al., 2002; Vesuvius – *Italy*, Carey and Sigurdsson, 1987) as well as about the wind distribution during the eruption (e.g. Miyakejima – *Japan*, Nakada et al., 2005). Furthermore, it is also possible to calculate the volume of deposits for each eruptive event from the isopach maps using specific calculation methods, e.g. Fierstein and Nathenson (1992) (Nakada et al., 2005).

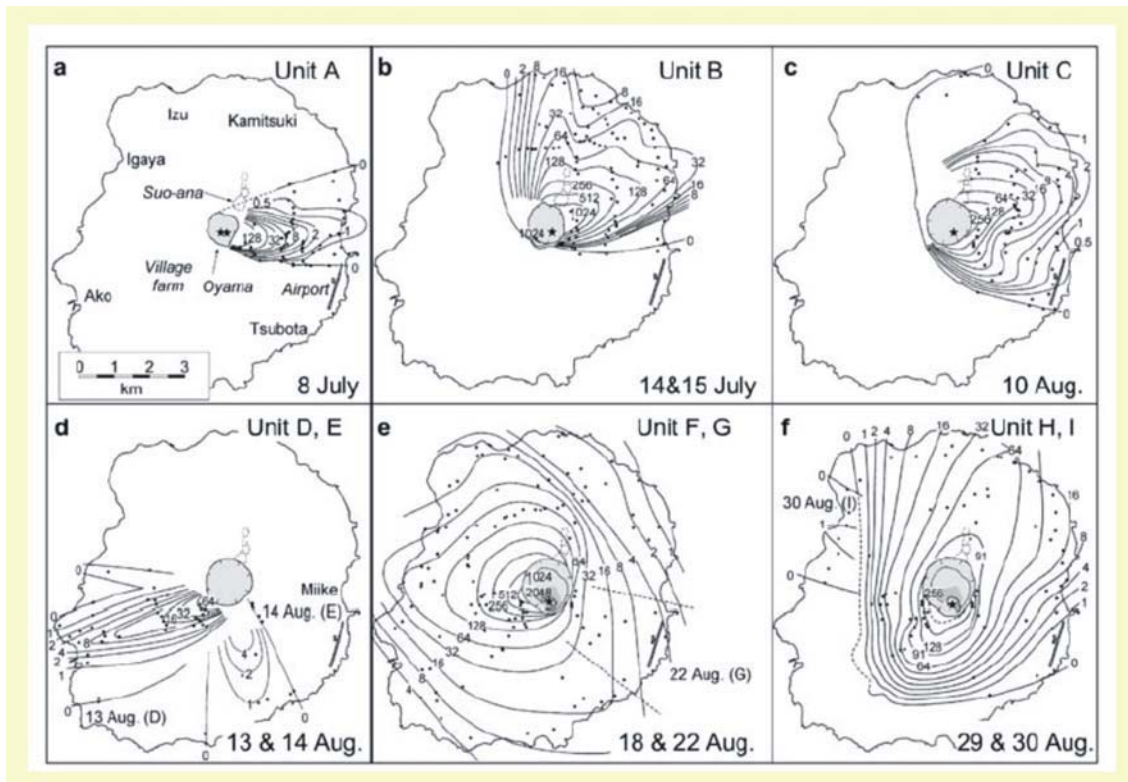


**Fig. 2.6:** Isopach maps of tephra during the July–August 2000 eruption of Miyakejima Volcano, Japan. Stars in the newly formed caldera represent the eruption craters. Contours are in millimeters.(Nakada et al., 2005)

## ❖ SEDIMENTOLOGY

Closer observations of the volcanic deposits may reveal the depositional regime of the erupted materials, discerning the eruptive style (e.g. Kos Plateau Tuff– *Greece*, Allen et al., 1999; Allen, 2001; Las Cañadas – *Tenerife*, Edgar et al., 2002) the number and duration of the different eruptive phases (e.g. Miyakejima – *Japan*, Nakada et al., 2005) and their temporal relationship (e.g. Valles – *U.S.A.*, Self et al., 1986) as well as the moment in which caldera collapse begun (e.g. Kos Plateau Tuff– *Greece*, Allen et al., 1999; Allen, 2001) (Fig. 2.7).

For example, changes in the nature of the depositional units (e.g. from mantle-bedded fallout throughout pyroclastic-density-current deposits to massive ignimbrites) may reflect changes in eruptive style from a stable column to the initiation of an oscillatory collapsing fountain, and further to a more stable collapsing fountain, coinciding with an increase in the mass flux (Fig. 2.7)(Carey and Sigurdsson, 1989; Neri and Dobran, 1994; Allen, 2001).

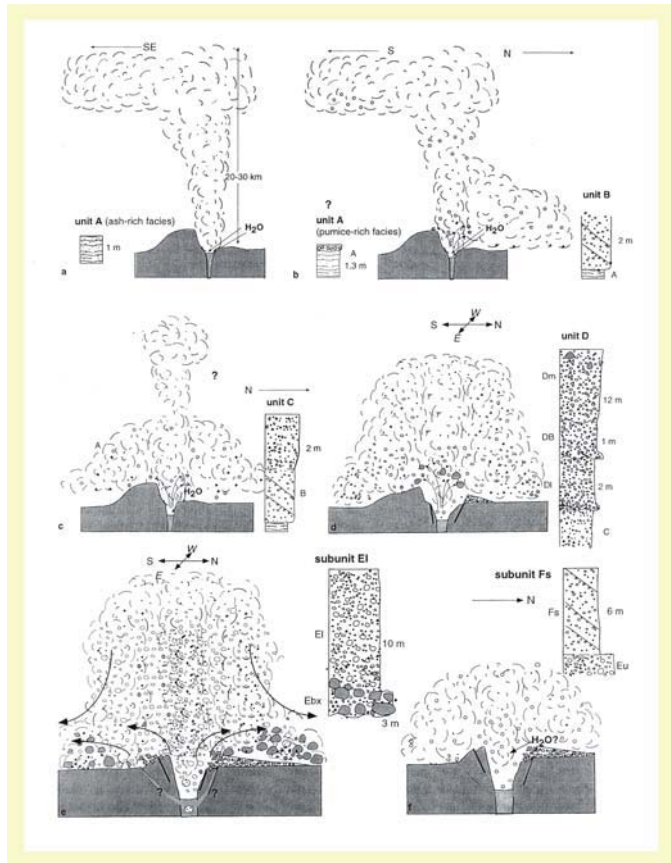


**Fig. 2.7:** Schematic representation of the Kos Plateau Tuff eruption, the major caldera-forming eruption in the eastern Aegean Sea. Thanks to the analysis of the stratigraphic column it is possible to reconstruct the eruption dynamics and phases. **(A)** Initiation of the eruption with a phreatoplinian column from which widespread fine-grained fallout is deposited. **(B)** The eruptive activity fluctuates between wet phreatomagmatic to dry explosive style, causing column collapse and generating a pyroclastic density current. **(C)** Explosive activity transitional between wet and dry generates a pyroclastic density current. **(D)** Eruption intensity increases and dominantly dry explosive activity prevailed. **(E)** Climax of the eruption marked by the disintegration of the vent and conduit walls and ejection of a large amount of coarse vent- and conduit-derived lithic clasts. Multiple vents were possibly initiated at this stage. **(F)** Further decline in the eruption intensity is recorded by a fine-grained, lithic-poor stratified pyroclastic-density-current deposit. (Modified from Allen, 2001)

## ❖ LITHOLOGY

The study of rock properties like the fragmentation, welding, cementation or alteration level as well as morphological and granulometry studies of the different components (e.g. pyroclasts, ashes, etc.) provide syn- and post-eruptive information. For example, angular and blocky in shape ash clasts that include predominantly tube pumice with some poorly vesicular pumice together with a widespread, sheet-like form, fine grain-size, grain-shape and good sorting may indicate a phreatoplinian deposition (e.g. Allen and Cas, 1998; Allen, 2001). Also related to the size of the clasts, the typical abundance and maximum size of dense lithic clasts in the ignimbrites may indicate for example the distance of the sources (Kuno et al., 1964; Wright and Walker 1977; Walker, 1985; McPhie, 1986). Additionally, the distribution of accidental lithics in pyroclastic units of caldera-forming eruptions provide important clues on the evolution of the vents(s), vent migration and transition from simple- to multiple-vent activity (Rosi et al., 1996 and references therein; Browne and Gardner, 2004). For example, a low

percentage of vent- and conduit-derived lithic clast, narrow range of lithic clast types and development of a sustained column suggest this opening phase involved a single vent (Fig. 2.7) (Wilson et al., 1980; Woods, 1988; Allen, 2001).

A further good example is the presence of a conspicuous layer of coarse vent- and conduit-derived lithic clasts (Fig. 2.8) in stratigraphic profiles of diverse caldera-forming eruptions. The identification of this lithic breccia at the base of voluminous ignimbrites and can be linked with the initiation of caldera collapse (e.g. Crater Lake - *U.S.A.*, Bacon, 1983; Minoan eruption - *Greece*, Bond and Sparks, 1976; Heiken and McCoy, 1984; Taupo ignimbrite - *New Zealand*, Wilson and Walker, 1985; Kos Plateau Tuff - *Greece*, Allen, 2001).

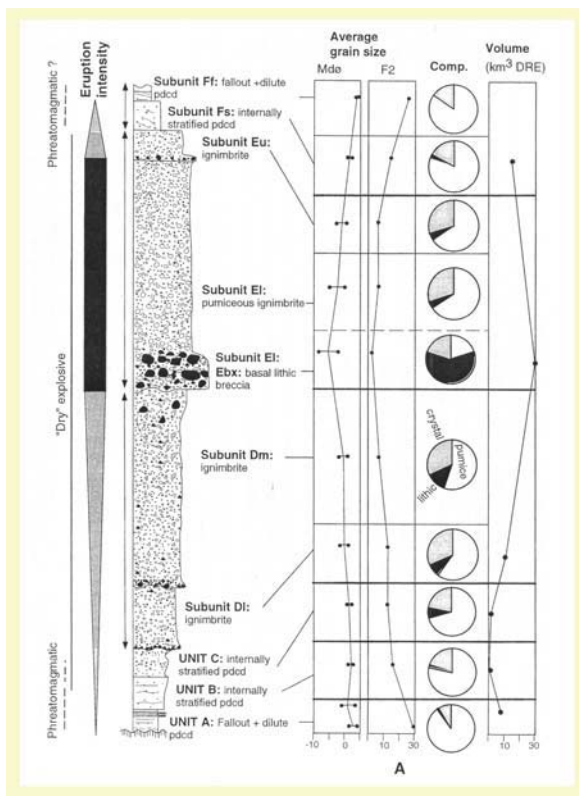


**Fig. 2.8:** Stratigraphy, textural characteristics and components of the Kos Plateau Tuff (KPT), eastern Aegean Sea. **(Left)** Simplified stratigraphic profile of the units and subunits of the KPT on Kos, indicating eruption style and waxing and waning phases. **(A)** Textural characteristics, components and volume of the various units and subunits. (Modified from Allen, 2001)

## ❖ PETROLOGY AND GEOCHEMISTRY

Finally, an exhaustive petrographical and geochemical work is useful to infer information about the magma chamber from which caldera formed. The study of whole rock and mineral geochemistry as well as a textural analysis may inform about the origin

of the extruded magma, its time of residence in the magma chamber (0), its physical properties (e.g. Menengai – *Kenya*, Leat et al., 1984) and volatile content (e.g. La Pacana – *Argentina*, Francis et al., 1989) and in some cases, also the magma chamber depth (i.e. pressure) (e.g. Long Valley – *U.S.A.*, Johnson and Rutherford, 1989) and temperature (e.g. Vesuvius – *Italy*, Cioni et al., 1999a, 1999b). Furthermore, this information may be useful to infer the internal structure of the magma chamber (e.g. magmatic mixing or mingling, magma chamber zonation or convection) (e.g. McDermitt – *U.S.A.*, Rytuba and McKee, 1984; Rum Central Igneous complex – *Scotland*, Troll et al., 2000) (Fig. 2.9) and the magma evolution, explosivity and rheology. Additionally, the study of major- and trace- elements abundances may help us to distinguish between different, apparently similar, depositional units (e.g. Ceboruco – *Mexico*, Nelson, 1980).

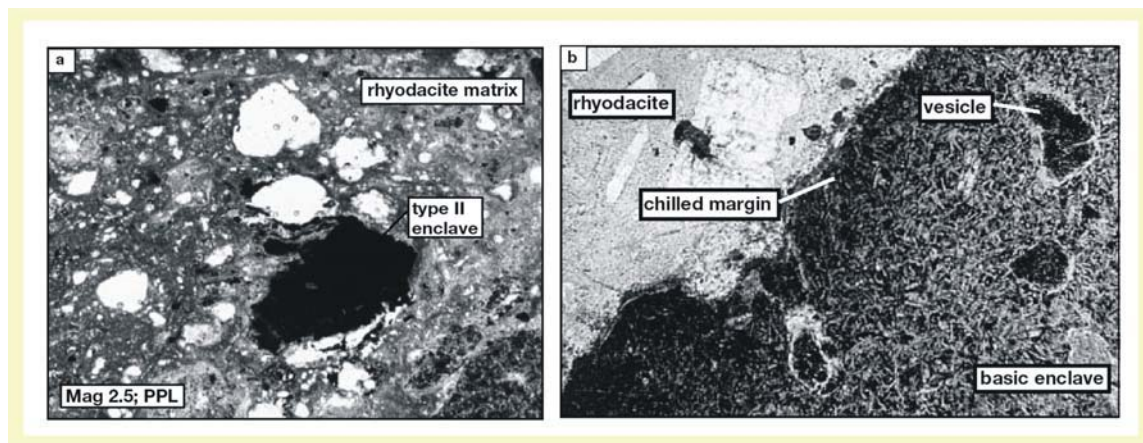


**Fig. 2.9:** Photographs of inclusions in rhyodacites of the Rum Central Igneous complex. (A) Type-II inclusions characterized by a dark aphyric, cryptocrystalline appearance representing magma frozen in the conduit or on eruption. (B) Type-III inclusions are always round and differ from type-II in having a microcrystalline texture with plagioclase lath morphologies characteristic quenching (Lofgren, 1980). This type is found throughout the rhyodacite implying repeated replenishments of the magma chamber by basic magma. (Modified from Troll et al., 2000)

Combining all the information coming from the different disciplines (stratigraphy, sedimentology, lithology, and petrology and geochemistry) it is possible to reconstruct partially the collapse caldera cycle (e.g. Rum Central Igneous complex – *Scotland*, Troll et al., 2000) (Fig. 2.10)

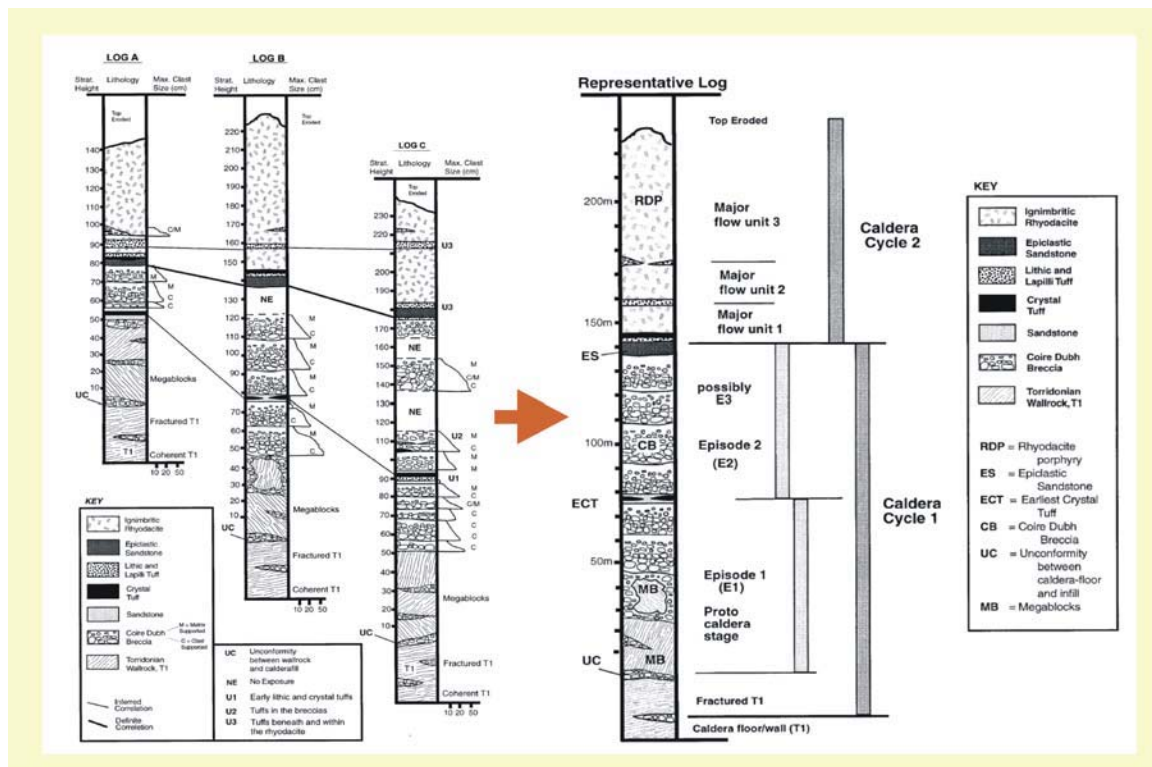


**Fig 2.10:** Stratigraphical logs of the caldera-infill succession of the Northern Marginal Zone in the Rum Central Igneous Complex in Scotland. The representative log permits to infer the caldera cycles and episodes marked by the caldera infill. (Modified from Troll et al., 2000)

## II.2.4 Study of hydrothermal, geothermal and ore deposits

Another excellent source of information when studying caldera collapse processes and their related deposits or structures, is the study of hydrothermal, geothermal and ore deposits.

As mentioned before (see section I.1.4) calderas and their associated volcanic activity are strongly related to these kind of natural resources (McKee, 1979). In fact, they are important controlling factors on many ore deposits and geothermal energy resources (Self et al., 1984; Guillou-Frottier et al., 2000; Lipman, 2000) especially because the structural features of collapse calderas favour thermal circulation and the formation of the deposits. For example, it is possible that large hydrothermal systems develop during a post-caldera resurgence stage when magma is injected at shallow levels. This provides a renewed heat source magmatic input of volatiles and metals and new structural pathways (Stix et al., 2003).

The study of the distribution of mineral deposits may provide information about the caldera structure and its surrounding since, in some cases, it can be associated with much later activity localized by caldera structures (Steven et al., 1974; McKee, 1979). Furthermore, the type of mineralization is related to the magma origin and composition (Lipman, 2000; Stix et al., 2003).

### II.2.5 Field data restrictions

Obviously, field work and consequently, field data is not exempt from important restrictions. On the one hand, *in situ* observations of eruptive processes are limited to the accessible parts of the eruptions, restricting observations to above-surface processes. Moreover, data of *in situ* observations can be collected only near an established observatory or in those places where volcanic activity has been somehow forewarned (Mader et al., 2004). Besides, field data of past volcanic events and caldera-forming eruptions is not free from considerable and limiting restrictions. Directly related to caldera collapse studies we can mention for example, that in some cases (e.g. Bolsena-Italy, Nappi, 1991) direct evidence for collapse is difficult to demonstrate because most of the area is now under water and the role of neotectonics has been very important (Nappi, 1991). Furthermore, when estimating volumes of extruded material, it is typical, especially during small eruptions characteristic of arc systems, a loss of a notable part of the total volume to the atmosphere, to be deposited as air-fall ash. Thus, volume estimates may err on the low side. On the other hand, the large-volume deposits from the epicontinental structures may commonly have a major component of intracaldera tuff, the volume of which may be difficult to estimate because the thickness is not known or the structural boundaries of the deeply subsided block are not well defined, or both (Smith, 1979). Additionally, in some cases thickness and areal distribution of deposits has to be inferred and consequently, volumes estimate is not possible or may have a considerable error (Varga and Smith, 1984).

Moreover, erosion plays also an important role when studying volcanic processes and it is maybe one of the most important sources of interpretation and also for examples, volume estimate errors (e.g. Turkey Creek – U.S.A., du Bray and Pallister,

1991). In some cases, erosion may control the interpretation of field observations (e.g. Koolau Kilauea and Mauna Loa – *Hawaii*, Walker, 1988).

Additionally, subsequent post-caldera volcanic activity or sedimentation processes may affect field observations (e.g. Platoro – *U.S.A.*, Lipman et al., 1996). For example, we can not infer in a volcanic area the distribution and vent localities because they are poorly exposed and interbedded with basin fill sediments (Self et al., 1986) or the topography of the caldera floor vary much over the past years due to repeated subsidence, erosion, post-collapse structural modifications and partial infilling events (e.g. *Kilauea-Hawaii*, Walker, 1988).

Furthermore the determination valid regional stratigraphic correlations are also full of critical difficulties and impediments. Deposits extruded during caldera-forming events are in most cases, enormous areal extensions of individual ash-flow sheets. In some cases, this leads to different names being applied to the same tuff sheet in widely separated parts of a volcanic field or they can exist miscorrelations between outflow tuff sheets and their intracaldera equivalents (e.g. Platoro – *U.S.A.*, Lipman et al., 1996). Moreover, it is also possible to misinterpret large coherent slide blocks and lithological mixed caldera-collapse breccias, leading to errors in the inferred stratigraphic sequence. It is also possible to failure trying to recognize entire calderas especially non-resurgent structures because later volcanic deposits may have buried them (Lipman et al., 1996).

## **II.3 STATE OF THE ART**

### **II.3.1 Introduction**

During more than a century, collapse calderas have been a major subject of interest in volcanological field studies. A great majority of these studies tend to offer a detailed descriptions of particular examples and to explain their origin from available field data (e.g. Grizzly Peak – *U.S.A.*, Fridrich et al., 1991). The number of relevant papers germane to collapse calderas is increasing year by year, and some of them are considered as guides for the other caldera studies (e.g. Williams, 1941; Smith and Bailey, 1968). These few field-based studies offer a generalised approach to the

---

understanding of caldera processes. On the one hand, these works are focused on comparing the main characteristics features (e.g. caldera structure, caldera morphology, composition of the extruded volcanic materials, etc) of caldera samples (e.g. Valles - *U.S.A*, Krakatau - *Indonesia*, Santorini – *Greece*) in order to find out the correct or most adequate criteria to classify them. On the other hand, some of these studies also include possible explanations for caldera dynamics (e.g. Williams, 1941). Lipman (1997) offered a comprehensive study of collapse calderas and proposed a general model of caldera structure and established the necessary nomenclature and definition of the different structural elements that characterize a caldera depression (see section II.3.4.3). This generalized model is an excellent basis for discussing main caldera structural elements and subsidence processes.

Moreover, in some cases, an exhaustive fieldwork may provide enough information to reconstruct an entire collapse caldera cycle, including pre-, syn- and post-caldera activity. For example, after a comprehensive review of field data Smith and Bailey (1968) proposed a general and simplified description of the whole caldera cycle for resurgent calderas (see section II.3.5). Also important is the study of Walker (1984) on post-caldera volcanic activity, in which the location (i.e. spatial distribution) of volcanic events after the caldera collapse may inform about the level of volcanic activity, the state of the magma chamber, the influence of the collapse structures, etc (see section II.3.6).

In section II.3.2, we offer a summary of the most important points exposed in the relevant work “Calderas and their origin” written by Williams in 1941. This comprehensive study has not always received the necessary attention, despite it offers the basis for an innumerable amount of subsequent works and today, some of the presented hypotheses and descriptions about collapse caldera processes may be still valid. Furthermore, we are going to introduce the structural parts of a collapse caldera according to Lipman (1997) (section II.3.3). This will facilitate the comprehension of posterior descriptions of field studies and both analogue and mathematical modelling results present in this work. Furthermore, we summarize the different classifications proposed for collapse calderas and introduce briefly the caldera cycle defined by Smith and Bailey (1968) (section II.3.5). We include also a summary of the results obtained by Walker (1984), since the nomenclature proposed by the author is also used in our database to characterize post-collapse activity of the revised calderas (section II.3.4.6).

---

Finally, we comment some results of other relevant general works also related to collapse calderas and field data analysis (section II.3.7).

### **II.3.2 “Calderas and their origin”**

In 1941, Williams presented with the work “Calderas and their origin” an insightful analysis of several aspects concerning collapse calderas. Since this revealing work became the basis for many investigations, we consider necessary to summarize the most important results obtained before continue commenting newer studies. The most outstanding points of Williams’s work are:

- **A proposal of caldera classification**
- **Presentation of the different theories of caldera formation**
- **List of factors favouring collapse**
- **Description of the collapse nature**

#### **❖ A PROPOSAL OF CALDERA CLASSIFICATION**

This works contains a first approach to subdivide and classify calderas trying to make a distinction based on eruption style and magma composition at representative volcanoes. The end-members of this classification slightly modified after Williams and McBirney (1979) are summarized in section II.3.4.2 .

#### **❖ PRESENTATION OF THE DIFFERENT THEORIES OF CALDERA FORMATION**

The author includes a short description of the different theories concerning collapse caldera formation existing at that time. As we consider that these theories may be useful for the comprehension of next sections, we proceed with a short summary of the most important points according to William’s abstracts (1941).

➤ **The “Crater elevation” theory**

According to this theory massive lavas might accumulate on gentle slopes and later, these might be arched to form high cones. The arching might produce wide tension fissures on the flanks and calderas on the summits. The life of this theory was very short then it was discarded within a few years.

➤ **The explosion theory**

The theory stated that large calderas are similar in origin to smaller craters and that the difference in size is merely a measure of the intensity of the explosions, which produce them. Consequently, calderas should form by explosive decapitation of former cones. Additionally, other authors like Escher suggested that caldera-forming explosions might originate at depth. Consequently, the deeper the explosion focus the greater the volume of lithic debris and the greater the proportion of fragments from the subvolcanic basements. This theory was abandoned due to the scarcity of such lithic debris in areas of caldera collapses.

➤ **The gas-coring and insliding theory of Escher**

In fact, Escher (1929) believed that if a large cylinder is drilled by explosion, insliding of the walls might take place forming depressions many width in km. In fact, it has often been observed that slumping of the walls both during and after eruptions enlarges craters. Furthermore, subsequently rise of magma may the convert the funnel-shaped depressions into flat-floored calderas.

➤ **Sandberg’s “Mantle-pipe” theory**

Again, this theory assumed that calderas and craters are formed in the same way and differ only in size. The arguments rested in the assumption that the original conduits of volcanic cones are of caldera proportions and that as activity continues with diminishing intensity the conduits decrease in size and calderas are slowly filled in.

---

➤ **Theories of internal solution**

According to this theory, volcanoes might enclose a large chamber of liquid lava, which might grow larger as a consequence of melting of the walls. If the magma remains inside the chamber, it would slowly crystallize to form a resistant core and erosion of the outer shell would reveal a “homogeneous dome volcano”. However, if the opening of the lateral vents drained much of the magma from the interior of the cone, the top of the solid shell might collapse to produce a caldera.

➤ **Wing Easton’s cell theory**

The theory suggested that volcanic conduits tap low levels on the roofs of inclined chambers. After the first eruption, the magma level falls and the gas pressure accumulates in the overlying space until the magma is again forced out of the conduit. Consequently, the magma level is lowered again and the process is repeated. As the cone grows higher and the volume of residual magma diminishes, the activity becomes more explosive and less effusive. When the magma level falls below a certain threshold, the conduit is effectively plugged with solid lava and debris, and the gases in the magma chamber are forced to escape through scattered fissures in the roof. Consequently, the fissures on the walls are widened by melting and generate new magma which slowly tends to percolate downward. The lowest part of the volcano consists of a solid skeleton with an infinite number of cells, differing greatly in size and shape, while the feeding chamber is gradually filled in with magma and the gases above the magma attain to increase tension. Finally, the structure might not be able to support the weight of the upper part of the volcano and it collapses either as a rigid block or gradually and piecemeal.

➤ **Collapse theories involving withdrawal of magmatic support**

This theory stated that collapse caldera form due to the removal of magmatic support, occasioned mainly by the withdrawal of magma to the surface and the injection of dikes at depth. However, the contraction of the magma body and changes of shape beneath the surface might lead to caldera collapse. Collapse does occur as a result of ring fracture stopping where the load of the volcanic edifice becomes too great for stability and the heavier crustal rocks sink into the lighter magma, but this cause of engulfment seems subordinate. It is principally the withdrawal of magma from the chamber which leads to crustal subsidence and the production of calderas, summit and

sector graben. In shield volcanoes magma chamber withdrawal occurs by abundant outpourings of lava from fissures far down the flanks. By contrast, in composite volcanoes evisceration is usually by the violent and rapid explosion of enormous volumes of pyroclastic material (Fig. 2.11). Independent on the mechanism the condition is that evisceration should occur very quickly to counteract possible magma chamber replenishment with equal speed from below. Consequently, an actual potential void is created in the upper part of the chamber and collapse roof is inevitable.

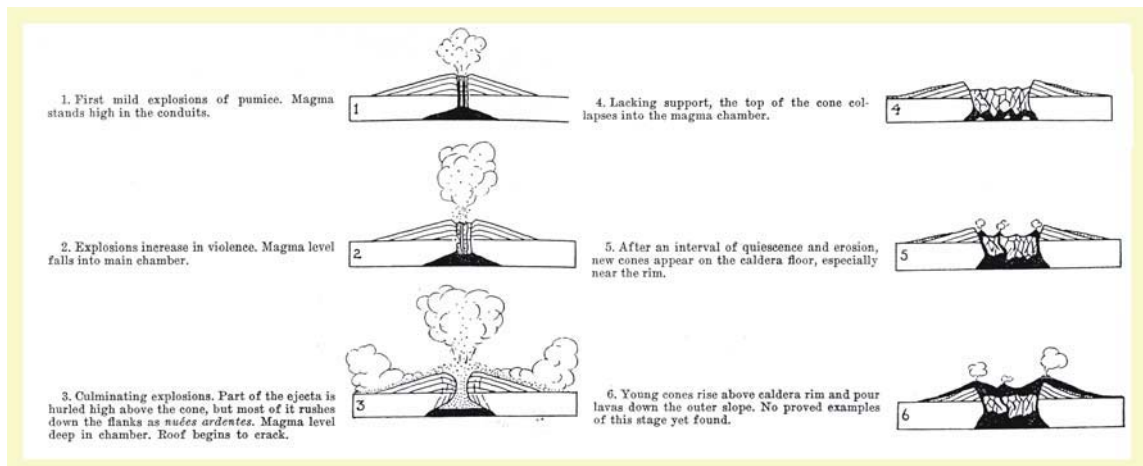


**Fig. 2.11:** Sketch representing the different step characterizing caldera evolution. Pumice eruptions, followed by collapse and growth of new cones on the caldera floor (In Williams, 1941 modified from van Bemmelen, 1929)

## ❖ LIST OF FACTORS FAVOURING COLLAPSE

The work of Williams (1941) also includes some observations about the factors favouring crustal collapse in general. These may be grouped as follows:

### ➤ Dimensions and morphology of the magma reservoir

Large magma reservoirs are the most probable to generate the enormous volumes of ejecta, which must necessarily be removed to withdraw enough support from the roof. Furthermore, a partial emptying of a prolate reservoir is less favourable to collapse than partial emptying of a broad, lenticular chamber. In fact, a steeply arched reservoir roof is more self-supporting than a widely domed roof.

➤ **Characteristics of the magma reservoir roof**

Another factor favouring are thin roofs, sufficiently impermeable to permit the accumulation of high gas and pressure. Moreover, heavy roofs, particularly, if these are underlain by light magma, will be particularly predisposed to engulfment by ring fracture stoping. Once such stoping begins, the rise of magma along the bounding fractures permits further settling by reducing friction on the sides of the block and by withdrawing material from below. Caldera collapse is also favored if the magma chamber roof presents zones of weakness (tectonic or volcanogenic) provided it retains sufficient coherence to allow the accumulation of high gas pressure.

➤ **Characteristics of the magma reservoir**

Caldera collapses may be also favored if a magma reservoir cut off from replenishment from below or with a magma chamber, which can only be refilled slowly. Obviously, to cause a mass deficiency at depth, magma must escape at the surface faster than it can enter.

➤ **Characteristics of the magma**

The magma should be capable of being discharged quickly. Two types are possible: fluid and hot basaltic magma, which can spread for long distances through narrow fissures and escape hurriedly in large volumes; or gas-rich, explosive magma. If the collapse is related to the contraction of a magma body during solidification, it will tend to be most pronounced above an acid magma body, since in general such magma loses more volume on crystallizing than basic magma. Obviously, the size of the body is important in this connection.

❖ **NATURE OF THE COLLAPSE**

The work of Williams (1941) concludes with a consideration about the nature of collapses. In the following paragraphs we present a summary of the most relevant conclusions and statements.

As mentioned before, the precise way in which a volcanic cone breaks down forming a collapse caldera depends on a diversity of factors: the nature of the reservoir roof (massive or incoherent, thin or thick), the shape and size of the reservoir, the rapidity of escape of the magma and the volume erupted, etc. Subsidence may take the form of a gentle downwarping and it may occur intermittently and produce stepwise collapse, or may take place in a sudden engulfment. Normally, sagging is more probable to happen where the reservoir roof consists of weak sediments or incoherent pyroclastic deposits whereas roofs of greater rigidity lead to abrupt collapses.

One important point of Williams considerations is to admit that much valuable information on the collapse caldera question can be obtained from comparison with mining subsidence. Mine studies indicate that the removal of material in mines cut in massive rocks causes the roofs of the stopes to spall, and if the mines are deep, the release of pressure may cause the roofs to split with explosive violence. Evidently, a similar phenomenon occurs when magma chambers are partly emptied by eruptions. In fact, for the enormous pressures at the plausible depths where magma chambers are located, small voids above the magma level will be rapidly enlarged.

Furthermore, in the formation of calderas by collapse the tendency will likewise be for the bounding fractures to spread upward at right angles to the outwardly dipping lavas and ashes of the cones. This process will be facilitated by the common alignment of joints in the same direction. The fractures will be steepest among massive lavas and most gently inclined among incoherent ashes. In general, also the fracture planes will become steeper at depth, and in their lower parts they will dip outward, in the manner of ring dikes.

Moreover, in mine studies, if an ore deposit lies at shallow depth, and its diameter is large compared with its depth, the roof usually caves in bodily. The same bodily collapse, or at least an engulfment of enormous blocks, is likely to happen in volcanic cones built above broad and shallow laccolithic magma chambers, especially if the chambers are rapidly evacuated by pumice discharge. By contrast, if the magma reservoir is broad and shallow and evacuation takes place gradually by a long series of pumice eruptions, the lower part of the roof will first fall into the reservoir and afterwards, that cracks will slowly extend upward, breaking the cover into a mass of small blocks. As the escape of magma continues and the support of the roof is further withdrawn, a critical stage may be reached at which the cover will founder as a block. Alternatively, the roof may subside in successive steps, producing a caldera with terrace

walls. The rapidity with which the magma chamber is evacuated determines, in large part, whether the roof drops telescopically or as a piston.

The collapse mechanism depends also on the number and size of vents perforating the roof before the collapse begins. A single and relatively narrow vent will not greatly weaken the roof over the reservoir and it will fail as a unit. But, if a cluster of vents penetrates the roof, failure is more probable to be piecemeal. Before the main, central dome collapses, the parasitic cones may be engulfed and the resultant caldera will then have a scalloped margin.

Furthermore, if the ore body is small in width but at considerable depth, subsidence is brought about mainly by the spalling process already mentioned and the sinking mass becomes a chaotic pile of fragments. Similarly in volcanic regions where relatively narrow cylindrical blocks have subsided, brecciated pipes are formed.

In caldera collapses where the original cones are composed dominantly of massive lavas the limiting faults will be sharply defined, but where a cone built chiefly of incoherent pyroclastic ejecta is concerned a series of concentric fractures will be formed and the caldera walls will show a terraced arrangement.

### **II.3.3 Caldera structure**

A caldera is characterized, considering a simple model, by the following structural and morphologic elements (Lipman, 1997):

- **Topographic rim**
- **Inner topographic wall**
- **Collapse collar**
- **Bounding faults (if present)**
- **Structural caldera floor**
- **Intracaldera fill**
- **Underlying magma chamber or solidified pluton**

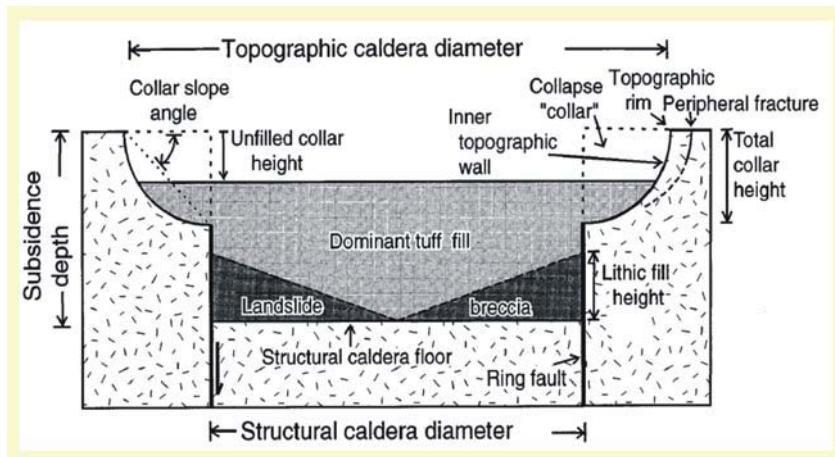


**Fig. 2.12:** Simplified model of plate (piston) caldera subsidence. Ring faults are arbitrarily shown as vertical, although they can dip steeply. The landslide breccia is shown schematically at the base of caldera fill to simplify the geometry, rather than the more actualistic complex interfingering that occurs in many calderas. (Lipman, 1997).

### ❖ TOPOGRAPHIC RIM

The topographic rim is the escarpment that separates the subsided area of the caldera from the undisturbed volcanic zone. The rim encloses both the subsided area and the area of scarp moved back due to rock falls and mass wasting (Fig. 2.12) (Lipman, 1997).

### ❖ INNER TOPOGRAPHIC WALL

The inner topographic wall is steep in its upper parts but tends to have a concave profile that flattens down slope. The upper parts of the inner topographic wall correspond first to fault scarp originated during roof subsidence. However, during and after caldera collapse landslides and rock falls may modify their morphology. In fact, scarps of individual landslides scallop the topographic walls of several large calderas and rock falls (Fig. 2.12) (Lipman, 1997).

### ❖ COLLAPSE COLLAR

Material removed by mass wasting and scarp retreat defines a collapse collar: the volume of rock lying between the topographic caldera wall and the structural caldera boundary (Fig. 2.12) (Lipman, 1997).

---

## ❖ **BOUNDING FAULTS**

Arcuate bounding faults (ring faults) are exposed at some deeply eroded calderas (mainly 5 km and greater in diameter), unambiguously defining plate (piston) subsidence (Lipman, 1997). The geometry of ring faulting in some eroded calderas is more complex at deep levels, recording increasingly coherent plate collapse as the eruption progressed (Fridrich et al., 1991). Ring faults can accommodate uplift, as well as subsidence, e.g., Lake City caldera, Colorado (Hon, 1987) and Cinque Denti caldera, Sicily (Mahood and Hildreth, 1986).

## ❖ **CALDERA FLOOR**

The geometry of the structural caldera floor within the subsided area has been well documented at only a few large ash-flow calderas, and the typical degree of disruption during subsidence remains uncertain. The structural floor is the subsided pre-caldera land surface, in contrast to the topographic caldera floor exposed at the surface within a young caldera (Lipman, 1997) (Fig. 2.12). Exceptional examples of structurally coherent caldera floors that subsided during a single large eruption are preserved in the Stillwater Range, Nevada (John, 1995), the eastern Sierra Nevada (Busby-Spera, 1984; Fiske and Tobisch, 1994), Questa and Organ Mountains areas in New Mexico (Seager and McCurry, 1988; Lipman, 1988), and the Tucson Mountains in Arizona (Lipman, 1993).

## ❖ **INTRACALDERA FILL**

The intracaldera fill consists of material erupted during and after the caldera-forming event deposited thanks to the subsidence of the magma chamber roof. The intracaldera fill is composed of ash-flow tuffs and interleaved caldera-wall slide breccias accumulated to multi-kilometre thickness within the collapsed area synchronously with caldera subsidence (Fig. 2.12). Additionally, most pre-Holocene calderas are partly to

completely filled by younger lavas and tuffs erupted from post-collapse caldera-related vents, sedimentary debris eroded from adjacent volcanic highlands, and volcanic deposits derived from separate volcanic centres. Such post-caldera deposits tend to conceal the primary volcanic structures, especially at non-resurgent calderas, impeding interpretation of subsidence processes or even the presence of some large calderas, e.g., Yellowstone caldera, Wyoming (Christiansen, 1984) and La Primavera caldera, Mexico (Mahood, 1980).

#### ❖ **SUBCALDERA MAGMA CHAMBER**

Several recent studies have inferred important roles for sills or shallow domical laccoliths of fine-grained hypabyssal rocks during caldera collapse (Gudmundsson, 1988b) and resurgence (Fridrich et al., 1991; du Bray and Pallister, 1991), including introducing a special category of “laccocaldera” (Henry and Price, 1989).

Magma chambers preserve as solidified plutons or batholiths. Such plutons have commonly been emplaced within a few kilometres of the regional volcanic surface, their roof zones protruding into the syn-eruptive fill of the associated caldera (summarized in Lipman, 1984). Accumulation of silicic low-density magma in a large shallow chamber, which can generate uplift and tensile stresses at the surface, could be important in initiating ring faulting and permitting caldera collapse (Gudmundsson, 1988b; Martí et al., 1994).

### **II.3.4 Classifications of collapse calderas**

#### *II.3.4.1 Introduction*

Calderas show a wide range of features as a response to the collapse process. It is therefore very difficult or almost impossible to classify them into well-defined types. However, nowadays there exist three different proposals of classifications based principally on field studies.

### *II.3.4.2 Eruption style and composition classification*

The first intents to subdivide and classify calderas tried to make a distinction based on eruption style and magma composition at representative volcanoes (Williams, 1941; Macdonald, 1972; Williams and McBirney, 1979). The end-members of this classification after Williams and McBirney (1979) are:

- **Krakatoan type**
- **Katmai type**
- **Valles type**
- **Hawaiian type**
- **Galápagos type**
- **Masaya type**
- **Atitlán type**

#### ❖ **KRAKATOAN TYPE**

The krakatoan type calderas are formed by the foundering of the tops of large composite volcanoes following explosive eruptions of siliceous pumice from one or more vents, or, in some instances, from fissures on the flanks. The volume of the ejecta is usually much less than 100km<sup>3</sup>. Examples: Krakatoa, Somma-Vesuvius (Italy), Santorini (Greece) and Suswa (Kenya).

#### ❖ **KATMAI TYPE**

The collapse results from drainage of a central magma reservoir to feed new volcanoes or fissure eruptions beyond the base of the cone.

**❖ VALLES TYPE**

Foundering takes place along ring fractures independent of pre-existing volcanoes because of and simultaneously with a discharge of colossal volumes of siliceous pumice, usually much more than 100 km<sup>3</sup>.

**❖ HAWAIIAN TYPE**

These calderas are formed by the collapse of the tops of shield volcanoes during late stages of growth. Prior tumescence is followed by subterranean drainage of basic magmas from beneath the summit region into rift zones and, in many cases, by flank eruptions of lava. Example: Kilauea.

**❖ GALÁPAGOS TYPE**

Collapse also formed by collapse during late stages of growth of basaltic shield but engulfment results from injection of magma and eruptions of lava from circumferential fissures near the summit and less frequently from radial fissures on the flanks of the shields. Examples: Sierra Negra, Fernandina.

From a genetic standpoint, the principal difference between Galapagos and Hawaiian shield volcanoes is in their profiles and in the geometry of their fissure systems. In fact, Galapagos shields are specially characterized by concentric fissures around the calderas and radial fissures on the flanks.

**❖ MASAYA TYPE**

The caldera collapse consists in a piecemeal cauldron subsidence of a broad shallow depression occupying most central portion of a low inconspicuous shield; eruptions from ring and radial fissures outside the caldera play no part, and nearly all the lavas are contained within the boundary scarps.

## ❖ **ATITLÁN TYPE**

These calderas are formed by cauldron subsidence unrelated to an earlier cone but associated with eruptions from volcanoes near the rim or from nearby fissures.

### *II.3.3.3 Morphological classification*

Alternatively to the prior considerations, Lipman (1997) presented a classification of calderas relating subsidence geometry and resulting structures to a few geometrically simplified end-member processes. These geometric end-members (Fig 2.13) are considered to cover the broad variety of caldera subsidence. However, many well-studied calderas involve subsidence processes intermediate between the idealized end-members. These end-members are:

- **Plate/piston subsidence**
- **Trap-door subsidence**
- **Piecemeal disruption**
- **Chaotic subsidence**
- **Downsag subsidence**
- **Funnel calderas**

Now we proceed to describe the different end-members. All the cited samples are those proposed by Lipman (1997).

## ❖ **PLATE/PISTON SUBSIDENCE**

Plate/piston collapse involves the subsidence of a coherent block of rock into a magma chamber that evacuates magma along a ring fault. The caldera floor may be variably faulted but the displacement along intracaldera floor faults is at least an order of magnitude less than that of the ring fault (Lipman, 2000). The intracaldera material erupted during the collapse should be planar without significant thickness variation

---

anywhere across the caldera floor. Examples: Lake City (Steven and Lipman, 1976) and Grizzly Peak (Johnson et al., 1989; Fridrich et al., 1991).

#### ❖ **TRAP-DOOR SUBSIDENCE**

Trap-door subsidence is bounded by a partial ring fault and by a hinged segment leading to a feature similar to “trap-door-like” structures. Such type of collapses may be related to smaller eruptions, an asymmetrical magma chamber, or regional tectonic influences. Examples: Bonanza (Steven and Lipman, 1976; Varga and Smith, 1984; Johnson et al., 1989), Three Creeks and Big John (Steven et al., 1984), Snowdon caldera (Howells et al., 1986), and Sakugi (Murakami and Komuro, 1993).

#### ❖ **PIECEMEAL DISRUPTION**

Piecemeal disruption refers to a caldera with numerous floor blocks and/or multiple collapse centres (Lipman, 1997, 2000). Complex small-displacement piecemeal faulting of subsiding caldera floors on a coarse scale has been interpreted as the dominant subsidence process for a few calderas (Branney and Kokelaar, 1994). This type of subsidence mechanism may have different possible origins. For example, a geometrically complex fracture system is usual at sites where multiple nested or overlapping collapses take place. These cause incremental subsidence during successive ash flow eruptions, probably observable in floors of overlapping caldera complexes that subsided recurrently at intervals of tens to hundreds of thousand years. Examples: Latera (Nappi et al., 1991), Kagoshima Bay area of southern Japan (Matumoto, 1943; Aramaki, 1984; Nagaoka, 1988).

#### ❖ **CHAOTIC SUBSIDENCE**

Some reviews (Williams, 1941; Yokoyama, 1983; Scandone, 1990) inferred that chaotic subsidence, marked by intense wholesale disruption and brecciation of caldera-floor rocks is an important caldera-forming process. Chaotic subsidence has been

interpreted as a process that generates low-density material within calderas that can account for the observed negative gravity anomalies (Yokoyama, 1983, 1987), and lithic breccias by collapse of the roof over a depressurising magma chamber (Scandone, 1990).

#### ❖ **DOWNSAG SUBSIDENCE**

Downsag subsidence occurs when ring faults either do not form or do not penetrate the ground surface (e.g. Cole et al., 2004). In its place, the rocks overlying the magma chamber deform by bending without fracture (e.g. Walker, 1984; Milner et al., 2002). Therefore, caldera walls are undistinguishable and the ground surface is slightly tilted towards the caldera collapse centre (Walker, 1984). Usually downsagging of the caldera floor occurs jointly by other collapse processes. Downsag often occurs immediately prior to formation of a completely or partially defined faulted caldera boundary (e.g. piston or trap-door collapse). Examples: Ichizuchi caldera (Yoshida, 1984). Other examples examples of downsag collapse are Taupo and Rotorua calderas (Walker, 1984; Milner et al., 2002).

#### ❖ **FUNNEL CALDERAS**

Funnel calderas are often identified by geophysical responses that are broadly “V” or “funnel” shaped (Cole et al., 2004). Such anomalies can be a result from severe downsag, piecemeal subsidence, or probably more commonly from recurrent subsidence during successive eruptions (Lipman, 1997). For these reasons, Lipman (2000) considers that “funnel calderas” should not be regarded as a separate end-member type, but that the shape may result from a variety of processes.

Small calderas (~2–4 km diameter at topographic rim) commonly have a funnel geometry, because enlargement by slumping of the inner wall into a really restricted vent is the dominant process in establishing the overall size of the subsided area. Such calderas are associated with explosive eruptions from a central vent, lack a bounding ring fault or a coherent subsided block, and probably overlie relatively small (and deep)

magma chambers. Examples: Nigorikawa and Sunagohara calderas (Ando, 1981; Yamamoto, 1992; Mizugaki, 1993) and Red Hills (Cunningham and Steven, 1979).

Some large young calderas, especially in Japan, have been inferred to have a funnel shape, based mainly on modelling of gravity anomalies (Yokoyama, 1983, 1987, 1991). Such funnel structures have been inferred to develop in relatively weak crusts of young island arcs, in contrast to ring fault and plate-subsidence of calderas in cratonic environments (Walker, 1984; Scandone, 1990).

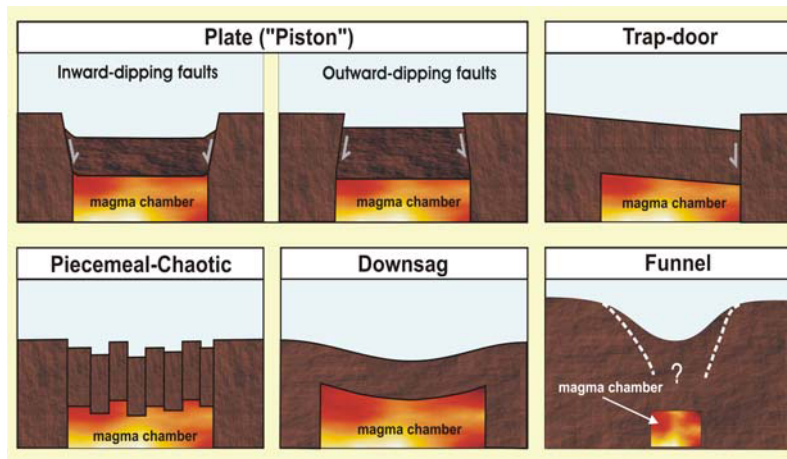


**Fig. 2.13:** Models of alternative subsidence geometries in relation to depth and roof geometry of underlying magma chamber (Modified from Lipman, 1997).

#### *II.3.3.4 Compositional classification*

Cole et al. (2004) proposed a compositional classification although they admitted that there is not a direct relationship between composition and the caldera type. Furthermore, many calderas may contain more than one composition (e.g. many rhyolitic calderas frequently contain some intermediate or mafic volcanism). The authors grouped the calderas towards the composition of the main eruptive magma:

- **Basaltic calderas**
- **Andesitic-dacitic calderas**
- **Peralkaline calderas**
- **Rhyolite calderas**

Now, we give a short description of the abovementioned end-members. Cited examples are those proposed by Cole et al. (2004).

## ❖ **BASALTIC CALDERAS**

These calderas are characteristic of oceanic intraplate hot spot locations, e.g. Hawaii (Walker, 1988). However, they also occur at some divergent plates boundaries in a mid-ocean ridge situation, e.g. East Pacific Rise (Fornari et al., 1984).

Basaltic calderas may be effusive or explosive. Effusive basaltic calderas are commonly related to shield volcanoes at hotspots (e.g. Hawaii, Galapagos Islands). In the case of Hawaii, magma intrusion and sills emplacement produce tumescence which generates an expansion and inflation at the top of the shield creating radial or concentric fractures at surface (Walker, 1988) and destabilizing the system. Subsequently, flank eruptions drain magma from the reservoir leading to a superficial caldera or development of a pit crater (Williams and McBirney, 1968; Decker, 1987). By contrast, calderas created by tumescence and magma withdrawal may be associated with minor explosive eruptions (Simkin and Howard, 1970; Decker, 1987; Walker, 1988). As an example the caldera collapse at Masaya Volcano was concurrent with explosive eruptions and the collapse is interpreted to have occurred along outward-dipping faults (Rymer et al., 1998).

## ❖ **ANDESITIC-DACITIC CALDERAS**

Andesitic-dacitic calderas are typical of continental margins, e.g., Crater Lake (Bacon, 1983) and of volcanoes on island arcs located on convergent plate boundaries, e.g. Tofua (Baker et al., 1971). Calderas related to andesitic–dacitic volcanism typically entail the destruction of stratocones. The best examples are the collapse of Mt. Mazama to form Crater Lake, USA (Williams, 1942; Bacon, 1983); Krakatoa, Indonesia (Self and Rampino, 1981; Simkin and Fiske, 1983), and Santorini, Greece (Druitt et al., 1999).

In all the cases the erupted magma was more silicic than the material of the volcanic edifice. This suggests that the magma related to the caldera-forming eruptions resided in the magma chamber long enough to become more evolved.

## ❖ PERALKALINE CALDERAS

These calderas are located on areas of high tectonic extension (rifting zones), e.g., calderas of the K'One volcanic complex (Cole, 1969; Acocella et al., 2002) or in areas of unusually high rates of localized extension in convergent margins, e.g., Mayor Island (Houghton et al., 1992).

Caldera forms generally in response to explosive activity (e.g. Schmincke, 1967; Mahood and Hildreth, 1983; Houghton et al., 1992; Martí and Gudmundsson, 2000). Frequently, after the caldera forming eruption lavas extrude from a central vent, filling the caldera depression (Mahood, 1984). In some cases, post-caldera lava extrusion is related to magma intrusion into the root zone of the caldera. This produces an uplift of the central part of the caldera floor, e.g. Suswa (Johnson, 1969), Pantelleria (Mahood and Hildreth, 1983; Mahood, 1984; Orsi et al., 1991).

The volcanic edifices associated with peralkaline calderas are normally shield-like (Mahood, 1984; Houghton et al., 1992) and go through stages of caldera collapse and caldera filling (similar to explosive basaltic calderas).

Peralkaline caldera collapses are moderate in size (most are <12 km in diameter), circular, and the roof subsides habitually few hundreds of meters.

## ❖ RHYOLITIC CALDERAS

Rhyolitic calderas are typically huge collapse depressions. They are usually >10 km in diameter and subsidence of the caldera floor is regularly >1 km. In some cases, these calderas are located in zones that have experienced volcanic activity over a substantial time period before the caldera-forming episode. Pre-caldera activity may involve lava flows, low shields, cones, domes and explosion craters, but have not developed a single large stratovolcano. The composition of these pre-caldera materials may range from basaltic to rhyolitic.

Rhyolitic caldera-forming eruptions are accompanied by the deposition of huge volumes of silicic ignimbrites (dacitic to high-silica rhyolite). In most cases post-caldera resurgence occurs, the central part of the caldera becomes uplifted as a structural dome.

This may be caused by the intrusion of magma in the underlying reservoir or post-caldera sill emplacement that often leads to further lava extrusion.

Some examples of rhyolitic calderas are the Valles caldera (Smith et al., 1961; Smith and Bailey, 1968; Heiken et al., 1986, 1990), Long Valley (Bailey, 1976), Cerro Galan (Francis et al., 1978, 1983, 1989) and Campi Flegrei (Barberi et al., 1991).

### II.3.5 A model of development of resurgent calderas

Using the Valles caldera as a model, but augmented by information from other cauldrons, Smith and Bailey (1968) recognized seven different stages in the development of resurgent cauldrons (Fig. 2.14). They are:

- **Regional tumescence and generation of ring fractures**
- **Caldera-forming eruptions**
- **Caldera collapse**
- **Pre-resurgence volcanism and sedimentation**
- **Resurgent doming**
- **Major ring fracture volcanism**
- **Terminal solfatara and hot-spring activity**

In the next lines we will describe shortly the different stages according to the definitions of Smith and Bailey (1968).

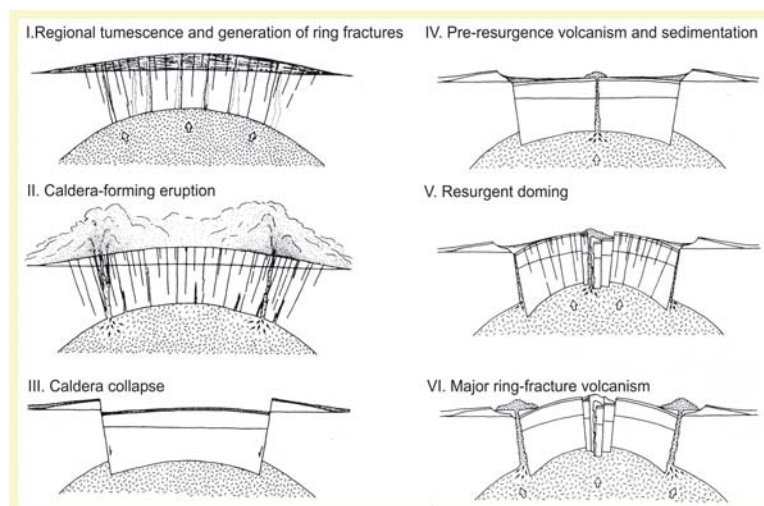


**Fig. 2.14:** Stages in the development of resurgent cauldrons. Example of the stages in the resurgent cycle of the Valles caldera (Modified from Smith and Bailey, 1968)

### ❖ REGIONAL TUMESCENCE AND GENERATION OF RING FRACTURES

The “regional tumescence” refers to the doming of an area larger than that circumscribed by the outer-ring fractures of a given cauldron. If this inflation progresses over a relatively long period of time it may lead to the formation of radial and concentric fracture, along which catastrophic ash-flow eruption eventually takes place. However, the authors recognize that doming and ring fracturing are not a necessary prelude to caldera formation in central volcanoes. However, they insist in the fact that even in some volcanoes of this type, concentric fractures did exist prior to the subsidence (e.g. Crater Lake – *U.S.A.*, Williams, 1941).

### ❖ CALDERA-FORMING ERUPTIONS

At some optimum time, regional tumescence culminates in the eruption of large volumes of ash flows from the domical-fracture system.

### ❖ CALDERA COLLAPSE

Although the authors treat the eruption and the collapse as separate stages, they recognize that the processes are logically concurrent, especially when very large volumes of materials are erupted. However, major collapse must follow as a consequence of the eruptive removal of magma; hence, final subsidence must follow the eruption. The authors insist on the idea that subsidence in resurgent cauldrons seems to take place along vertical steeply inclined ring faults, i.e. the collapse caldera is bounded by steep and almost vertical walls.

---

### ❖ **PRE-RESURGENCE VOLCANISM AND SEDIMENTATION**

The period immediately after the caldera collapse is a time of extreme disequilibrium both in the magma chamber and within the caldera depression. On the one hand, the steep and unstable walls of the caldera undergo caving, avalanching and gravity sliding. Furthermore, with partial restoration of magma pressure, this coarse sedimentation appears together with pyroclastic and lava eruptions. In most cases, at this time, lakes may also begin to form on the caldera floor.

Normally, the duration of this stage is short. In some calderas (e.g. Valles and Creede calderas) the related deposits are well represented in the stratigraphic column, however, in other cases, they are indistinguishable from those deposits characteristics of the resurgent doming stage.

### ❖ **RESURGENT DOMING**

In most cases, the cauldrons studied by the authors have well-defined, central resurgent domes. Longitudinal, radial or apical grabens or other distension faults characterize these domes. In some calderas (e.g. Valles and Timber Mountain) this doming was accompanied by ring fracture volcanism and intrusion and/or effusion along the graben or other fractures in the dome. The time and rate of uplift of the dome is extremely important to infer the causes for uplift.

### ❖ **MAJOR RING FRACTURE VOLCANISM**

The authors affirm that volcanism from the moat or ring fracture zone, following formation of the resurgent dome, is known in all cauldrons they studied. This stage is the one of greatest post-subsidence surface-volcanic activity, and it has a longer duration than the other stages, except perhaps the regional tumescence phase. The volcanoes of this stage are commonly interbedded with or overlie the undeformed lake sediments and caldera fill that accumulated after resurgence. Much of the fill may be derived from pyroclastic eruptions of this stage.

## ❖ **TERMINAL SOLFATARA AND HOT-SPRING ACTIVITY**

Hot-springs and solfataras are probably active throughout most of the cauldron cycle, and it may be argued that this stage overlaps all others. However, it becomes uniquely characteristic only after all eruptions have ceased. Then, it constitutes the terminal stage of disappearing volcanic activity, a stage reached by all volcanoes.

The long duration of this stage in epicontinental cauldrons suggests long-lived hydrothermal systems and major ore-forming potential.

In order to summarize the principal concepts of their work, the authors state that major post-subsidence volcanism has followed resurgent doming, and either minor or no post-subsidence surface-volcanic activity preceded doming. In fact, surface volcanism during doming occurred in few of the studied cauldrons, but was minor except for the Valles caldera.

### **II.3.6 Post-caldera volcanic activity classification**

After a literature survey at 160 Quaternary calderas in various parts of the world, Walker (1984) intended to investigate the distribution of post-caldera vents as a possible indicator of caldera origin. The survey was no comprehensive but probably included a sufficiently large sample to be representative. Only morphological youthful calderas exceeding 1 mile (1.61 km) across were included and strongly asymmetric features (e.g. Valle del Bove), which may be landslide scars were excluded. The author made an attempt to categorize the vent distribution in the 90 examples in which post-collapse younger vents were most clearly displayed. The proposed categories of post-caldera volcanic activity are:

- **Type-C: A single vent occupies a central or near-central position (Fig. 2.15 A).**

**Examples:** Vulcano (Walker, 1984) and Vico (Walker, 1984).

- **Type-L: Vents are distributed in a defined straight line or linear zone (Fig. 2.15 B).**

**Examples:** Hakone (Kuno, 1950; Nakamura, 1977), Karkar, Kilauea, Santorini (Walker, 1984), Tengger (Walker, 1984) .

➤ **Type-M : A single vent occurs at or near the caldera margins (Fig. 2.15 C).**

**Examples:** The marginal vent position is ambiguous, it could be equally related to a line transecting the caldera or to a ring fracture paralleling the caldera rim. The author does not offer examples for this postactivity type.

➤ **Type-R : Vents occur along an arcuate line paralleling the caldera margin (Fig. 2.15 D).**

**Examples:** Deception Island (Baker et al. 1975), Masaya , Mendeleev, Okmo (Byers, 1959) , Rabaul (Heming, 1974), Sete Cidades (Zbyszewski et al., 1959), Valles (Smith et al., 1961), Daisetu (Kuno, 1962), Usu (Ishiwaka, 1964) and La Primavera (Mahood, 1980).

➤ **Type-S : Vents are scattered widely within the caldera (Fig. 2.15 E).**

**Examples:** Newberry (Williams, 1935; Higgins, 1973), Nisyros (Di Paola, 1974), Pico Alto (Self, 1976), Phelgreaun Fields, Pantelleria (Villari, 1971).

Shortly, the most noteworthy features revealed by this survey are the scarcity of examples of type-R (i.e. few calderas show positive evidence for possessing a ring fault that has guided subsequent eruptions) and the abundance of type-L calderas (i.e. a linear zone crossing a caldera possibly related to the regional stress field is a more fundamental line of weakness than any possible ring fault and not subdued as a result of caldera formation). The overall conclusions from this survey are, first, that for most calderas there is a lack of positive evidence from the post-caldera vent distribution for the existence of a ring fracture and, second, the prevalence of caldera types C, L and S suggest that the conditions that determined the pre-caldera vent position commonly continued operating after caldera formation as though no major new deep-extending lines of weakness were then generated (Walker, 1984).

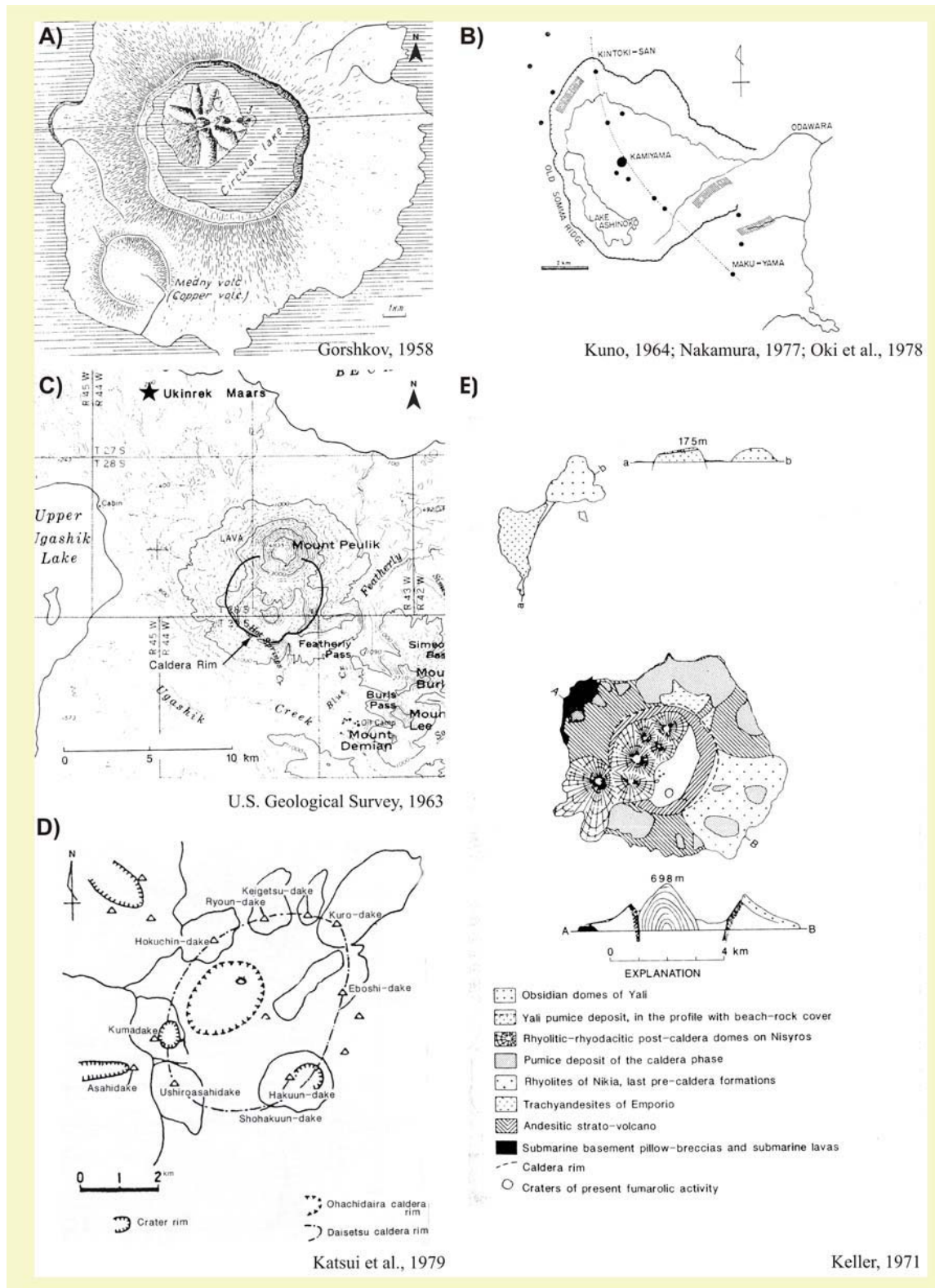


**Fig. 2.15:** Caldera samples with the different types of post-caldera volcanic activity. **(A)** Sketch showing the structure of Tao – Rusyr caldera. The central post-caldera vent indicates an A-type activity. **(B)** Sketch map of Hakone caldera. Small dots represent parasitic cones and large dots main post-caldera cones. Evidently, this distribution corresponds to an L-type activity. **(C)** Topographic map showing Peulik Volcano and the inferred outline of Ugashik caldera. Obviously, it corresponds to a M-type post-caldera volcanic activity. **(D)** Simplified structure of the composite Daisetsu volcano. Many domes extruded along the caldera rim corresponding to a R-type post-caldera volcanic activity. **(E)** Geological interpretation of Nisyros – Yali group, the post-caldera activity if of type-S.

### II.3.7 Other relevant works

#### II.3.7.1 Relationship between the caldera area and the volume of extruded deposits

Other important works related to field data on collapse calderas are that of Smith (1979) and Spera and Crisp (1984). From all the interesting results presented in these works we will focus on those related to the analysis of the relationship between the caldera area  $A_c$  and the volume of extruded deposits  $V_m$  (Fig. 2.16). Both works indicate that although  $A_c$  varies by a factor  $>10^4$  and  $V_m$  slightly  $<10^4$ ,  $\log A_c$  correlates positively with  $\log V_m$ . Consequently, in an order of magnitude sense, there is a positive correlation between the volumes of ash flow sheets and the areas of their associated calderas.

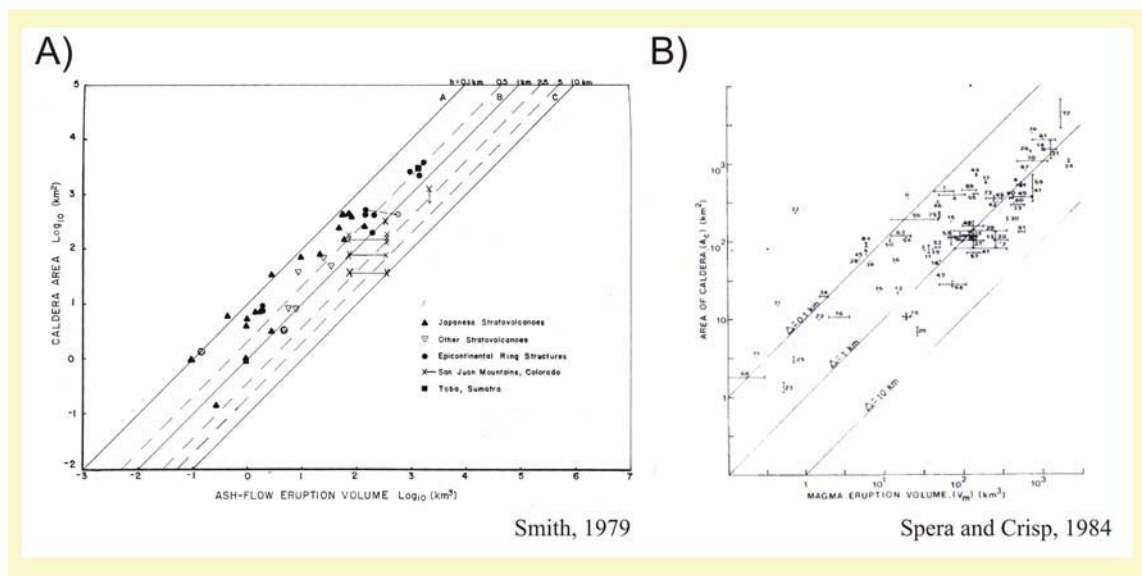


**Fig. 2.16:** Plots of the caldera area  $A_c$  versus ash-flow magma eruption volume. Lines are drawn to indicate various depth of drawdown ( $\Delta$  or  $h$ ), assuming the magma chamber has a cylindrical shape ( $\Delta = V_m / A_c$ ). (A) Error bars represent best estimates, not necessarily true error. If area and volume are given in the literature as exact number, they are plotted as points. Older systems should inherently have more error than younger ones. Volumes for ocean island ash flows, such as Kikai (point 32), are underestimates due to loss of ash in the ocean. In some cases, ash flow volume is small because subterranean withdrawal of magma also contributed to caldera collapse (Modified from Smith, 1979 and Spera and Crisp, 1984).

### III.3.7.2 Ice-melt and mining subsidence studies applied to collapse caldera processes

In this section it is also interesting to present one important point included in the work of Branney (1995) and subsequently partially commented by Roche et al. (2000): the application of ice-melt and mining subsidence studies to the understanding of caldera collapse structures.

#### III.3.7.2.1 Ice-melt subsidence studies

Branney (1995) explained that natural pits formed when blocks of ice buried in unconsolidated sediments melt are partially similar to analogue models on collapse calderas. These natural pits are an additional source of information because their fault geometries, including hairline fractures and dip orientations, are clearly discernible and because they show several features that occur at calderas but which have not yet been reproduced experimentally (Branney, 1995).

Figure 2.17 illustrates some examples of structures in ice-melt collapse pits in unconsolidated sediments.

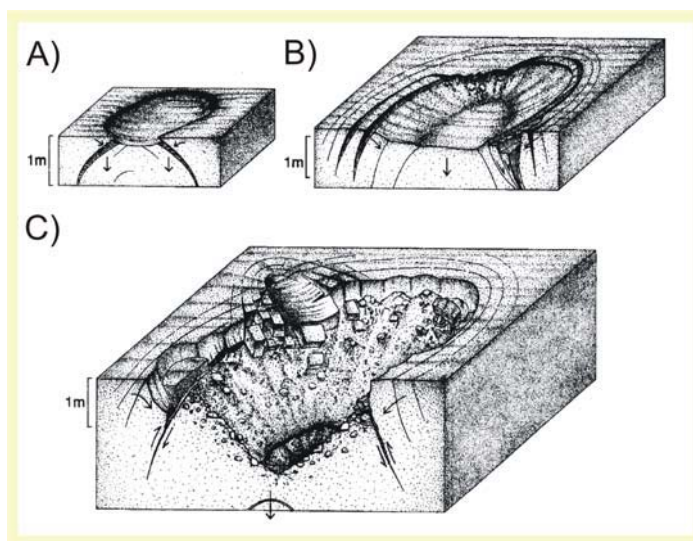


**Fig. 2.17:** Structures in ice-melt collapse pits in unconsolidated sediments. Relationship between downsag, outward-dipping ring fractures and vertical to inward-dipping pit walls are shown at different stages of subsidence. **(A)** Small, immature pit, formed by collapse of a circular block on an outward-dipping ring fault. **(B)** Downsag at a larger, more mature pit has caused peripheral extension leading to multiple ring fractures. **(C)** Deep collapse pits acquire a funnel shape. Overhanging walls fail as soon as they develop, producing near-vertical and inward-dipping pit walls. (Modified from Branney, 1995)

---

The main structural features may be summarized as follows (Branney, 1995):

- Initial ring and arcuate faults dip outwards. These faults deep outward even at depth, and they tend to steepen with depth, just as in the experiments of Sanford (1959) and Komuro (1987).
- Most pits have sets of multiple concentric ring fractures, which originate as a result of peripheral radial (centripetal) outer arc extension associated with downsag flexuring. This extension may produce also peripheral arcuate grabens and causes arcuate ring fractures to dilate, producing upward-flaring crevasses.
- Many of smaller pits have a single ring fault that dips outwards and surrounds a single down-dropped block that is coherent, at least at surface.
- The pits widen progressively during subsidence and their structural complexity increases from small diameter, immature pits with a ring fault to larger mature pits with complex faulted margins and floors. They become increasingly piecemeal as they grow.
- Rare, small trap-door-shaped pits have a horseshoe-shaped fault opposite a monoclinial hinge. These become more symmetrical as subsidence progresses, the horseshoe faults elongating into rings.
- Pit enlargement occurs by the formation of new outward-dipping to vertical ring fractures outside the pit, followed by the subsidence and inward tilting up to 90° of the enclosed ring-shaped or arcuate blocks of sediment.
- Pit enlargement also occurs by collapse of unstable pit walls.
- The deeper pits with higher walls, smaller ratios of diameter to subsidence depth and abundant collapse debris have similarities to calderas with thick fills and abundant mesobreccias and megabreccias, whereas the less deep pits are more similar to shallow calderas, or calderas in the early stages of collapse.

### III.3.7.2.2 Mining subsidence studies

Additionally to ice-melt subsidence studies, mining subsidence structures and scaled experimental models of subsidence (Sanford, 1959; Whittaker and Reddish, 1989) provide a useful analogue for caldera collapse in the absence of tumescence or regional tectonism (pure caldera collapse) (Branney, 1995).

Further papers reinforced the idea introduced by these authors: the relationship between the geometry of the magma chamber and its depth controls the collapse structure and type.

Two-dimensional subsidence in mining is characterized by three parameters, which provide enough information to classify the different collapses types (Fig. 2.18):

- Angle of draw,  $\theta$  ( $\sim 35^\circ$ ), localized between the vertical and the lines that draw from the edges of the cavity and delimit the collapse depression at surface
- Roof width,  $w$
- Roof thickness (depth),  $h$

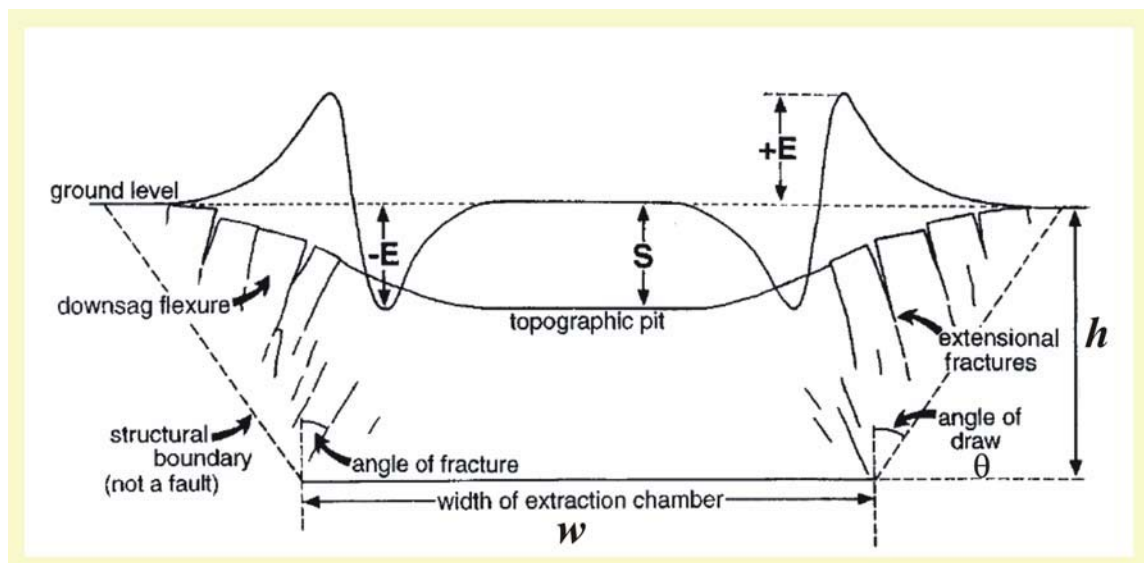


**Fig. 2.18:** Generalized mining subsidence structure showing strain profiles for the ground surface. **+E** Maximum extension; **-E** Maximum compression; **h** Roof thickness (In Branney, 1995 modified from Whittaker and Reddish, 1989).

From these parameters it is possible to distinguish three cases of mining subsidence depending on the *roof aspect ratio* ( $\mathbf{R}=\mathbf{h/w}$ ): subcritical, critical and supercritical. The critical aspect ratio is given by:

$$\tan \theta = \frac{(w/2)}{h} = \frac{1}{(2R)} \quad [2.1]$$

For  $\theta = 35^\circ$ , the critical value for  $\mathbf{R}$  is 0.7. The three different cases are (Fig 2.19):

- **Subcritical case,  $\mathbf{R}>0.7$ :** There is a single point of maximum compression located at the centre of the depression.
- **Critical case,  $\mathbf{R}=0.7$ :** There are two points of maximum compression and a single point of no deformation at the centre.
- **Supercritical case,  $\mathbf{R}<0.7$ :** There are two points of maximum compression and an undeformed zone of finite width in between.

The model distinguishes between three different areas: extensional (**E**), compressional (**C**) and non-deformed (**N**). The width of the marginal deformed zone (extensional and compressional) are constant for a given  $\theta$  and  $h$ , and do not depend on  $w$ . For low values of  $\mathbf{R}$ , there is a central non-deformed zone bounded by marginal deformed zones. By contrast, for high values of  $\mathbf{R}$  the entire depression is affected by surface deformation.

Additionally, it is possible to define the “structural boundary” of a caldera, which is considered as the outer limit of subsidence and related deformation, i.e. the deformation front that separates subsided rocks from enclosing non-subsided rocks (Fig. 2.18). The enclosed volume is known as the “zone of influence” (Whittaker and Reddish, 1989). The structural boundary itself is not a discrete fault, but of a cryptic limit of deformation (downsag and microfaulting). Volcanologists commonly assume that the structural boundary of a caldera is a ring fault, but this may not always be the case (Branney, 1995). In some cases, there can be multiple faults and subsidence involving flexure and microfaulting that extend outside the ring faults to a more cryptic

boundary (Fig. 2.20). For example, Biblis Patera and Alba Patera on Mars (Hodges and Moore, 1994) exhibit concentric arcuate and ring fractures, and changes of slope, several kilometres outside their caldera walls, indicative of peripheral extension and downsag within an outlying cryptic structural boundary.

The structural boundary is usually “funnel-shaped” and typically dips inwards at an angle approximately  $55^\circ$  from the horizontal and the complementary angle corresponds to the “angle of draw” (Fig. 2.18). However, this dip angle is mainly influenced by the rheology of the rock.

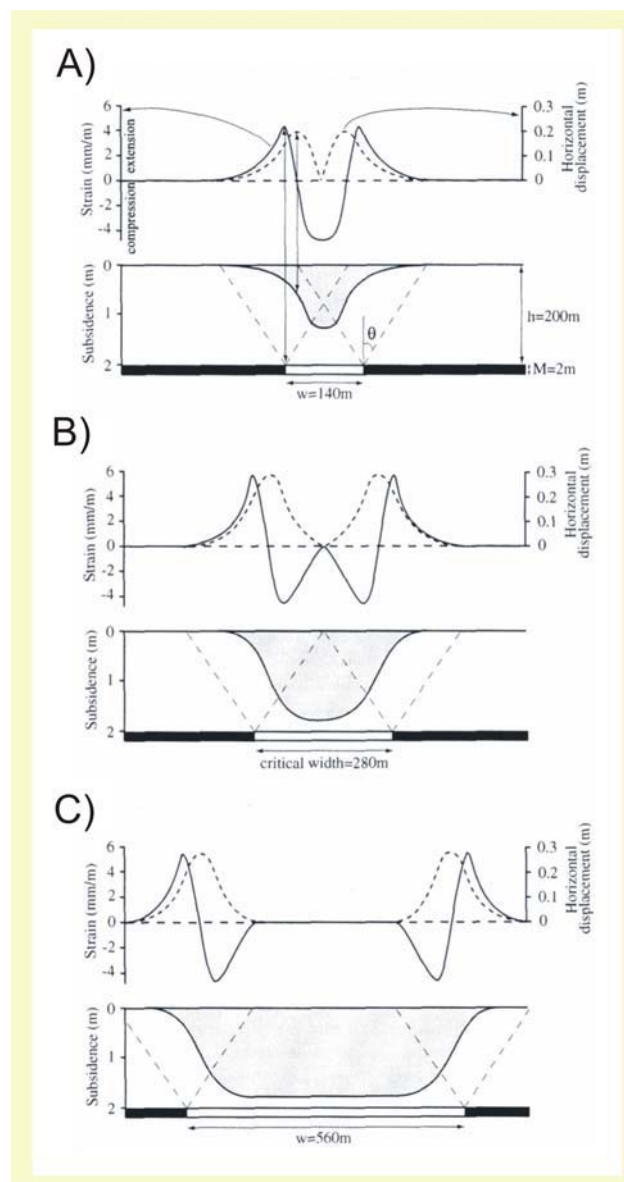


**Fig. 2.19:** Model for subsidence, horizontal displacement, and strain at the surface caused by a rectangular cavity 2 m high and 200 m deep. **(A)** Subcritical case, **(B)** Critical case, and **(C)** Supercritical case. The angle of draw  $\theta$  is  $35^\circ$ . (Modified from Whittaker and Reddish, 1989)

### III.3.7.2.3 Main results

After comparing ice-melt collapse structures, mining subsidence structures, scaled subsidence models and evidence from over 50 calderas Branney (1995) concluded that:

- Simple caldera collapse without magmatic inflation may produce complex deformation geometry, including downsag, multiple outward-dipping to vertical arcuate faults and ring faults, and zones of extension and compression. Caldera scarps formed on outward-dipping faults are so unstable they rendered vertical to inward-dipping as subsidence proceeds.
- Downsag is a cause of ring faulting (e.g. La Primavera – *Mexico*, Mahood, 1990, Yokoyama and Mena, 1991; Tavua – *Fiji*, Setterfield et al., 1991) and arcuate faulting at calderas because it causes radial extension near the margin of subsidence (Fig. 2.17 B and Fig. 2.18). This interpretation requires the faults to be extensional, which is commonly the case at calderas. These models also show a zone of surficial compression that lies inside the peripheral zone of extension (Fig. 2.18) and this may account for syn-subsidence folds recorded at some caldera floors (e.g. Sabaloka – *Sudan*, Almond, 1971; Almond and Ahmed, 1993; Olympus Mons – *Mars*, Mouginiis-Mark and Robinson, 1992). Extension associated with downsag is indicated by arcuate graben and dilatational fissures at several calderas (e.g. Scafell - *U.K.*, Branney and Kokelaar, 1994).
- Occurrences of ice-melt pits showing downsag with well-developed ring fractures across which there is little to no downthrow suggests (Branney and Gilbert, 1995) suggest that ring fractures can form as a response to downsag, rather than the downsag being a consequence of ring fault geometry. Downsag may precede faulting and/or may develop simultaneously with outward-dipping faults. In some cases, downsag occurs without ring fault-type subsidence (e.g. Kumseongsan – *Korea*, Branney, 1995).

- 
- As caldera subsidence proceeds, any initial outward-dipping ring and arcuate faults may be reactivated and cut by inward-dipping faults at shallow levels as a result of the collapse of unstable, overhanging to vertical calderas and crevasse walls, as occurred with the mature ice-melt collapse pits (Fig. 2.17 B and C).
  - Caldera enlargement may arise by progressive downsag and initiation of new extensional ring fractures outside an initial collapse depression (Fig. 2.20), in addition to surficial degradation of oversteep caldera walls. Calderas that have widened by progressive downsag and faulting will have piecemeal floor cut by arcuate faults, possibly surrounding a more coherent, central block.
  - The proposed caldera model (Fig. 2.20 bottom) reconciles aspects of the Japanese funnel-shaped caldera model (Aramaki, 1984; Sawada, 1984) with some aspects of the ring fault caldera mode (Clough et al., 1909; Lipman, 1984). Ring fractures are compatible with the idea that structural boundaries are funnel-shaped, that the diameter of the low-density caldera fills may decrease with depth (due to the combined effects of downsag and wall retreat), and caldera floors may include gradations between coherent and brecciated (piecemeal).
  - There are a great variety of caldera types, and some important factors controlling their structural development are not represented by ice-melt collapse pits, mining and experimental models. These include variations in thickness of the caldera floor, strain rate, intrusion of magma and tumescence, regional tectonic stress, and pre-existing and syn-volcanic regional faults. The latter may account for features that are rare at the ice-melt collapse pits, such as rectilinear and highly asymmetrical trap-door shapes.
  - Calderas with very thick massive fills probably have larger ratios of subsidence depth to caldera floor thickness than is typical in mining subsidence and, for these, the mining subsidence model (Fig. 2.18) has most relevance to the early stages of caldera collapse—that is before high caldera walls develop.

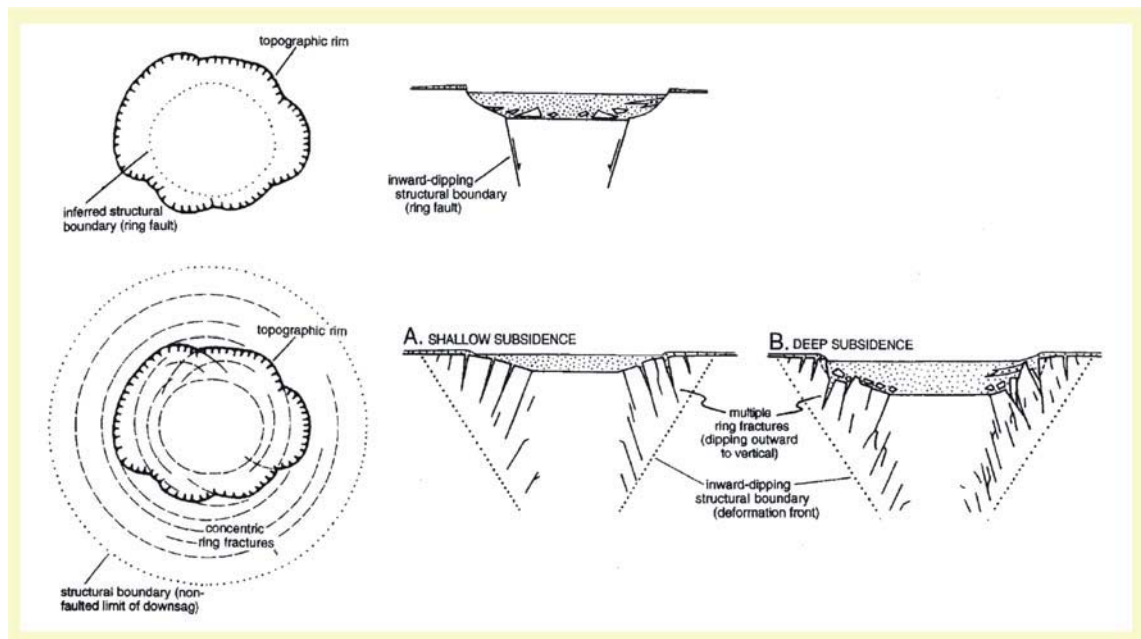


**Fig. 2.20:** Alternative possible caldera structures (schematic) **(Top)** Coherent collapse on a single inward-dipping ring fault followed by topographic enlargement due to landsliding (e.g. Lipman, 1984). The structural boundary is a ring fault whose geometry poses a space problem requiring substantial magmatic inflation. **(Bottom)** Downsag with concentric outward-dipping arcuate and ring fractures, based on evidence cited in Branney's work (1995). Caldera diameter may increase by progressive downsag and initiation of concentric ring fractures outside the first-formed pit, in addition to the failure of caldera scarps. Outermost ring fractures may have negligible downthrow. Deeply subsided calderas (B) develop steep walks by surficial collapse of scarps sited at outward-dipping faults. The structural boundary encloses ring fractures and may even enclose embayments. Possible effects of resurgence and regional tectonism are omitted, and caldera fill (stipple on cross-sections) is omitted from the plan views (left) to show caldera floor fractures.

### II.3.8 Summary of previous results and commented works

In order to facilitate the comprehension and understanding of the rest of this chapter, we consider necessary to present a schematic summary of the most important aspects commented in this section. Figure 2.21 offers a sketch summing up the different aspects and topics commented in this section concerning the state of the art of collapse calderas.

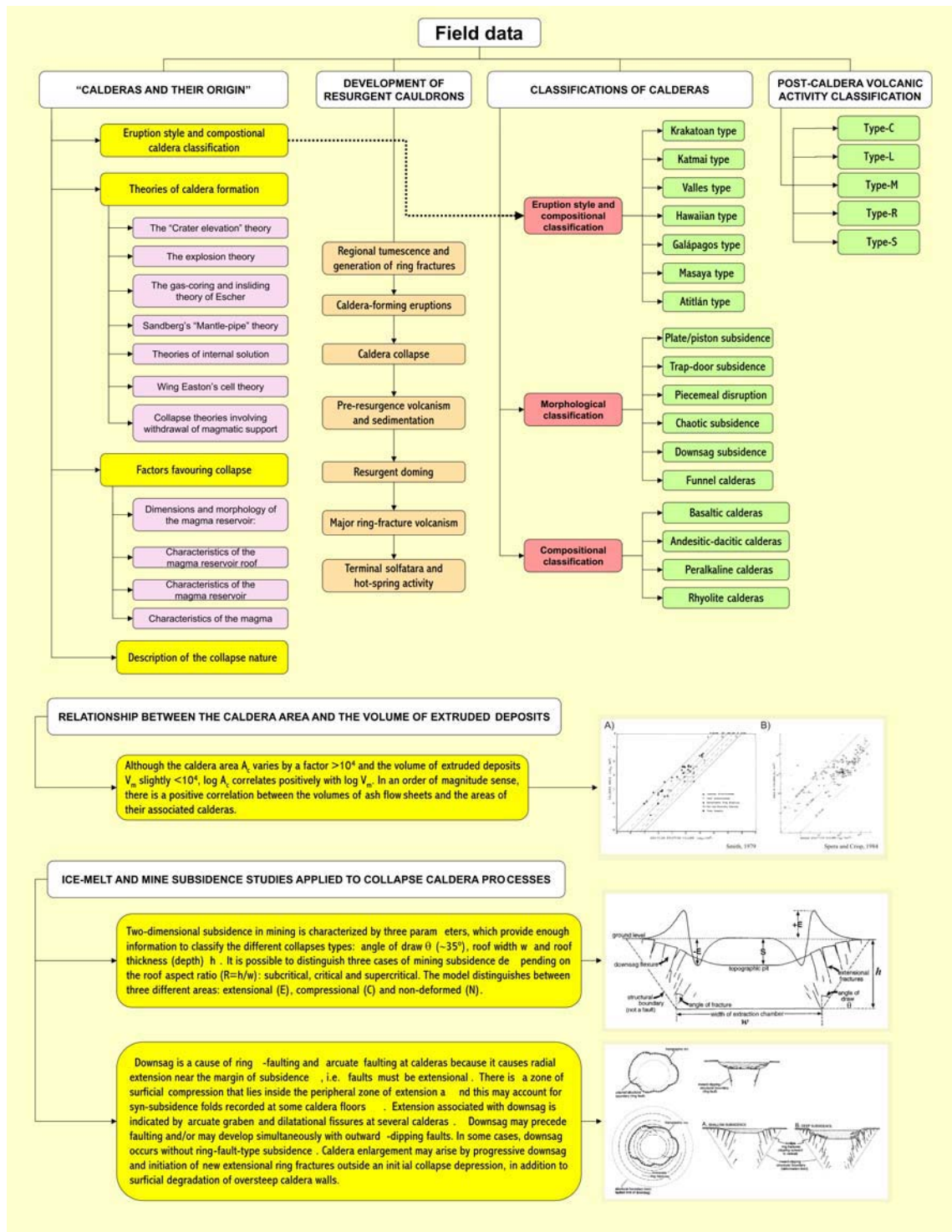


Fig. 2.21: Sketch summing up the different aspects and topics commented in this section concerning the state of the art of collapse calderas.

---

## **II.4 WORLDWIDE CALDERA INFORMATION**

### **II.4.1 Introduction and objectives**

As mentioned earlier (see section II.1.2), this section deals with our compilation of results from representative fieldwork done on collapse calderas, fusing the work of Newhall and Crisp (1981) with information available from web pages of IAVCEI and the Smithsonian Museum of Natural History (<http://www.iavcei.org/> and <http://www.volcano.si.edu/>, respectively). The ultimate scope of this compilation is the development of a world-wide database on calderas, the CCDB: The Collapse Caldera DataBase. The objectives of this extensive data compilation are diverse. First, it should be a useful and accessible tool for studying collapse calderas. Consequently, one of the main purposes is the creation of a webpage (the CCDB webpage) and publication of the database on the www. There, users will be able to access (after previous registration and provision with a username and password) the current database version, to propose possible corrections or updates and to exchange information with other registered users. The second aim of the first version of the data base, is to perform an analysis of the included information and data. We are looking for general trends or relationships between specific aspects concerning collapse calderas, e.g. structure, magma composition, size, etc.

Furthermore, we want to check existing collapse caldera classifications (see section II.3.4 for more details) and to compare our results with those from the studies summarised in section II.3.7.

### **II.4.2 CCDB: Collapse caldera database**

After revising more than 200 studies based on field observations at collapse calderas and their related tectonic and geological setting, we created the collapse caldera database (CCDB) in Microsoft Access<sup>®</sup>. The data base currently includes information on about 280 calderas world-wide. It is open for subsequent up-dates and up-grades. In fact,

the CCDB includes a formulary that will facilitate the incorporation of new data on calderas with their corresponding characteristics and attributes into the database (Fig. 2.22). Furthermore, we link the CCDB with a GIS application in ArcGIS® 9.1 (Fig. 2.23) This allows us to represent the calderas on a world map in order to study the spatial distribution of certain specific features or attributes. In the next section (II.4.3), we provide an accurate description of the database architecture and functionality.

**CALDERA DATABASE : CCDB** CALDERA search Ugashik

IDCaldera: CALDERA **1102-13** Ugashik Latitude: 57.751 World region: 11

Age: 40 ka Age interval: 2 Longitude: -156.368 Subregion: 1102

---

**CALDERA PROPERTIES** **DEPOSITS PROPERTIES**

Dim max (km)  Calculated Area (Dmin\*Dmax\*PI/4): 23.5619475 Dimension interval: 2

Dim min (km)  Calculated area: 23.5619449 Area (km2) (from ref):

Dimensions: 5 x 6 Subsidence (km):

Collapse type: ?  Incremental  Volume (km3) (from ref):

Collapse classification: ? **DEPOSITS PROPERTIES**

Deposit name:

Deposits thickness (km):

Volume of deposits (km3):

Interval of volume ?

Volume of magma (km3):

Interval of volume ?

---

**MAGMA CHAMBER PROPERTIES**

Chamber depth (km):  Roof aspect ratio:  Composition ? General composition ?

---

**PRE-CALDERA ACTIVITY** **POST-CALDERA ACTIVITY**

Pre-caldera edifice: STR  Edifice type: 2 Pre-caldera doming

Collapse precursor: ?  Precursor type: ? Resurgence:

Post-caldera activity: M

---

**LOCAL, REGIONAL AND PLATE TECTONICS**

Tectonic setting description: Compression, subduction zone, boundary between two subducting lithospheric segments Tectonic setting: SC Regional faults:  Condition local structures:

Crustal type: Cd IF

---

**REFERENCES** **COMMENTS:**

IDReferer	Reference
M20	Miller and Smith (1987): Geology 15, 434-438
Kc7	Kienle and Swanson (1983): JVGR 17, 393-432
Fc8	Fliedner and Klemperer (2000): EPSL 179, 567-579
N4	Newhall and Dzurisin (1988): USGSB 1855, 1108pp.
*	

**PHOTOGRAPHY:**  
Ugashik

Registro: 1 de 4

Fig. 2.22: Screen-shot the formulary included in the database.

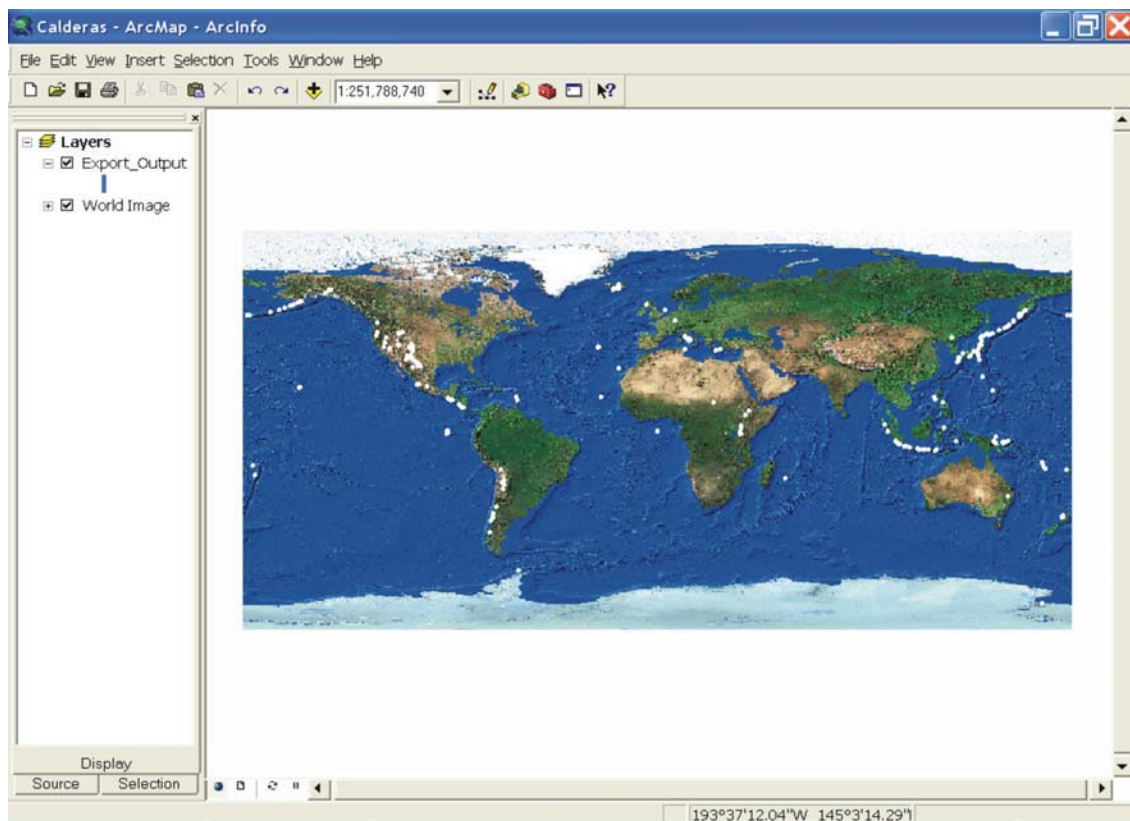


**Fig. 2.23:** Screen-shot of the ArcMap® project, which links the database to the GIS application. White dots in map indicate locations of the calderas included in the database.

## II.4.3 CCDB structure

### II.4.3.1 General aspects

Prior to the creation of any database it is necessary to define its architecture. Databases are composed of so-called “*FIELDS*”. In each field we are able to introduce a specific type of information, from text to numbers, passing through arithmetic operations. Since databases usually involve considerable amounts of information it is very useful to group the different fields into specific topics. These main groups are hereafter termed “*SECTIONS*” (Fig. 2.24). Additionally, each section may be composed of one or more fields that can be sub-grouped into different “*FIELD SETS*” (Fig. 2.24). Figure 2.24 illustrates the architecture of the CCDB. Summarising, the database is subdivided into “*SECTIONS*”, each section is in turn subdivided in “*FIELD SETS*” and each field set may include one or more “*FIELDS*”.

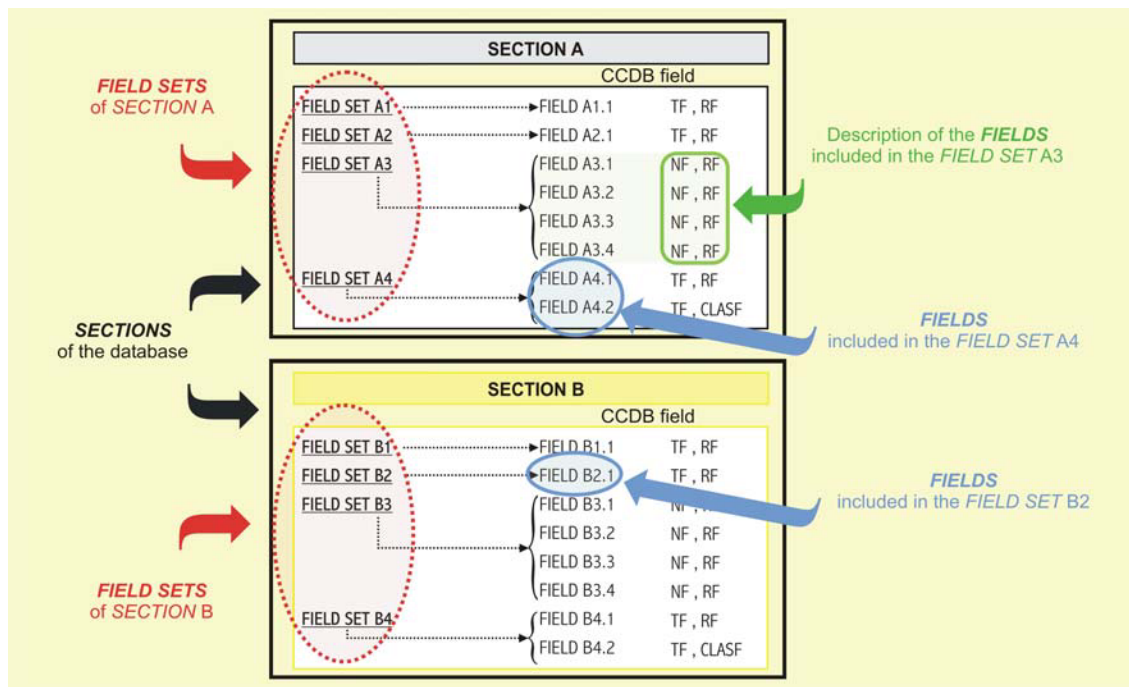


Fig. 2.24: Sketch of the CCDB architecture.

#### II.4.3.2 Field types included in the database

We mentioned earlier that each *FIELDS* constituting the CCDB is able to introduce a specific type of information. As a result, we are able to classify the *FIELDS* according to the type of information they record. According to the type of information stored in the *FIELD*, we distinguish three different types of *FIELDS*:

- **Numerical field (NF):** Information recorded in the field is numerical
- **Text field (TF):** Information recorded in the field is a text string
- **Yes/No field (YNF):** Information is Yes or No

Moreover, due to the complexity of the database and considering that the information included in each *FIELD* comes from diverse sources, we deem it necessary to perform a second classification of the *FIELDS* according to the source of information they contain. These are:

- **Reference field (RF):** Information comes directly from the consulted references.
- **Classification field (CLASF):** Information in these fields results from classifying the information of the “**Reference fields**” in simplified groups according to prior defined criteria.
- **Inferred field (IF):** Information is inferred combining consulted references related to collapse calderas and additional references concerning the area where calderas are located. Before recording the information in these fields, we define and establish certain criteria. The information of these fields is directly used to further classifications.
- **Calculated field (CALF):** Information is the result of a calculation performed with the information from the other fields, mainly RF fields.

#### *II.4.3.3 CCDB structure and included fields*

We have to define *SECTIONS* such that we are able to group all *FIELDS* of the CCDB in a specific *SECTION*. We have thus defined the following *SECTIONS* (Fig. 2.25):

- **Caldera properties**
- **Deposits properties**
- **Magma chamber properties**
- **Pre-caldera activity**
- **Post-caldera activity**
- **Local, regional and plate tectonics**
- **References**

Figure 2.25 represents a sketch of the CCDB structure with the representation of all *SECTION*, their corresponding *FIELD SETS* and *FIELDS*. In the following pages we will describe shortly the content of each CCDB *SECTION*, as well as, the included *FIELD SETS* and *FIELDS*.

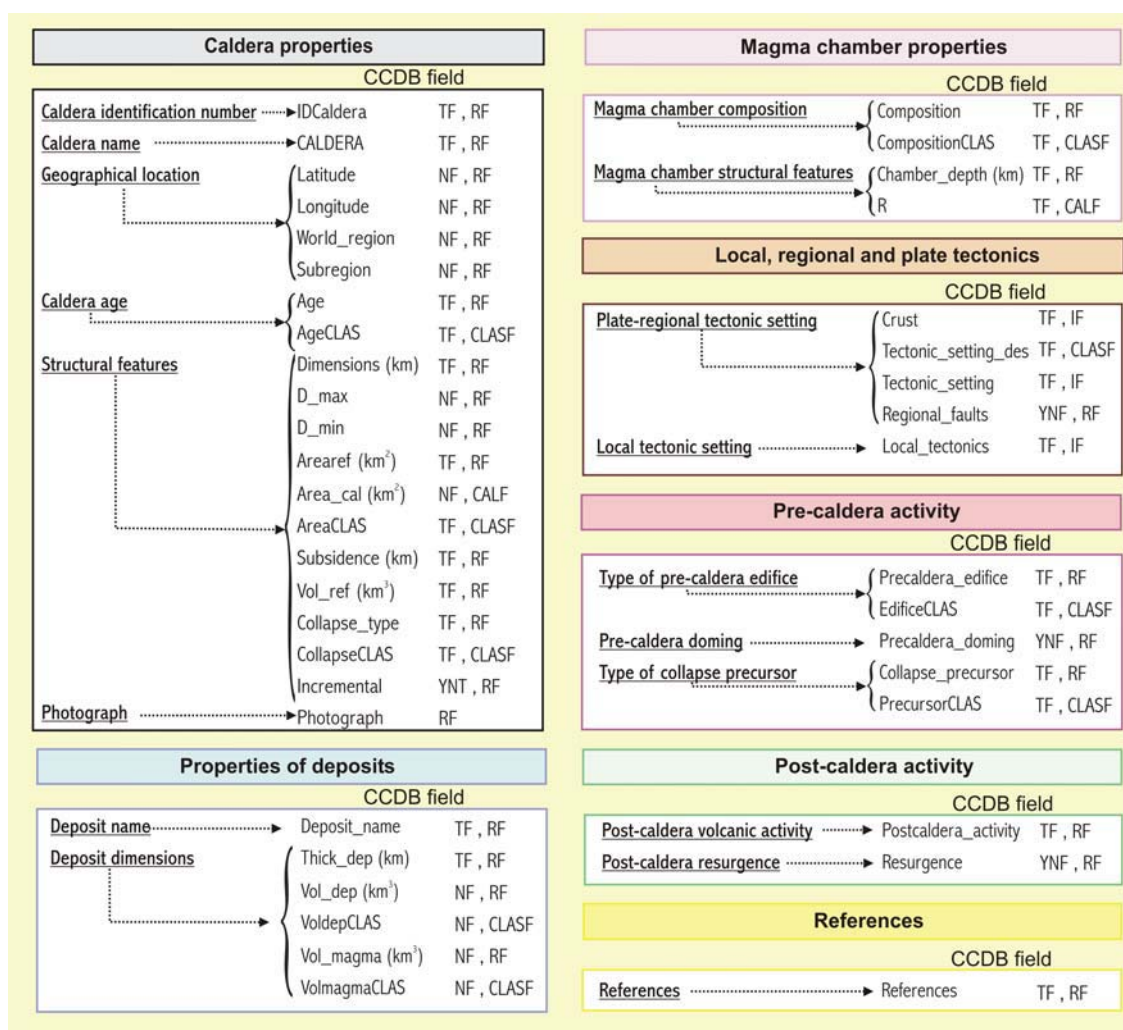


**Fig. 2.25:** Sketch of the CCDB architecture. The database is divided into seven main sections, which include information about the caldera, the deposits and magma chamber properties, the pre- and post-caldera activity, the local, regional and plate tectonics and interesting references. In each section, field sets are shown in bold and underlined, whereas the names of the included fields have been printed in a normal font. On the right side of each of the field we added the code to characterise each of the fields according to the classification of section II.4.3.2. **CALF** Calculated field; **CLASF** Classification field; **IF** Inferred field; **NF** Numerical field; **RF** Reference field; **TF** Text field; **YNF** Yes/No field.

## ❖ CALDERA PROPERTIES

This *SECTION* describes the information necessary to characterize the caldera samples recorded in the CCDB as geological structures. Therefore, we should keep in mind that collapse calderas are depressions with their corresponding dimensions, age, volume, etc. Consequently, the field sets have to include the following fields:

### ➤ Caldera identification number

Only the *FIELD* “IDCaldera” (TF, RF) is included in this *FIELD SET*. In this *FIELD* we correlate each caldera sample of the CCDB with an identification number that corresponds to the number assigned to their active vent(s) in the “Catalogue of active volcanoes of the world” (CAVW) or as modified by Simkin et al. (1981). The scheme to assign these identification numbers is summarised in Figure 2.26. Since not all calderas included in our database are recorded in previous studies some modifications have been introduced.

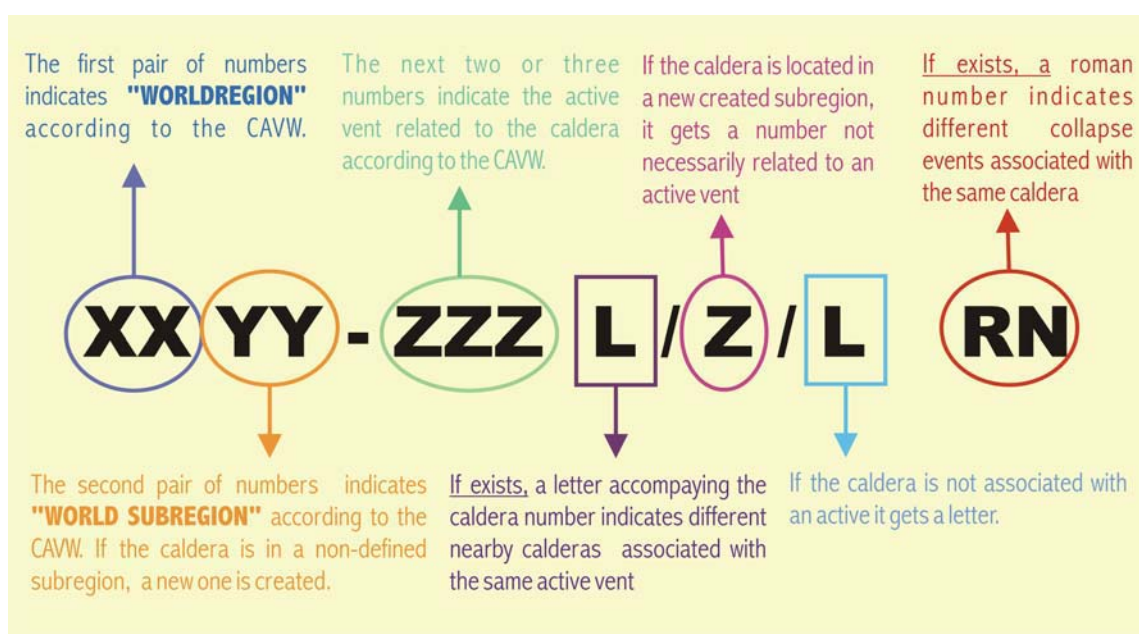


**Fig. 2.26:** Schematic explanation of the components of the caldera identification number. The different world regions and their corresponding subregions are listed in Appendix III.

### ➤ Caldera name

This *FIELD SET* includes the *FIELD* “CALDERA” (TF, RF) recording the name of the corresponding sample caldera. In general, caldera names used are listed in the “Catalogue of Active Volcanoes of the World” (CAVW) (IAVCEI, 1951-present), “Data Sheets of the Post-Miocene Volcanoes of the World” (IAVCEI, 1973-present), “Volcanoes of the World” (Simkin et al., 1981) or “Historical unrest at large calderas of the world” (Newhall and Dzurisin, 1988). Calderas not listed in these publications are referred to by their most commonly used name. In some cases, calderas have the same name as that of their most active vent.

### ➤ Geographical location

The fields “Latitude” (NF, RF), “Longitude” (NF, RF), “World\_region” (NF, RF) and “Subregion” (NF, RF) are included in this *FIELD SET*. The first two *FIELDS* provide the latitude and the longitude (in degrees) of the calderas. The other two *FIELDS* indicate the world region and more precisely also the sub-region where the caldera sample is located at. The designation of the different world regions and sub-regions is in agreement with the definition proposed by Simkin et al. (1981) and afterwards modified by Newhall and Dzurisin (1988). Figure 2.27 represents the outlines of the 20 regions of the world. Some calderas are located in non-defined subregions (e.g. Glencoe -U.K. Moore and Kokelaar, 1997, 1998; Raman Yotam – *Israel*, Eyal and Peltz, 1994) which resulted in the definition of new sub-regions (e.g. the subregion 0106 corresponding to the U.K. or the 0107 to Israel) not marked in the map of Figure 2.27. The list with the different world regions, their corresponding sub-regions, as well as an enlarged image of this map is compiled in Appendix II.

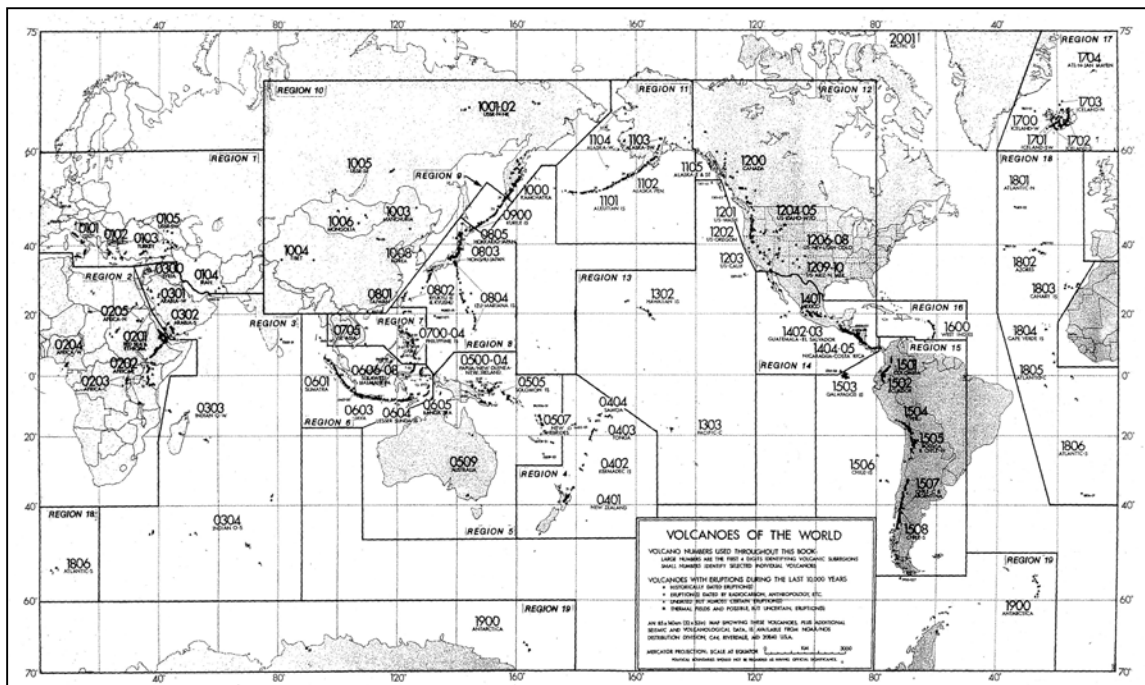


**Fig. 2.27:** Outlines of the 20 world regions defined by Simkin et al. (1981) and modified by Newhall and Dzurisin (1988). The lists with the different world regions and their corresponding subregions, as well as an enlarged image of this map are compiled in Appendix II and III, respectively.

➤ **Caldera age**

In connection with the age of the caldera samples, the database has two different *FIELDS*: “Age” (TF, RF) and “AgeCLAS” (TF, CLASF). The *FIELD* “Age” records all existing information regarding caldera age. In most cases, authors are able to provide a precise age (e.g. “114 ka” La Vecchia – *Italy*, Newhall and Dzurisin, 1988 and references therein). However, for some caldera samples, it is not possible to assign an accurate age, therefore, some authors give only the geological time period (e.g. “Late Miocene-Early Pliocene” Los Azufres – *Mexico*, Ferrari et al., 1991) and in other cases, an age interval (e.g. “5.59-1.79 ka” Dorobu – *Japan*, Miura and Tamai, 1998). Evidently, if we do not homogenize this information, although being necessary for the database, it is useless for field data analysis. Therefore, in order to allow the subsequent analysis and to facilitate the resulting interpretations we homogenise the information by classifying the calderas in different categories according to their age. This classification is recorded in the *FIELD* “AgeCLAS”. The classification criteria, as well as, the different categories are explained in section II.5.4 and listed in Appendix II.

➤ **Structural features**

This *FIELD SET* groups all the *FIELDS* recording information about the structural features of the caldera samples. On the one hand, the *FIELD* “Dimensions (km)” (TF, RF) records available data about the dimensions of the caldera structure at surface. Sometimes, the dimensions of the collapse depression are difficult to define, and consequently, authors are only allowed to give an approximate interval (e.g. “6- 7 km” Pine Canyon - *U.S.A.*, Henry and Price, 1989) or a minimum diameter (e.g. “>20 km” Silverton – *U.S.A.*, Lipman, 1975, 1984). Furthermore, if the caldera has two rims authors give both, the outer and the inner one (e.g. “4 x 7 (outer) 2.5 x 3 (inner)” Agua de Pau- *Azores*, Newhall and Dzurisin, 1988 and references therein). Consequently, we introduce two additional *FIELDS*: “D<sub>max</sub> (km)” (NF, RF) and “D<sub>min</sub> (km)” (NF, RF). These represent, in that order, the maximum and minimum diameter of the caldera depression at surface. In the case of calderas with two rims, we put in these two *FIELDS* the dimensions of the outer rim. Furthermore, if an interval is given, we assume that the lower limit corresponds to D<sub>min</sub> and the upper to D<sub>max</sub>.

Moreover, the *FIELD SET* “Structural features” also includes the *FIELDS* “Area\_ref (km<sup>2</sup>)” (TF, RF) and “Vol\_ref(km<sup>3</sup>)” (TF, RF), which record the area and the volume of the caldera depression provided by the consulted references. However, in most cases, the authors do not give

the calculated area only the caldera dimension. Therefore, we include a further *FIELD* called “Area\_cal (km<sup>2</sup>)” (NF, CALF). Information included in this *FIELD* is the result of calculating the area of the caldera using the information contained in the *FIELDS* “D<sub>max</sub>” and “D<sub>min</sub>” . For this, we consider that:

$$A_c = \pi (D_{\max}/2) (D_{\min}/2) \quad [2.1]$$

where  $A_c$  is the area of the collapse depression at surface in km<sup>2</sup> . Theoretically, the values contained in this field should coincide with those of the field “Area\_ref (km<sup>2</sup>)” (e.g. “Area\_cal (km<sup>2</sup>)” = 241.9 km<sup>2</sup> vs. “Area\_ref (km<sup>2</sup>)” =240 km<sup>2</sup> , Soledad - *South America*, Redwood, 1987) but this is not always the case (e.g. “Area\_cal (km<sup>2</sup>)” = 1237 km<sup>2</sup> vs. “Area\_ref (km<sup>2</sup>)” =707±25 km<sup>2</sup> , Mc Dermitt - *U.S.A.*, Spera and Crisp, 1981 and references therein; Rytuba and McKee, 1984). One possible explanation for this is that with equation 2.1 we approximate the plan view shape of the caldera to a circumference (if  $D_{\max} = D_{\min}$  ) or to an ellipse (if  $D_{\max} \neq D_{\min}$  ). Obviously, this is not necessarily true for all caldera samples of the database, as some of them have irregular morphologies (e.g. Kumano – *Japan*, Miura, 1999). However, we consider that calculating the area with equation 2.1 is, at least, a good approximation for those calderas from which we do not have direct information about their area.

The *FIELD* “AreaCLAS” (NF, CLASF) corresponds to the classification of the calderas according to their dimensions in km<sup>2</sup>. We define certain intervals specified in Appendix II and explained in section II.5.4.

Additionally, the field “Subsidence (km)” (TF, RF) registers the amount of caldera subsidence during the collapse process.

The last two *FIELDS* of this *FIELD SET* are: “Collapse\_type” (TF, RF) and “Incremental” (YNF, RF). In the first one, we try to organize the calderas according to the morphological classification proposed by Lipman in 1997 (see section II.3.4.3). Appendix II includes a list of the different possibilities of this field. In the *FIELD* “Incremental” we mark those calderas with evidences of an incremental collapse process, i.e. caldera subsidence took place in different pulses. Noticeably, if this field is not marked, it does not necessarily mean that the caldera subsided suddenly and in one single event. It may happen, that although caldera collapse was incremental, there is no information or data about that in the revised bibliography.

➤ **Photograph**

The *FIELD* “Photograph” (RF) contains the links to the images of the corresponding calderas. Most of these photographs have been obtained with the program Google Earth® (<http://earth.google.es>).

❖ **DEPOSITS PROPERTIES**

A good knowledge of the extruded deposits may inform us about the magnitude of the collapse event, on the possible collapse mechanisms. All the information regarding the volcanic deposits may be divided in the following *FIELD SETS*:

➤ **Deposit name**

The unique *FIELD* included in this group is called “Deposit\_name” and records the names of the stratigraphic unit associated with the corresponding caldera-forming event.

➤ **Deposit dimensions**

We include in this *FIELD SET* the *FIELDS* “Thick\_dep (km)” (TF , RF) thickness of the deposits in km (intra- and, in some cases also, extracaldera), “Vol\_dep (km<sup>3</sup>)” (TF , RF) volume in km<sup>3</sup> of the extruded deposits during the caldera-forming event and “Vol\_magma (km<sup>3</sup>)” (TF , RF) volume in km<sup>3</sup> of magma extruded during the eruptive event. Moreover, the *FIELD* “VoldepCLAS” (TF , CLASF) and “VolmagmaCLAS” (RF, CLASF) correspond to a classification of the calderas according to the volume of the extruded deposits or magma, respectively. There exist eight different categories for both *FIELDS*, all listed in Appendix II and explained in section II.5.4.

❖ **MAGMA CHAMBER PROPERTIES**

The chemical, mechanical and physical properties of the magma chamber and of the erupted magma during a caldera-forming event may be useful to understand possible

caldera collapse triggers and subsidence mechanisms. Therefore, we record the pertinent information in the following *FIELDS*:

➤ **Magma chamber composition**

This *FIELD SET* comprises the *FIELDS*: “Composition” (TF , RF) and “CompositionCLAS” (TF , CLASF). The first one records the composition of the extruded deposits during the caldera-forming event. The second corresponds to the classification of the calderas according to the composition of the extruded materials. The defined categories are commented in section II.5.4. Appendix II includes a list of the different possibilities of this field.

➤ **Magma chamber structural features**

This group includes the *FIELDS* “Chamber\_depth” (TF, RF) and “R” (TF , CALF). In the first one, we record the available information about the depth of the magma chamber during the caldera-forming event. Normally, this is not a single value but an interval defined by  $P_{min}$  (minimum magma chamber depth) and  $P_{max}$  (maximum magma chamber depth). The *FIELD* “R” provides the roof aspect ratio of the magma chamber, i.e. the ratio between the magma chamber depth or thickness of the overlying roof and the magma chamber width. We calculate the roof aspect ratio interval as follows:

$$P_{min} / D_{max} \leq R \leq P_{max} / D_{min} \quad [2.2]$$

where  $D_{max}$  and  $D_{min}$  are the maximum and minimum diameter of the caldera included in the fields “ $D_{max}$  (km)” and “ $D_{min}$  (km)”, respectively.

❖ **LOCAL, REGIONAL AND PLATE TECTONICS**

In this *SECTION*, the database records information concerning the local, regional and plate tectonics of the area where the collapse caldera is located.

In their comprehensive work, Newhall and Dzurisin (1988) listed the regional tectonic setting for those calderas where local tectonic structure or pattern of unrest was consistent with the regional tectonic setting. However, they found that in some cases, the local tectonic features differed from those of the regional pattern (for example, an

extensional graben along a regionally convergent plate margin, or local shear in a region of tectonic extension). Therefore, for several of the calderas they indicated the local, or both local and regional, tectonic settings. We can see that the authors distinguished only between local and regional tectonic contexts, however the definition and limits they considered for both scales is not clear. In a first attempt, we tried to continue with the method of Newhall and Dzurisin (1988) but soon we found some difficulties. Their methodology was not descriptive enough for a further analysis, as they merged stress field information with data about regional structure, etc. In our database we try to compile a more accurate description to characterize precisely the maximum number of calderas. However, we also need that the included information is not very complicated, in order to facilitate a good and efficient field data analysis. Therefore, we have had to find a compromise between an overly accurate database and a useful and easy-to-manage data compilation. In previous sections, we proposed that factors influencing volcanic cycles may be divide in three main groups depending on their scale: plate, regional or local. Here, we try to preserve this distinction in order to be coherent throughout all this work. Consequently, we have decided to divide the information about the tectonic setting in two groups considering plate-regional and local tectonic setting.

➤ **Plate-regional tectonic setting**

Here we distinguish the *FIELDS* “Tectonic\_setting\_des” (TF , RF), “Tectonic\_setting” (TF , IF) and “Crust” (TF , IF). In the first one, we include, following the indications of the consulted references, a short description of the tectonic context in which each collapse calderas is located. In some cases, only plate tectonics is described (e.g. “Back-arc rifting” Santorini-*Greece*); in others, comments on regional or local structures are also included (e.g. “Island arc collision and regional strike-slip faults and associated extension” Pinatubo- *Philippines*). For those calderas also integrated in the work of Newhall and Dzurisin (1988) we maintain the description of the tectonic setting given by these authors and first adding, in some samples, comments from other additional sources. However, this field presents two important weaknesses. On the one hand, the field records several types of information. On the other, included data can be extremely subjective. The main source of this subjectivity is the definition and interpretation of the different tectonic settings, which may vary slightly from author to author (see section II.5.4). Furthermore, in other cases, available information do not discriminate between distinct tectonic settings and consequently it is

difficult to decide between one of the different possibilities, e.g. Italian volcanic zones (see section II.5.4). These kinds of uncertainties become an important problem during the elaboration of the database. Therefore, we have created the *FIELD* “Tectonic\_setting” in order to homogenize the information coming from the consulted references. This *FIELD* only records the plate tectonic setting regardless of stress fields or regional structures. First, we establish a unique definition of the diverse tectonic settings, based on the information obtained from the literature on plate tectonics consulted for this work (e.g. Condie, 1993; Kearey and Vine, 1996) (see section II.5.4). Afterwards, we try to reclassify the calderas included in the CCDB according to the new-defined tectonic settings. Appendix II lists all the different possibilities we can find in the field and in section II.5.4 includes an explanation of the criteria applied to define the different tectonics settings.

Also related to plate tectonics is the type of crust where the collapse caldera is located. As we mentioned before (see section I.1.2), the type of crust plays an important role in defining volcanic cycles and caldera-forming eruptions. The field “Crust” records the composition of the crust, as well as, its thickness at the area where the collapse caldera is located.. In Appendix II are listed all the different possibilities we can find in the field “Crust”.

The last *FIELD* “Regional\_faults” (YNF , RF), records the existence of regional faults that may affect the magmatic system or the caldera structure before or after the caldera collapse. Notice, that if this *FIELD* is not marked it does not necessarily mean that there is not a regional fault near or along the caldera structure. It can happen that there is no information or data about that in the revised references.

### ➤ **Local tectonic setting**

We include in this *FIELD SET* the *FIELD* “Local\_tectonics” (TF, IF). Additionally to the regional-plate tectonic setting, it is interesting and necessary to study the local tectonics restricted to small-scale structures (from regional to local), which may also control caldera collapse or magma extrusion. We define the information included in the *FIELD* “Local\_tectonics” as the condition or nature of the structures (e.g. extensional, compressional, etc.) affecting the caldera or the magmatic system responsible of the caldera-forming eruption. In some cases, the nature of the local structures is a direct consequence of the regional-plate tectonic setting, e.g. areas of continental rifting (extensive stress field) produce extensional faults. In other cases, they do not agree, for example areas of convergent plate margin (compressive stress field) with local graben structures (extensive origin). In Appendix II are listed all the different possibilities we can find in

this *FIELD* and section II.5.4 includes a more accurate description of the criteria applied for establishing the different conditions of local structures.

#### ❖ **PRE-CALDERA ACTIVITY**

A significant aspect necessary to clarify the mechanisms of caldera collapse processes is to understand possible signals occurring during the pre-caldera activity in the area. Therefore, we collect relevant information related to pre-collapse activity grouped in the following *FIELD SETS*:

##### ➤ **Type of pre-caldera edifice**

This *FIELD SET* includes the *FIELDS* “Edifice” (TF , RF) and “EdificeCLAS” (TF , CLASF). The first one records the type of volcanic edifice (e.g. shield volcano, stratovolcano, composite volcano, etc.) existing prior to the caldera-forming event or in some cases, also its absence. In Appendix II are listed all the different possibilities we can find in this field. Furthermore, the field “EdificeCLAS” offers a simplified classification of the caldera samples according to the type of pre-caldera edifice. It considers different categories also listed in Appendix II and explained in section II.5.4.

##### ➤ **Pre-caldera doming (tectonic or magmatic)**

The unique *FIELD* included in this *FIELD SET* is called “Pre-caldera\_doming” (YNF , RF). Here we record the existing information about tectonic or magmatic tumescence or doming periods prior to the caldera-forming eruption. In most cases, due to the scarcity of information we are not able to elucidate the origin of the doming process. Therefore, we record the existing information about the process of doming regardless of its origin. Notice, that if this field is not marked it does not essentially mean that there was not a local doming prior to the caldera-forming event. It can happen that although caldera collapse could be preceded by local tumescence there is no information or data about that in the revised references.

##### ➤ **Type of collapse precursor**

This *FIELD SET* is composed of two different *FIELDS* “Precaldera\_precursor” (TF , RF) and “PrecursorCLAS” (TF , CLASF) that document possible information about the triggers or precursors of the caldera-forming event. In most cases, there are indices of pre-caldera plinian eruptions and for other caldera samples ring faults apparently started the eruption. In the *FIELD* “Precaldera\_precursor” is included an accurate description of the possible triggers and the *FIELD* “PrecursorCLAS” corresponds to a simplified classification of the caldera samples according to the type of triggers or precursors. All the different possibilities we can find in both fields are listed in Appendix II. Furthermore, the classification criteria of the “PrecursorCLAS” field are explained in section II.5.4.

## ❖ **POST-CALDERA ACTIVITY**

A caldera collapse does not imply necessarily the end of the volcanic activity in an area. By contrast, a great majority of caldera-forming events are only an intermediate stage in the evolution of a specific volcanic system. Therefore, it is interesting to study the type of post-caldera activity that takes place after the caldera-forming event. *FIELDS* included in this *SECTION* may be grouped in:

### ➤ **Post-caldera volcanic activity**

After the investigation of Walker (1984) summarized in section II.3.6, it is evident that the study of the post-caldera activity is useful to understand the state of the volcanic system after the caldera-forming event and also the internal aspect of the structures generated during the caldera collapse. Therefore, the *FIELD* “Postcaldera\_activity” (TF, RF) records those calderas with enough data on the type of activity that takes place after the caldera-forming event, according to the classification performed by Walker (1984). In Appendix II are listed all the different possibilities we can find in this *FIELD*.

### ➤ **Post-caldera resurgence**

In some cases, caldera-forming eruptions are followed by resurgence periods. Therefore, in the *FIELD* “Resurgence” (YNF, RF) we mark those samples in which there exist evidences of further resurgence or intracaldera doming. Again, if this *FIELD* is not marked, it does not strictly mean that there was not any local doming after the caldera-forming event. In such a case, although

local resurgence might have followed caldera collapse there is no information or data available on this matter in the revised literature.

## ❖ REFERENCES

This *SECTION* contains only the *FIELD* “References” (TF, RF) included in the *FIELD SET* with the same name. This *FIELD* lists for each caldera all the consulted references. References are assigned to an identification number composed of a capital letter and a number. The capital letter corresponds to the initial of the first author surname, the number has any particular meaning, and it indicates only when the reference was introduced in the database. Furthermore, those articles with a “c” in their identification numbers are references about plate tectonics of the area where the caldera is located; this works are not necessarily directly related to the caldera. All references cited in the database are also included in part VII and listed in Appendix II.

### II.4.4 On-line database

Unfortunately, communication and data exchange between different scientific groups is still scarce and sometimes also unsatisfactory. With this in mind, the final and better use of this database is to convert it into an open and accessible tool for everybody working on collapse calderas. It is hence proposed to develop of a web page where the database will be accessible to everybody. We are interested in the communication between research groups in order to streamline data and knowledge exchange. The web page is going to be structured in three main areas (Fig. 2.28):

- **CCDB**
- **Register**
- **CCDB Community**

## ❖ **CCDB**

This section will be open to everybody and consists of a short introduction, explanation and user's manual of the calderas database. In this section, it will explain the different fields included in the database, the type and sources of information, the database structure and the objectives of the CCDB.

## ❖ **REGISTER**

Persons interested in the database should register in order to obtain a user name and a password. These will be necessary to receive the CCDB and to enter in the third section: *CCDB Community*. Registration is only for security reasons to avoid any misuse of the database and non-controlled modifications. Users will be asked to introduce their name and surname, as well as the information of their institute or organization. This will be also useful to create a new database of scientists working on calderas and may facilitate further personal contacts or information exchange between them.

## ❖ **CCDB COMMUNITY**

In the *CCDB Community* section the web page visitors will be able to suggest updates and corrections of the database, to send news about event or publications related to caldera collapse studies or to enter in the CCDB Forum. The principal objectives of this section are twofold. First, to maintain the collapse caldera database as updated as possible with the incorporation of new information and data. Second, to give the CCDB users the possibility of asking or consulting aspects related to caldera collapse processes to other CCDB members.



**Fig. 2.28:** Screenshots of the CCDB web page prototype. Three different sections compose the web page. The first one, called *CCDB*, will be open to any user and consists of a short introduction, explanation and user's manual of the calderas database. A second section, *Register*, will house a registration form. Users interested in the database should register in order to obtain a user name and a password. These will be necessary to receive the CCDB and to enter in the third section: *CCDB Community*. Registration is only for security reasons in order to avoid any misuse of the database and non-controlled modifications. In the *CCDB Community* people will be able to suggest updates and corrections of the database, to send news about event or publications related to caldera collapse studies or to enter in the CCDB Forum.

The CCDB web page will have a webmaster, who represents the only person eligible to modify, update and correct the database and to keep the CCDB in good working order. With a username and password, each CCDB member will be able to connect with the Webmaster to inform him about collapse caldera news, updates or corrections. Of course, published or accepted works should support each correction or update. Once updated or corrected the webmaster will inform all CCDB users about the new database version.

The existence and good working of such a kind of database and community of learning will be a great advance on collapse caldera studies and in improving communication and information exchange between research groups.

## **II.5. FIELD DATA ANALYSIS**

### **II.5.1 Introduction and objectives**

In this section, we present an exhaustive analysis of the database information in order to find possible general trends and to distinguish between different caldera types or groups for a further determination of a common physical scenario. In further chapters of this work, the combination of these results with subsequent analogue and numerical models will be crucial to propose a genetic classification of calderas.

### **II.5.2 Methodology**

In order to perform the analysis of the field data, we will follow the steps described below:

- **Selection of the *CHARACTERISTICS***
  - **Definition of the *CATEGORIES***
  - **Creation of the *CCDB DATA TABLE***
  - **Analysis of the *CCDB DATA TABLE***
  - **Concluding results and remarks**
- 
- ❖ **SELECTION OF THE *CHARACTERISTICS***

Firstly, we define those features (e.g. caldera age and size, composition of the erupted material, etc.) that will be considered in the field data analysis. We call them “*CHARACTERISTICS*” in order to differentiate them from the rest of features included in the database. These *CHARACTERISTICS* have to fulfil certain requisites to be adequate for the analysis.

## ❖ DEFINITION OF THE *CATEGORIES*

The next step consists in the identification of those *FIELDS* in the database that record all the information concerning the selected *CHARACTERISTICS*. Subsequently, we study the type of information recorded in these *FIELDS*.

If a specific field contains a continuum spectrum of numeric data (e.g. the field “Area\_cal (km<sup>2</sup>)”), we try to simplify the information defining specific intervals called “*CATEGORIES*”. After that, we reclassify the information of the field in the new-defined categories. The information related to the reclassification is recorded in a new-created field called “*CLASSIFICATION FIELD*”. In order to distinguish these *CLASSIFICATION FIELDS* from the other fields included in the database, they get a special name. This is composed of the name of the *CHARACTERISTIC* plus the suffix “CLAS” (e.g. AreaCLAS).

In some cases, information regarding a *CHARACTERISTIC* does not get to be a continuum spectrum of numeric values but the list of possible options is quite long. For example, the field “Composition” (Composition of the extruded magma or deposits during the caldera-forming event) may record more than 40 different compositions. Since this is also unworkable for the field data analysis, we try to group all possibilities in a few representing groups, i.e. *CATEGORIES*. Again, the reclassification of the information in the new-created *CATEGORIES* is recorded in a *CLASSIFICATION FIELD*. The assignment of the *CLASSIFICATION FIELD*'s name follows the abovementioned rule (e.g. “CompositionCLAS”).

If the information regarding a *CHARACTERISTIC* is restricted to a small number of options, we assume that these are the *CATEGORIES*. We perform the analysis directly without reclassifying the information in a *CLASSIFICATION field*.

Finally, if the information concerning a *CHARACTERISTIC* is recorded in an **IF FIELD** we assume that the different options included in the *FIELD* are the *CATEGORIES* and no *CLASSIFICATION FIELD* is created. Remember that all data included in **IF FIELDS** is assigned according to our criteria and the information from consulted references related to the collapse caldera and the area where this is located. Before recording the information we define the suitable *CATEGORIES* consequently, we do not need to reclassify the information as is the case of other *FIELDS*.

## ❖ CREATION OF THE *CCDB DATA TABLE*

Once defined the different *CHARACTERISTICS* and their corresponding *CATEGORIES* we create a table, called “*CCDB DATA TABLE*”. In the *CCDB DATA TABLE* we try to compile all the information concerning the chosen *CHARACTERISTICS* and related *CATEGORIES*. Thanks to this table we are able to study independently each *CHARACTERISTIC* but also the interaction of two different *CHARACTERISTICS*.

## ❖ ANALYSIS OF THE “*CCDB DATA TABLE*”

Once the *CCDB DATA TABLE* has been created, we proceed with its analysis. On the one hand, we study how many calderas included in the CCDB are classified in each *CATEGORY* of a *CHARACTERISTIC*. On the other hand, we investigate how many calderas included in a *CATEGORY* of the *CHARACTERISTIC* “A” are classified in a specific *CATEGORY* of the *CHARACTERISTIC* “B”.

### II.5.3 Selection of the *CHARACTERISTICS*

#### II.5.3.1 Conditions for the selection of *CHARACTERISTICS*

Once finished the CCDB version used in this work, it is necessary to determine those features that will be considered in the field data analysis. As mentioned in the previous section (see section II.5.2), we call them “*CHARACTERISTICS*” in order to differentiate them from the rest of features included in the database. However, before choosing the definitive *CHARACTERISTICS* we should be sure that they fulfil certain requisites necessary for a correct analysis. These conditions are:

- **Information about the collapse mechanism and controlling factors**
- **Minimum number of calderas with information**
- **Objectivity of the recorded information**
- **Comparability of the recorded information**

---

## ❖ INFORMATION ABOUT THE COLLAPSE MECHANISM AND CONTROLLING FACTORS

The first requisite is obvious. The analysis of the selected feature should provide information about the collapse mechanism or/and the controlling factors prior or during the caldera collapse, and also for a further genetic classification proposal. Consequently, features such as the caldera or the deposit name, the latitude and longitude are excluded. Considering this, we are able to make a preliminary selection of those *CHARACTERISTICS* we are interested to study.

## ❖ MINIMUM NUMBER OF CALDERAS WITH INFORMATION

Once the preliminary *CHARACTERISTICS* are selected, we identify the corresponding *FIELDS*. In order to establish the definitive *CHARACTERISTICS* we are obliged to study the information recorded in the *FIELDS*. We control if the included information fulfills certain criteria. The first condition is that the *FIELD* regarding the *CHARACTERISTIC* should contain data for a considerable high number of calderas. In order to control if this requisite is fulfilled, we define two new parameters. Firstly, we identify **N** as the total number of calderas with information on a specific *FIELD*. Secondly, since in some cases not all the available information is useful for the analysis, we also define **N<sub>ANA</sub>**. This parameter represents the total number of calderas that contain information valid for the CCDB data analysis. Evidently,  $N_{ANA} \leq N$ . Due to scarcity of data, not all the *FIELDS* included in the database satisfy the criteria of having a considerable high number of calderas with information. Once introduced all data in the CCDB we notice that several *FIELDS* remain almost empty for approximately all included calderas (e.g. the *FIELDS* “Chamber\_depth (km)”: depth of the magma chamber; and “R”: roof aspect ratio of the magma chamber). In both cases, we have information on only about 27 calderas (**N** = 27), less than the 10% of the total recorded samples (283). Therefore, although both *FIELDS* could be an interesting source of information, it is obvious that such a low **N** value is insufficient for the analysis we try to perform. However, it is evident that due to scarcity of data we

cannot be too strict when defining a minimum **N** and also **N<sub>ANA</sub>** values to empower the *FIELDS* to take part in the field data analysis. After careful considerations, we establish that every field included in the analysis should have information for at least a fourth of the total recorded calderas (**N**, **N<sub>ANA</sub>**  $\geq 70$ ). We assume that this is not a very high value but in some case, insufficiency of data obliges us to accept this threshold. However, we will take into account these low **N<sub>ANA</sub>** values during the analysis and also when drawing the final conclusions. Again, we insist on the CCDB to be a dynamically changing database, which should be updated time by time, in order to improve the analytical studies presented in this work.

#### ❖ OBJECTIVITY OF THE RECORDED INFORMATION

The next requisite refers to the need of objectivity in the studied data. This is for example the case of the *FIELD* “Tectonic\_setting\_description”. As we have already mentioned in section II.4.3, this *FIELD* includes a short description of the tectonic context in which the collapse caldera is located according to the consulted references. However, the information ranges from plate tectonics (e.g. “Back-arc rifting” Santorini – *Greece*, Newhall and Dzurisin, 1988 and references therein) to regional or local structures (e.g. “Regional strike-slip faults” Pinatubo - *Philippines*; “Listric faults” Bolsena – *Italy* Newhall and Dzurisin, 1988 and references therein). Consequently, this *FIELD* presents two important weaknesses. On the one hand, the field records several types of information. On the other, included data can be extremely subjective. The main source of this subjectivity is the definition and interpretation of the different tectonic settings, which may vary slightly from author to author. Since the main source of subjectivity is the definition and interpretation of each tectonic setting we have to create a new *FIELD* (“Tectonic\_setting”) using own definitions and reassign each caldera sample to a tectonic setting following our own criteria. Thus, we have, at least, a control of the “subjectivity”. As a result, the new created *FIELD* is useful for the analysis if it fulfils the other requisites.

## ❖ COMPARABILITY OF THE RECORDED INFORMATION

The last condition is that information recorded in the *FIELDS* has to be comparable among the different calderas included in the CCDB. This forces us to neglect fields like “Age” or “Dimensions”, when the information is introduced as intervals, minimum or maximum values, etc. However, as we will see, these fields become useful after to specific modifications, information is reclassified into *CLASSIFICATION FIELDS*.

### II.5.3.2 Selected *CHARACTERISTICS*

Finally, taking into account the defined criteria, we consider that the analysis may be performed using the *CHARACTERISTICS* summarized in Table 2.1.

## II.5.4 Definition of the *CATEGORIES*

This section, describes the motivations for choosing each of the *CHARACTERISTICS* for the definitions of the different *CATEGORIES*.

### ❖ CALDERA PROPERTIES

#### ➤ World region

We consider that it is interesting to study the spatial distribution of the calderas and also to try to infer a possible relationship between the geographical location and the rest of *CHARACTERISTICS*. Therefore, we define first the *CHARACTERISTIC* “World region”. Information included in the corresponding *CLASSIFICATION field* “World\_region” fulfils all conditions. First of all, there is information on all calderas included in the database, i.e.  $N = 283$ . Furthermore, the information is clearly objective and comparable, since geographical location of calderas is unique and we assign the world regions according to the well-defined world sections of Simkin et al. (1981) and Newhall and Dzurisin (1988). The *CATEGORIES* corresponding to the *CHARACTERISTIC* “World region” coincide with the 20 world regions outlined in figure 2.27 and listed in Appendix II. Moreover, since all the information in the *CLASSIFICATION field* is useful the total number of analysed calderas  $N_{ANA}$  is also 283.

<i>CHARACTERISTIC</i>	<i>FIELD/S CLASSIFICATION FIELD</i>	<i>Location in the CCDB</i>	
		<i>FIELD SET</i>	<i>SECTION</i>
World region	World_region	Geographical location	Caldera properties
Age	Age AgeCLAS	Caldera age	Caldera properties
Dimensions (Equivalent diameter $D_{CIR}$ )	Area_cal (km <sup>2</sup> ) + Area_ref (km <sup>2</sup> ) AreaCLAS	Structural features	Caldera properties
Collapse type	Collapse_type CollapseCLAS	Structural features	Caldera properties
Volume of extruded deposits	Vol_dep (km <sup>3</sup> ) VoldepCLAS	Deposit dimensions	Properties of deposits
Volume of extruded magma	Vol_magma (km <sup>3</sup> ) VolmagmaCLAS	Deposit dimensions	Properties of deposits
Composition of extruded magma	Composition ComposititionCLAS	Magma chamber composition	Magma chamber properties
Crustal type	Crust	Plate-regional tectonic setting	Local, regional and plate tectonics
Tectonic setting	Tectonic_setting	Plate-regional tectonic setting	Local, regional and plate tectonics
Existence of relevant regional faults	Regional faults	Plate-regional tectonic setting	Local, regional and plate tectonics
Condition of the local structures	Local tectonics	Local tectonic setting	Local, regional and plate tectonics
Type of pre-caldera edifice	Pre-caldera edifice EdificeCLAS	Type of pre-caldera edifice	Pre-caldera activity
Type of collapse precursor	Collapse_precursor PrecursorsCLAS	Type of collapse precursor	Pre-caldera activity
Type of post-caldera volcanic activity	Postcaldera_activity	Post-caldera volcanic activity	Post-caldera activity

**Table 2.1:** *CHARACTERISTIC* considered in the field data analysis. Furthermore, we indicate the *FIELDS* and *CLASSIFICATION FIELDS* that record all the information regarding the different *CHARACTERISTICS*. Moreover, we added the information related to the location of these fields in the database according to figure 2.25.

➤ **Age**

A further *CHARACTERISTIC* considered in this study is the age of the collapse caldera. We want to know if there is a preferential time period for caldera-forming events. Also, we will be able to find out if other *CHARACTERISTICS* are typical in calderas of certain ages. Moreover, we can calculate the frequency of caldera-forming eruptions during the last tens of Ma. The information is recorded in the *FIELD* "Age" and it fulfils the minimum **N** value (**N** = 216) and the required objectivity. However, it does not accomplish one of the main conditions, which is data comparability. For example, for some calderas we have information only about the geological time period (e.g. "Late Quaternary" Longonot – *Africa*, Williams et al., 1984; Newhall and Dzurisin, 1988 and references therein) and in other cases an age interval (e.g. "5.59-1.79 ka" Dorobu-*Japan*, Miura and Tamai, 1998). Evidently, if we do not homogenize this information, it is useless for the field data analysis. Those calderas with a specific age generate a continuum spectrum of data, which is more useful when it is divided in specific interval. Taking all this into account, we define certain age intervals, i.e. "Age" *CATEGORIES*, and classify the values of the field "Age" in these new categories. Thus, information becomes comparable and allows us to use the *CHARACTERISTIC* "Age". Once classified, we record the information in the *CLASSIFICATION field* "AgeCLAS". Nevertheless, the main problem when defining the *CATEGORIES* is that the age of a caldera may range from few hundreds of years to several tens of million years. Evidently, the definition of the intervals should be accurate enough to represent the age distribution of the calderas included in the CCDB but, of course, not too extensive in order to facilitate further analysis of the results. In a first attempt, we tried to establish the intervals following a logarithmic rule, i.e. < 1 ka, 1 – 10 ka, 10 – 10<sup>2</sup> ka, 10<sup>2</sup> – 10<sup>3</sup> ka, 10<sup>3</sup> – 10<sup>4</sup> ka (1- 10 Ma), 10<sup>4</sup> – 10<sup>5</sup> ka (10 – 100 Ma) and > 10<sup>5</sup> ka (>100Ma). However, this classification has some disadvantages. The last interval is too long in duration and consequently, all the information provided by the calderas within this interval (around 50 samples) gets lost. Furthermore, we consider that 1 ka for the first interval is not long enough considering that we are dealing with geological structures. As a consequence, we modify this first classification proposal as follows. Firstly, we consider that the interval of young calderas should be extended to 5 ka, a more reasonable time scale for geological structures but at the same time, also reasonable for human scale. Consequently, we modify also the second and third interval to obtain a better distribution of the age information. In order to take the maximum advantage of the information provided by the calderas samples, we also divide the period of "10 – 100 Ma" in three different intervals. Since the number of calderas older than 50

Ma is very low, and consequently, information is scattered, we assume that establishing the upper threshold at this age, only a few information gets lost. In fact, the elimination of *CATEGORIES* that do not provide additional information leads to a more accurate classification. Finally, the “Age” *CATEGORIES* are: “<5 ka”, “5 – 50 ka”, “50 - 100 ka”, “100 ka – 1 Ma”, “1 – 10 Ma”, “10 – 25 Ma”, “25 - 50 Ma”, “> 50 Ma”. In the case that the age interval falls between two different “Age” *CATEGORIES* (e.g. “5.59-1.79 ka” Dorobu – *Japan*, Miura and Tamai, 1998), we calculate the mean value and assign that caldera sample to the *CATEGORY* according to the mean value of its age. Moreover, those calderas with unknown age or for which only a minimum or maximum age value is indicated, are included in the *CATEGORY* “?”. Calderas included in this *CATEGORY* are not included in the field data analysis. Therefore, from the 216 calderas with information recorded in the *CHARACTERISTIC field* “Age” (N = 216), only 177 are included in the *CLASSIFICATION field* “AgeCLAS” (N<sub>ANA</sub> = 177).

### ➤ **Dimensions**

The dimension of calderas is an important parameter. A special interest lies with the question as to whether a particular size is favoured over another. Therefore, we define the dimension as the next *CHARACTERISTIC*. Since calderas are, in most cases, well-defined structures, it is relatively easy to estimate their dimensions, specially their diameter at surface. However, the main problem when dealing with caldera dimension is that caldera diameter is not a useful parameter for comparison. The principal reason is that calderas plan view shapes may vary from circular ( $D_{\max} = D_{\min}$ ) to elliptical ( $D_{\max} \neq D_{\min}$ ). This implies that we cannot compare the diameters of the calderas with different shapes. Consequently, we have to find out a parameter related to caldera dimensions, which allows us to compare the dimensions of all calderas regardless of their morphology. We believe that the best choice is to consider the area of collapse. As mentioned before (see section II.4.3), this information is recorded in two different fields: “Area\_ref (km<sup>2</sup>)” and “Area\_cal (km<sup>2</sup>)”. The first one records the area provided by the consulted references. The second, the area calculated with Equation 2.1 using the information contained in the *FIELDS* “D<sub>max</sub>” and “D<sub>min</sub>” (see section II.4.3). For the *FIELD* “Area\_ref (km<sup>2</sup>)” N is 76 and for “Area\_cal (km<sup>2</sup>)”, 237. Now, we have to select one of them. Undoubtedly, there exist two possibilities, either to accept the field “Area\_cal (km<sup>2</sup>)” with the highest N value or to add the information of both *FIELDS*. The first option clearly fulfils all requisites, as we have enough calderas with information, and the available data are objective and comparable. By contrast, if we add the information of both *FIELDS* we have to take into account that the information has been obtained from two different

sources, and we have to be sure that none representative discrepancies exist between them. For this reason, we define first the *CATEGORIES* of the *CHARACTERISTIC* “Dimensions”.

We assume that dealing with areas is not always intuitive. Therefore, we define an equivalent diameter  $D_{CIR}$  to make the analysis more understandable. This new parameter corresponds to the diameter of a circumference with the same area than that of the studied caldera (Fig. 2.29). In fact, classification of calderas according to  $D_{CIR}$  is equivalent to do it with the caldera area but the expression of the categories is more comprehensive and intuitive.

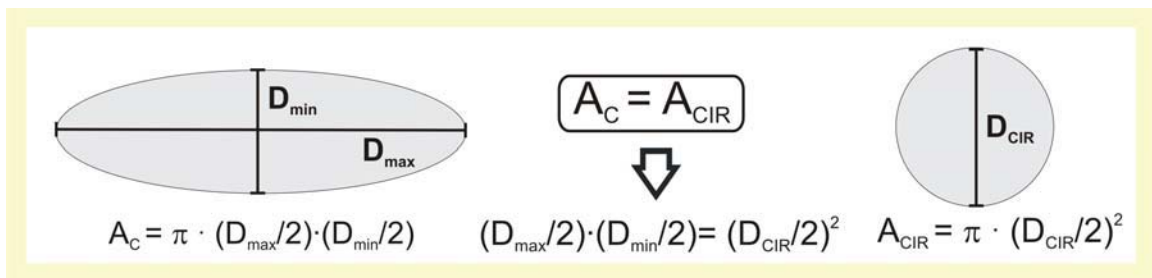


**Fig. 2.29:** Sketch of the equivalent diameter  $D_{CIR}$  definition.  $A_C$  Caldera area;  $A_{CIR}$  Circle area;  $D_{max}$  Maximum caldera diameter ;  $D_{min}$  Minimum caldera diameter.

Finally, the *CATEGORIES* of the *CHARACTERISTIC* “Dimensions” are defined such that  $D_{CIR}$  is: “<5 km” (19.63 km<sup>2</sup>), “5 – 10 km” (19.63 – 78.54 km<sup>2</sup>), “10 – 25 km” (78.54 – 490.87 km<sup>2</sup>), “25 – 50 km” (490.87 – 1963.5 km<sup>2</sup>) and “> 50 km” (> 1963.5 km<sup>2</sup>). Moreover, those calderas with unknown dimensions or for which only a minimum or maximum area value is indicated, are assigned to the *CATEGORY* “?”.

Once defined the corresponding *CATEGORIES*, differences between the values of the *FIELDS* “Area\_ref (km<sup>2</sup>)” and “Area\_cal (km<sup>2</sup>)” become, in most cases, irrelevant. Independently from which *FIELD* we take the information, the caldera sample is classified in the same *CATEGORY*, even for those samples with relatively high differences (e.g. “1500±45 km<sup>2</sup>” ( $D_{CIR} = 43.8$  km) in the *FIELD* “Area\_ref (km<sup>2</sup>)” and “942 km<sup>2</sup>” ( $D_{CIR} = 34.6$  km) in the *FIELD* “Area\_cal (km<sup>2</sup>)” Bursum-*U.S.A*, Spera and Crisp, 1981, Elston, 1984; Ratté et al., 1984). There are only two samples for which we had to choose between the information of one of the two *FIELDS*, La Garita - *U.S.A* and Gila Cliff Dwelling - *U.S.A*. In both cases, we decided to take the values of the “Area\_cal (km<sup>2</sup>)” field, because those of the “Area\_ref (km<sup>2</sup>)” are too low or too high, respectively. The dimensions of La Garita caldera are 35 × 75 km (Lipman, 1984, 1997) according to Equation 2.1 this corresponds to an area around 2000 km<sup>2</sup>. In contrast, the consulted reference (Spera and

Crisp, 1981 and references therein) assigns only around 1052 km<sup>2</sup>. The case of the Gila Cliff Dwelling caldera is reverse. It is an approximately circular caldera with a diameter of 20 km (Elston, 1984; Ratté et al., 1984). The area according to Equation 2.1 is around 315 km<sup>2</sup>, however the consulted reference assigns (Spera and Crisp, 1981 and references therein) more than 1400 km<sup>2</sup>. Furthermore, the information concerning  $D_{\max}$  and  $D_{\min}$  come from newer references (Elston, 1984; Ratté et al., 1984), which are assumed to be updated in comparison with that consulted for the information in the field “Area\_ref (km<sup>2</sup>)” (Spera and Crisp, 1981 and references therein). Taking all these considerations into account, we decided to add the information of both *FIELDS* ( $N_{ANA}=256$ ).

The classification of the calderas according to their equivalent diameter, i.e. dimensions in km<sup>2</sup>, is recorded in the *CLASSIFICATION FIELD* “AreaCLAS”.

### ➤ Collapse type

Lipman (1997) presented a classification of calderas relating subsidence geometry and resulting structures to a few geometrically simplified end-member processes. However, no previous studies exist associating these end-members with other features described here, e.g. the tectonic context. Therefore, we consider interesting to design the “Collapse type” as the next *CHARACTERISTIC*. In the CCDB all information regarding the type of caldera collapse is recorded in the *FIELD* “Collapse\_type” ( $N=109$ ). In this field we can see that there exists more possibilities than those proposed by Lipman (1997). However, we decided to simplify and homogenize the information using only his terminology. Subsequently, we create the *CLASSIFICATION FIELD* “CollapseCLAS” in which the existing information regarding the type of caldera collapse is reclassified in the following *CATEGORIES*:

1. Plate/piston subsidence
2. Trap-door subsidence
3. Piecemeal disruption
4. Chaotic subsidence
5. Funnel calderas
6. Others: Those calderas involving subsidence processes intermediate between the idealized end-members

Contrary to the classification proposed by Lipman (1997) (see section II.3.4.3), we do not consider downsag subsidence as a *CATEGORY* of the *FIELD* "Collapse\_type". In fact, downsagging can be combined with other subsidence types as for example is the case for some of the examples cited by Branney (1995; Table 1). Some of the calderas represented in that table have subordinate downsagging of caldera floors bounded by well-developed ring faults, and others are asymmetrical hinged trap-door calderas as defined by Lipman (1997) with incomplete ring-faults. Consequently, we assume that some of the calderas included in the above mentioned *CATEGORIES* can have a downsag component but we consider that the above mentioned subsidence geometries and mechanisms are the most ones.

Moreover, calderas with unknown collapse type, are assign to the *CATEGORY* "?". After reclassifying the information of the *FIELD* "Collapse\_type" in the new *CATEGORIES* of the *CLASSIFICATION FIELD* "CollapseCLAS" the total number of calderas with information is 93 ( $N_{ANA} = 93$ ). The *CHARACTERISTIC* "Collapse type" fulfils all requisites, a high number of calderas samples with information, as well as, objectivity and comparability of the information.

## ❖ **PROPERTIES OF DEPOSITS**

### ➤ **Volume of extruded deposits and magma**

We also consider important to know if there is a preferential value of extruded deposits or magma volume. Therefore, these features are defined as *CHARACTERISTICS*, too. Due to the direct relationship between the volume of extruded deposits and the volume of extruded magma, information provided by analysing both *CHARACTERISTICS* is expected to be similar. However, it is, in most cases, complementary. In fact, for some calderas we know the volume of the extruded deposits but not that of the extruded magma or vice versa. Subsequently, we could combine both data sets but the main problem is that there is not a unique way to transform deposit volumes into magma volumes (since it depends on different parameters such as density, porosity, etc.). Therefore, we prefer to analyse both *CHARACTERISTICS* separately.

In the CCDB, *FIELDS* recording the information about deposits and magma volume are "Vol\_dep (km<sup>3</sup>)" ( $N = 104$ ) and "Vol\_magma (km<sup>3</sup>)" ( $N = 76$ ), respectively. These contain a wide spectrum of values which should be divided in the specific *CATEGORIES*, the same for both *CHARACTERISTICS*: "<10 km<sup>3</sup>", "10-50 km<sup>3</sup>", "50-100 km<sup>3</sup>", "100-500 km<sup>3</sup>", "500 – 1000 km<sup>3</sup>", "1000 - 2000 km<sup>3</sup>", ">2000 km<sup>3</sup>". In addition, those calderas with unidentified volume of the

extruded deposits or magma, or with a minimum or maximum value are assigned to the *CATEGORY* “?”. The classification of the calderas according to extruded deposits and magma volume is recorded in the *FIELDS* “VoldepCLAS” ( $N_{ANA} = 89$ ) and “VolmagmaCLAS” ( $N_{ANA} = 70$ ), respectively.

## ❖ MAGMA CHAMBER PROPERTIES

### ➤ Composition of extruded materials

We define as the next *CHARACTERISTICS* the composition of the extruded material. The reasons for this are twofold. On the one hand, considering that composition influences and controls magma physical properties, the study of the composition of the extruded materials during caldera-forming eruptions may help us to understand the collapse mechanisms or the controlling factors. Moreover, the composition of the extruded materials during a caldera-forming eruption has been also used to classify collapse calderas compositionally (Cole et al., 1995). Therefore, we consider necessary to revise the compositional information registered in the database in order to find out whether this compositional classification is valid or not.

Information regarding the composition of the extruded materials during the eruption is recorded in the *FIELD* “Composition” ( $N = 225$ ). Furthermore, objectivity of compositional analysis and the existing standard definitions of the different compositional fields guarantee that this *CHARACTERISTIC* also accomplish data objectivity. However, the main problem appears when trying to compare the information recorded in the field. In most cases, consulted references provide a precise composition, e.g. rhyolite (e.g. Golovnin – *Kurile Islands*, Newhall and Dzurisin, 1988 and references therein; On-take – *Japan*, Newhall and Dzurisin, 1988 and references therein) or dacite (e.g. Okmok – *Aleutian Islands*, Newhall and Dzurisin, 1988; Orafajokull – *Iceland*, Newhall and Dzurisin, 1988). By contrast, for other calderas, the field gives only information about the percentage of  $\text{SiO}_2$  content (e.g. “68-70%” Summitville – *U.S.A.*, Lipman, 1974, 1984), if the composition is silicic (e.g. Torfajokull – *Iceland*, Newhall and Dzurisin, 1988 and references therein) or mafic (e.g. Aoba – *New Hebrides*, Newhall and Dzurisin, 1988 and references therein), etc. As a consequence of this great diversity of compositions and types of information we avoid the use of the field “Composition” for the field data analysis. In order to make information comparable and applicable to the analysis, we decided to classify the compositions into the main rock suites subalkaline and alkaline. The types of rocks included in each of these main groups are represented

---

in a TAS diagram (Total alkali-silica diagram) (Fig. 2.25 A). The irregular red dashed line separates the compositional areas covered by both rock suites. Furthermore, subalkaline rocks have been subdivided into the calc-alkaline and tholeiitic suites. Tholeiitic rocks show stronger enrichment in Fe relative to Mg than do calc-alkaline rocks and generally have less variation in silica, whereas the calc-alkaline suite shows enrichment in silica and alkalis with differentiation (Fig. 2.25 B). In Table 2.2 are represented the different *CATEGORIES* considered for the *CHARACTERISTIC* "Composition". In addition to the division into calc-alkaline, alkaline and tholeiitic, we distinguish also for the first two compositions between mafic, intermediate and felsic and also two ranges from mafic to felsic and from intermediate to felsic. Additionally, to these eleven *CATEGORIES* we also consider the option "others" which includes those calderas with compositions ranging from calc-alkaline to alkaline. If magma composition is given as SiO<sub>2</sub> percentage or as silicic, felsic, intermediate or mafic, information is ambiguous and the composition could be sorted both into the subalkaline and calc-alkaline *CATEGORY*. Sometimes, this ambiguity may be solved comparing the composition of those calderas with that of nearby calderas (e.g. "Silicic" Ijen – *Java*, Newhall and Dzurisin, 1988 and references therein; "Dacite" Prahu – *Java*, Newhall and Dzurisin, 1988 and references therein). However, if the ambiguity persists we assign the caldera sample to the *CATEGORY* "?" (e.g. St. Andrew Strait – *New Guinea*, Newhall and Dzurisin, 1988 and references therein). Additionally, we classify also into the *CATEGORY* "?" those calderas whose composition is not yet known. Finally, the classification of the recorded calderas according to composition of the extruded material is recorded in the *CLASSIFICATION FIELD* "CompositionCLAS" ( $N_{ANA} = 224$ ).

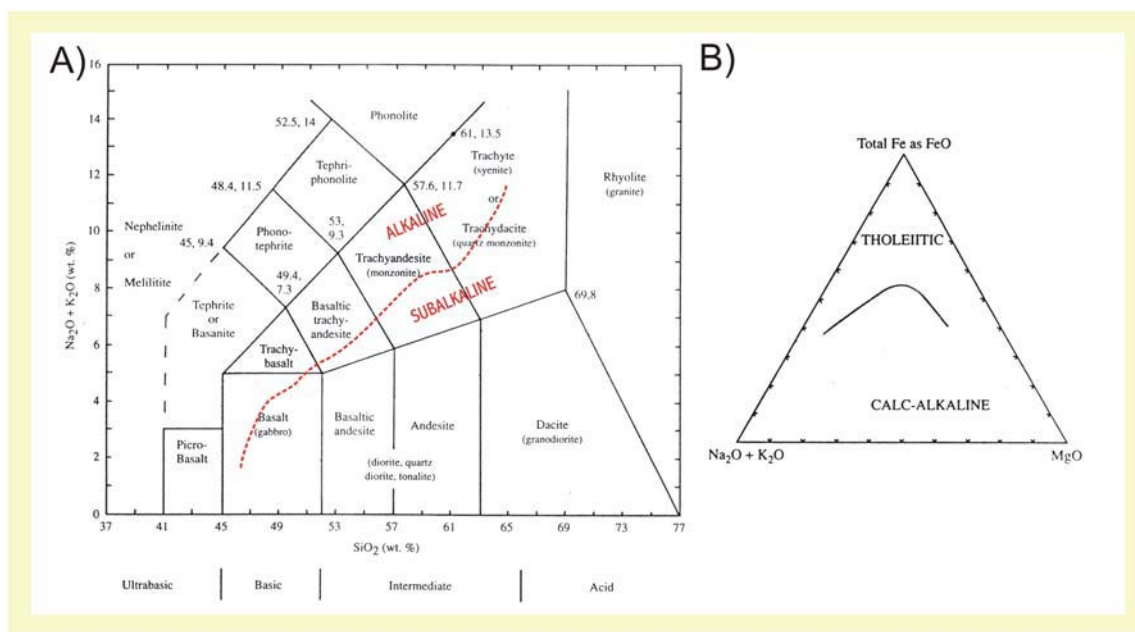


**Fig. 2.30: (A)** IUGS (International Union of the Geological Sciences) classification of aphanitic and glassy volcanic rock types. Coordinates of critical points are indicated as, for example,  $\text{SiO}_2$  wt.% = 69 and  $(\text{Na}_2\text{O} + \text{K}_2\text{O})$  wt. % = 8 at the common corner trachyte, rhyolite, and dacite. The distinction between trachyte ( $Q < 20\%$ ) and trachydacite ( $Q > 20\%$ ) is based on the amount or normative quartz,  $Q$  from a recalculation in which  $Q + An + Ab + Or = 100$ . The amount of olivine,  $Ol$ , in the rock distinguish tephrite ( $<10\%$ ) from basanite ( $>10\%$ ). Rock-type names for more or less corresponding common phaneritic rocks are indicated in parentheses. Irregular red dashed line separates the fields of subalkaline and alkaline rock suites. **(B)** Division of the subalkaline rocks into tholeiitic and calc-alkaline rock suites. AFM diagram in terms of alkalis ( $\text{Na}_2\text{O} + \text{K}_2\text{O}$ ), total FeO, and MgO. Solid line separates fields of tholeiitic rocks from calc-alkaline rocks. (Modified from Best and Christiansen, 2001)

		<u>CATEGORY</u>			<u>CATEGORY</u>
<b>SUBALKALINE</b>	Calc-alkaline composition $\Rightarrow$	<i>Mafic</i> <i>Intermediate</i> <i>Felsic</i> <i>Intermediate-felsic</i> <i>Mafic-felsic</i>	<b>ALKALINE</b>	Alkaline composition $\Rightarrow$	<i>Mafic</i> <i>Intermediate</i> <i>Felsic</i> <i>Intermediate-felsic</i> <i>Mafic-felsic</i>
	Tholeiite composition $\Rightarrow$	<i>Tholeiitic</i>			<i>Mafic-felsic</i>

**Table 2.2:** Classification of the main compositional groups considered in the statistical analysis and the corresponding subgroups and compositions.

---

## ❖ LOCAL, REGIONAL AND PLATE TECTONICS

### ➤ Crustal types

Here, we consider crustal types the next *CHARACTERISTIC*. The corresponding *FIELD* is “Crust”, which accomplishes the minimum **N** value (**N** = 273) necessary for a representative analysis. As we mentioned in section II.4.3, this *FIELD* is of type **IF**, i.e. for each caldera sample the crustal type is assigned according to the information extracted from references related to the collapse caldera and to the area where the caldera is located. Furthermore, the assignation of the crustal types is carried out according to our criteria, in order to homogenize the recorded information and maintaining coherence. Otherwise, the information included in the field “Crust” would not accomplish the required requisites of objectivity and comparability. Consequently, the next and most difficult task concerning the *FIELD* “Crust” is to define these criteria and subsequently, the corresponding *CATEGORIES*. Therefore, we have to think about the principal aspects defining crustal types, which are composition and thickness (see section II.5.4). The first influences the composition and also the physical properties of the magma (Best and Christiansen, 2001). The second may also modify magma composition and defines, as well, the mechanical behaviour of the crust and controls the magma storage capacity (Turcotte and Shubert, 2002). Therefore, when defining the *CATEGORIES* of the *CHARACTERISTIC* “Crustal types”, we have to take into account both composition and thickness. From the references included in this review we propose following *CATEGORIES*:

1. Thick continental crust (> 30-35 km of thickness)
2. Thin continental crust (< 30-35 km of thickness)
3. Thick transitional crust (>20-25 km of thickness)
4. Thin transitional crust (< 20-25 km of thickness)
5. Thick Oceanic crust (> 10-15 km of thickness)
6. Thin Oceanic crust (< 10-15 km of thickness)

Continental crust is silicic (granitic) while oceanic crust is more mafic and primarily basaltic in composition. The transitional crust has an intermediate composition between the continental and the oceanic crust. Although the main common crustal divisions are: oceanic, transitional and continental, it is typical to find zones of continental thinned crust for examples in areas of continental rifting or very thick transitional crust in highly evolved island arcs. Regarding the

oceanic crust there are also some examples where the crustal thickness is above the mean value, like in Iceland or the Lesser Antilles (Condie, 1993; Kearey and Vine, 1996). In order to illustrate such thickness differences in continental, oceanic or transitional crust, figure 2.31 and 2.32 show different seismic profiles. Consequently, we maintain that an accurate classification has to take into account both parameters: thickness and composition. The thickness thresholds from thick to thin are established according to the definition of Condie (1993), who assumes that oceanic crust ranges from 5 to 15 km thick, transitional crust from 15 to 30 km and continental crust from 30 to 50 km. Moreover, those calderas with undefined or unknown crustal type are assigned to the *CATEGORY“?”*.

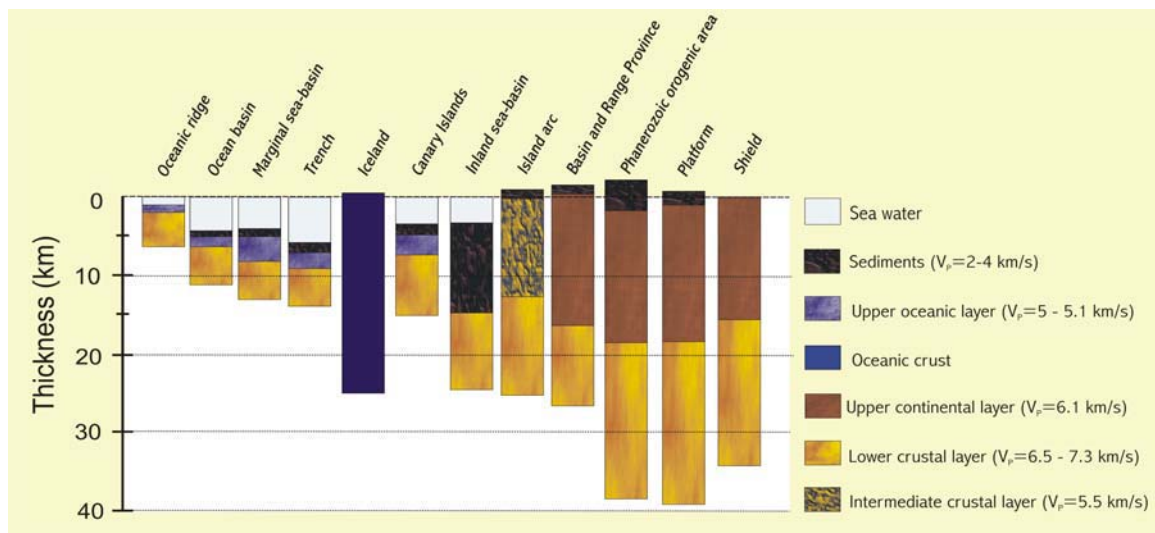


**Fig. 2.31:** Seismic sections of various crustal types according to the classification by Condie (1993). The seismic section for the Canary Island has been extracted from Watts (1994). For the case of Iceland we illustrate only the crust thickness according to Best and Christiansen (2001).  $V_P$  corresponds to the P-wave velocity of the layer. (Modify from Condie, 1993)

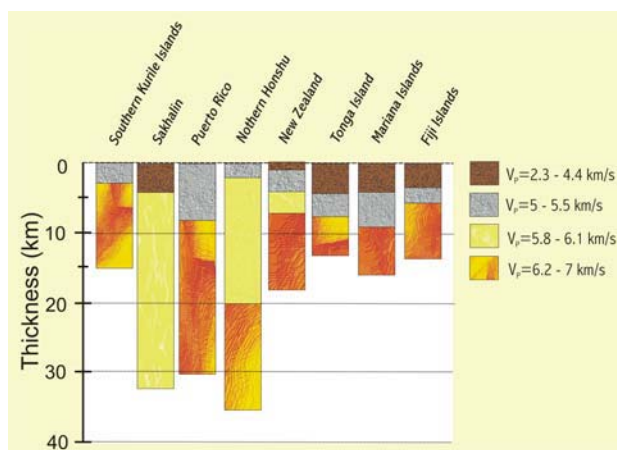


**Fig. 2.32:** Seismic sections of island arcs according to the classification of Condie (1993).  $V_P$  corresponds to the P-wave velocity of the layer. (Modified from Condie, 1993)

Some calderas recorded in the CCDB are difficult to classify into one of the different crustal types or *CATEGORIES*. The major problems appear classifying island arcs. Their composition should be theoretically transitional (Condie, 1993) However, these may range from almost oceanic (e.g. Western Aleutians) to practically continental (e.g. Japan) (Condie, 1993; Kearey and Vine, 1996). Thus, the Aleutian arc, although being an island arc could be considered, from a compositional stand point, an oceanic crust rather than intermediate as, for example, the Izu-Osawa arc (Fliedner and Klemperer, 2000).

In most cases, due to the scarcity of data it is very difficult to define the type of crust (e.g. Gaua, Aoba, Ambrym). In these cases, we assign the type of crust extrapolating the information from the tectonic setting and the bathymetric information. Of course, there can be some errors in the interpretations, so it is pointed out again the necessity of this database to be dynamic and continuously updated.

For a large number of calderas, we have used the information existing from general maps of crustal thickness. This is the case of the calderas in the USA (Condie, 1993) and or those in 45 the Caribbean region (Case et al., 1984). The accuracy of the observations is then strongly dependent on the precision of this kind of maps. Occasionally, we can contrast the information of the maps with other specific works (e.g. Riciputi et al., 1995) but this is not always possible. In other cases, we have found specific information about the area where the caldera sample is located (e.g. Kamimura et al., 2002; Hasegawa et al., 2005).

Finally, since the *FIELD* "Crust" is of type IF, we do not generate a *CLASSIFICATION field*. Furthermore, the information contained in the field "Crust" is used in the field data analysis without any further modification. Consequently,  $N_{ANA} = N = 273$ .

### ➤ Tectonic setting

Another feature that controls directly or indirectly collapse caldera processes, is the tectonic setting. Consequently, we define it also as *CHARACTERISTIC*. As we have already mentioned in section II.4.3, two *FIELDS* of the database contain information about the tectonic setting where collapse calderas included in the CCDB are located: "Tectonic\_setting\_des" (TF , RF) and "Tectonic\_setting" (TF , IF). However, the main problem of the first *FIELD* is the combination (mixture) of different types of information (no comparability of data) and data subjectivity. By contrast, in the second *FIELD*, information coming from the consulted references and from "Tectonic\_setting\_des" has been filtered and homogenized following the specific and unique criteria set out below. Since the latter field fulfils the requisites of data comparability, objectivity

and minimum  $N$ , we select it as the source of information for the *CHARACTERISTIC* "Tectonic\_setting". Similar to the *FIELD* "Crust", the *FIELD* "Tectonic\_setting" is of type **IF**, consequently, it is not necessary to generate a *CLASSIFICATION field* and  $N_{ANA} = N = 243$ .

Now, we define the corresponding *CATEGORIES* but this is not an easy task. After studying the available collapse calderas and the corresponding references, we conclude that the tectonic settings in which calderas may appear may be classified into the *CATEGORIES* indicated in figure 2.33.

Notice, that assume as a possible tectonic setting oceanic ridges although none of the caldera sample in the database is classified in this *CATEGORY*. The reasons for this are diverse. Firstly, we consider that ocean ridges are important and significant tectonic settings in volcanic cycles. Therefore, it can be that although the CCDB does not included any sample in areas of oceanic ridges it is possible that future updating includes some calderas. The second reason is that maybe the fact that in strict oceanic ridges there do not exist collapse calderas (as far as we have recorded in the database) has a specific meaning in terms of collapse mechanism. Consequently, we decided to include this *CATEGORY* leaving open the possibility of recording calderas on oceanic ridges.

Probably, the most difficult task in this part is to find the correct definition for the *CATEGORIES* "Chilean-type subduction" (C-type subduction) and "Mariana-type subduction" (M-type subduction), i.e. to classify the subduction types. Nowadays, there is still not a clear and well-defined classification of this kind of convergent margins. Some authors propose a simple classification suggesting that Mariana-type subduction zones are characterized by the subduction of an old and dense oceanic crust under another oceanic crust with the overriding plate moving away from the active trench. Furthermore, some authors expand this definition arguing that this subduction zones are also characterized by active back-arc basins under extension, as well as, high subduction angles (Strahler, 1997) and steeply deeping Benioff zones (Uyeda, 1982). By contrast, in Chilean or Andean-type subduction zones the descent of the subducting slab is more difficult since this is younger, less dense and consequently, more buoyant. Furthermore, the overriding plate moves towards the trench, creating compression in the volcanic front (Carey, 2005). Additionally, other references defend the idea that at these subduction zones subduction angles are low, there exist no active back-arc basins (Strahler, 1997) and the Benioff zone is shallow and gently deeping (Uyeda, 1982; Carey, 2005). In general terms, the criteria defining the mode of subduction should consider the state of stress and nature of coupling in the back-arc region, the subduction rate, and the dip of the Benioff zone. In fact, data about the range of subduction rates and Benioff zone dips indicate that the definitions of Chilean-type and Mariana-

type subduction are end-members in a continuum of subduction types. This leads to some problems when trying to classify the different tectonic setting of calderas.

Almost the rest of the tectonic setting “Island arc collision”, “Back-arc rifting”, “Continental rifting” and “Oceanic ridge” are well defined (Carey, 2005) and their identification does not present controversies. Further problems appear when designing “Hotspots”. Hotspot are anomalous areas of surface volcanism that cannot be directly associated with plate tectonic processes (Kearey and Vine, 1996; Turcotte and Schubert, 2002; Carey, 2005). Normally, hotspots occur both in the ocean and in the continents. These lie well within in the middle of plates and/other at or near an ocean ridge. Some hotspots have been well-studied and recognized as unique and dominant tectonic setting (e.g. Yellowstone – *U.S.A*, Spera and Crisp, 1981 and references therein) but in other cases, overlapping structures like hotspots close or over ocean ridges make us to think about which one of the two tectonic settings is the most relevant for the area. For example, due to the hotspot, the volcanism that forms Iceland is much more voluminous than normal ocean ridge volcanism. This volcanism resulted in a thick oceanic crust and the elevation of Iceland above the sea level. Consequently, we decided also to distinguish between intraplate hotspots and those close to an oceanic ridge.

However, problems concerning this *CHARACTERISTIC* are not restricted to the definition of the tectonic settings. In certain circumstances, due to the scarcity or ambiguity of the available information, it is difficult or almost impossible to decide objectively between one of the existing possibilities. This is, for example, the case of Italy. The models that are generally invoked to explain the origin of volcanism in central Italy consider two possibilities (Savelli, 2000): (1) subduction of Adriatic lithosphere and back-arc asthenospheric mantle updoming (Thompson, 1977; Di Girolamo, 1978; Peccerillo, 1985; Doglioni, 1991; Keller et al., 1994), or (2) an intracontinental rift environment unrelated to subduction, as in east Africa and the Eifel district (e.g. Cundari, 1979; Stoppa and Lavecchia, 1992 and references therein; Decandia et al., 1998). For this kind of situations we define the *CATEGORY “?”*. Since we are not able to decide objectively between one of the possible settings, we prefer to assign “?” in order to avoid influencing the field data analysis. This *CATEGORY “?”* is also thought to be the option for those calderas with unknown tectonic setting.

In most cases, we have found information about the tectonic setting of the caldera (e.g. Toba – *Sumatra*, Katili, 1975; Malod and Kemal, 1996; Elburg et al., 2005) but in others, we have to extrapolate the information from references of the specific area or from nearby calderas.

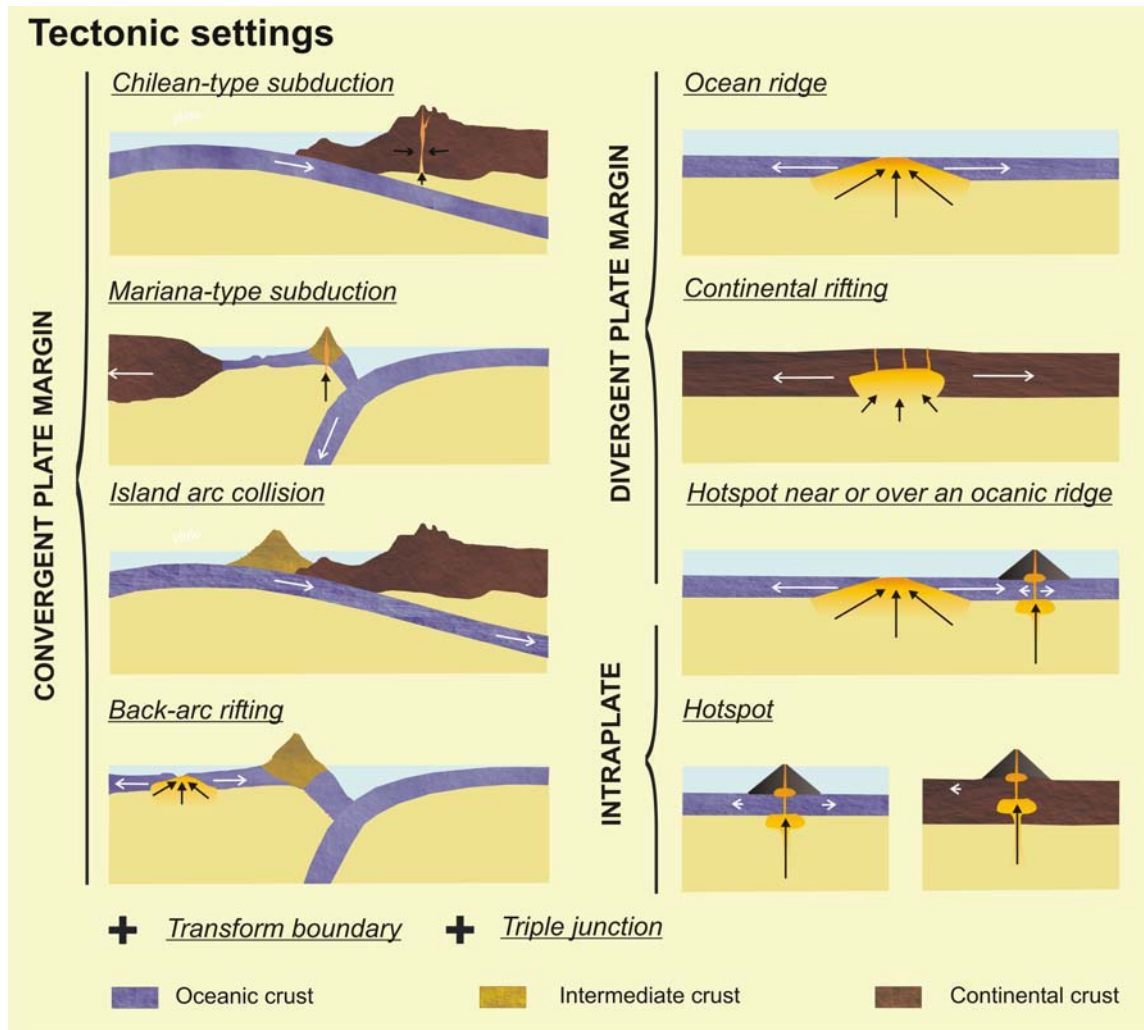


Fig. 2.33: Sketch of the different tectonic settings collapse calderas may take place.

### ➤ Existence of relevant regional faults

A further interesting feature and consequently, *CHARACTERISTIC*, is the presence of relevant regional faults close or intersecting the considered collapse caldera structures. Under this topic we include those faults that may affect either caldera structure or the magmatic system prior, during or after the collapse event. This information is recorded in the *FIELD* "Regional\_faults" (YNF, RF) (N =124). The recorded information is clearly objective and comparable. We consider only the information provided by those calderas with regional faults.

➤ **Condition of the local structures**

The last characteristic included in the section “Local, regional and plate tectonics” refers to the local structural setting. We are interested in the type and condition of the structures surrounding the collapse caldera or the magmatic system responsible for the caldera-forming eruption. As we commented before (see section II.4.3), this information is recorded in the field “Local\_tectonics”.

Although, the condition of the local structures and the local state of stress are intimately related aspects, as we will explain later, it is very important to maintain them separated. Figure 2.34 illustrates the different *CATEGORIES* of this *CHARACTERISTIC* “Condition of the local structures”: “Extensional”, “Compressional”, “Shear”, “Shear-compressional”, “Shear-extensional”.

In the case of ideal structures, the relationship between the latter and the local stress field is direct, i.e. it is easy to extrapolate the local stresses from the condition of the local structures (Fig. 2.34 A). We include mainly in the *CATEGORY* “Extensional” normal faults but also ideal graben structures, both kinds of structures clearly related to extensional stress fields (Fig. 2.34 A I). In the *CATEGORY* “Compressional” we include principally thrust faults and horst-like structures associated with compressional stress fields (Fig. 2.34 A II). The *CATEGORY* “Shear” records those calderas with associated transform structures related to shear stress fields (Fig. 2.34 A III). Between these three structural end-members, we can find more complex structures like strike-slip duplexes (Fig. 2.34 B and C). In these cases, displacement along strike-slip faults with bends or stepovers produces a complex zone of deformation. Such structures may be extensional or contractional, depending on whether they form at an extensional or a contractional bend or stepover. Such local structures are classified into the *CATEGORIES* “Shear-extensional” or “Shear-compressional”, respectively. Additionally, faults submitted to forces neither perpendicular (pure extension or compression depending on the direction) nor parallel to the strike line of the fault, i.e. a oblique force, are also associated with a combined stress field: shear-extensional or shear-compressional (Fig. 2.35). The applied force  $F$  can be expressed in terms of its normal component and its shear component.

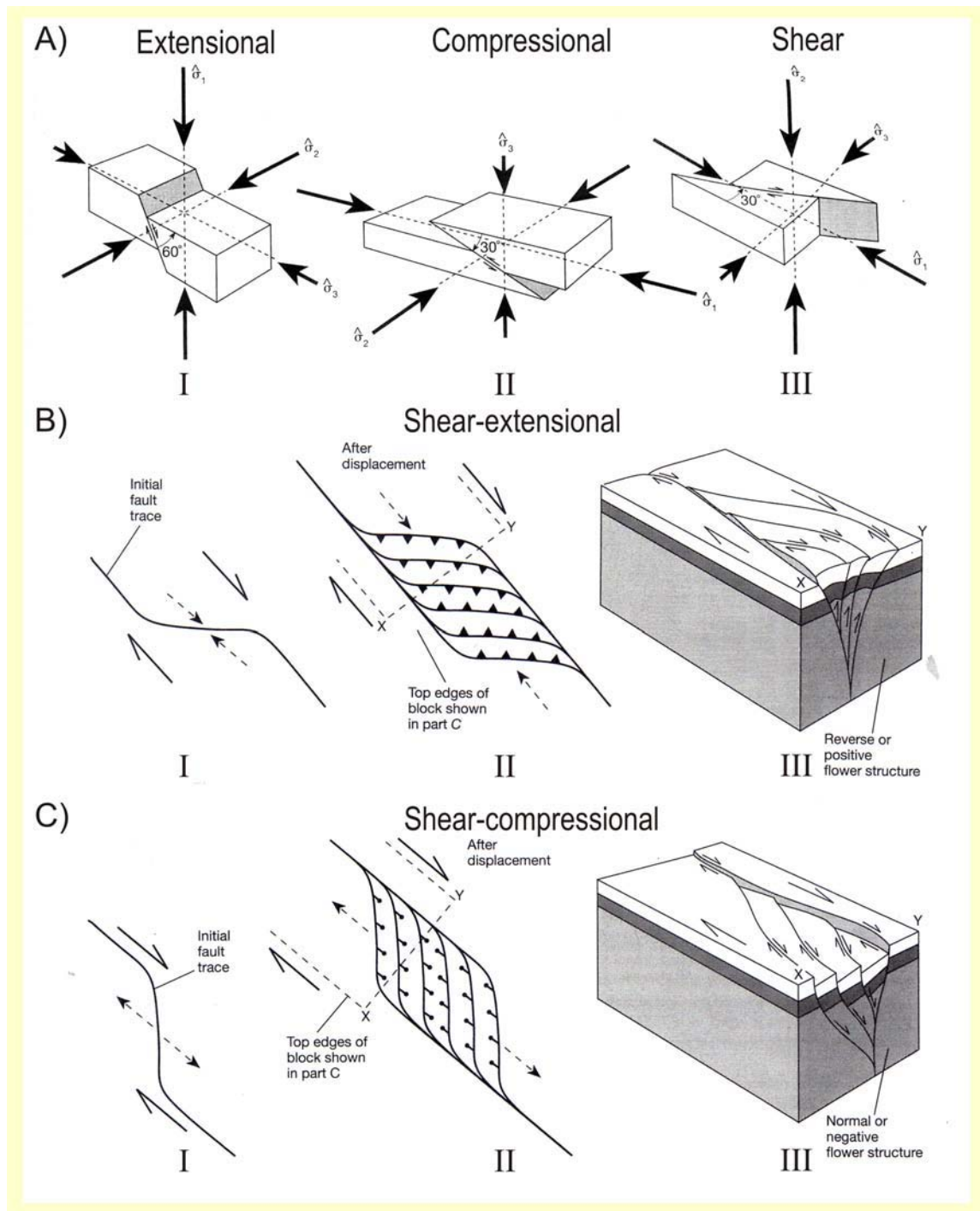


**Fig. 2.34:** (A) Sketch showing the relationship between the orientation of the principal stresses and the different ideal fault types. I Normal fault with maximum compressive stress vertical. II Thrust fault with minimum compressive stress vertical. III Strike-slip fault with intermediate compressive stress vertical. (B) Formation of an extensional duplex at an extensional (releasing) bend. Large arrows indicate the dominant shear sense of the fault zone; small arrows indicate the sense of the strike-slip and normal components of motion on the fault splays. I Extensional bend on a dextral strike-slip fault. II An extensional duplex developed from the bend in part I. III A block diagram showing a normal, negative, flower structure in 3-D. The block faces are vertical planes along the dashed lines in part II. (C) Formation of a contractional duplex at an contractional (restraining) jog. Large arrows indicate the dominant shear sense of the fault zone; small arrows indicate the sense of the strike-slip and normal components of motion on the fault splays. I Contractional bend on a dextral strike-slip fault. II A contractional duplex developed from the bend in part I. III A block diagram showing a reverse, positive, flower structure in 3-D. The block faces are vertical planes along the dashed lines in part II. (Modified from Twiss and Moores, 1992)

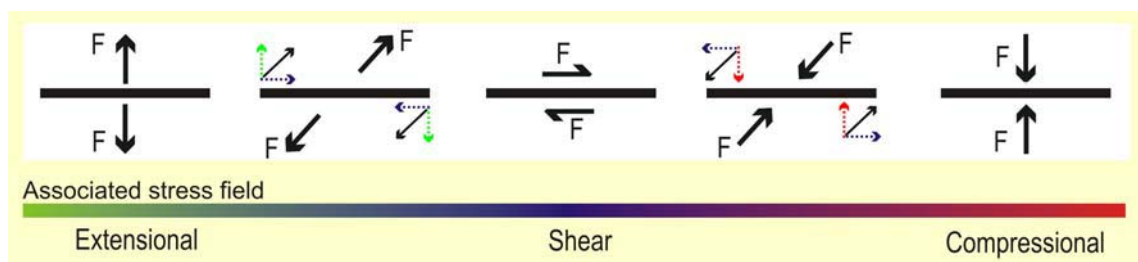


**Fig. 2.35:** Sketch of the different situations regarding at which angle a force acts on a surface and the associated stress field. The force may act perpendicular or parallel to the surface or oblique. In the latter case, the force can be expressed in terms of its normal component and its shear component.

There exist a close relationship between the type or condition of structures and the local stress field. Consequently, up to here, it has no sense to separate one from the other. However, in some cases, there exists an intersection between two structural families (e.g. Montefiascone – *Italy*, Nappi et al., 1991). Since some author (e.g. Nappi et al., 1991) assume that this phenomenon creates a favourable path for magma ascent and points of structural weakness, we consider necessary to classify the corresponding calderas in an additional *CATEGORY* : “Intersection of faults”. In most cases of fault intersection, we do not have enough information about the related stress field., It would be thus necessary to conduct more precise fieldwork on mechanical stress to study fault displacement, orientation and relative motion of the intersecting faults. However, structurally speaking, we consider fault intersection more important than the associated stress field and necessary the creation of the *CATEGORY* “Intersection of faults”. However, since information included in this *CATEGORY* is not related the stress field, the *CHARACTERISTIC* “Condition of the local structures” has to refer to the type of structures surrounding the caldera and not to the associated stress field.

The related *CHARACTERISTIC FIELD* is “Local\_tectonics” (RF, IF) and  $N_{ANA} = N = 229$ .

## ❖ PRE-CALDERA ACTIVITY

### ➤ Type of pre-caldera edifice

In order to understand the full caldera process it is necessary to characterize also pre-caldera volcanism. In this sense, we want to know if there exist a preferential type pre-caldera edifice(s) present in caldera-forming eruptions or not. Information regarding the type of pre-caldera edifice is recorded in the *FIELD* “Edifice”. An important problem when dealing with the information

recorded in this *FIELD* is that the bibliography proposes a too extensive number of edifice types that would complicate the statistical analysis. Therefore, we have reclassified them into six main *CATEGORIES*:

1. Volcanic edifice (various): Cones, basaltic volcanoes and simple volcanic edifices
2. Stratovolcanoes and stratocones
3. Shield volcanoes
4. Lava flows and domes
5. No previous edifices, calderas or caldera clusters
6. Other structures not included in the other five groups like pyroclastic plateaus,...

Moreover, calderas with unknown type of pre-caldera edifice are assigned to the *CATEGORY* “?”. Information regarding this reclassification is recorded in the *CLASSIFICATION field* “EdificeCLAS” with a total of 165 calderas to be analysed ( $N_{ANA} = 165$ ). We can see that the *CHARACTERISTIC* “Type of pre-caldera edifice” fulfils the entire requisite: a number of calderas with information enough high, and objectivity and comparability of data.

#### ➤ **Type of collapse precursor**

Since caldera collapse triggers are still controversial we consider that the type of collapse precursor has to be consider as *CHARACTERISTIC* and consequently, incorporated into the field data analysis. All the information concerning caldera collapse triggers observed in the *FIELD* is recorded in the *FIELD* “Collapse\_precursor” with a total of 83 calderas with information ( $N = 83$ ). In order to simplify the recorded information we classify it in the following *CATEGORIES*:

1. Previous volcanic eruptions: Basaltic eruptions, Plinian eruptions, etc.
2. No previous volcanic eruption or ring fractures trigger the volcanic event
3. Other eruption triggers like interaction of regional fractures with the magma chamber or interaction of magma with water

Similar to other *CHARACTERISTICS* we include also the *CATEGORY* “?” for those calderas with unknown collapse precursor. Moreover, the *CLASSIFICATION field* “PrecursorCLAS” ( $N_{ANA} = 72$ ), fulfils the entire requisite, an enough high number of calderas with information and objectivity and comparability of the results.

## ❖ POST-CALDERA ACTIVITY

### ➤ Type of post-caldera volcanic activity

We mentioned in section II.3.6 that Walker (1984) intended to investigate the distribution of post-caldera vents as a possible indicator of caldera origin. The author made an attempt to categorize the vent distribution in some calderas. Now, we consider necessary to compare the information contained in the CCDB with that of Walker (1984). Consequently, we define the next *CHARACTERISTIC* as “Type of post-caldera volcanic activity”. The corresponding information is recorded in the *FIELD* “Postcaldera\_activity” (**N** = 99). Initially, we tried to maintain the same classification than Walker (1984), but finally, we have added four further types of post-caldera volcanic activity. This allows us a more accurate description in those cases in which activity is more complex. Therefore, we propose the following *CATEGORIES* for the *CHARACTERISTIC* “Type of post-caldera volcanic activity”:

1. Type-C : A single vent occupies a central or near-central position.
2. Type-L : Vents are distributed in a clearly defined straight line or linear zone.
3. Type-M : A single vent occurs at or near the caldera margins.
4. Type-R : Vents occur along an arcuate line paralleling the caldera margin.
5. Type-S : Vents are scattered widely within the caldera.
6. Type-CaR : Central vent and multiple vents located at the caldera margins
7. Type-CC: Caldera collapse
8. Type-Ms: Multiple vents at or near the caldera margins
9. Type-Rs: Vents controlled by regional structures

The first five *CATEGORIES* correspond to the classification of Walker (1984), the other four are the new ones created for this work. Since we accept the options of the *FIELD* “Postcaldera\_activity” as the *CATEGORIES*, we do not generate a *CLASSIFICATION FIELD* and **N** = **N<sub>ANA</sub>** = 99.

### II.5.5 Construction of the “*CCDB DATA TABLE*”

To summarize and correlate all the information recorded in the *CCDB* we elaborate a table called “*CCDB DATA TABLE*”. The main steps for its construction are:

- **Definition of the *CCDB DATA TABLE* architecture**
- **Definition of the *CCDB DATA TABLE* content**
- **Treatment of the *CCDB DATA TABLE* content**
- **Analysing the *CCDB DATA TABLE* content**

#### ❖ **DEFINITION OF THE *CCDB DATA TABLE* STRUCTURE**

The table is composed by main columns, secondary columns, main rows, secondary rows, sectors, diagonal sectors and squares (Fig. 2.36). The headings of both main columns and main rows correspond to the name of the analysed *CHARACTERISTICS*. By contrast, headings of both secondary columns and secondary rows correspond to the name of the studied *CATEGORIES*. In short, each main column or row contains the information about one *CHARACTERISTICS* and each secondary column or row records the information about one specific *CATEGORY*.

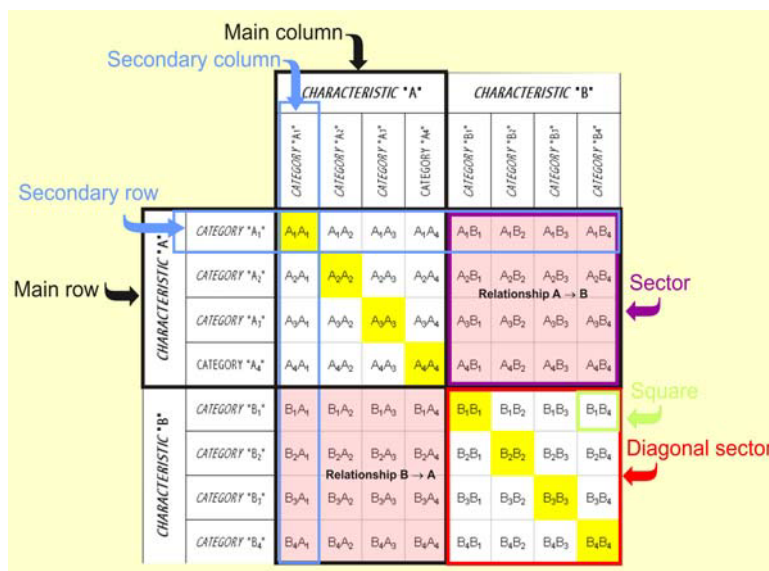


**Fig. 2.36:** Sketch of the *CCDB DATA TABLE* structure. Main components of the table are specially marked: main column, secondary column, main row, secondary row, sector, diagonal sector and square. As represented in the figure, the headings of both main columns and main rows correspond to the name of the analysed *CHARACTERISTICS*. By contrast, headings of both secondary columns and secondary rows correspond to the name of the corresponding *CATEGORIES*. From the sketch represented in this figure, it is evident that the *CCDB DATA TABLE* is diagonal symmetric.

The intersection of a main column and a main row results defines a sector. If both refer to the same *CHARACTERISTIC*, the sector is redefined as “diagonal sector” (Fig. 2.36). The ultimate components of the *CCDB DATA TABLE* are the “squares” (Fig. 2.36). The number of squares per sector depends on the number of *CATEGORIES* (secondary rows or columns) included in each *CHARACTERISTIC* (main rows or columns). A sector defined by the intersection of two different *CHARACTERISTICS* with x and y *CATEGORIES*, respectively, has a total number squares equal to  $x \times y$ .

Finally, considering all the *CHARACTERISTICS* listed in Table 2.1 we analyse 13 different *CHARACTERISTICS*, i.e. the table is composed by 13 main rows and columns (Fig. 2.37). Moreover, counting all the *CATEGORIES* included in the different *CHARACTERISTICS* the number of secondary columns and rows amounts to 98. We can observe the structure represented in figure 2.36 and the resulting table in figure 2.37, the *CCDB DATA TABLE* is diagonal symmetric.

**Fig. 2.37:** Structure of the *CCDB DATA TABLE*. In different colours are marked the main rows and columns corresponding to the analysed *CHARACTERISTICS*.

## ❖ DEFINITION OF THE *CCDB DATA TABLE* CONTENT

Once defined the structure we fill the *CCDB DATA TABLE* with the corresponding information. We fill the table sector by sector, and in more detail, square by square. Since diagonal sectors are the result of the intersection between two main columns of the same *CHARACTERISTIC*, included information is restricted to this *CHARACTERISTIC*. Moreover, data contained in the rest of the sectors gives information on the existing relationship between two different *CHARACTERISTICS*.

Squares are filled in with numbers or patterns. Since diagonal sectors are defined as the intersection of a main column and row referring to the same *CHARACTERISTIC* “A”, they have information only in the squares located in the diagonal of the table (Fig. 2.36, squares  $A_1A_1$ ,  $A_2A_2$ ,  $A_3A_3$  and  $A_4A_4$ ). Each of the numbers in the squares of the diagonal sectors are referred as **CS (Calderas)** and indicate how many calderas included in the CCDB are in the different *CATEGORIES* “A<sub>1</sub>”, “A<sub>2</sub>”, “A<sub>3</sub>” or “A<sub>4</sub>” of the referred *CHARACTERISTIC* “A”. Additionally, the sum of the values contained in these squares corresponds to the total number of calderas included in the database:  $A_1A_1 + A_2A_2 + A_3A_3 + A_4A_4 = 283$ . Consequently, the analysis of the diagonal sectors informs us about distribution of the calderas in the *CATEGORIES* of the individual *CHARACTERISTICS*. However, to get information about how calderas are distributed according to the relationship between two different *CHARACTERISTICS* we have to complete the rest of the table.

In the other sectors, defined as the intersection of a main column and row referring to two *CHARACTERISTICS* “A” and “B”, the numbers in the squares show a certain relationship between the *CATEGORIES* of both *CHARACTERISTICS*. From figure 2.30 we can see that this relationship can be from “A” to “B” (i.e. the main row corresponds to the *CHARACTERISTICS* “A” and the main column to the *CHARACTERISTICS* “B”) or from “B” to “A” (i.e. the main row corresponds to the *CHARACTERISTICS* “B” and the main column to the *CHARACTERISTICS* “A”). We will see later that both relationships may be important when interpreting the table.

In order to fill in each square of the table, we perform a series of queries in the database. For example, if we want to know how many calderas are in the *CATEGORY* “A<sub>1</sub>” of the *CHARACTERISTICS* “A” and also in the *CATEGORY* “B<sub>1</sub>” of the *CHARACTERISTICS* “B” we will perform a combined query using the information of the *FIELDS*. figure 2.38 shows an example of the required query to find the number of calderas in the *CATEGORY* “ $D_{CIR} < 5$  km” of the *CHARACTERISTIC* “Dimensions” and at the same time in the *CATEGORY* “< 5 ka” of the *CHARACTERISTIC* “Age”. As we can see in figure 2.38 the result of the query is 14. The obtained number is introduced in the corresponding square of the *CCDB DATA TABLE* (Fig. 2.39).

Thus, the relationship *CHARACTERISTIC* “A” to *CHARACTERISTIC* “B” (Fig. 2.30), indicates how are distributed in the *CATEGORIES CHARACTERISTIC* “B” those calderas included in each of the *CATEGORIES* of “A”.

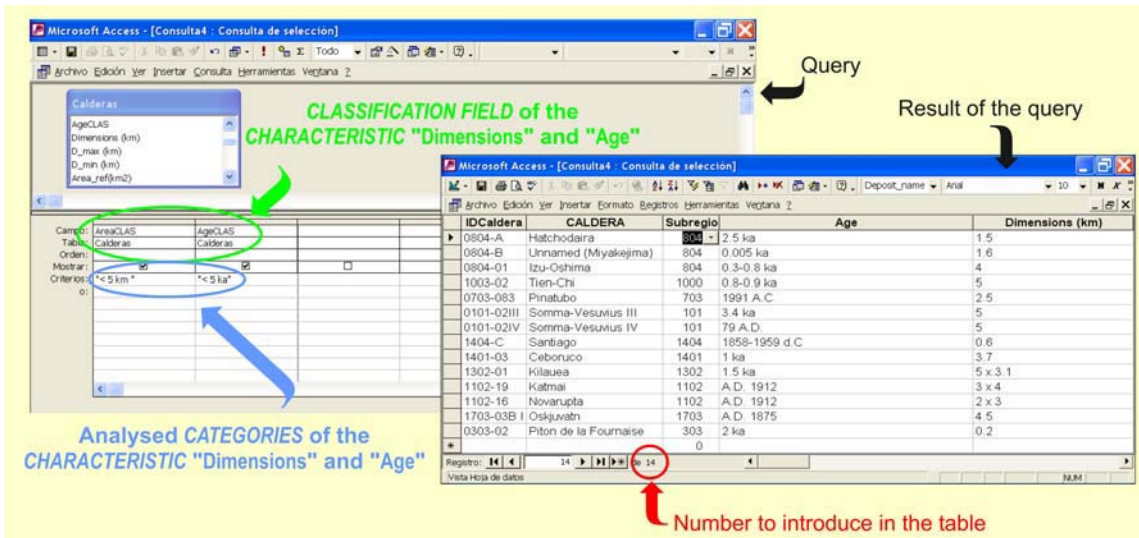


Fig. 2.38: Example of one of the queries necessary to obtain the numbers for the CCDB DATA TABLE.

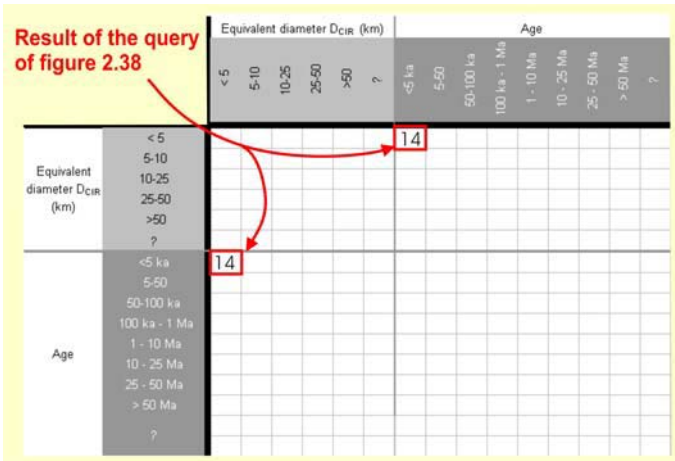


Fig. 2.39: Performing the query of figure 2.28, the obtained result is introduced in corresponding squares of the CCDB DATA BASE. Since the table is symmetric we have to introduce the value twice. One in the sector defined as the intersection of the CHARACTERISTIC "Dimensions" as row and the CHARACTERISTIC "Age" as column and a second value in the sector defined by the intersection of the CHARACTERISTIC "Age" as row and the CHARACTERISTIC as column "Dimensions".

We repeat this process for each square until the entire table is completed (Fig. 2.40)



Fig. 2.40: Image of the CCDB DATA TABLE with the information obtained from the queries performed in the database. In different colours are marked the main rows and columns corresponding to the analysed CHARACTERISTICS.

## ❖ TREATMENT OF THE *CCDB DATA TABLE* CONTENT

In order to extract easily and systematically the information of the *CCDB DATA TABLE*, we have decided to normalize the data according to the following methodology.

The method is based on the study of the results by *CATEGORIES* and rows. We examine the values in the following type of sets  $A_1B_1 - A_1B_4$ ,  $A_1C_1 - A_1C_4$ ,  $B_1A_1 - B_1A_4$ , etc. (Fig. 2.36). We analyse how the calderas in a specific *CATEGORY* “A<sub>1</sub>”, “B<sub>1</sub>”, etc., are distributed in the different *CATEGORIES* “B<sub>1</sub>” – “B<sub>4</sub>”, “C<sub>1</sub>” – “C<sub>4</sub>”, etc., of the other *CHARACTERISTICS*. We will see that although applying the method only to rows, due to the table symmetry no information gets lost. Figure 2.41 describes and illustrates the steps followed in the analysis of the *CCDB DATA TABLE*.

Firstly, we shade in grey those squares which correspond to calderas with unknown or undefined information, i.e. those included in the *CATEGORIES* “?” in the different *CHARACTERISTICS*. In the next step, we chose the maximum values inside each of the groups **MVR** (Maximum value of the row in one specific *CHARACTERISTICS*) (Fig. 2.41). Once defined the maximum value we establish four intervals which will be designed as “Low”, “Low-Medium”, “Medium-High” and “High”. A colour “yellow”, “green”, “orange” and “red” is assigned to each interval, respectively. The limits of these intervals are established as indicated in Figure 2.41. We take the maximum value (**MVR**) and divide it by four, this giving us the upper limit of the “Low” interval and the lower limit of the “Low-Medium” interval. Evidently, the lower limit of the “Low” interval is “0”. The upper limit of the “Low-Medium” interval and the lower limit of the “Medium-High” interval is the **MVR** divided by 2. Finally, the upper limit of the “Medium-High” as well as the lower limit of the “High” interval is the **MVR** multiply by  $\frac{3}{4}$ . In fact, this process is a normalization per rows considering four intervals of values. We repeat this process until all the squares with a number are tinted. Those without calderas marked with a dash remain in white colour. In the case of the values located in the diagonal, the normalization is performed diagonally. Once the table is coloured (Fig. 2.42) we proceed with the field data analysis.

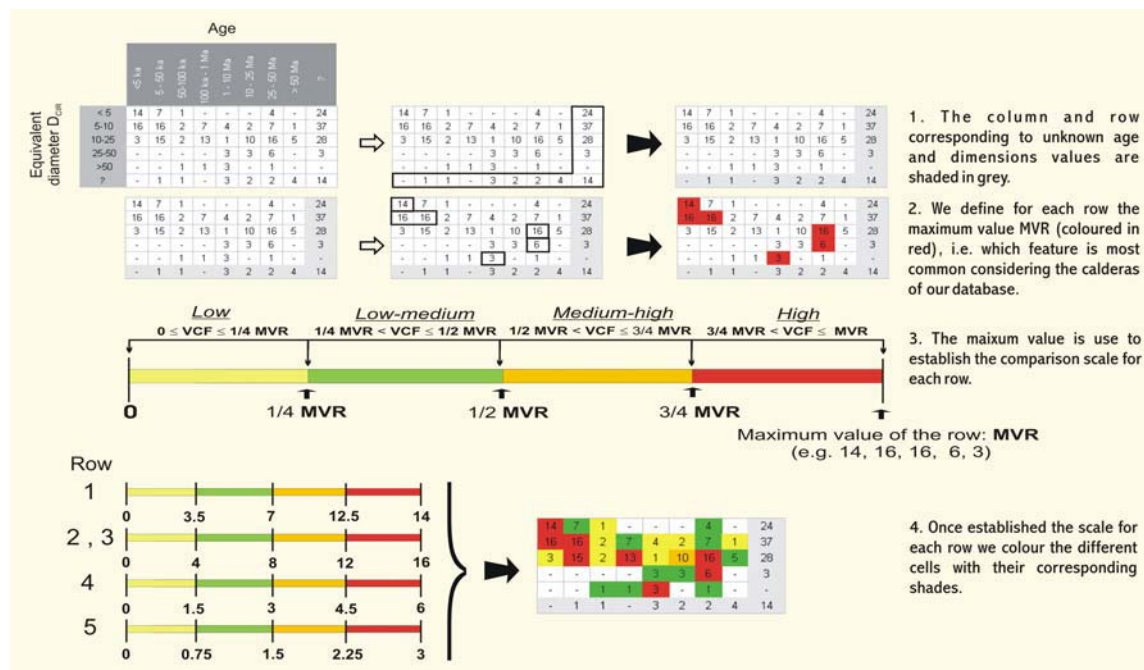


**Fig. 2.41:** Descriptions and illustrations of the different steps necessary to perform the *MAXIMUM NORMALIZATION* in order to analyse the information of the *CCDB DATA TABLE*. **MVR** Maximum value of the row in each sector.

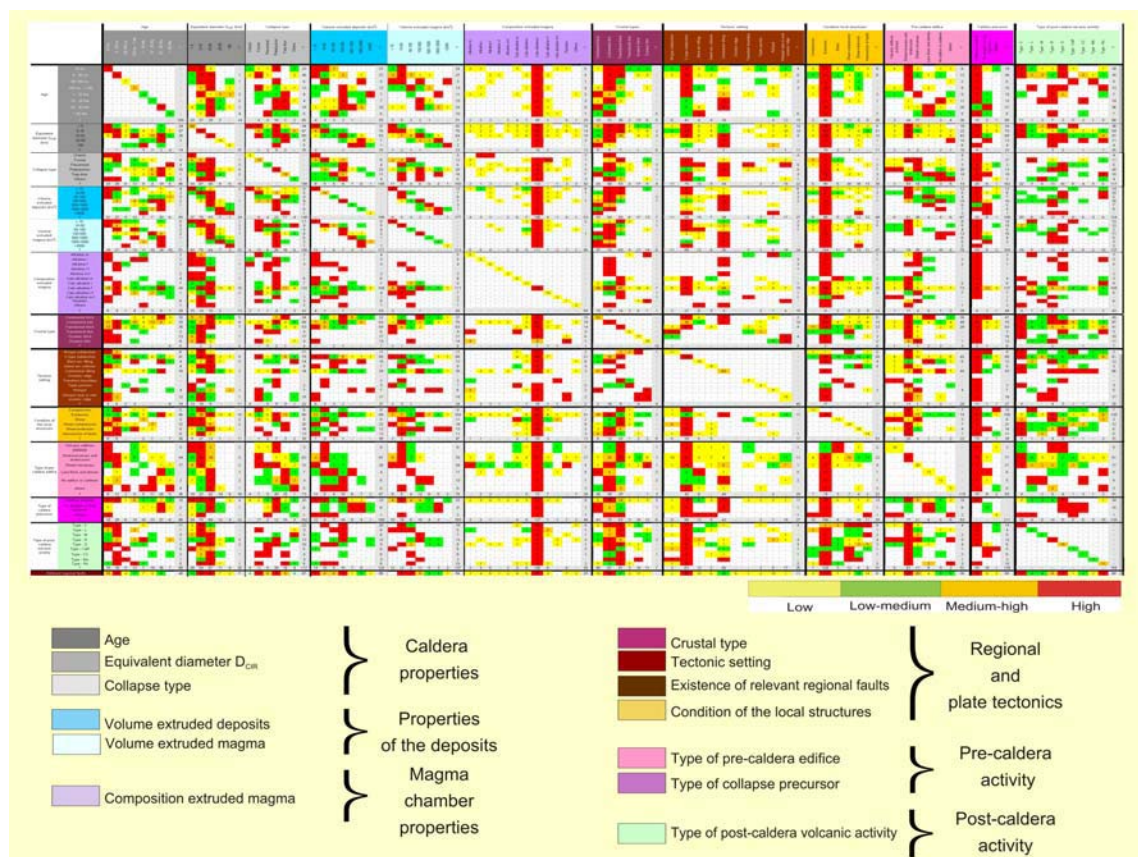


**Fig. 2.42:** Image of the *CCDB DATA TABLE* once coloured. Different colours at the heading of the main rows and columns indicate different *CHARACTERISTICS*. Yellow, green, orange and red colours of the squares correspond to the intervals assigned by the *MAXIMUM NORMALIZATION*. In Appendix IV is included an enlarged version of the coloured *CCDB DATA TABLE*.

## ❖ ANALYSING THE *CCDB DATA TABLE* CONTENT

Now it is evident why we need the table to be symmetric. The normalization per rows in a symmetric table provides us both relationships *CHARACTERISTICS* “A” to *CHARACTERISTICS* “B” and vice versa. In fact, this information can be equivalent or complementary. For example, if we look the boxes corresponding to the relationship “Dimensions” vs. “Age” (*CATEGORIES* of the *CHARACTERISTICS* “Dimensions” in rows and *CATEGORIES* of the *CHARACTERISTICS* “Age” in columns) the coloured pattern inform us about the age of the calderas located in the different *CATEGORIES* of the *CHARACTERISTIC* “Dimensions”. By contrast, the relationship “Age” vs. “Dimensions” (*CATEGORIES* of the *CHARACTERISTICS* “Age” in rows and *CATEGORIES* of the *CHARACTERISTIC* “Dimensions” in columns) give us the dimensions of those calderas located in the different *CATEGORIES* of the *CHARACTERISTICS* “Age”.

In the table of Figures 2.37, 2.40 and 2.42 the *CHARACTERISTIC* “World region”, in charge of the spatial distribution of calderas, is not included. We decided to maintain it apart from the main *CCDB DATA TABLE* and to generate a second table specially focused on the study of the spatial distribution. Consequently, the table of Figure 2.43 (*CATEGORIES* of the *CHARACTERISTIC* “World region” in columns and the other *CHARACTERISTICS* in rows) inform us about the spatial distribution of the different *CATEGORIES* belonging to the other *CHARACTERISTICS*. By contrast, the table of Figure 2.44 (*CATEGORIES* of the *CHARACTERISTIC* “World region” in rows and the other *CHARACTERISTICS* in columns), informs us about the different *CATEGORIES* belonging to the other *CHARACTERISTICS* in each world region.

Once generated the main *CCDB DATA TABLE* and those referring to the spatial distribution, we proceed with the analysis and summary of the results obtained.

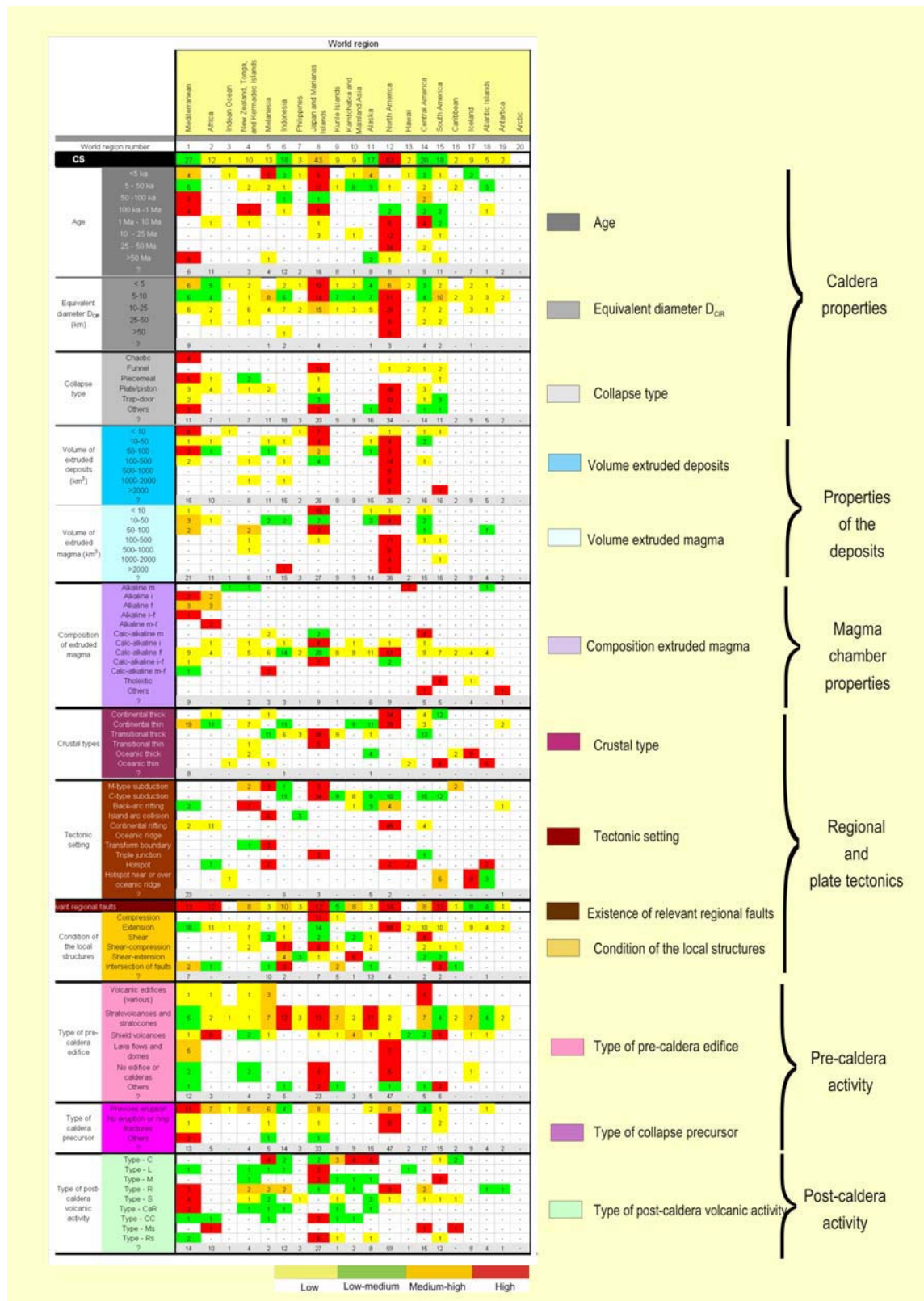


**Fig. 2.43:** Image of the *CCDB DATA TABLE* special for the *CHARACTERISTIC* "World region". In this table we have the necessary information to study how the different *CHARACTERISTICS* are distributed over the world.

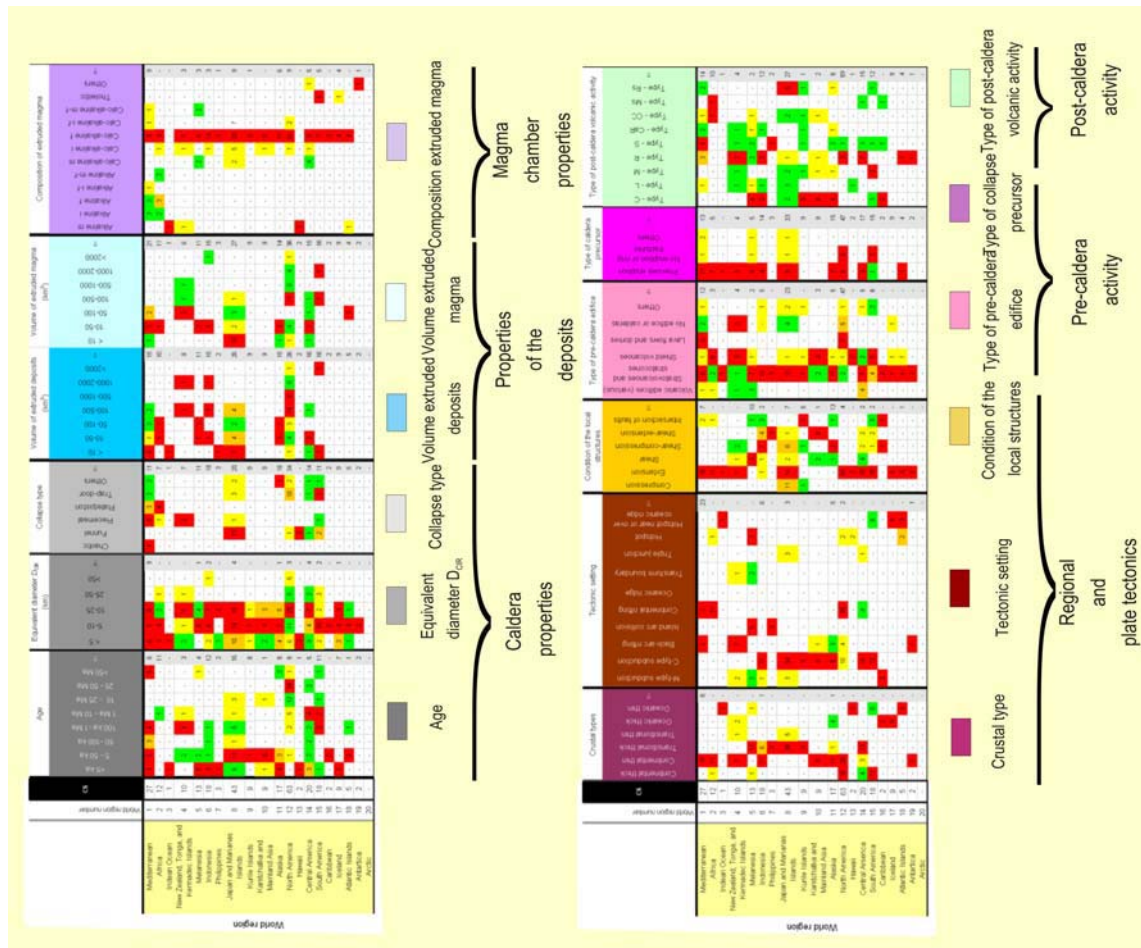


**Fig. 2.44:** Image of the *CCDB DATA TABLE* special for the *CHARACTERISTIC* “World region”. In this table we have the necessary information to study the different *CHARACTERISTICS* in the defined world regions.

## II.5.6 Results obtained with the *CCDB DATA TABLE*

### II.5.6.1 Results obtained for the individual *CHARACTERISTICS*

In this section, we proceed to analyse the results obtained individually for each *CHARACTERISTIC*. Results are represented as follows:

- **Histograms:** The most representative results obtained with the *CCDB DATA TABLE* are also represented with histograms. In the histograms we do not include those calderas in the *CATEGORY* “?”. The percentage of calderas in each of the *CATEGORIES* is calculated considering  $N_{ANA} = 100\%$ . Furthermore, in some cases we also add to the respective bars the number of calderas **CS** in the corresponding *CATEGORY*.
- **Sections of the *CCDB DATA TABLE*:** We assume that to deal with the whole “*CCDB DATA TABLE*” is not practical. Therefore, we represent again that section of the table we need for commenting the corresponding results.

### ❖ **CALDERA PROPERTIES**

- **World region**

Information recorded in the database show that calderas are worldwide distributed in areas of active volcanism or with past volcanic activity (Fig. 2.45).

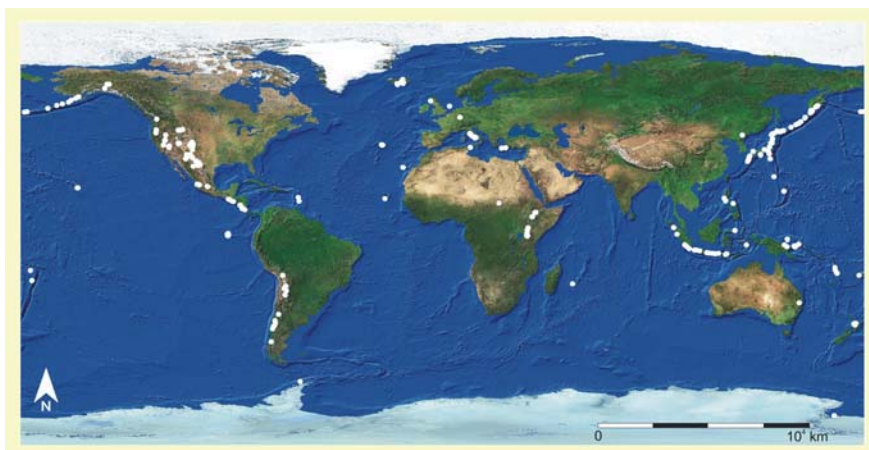


**Fig. 2.45:** World map with the location of the collapse calderas (white circle) included in the database.

In Figure 2.46 we plot the results for the classification of calderas according to the *CATEGORIES* commented in section II.5.4, i.e. world sections defined by Simkin et al. (1981) and afterwards modified by Newhall and Dzurisin (1988). Results may be summarized as follows:

- The geographical distribution of calderas has two important peaks in the Mariana trench (**CS = 43**) and the North America (**CS = 63**) regions, with 15.2 % and 22.3 %, respectively. The Mediterranean region is also characterized by a relatively high number of calderas (**CS = 27**), which comprises the 9.5 % of the total number of analysed calderas with world region information  $N_{ANA}$ .
- World areas such as Africa, Melanesia or Central and South America house a lower, but also considerable, percentage of calderas, namely, between the 7.1% and 3.2 % (**CS 17-20**). Extremely few examples of natural calderas are located in regions like the Indian Ocean (0.4%, **CS = 1**), the Caribbean (0.4 %, **CS = 1**) or Antarctica (0.7 %, **CS = 2**).

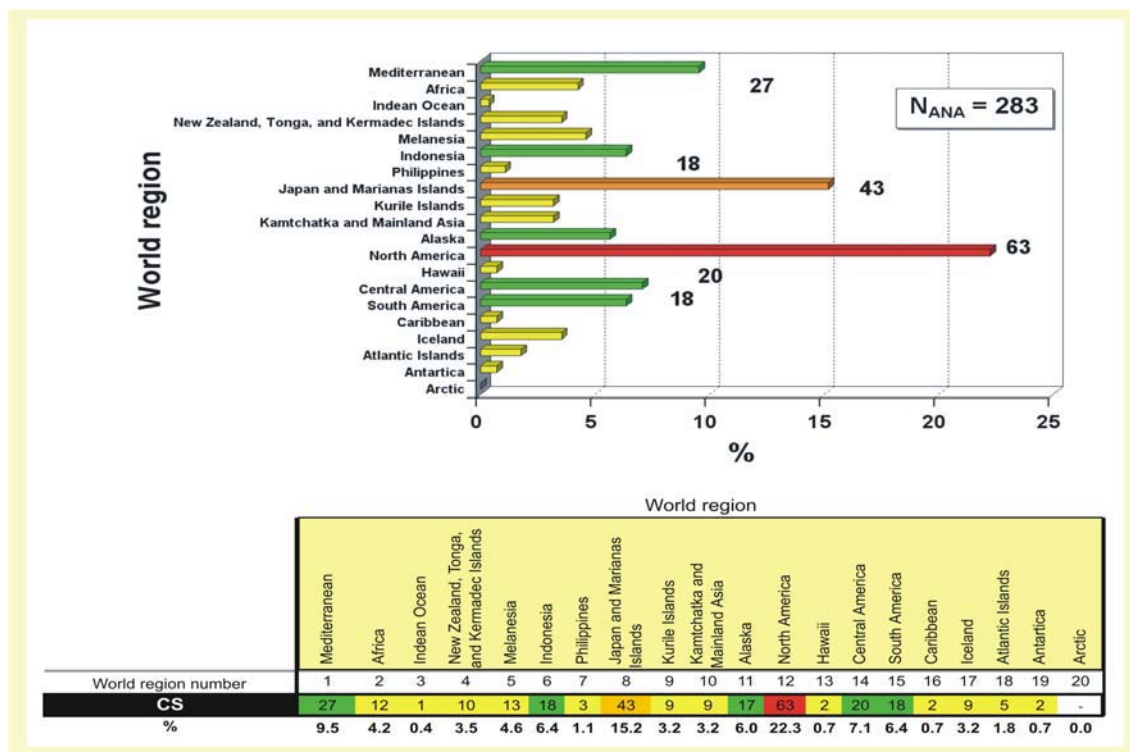


**Fig. 2.46:** Results for the worldwide distribution of the calderas included in the CCDB. Colours correspond to the “*MAXIMUM NORMALIZATION*”. **(Top)** Histogram showing the percentages of calderas located in the different *CATEGORIES* of the *CHARACTERISTIC* “World region”. Bold numbers at the right of the bars indicate the number of calderas included in the world region or *CATEGORY CS*.  $N_{ANA}$  at the left top corner indicates total number of calderas with information about the *CHARACTERISTIC* “World region”. Furthermore, the colours correspond to the “*MAXIMUM NORMALIZATION*” and are in agreement with those of the “*CCDB DATA TABLE*” section represented below. **(Bottom)** Section of the “*CCDB DATA TABLE*” represented in Figure 2.43. Here are represented the number of calderas included in each world region or *CATEGORY CS*.

## ➤ Age

Information recorded in the database about the age of collapse caldera shows that these structures occur during all geological periods. Figure 2.47 exposes the percentage of calderas comprised in the proposed *CATEGORIES*. We can observe that:

- Calderas are structures that cover a wide range of ages, from 0.005 ka (Miyakejima eruption in 2000, Geshi et al., 2002; Nakada et al., 2005) to 93.6 Ma (West Fork – *Alaska*, Bacon et al., 1990). There exist also Late Precambrian examples like Ramat Yotam caldera (548 Ma) (Eyal and Peltz, 1994).
- The age distribution has three peaks corresponding to the *CATEGORIES* “< 5 ka” (18.7%, CS = 33), “5 – 50 ka” (22%, CS = 39) and “25 – 50 Ma” (20.3%, CS = 36).

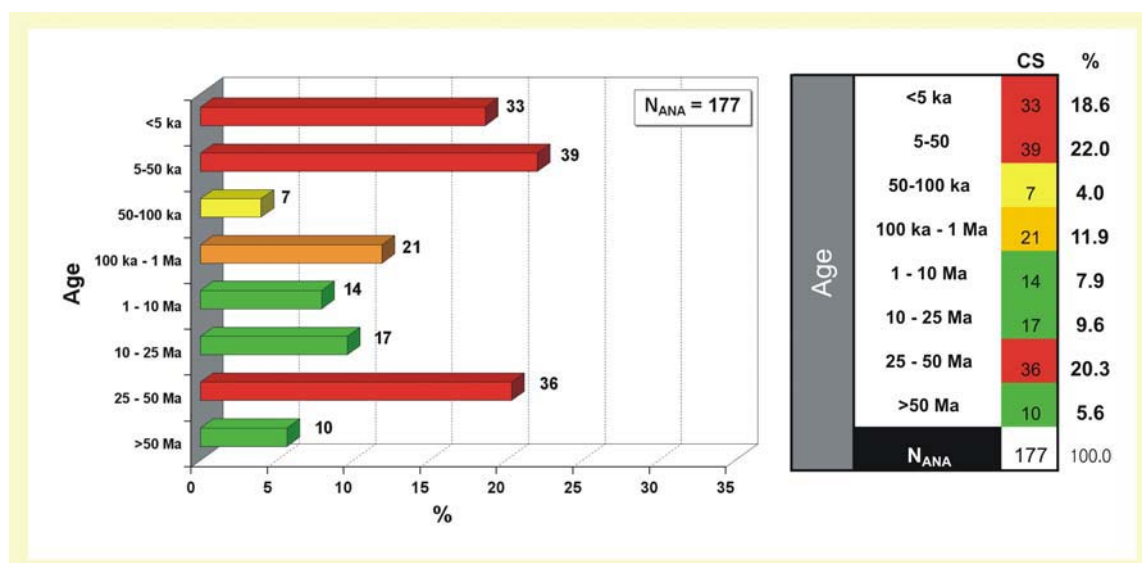


**Fig. 2.47:** Results for the age distribution of the calderas included in the CCDB. Colours correspond to the “*MAXIMUM NORMALIZATION*” (Left) Histogram showing the percentages of calderas located in the different *CATEGORIES* of the *CHARACTERISTIC* “Age”. Bold numbers at the right of the bars specify the number of calderas included in this age interval or *CATEGORY CS*. **N<sub>ANA</sub>** at the left top corner indicates total number of calderas with information about the *CHARACTERISTIC* “Age”. (Right) Representation of information included in the “*CCDB DATA TABLE*” of Figure 2.42. Here are represented the number of calderas included in each *CATEGORY CS*.

Comparison of the age of calderas with their location (Fig. 2.48):

- Calderas included in the *CATEGORY* “< 5 ka” do not have a preferential spatial location. These are, more or less, worldwide uniformly distributed with to moderate maximums at

the Melanesia and the Japan and the Marianas Islands. However, differences with other regions consist of one or two calderas.

- The distribution of calderas with an age comprised in the interval “5 – 50 ka” (**CS** = 39) has a moderate maximum in Japan and the Marianas Islands (28,2%, 11 samples).
- Calderas in the intervals “10 – 25 Ma” and “25 – 50 Ma” (**CS** = 17 and **CS** = 36, respectively) are principally localized in North America (70.6%, 12 samples and 94.4%, 34 samples, respectively).

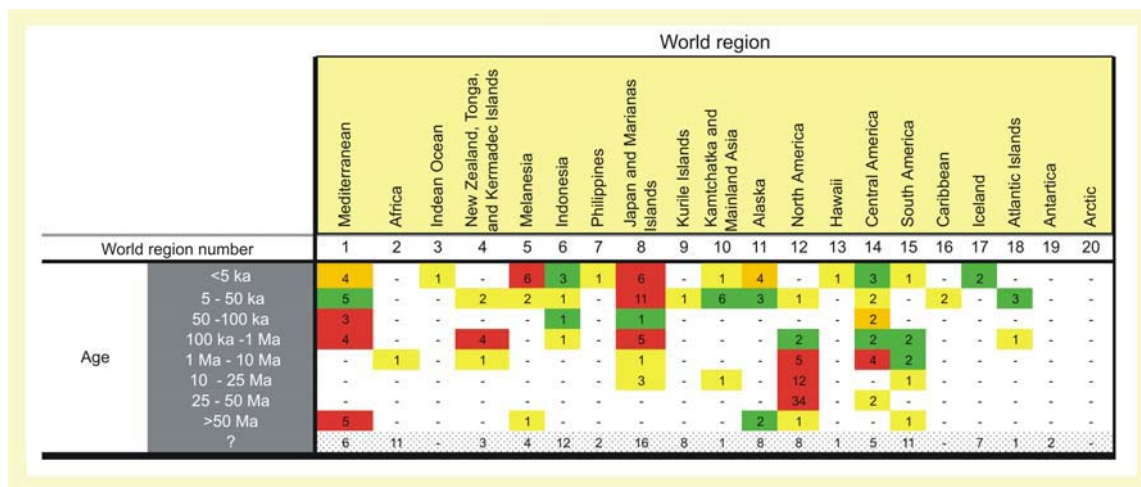


Fig. 2.48: Representation of information included in the “CCDB DATA TABLE” of figure 2.43 comprising the spatial distribution of calderas in each *CATEGORY* of the *CHARACTERISTIC* “Age”. The colours correspond to the “MAXIMUM NORMALIZATION”.

Now it would be interesting to find out the reason for these preferential spatial distributions. However, we have to wait till the end of the field data analysis in order to dispose of more information.

The *CHARACTERISTIC* “Age” may also provide information about the frequency of caldera-forming eruptions  $f_{CFE}$  during the last 50 Ma. Consequently, we assume that:

$$f_{CFE} = \mathbf{CS} / t_{INT} \tag{2.3}$$

where **CS** is the number of calderas comprised in each age interval or *CATEGORY* and  $t_{INT}$  is the time length in ka covered by each interval or *CATEGORY*. Results obtained are illustrated in Figure 2.49. We can observe that the frequency of caldera-forming eruptions increases exponentially to

the present days. Furthermore, calculated values indicate seven caldera-forming eruptions every thousand years during the last 5 ka.

Of course, this analysis is a simplification but clearly reflexes the “life” of collapse calderas as visible structures on the field and the restrictions when analysing geologic structures due to erosive and deformation processes, which avoid us to observe the complete geologic record.

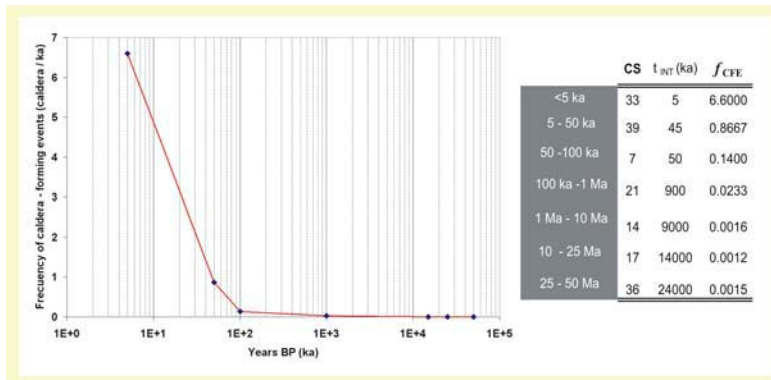


**Fig. 2.49:** Results obtained for the calculus of the frequency of caldera-forming eruptions  $f_{CFE}$  during the last 50 Ma. **CS** Number of calderas comprised in each age interval or *CATEGORY* ;  $t_{INT}$  Number of ka covered by the *CATEGORY*.

➤ **Dimensions (Caldera equivalent diameter  $D_{CIR}$ )**

Figure 2.50 illustrates all the information recorded in the CCDB regarding the *CHARACTERISTIC* “Dimensions”.

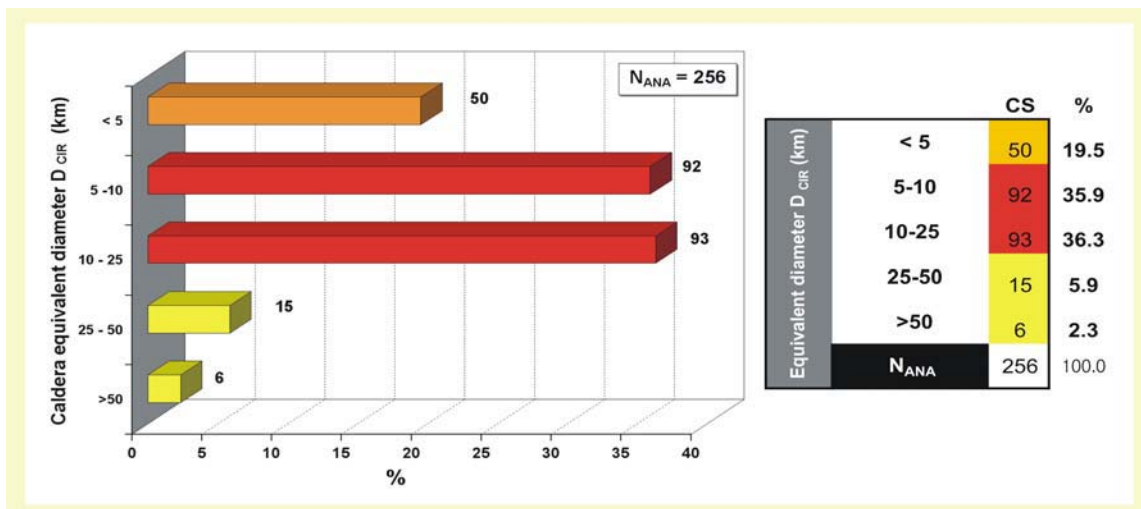


**Fig. 2.50:** Results for the dimensions distribution of the calderas included in the CCDB. Colours correspond to the “*MAXIMUM NORMALIZATION*”. **(Left)** Histogram showing the percentages of calderas located in the different *CATEGORIES* of the *CHARACTERISTIC* “Dimensions”. Bold numbers at the right of the bars specify the number of calderas included in this *CATEGORY* **CS**.  $N_{ANA}$  at the left top corner indicates total number of calderas with information about the *CHARACTERISTIC* “Dimensions”. **(Right)** Representation of information included in the “*CCDB DATA TABLE*” of Figure 2.42. Here are represented the number of calderas included in each *CATEGORY* **CS**.

- Calderas vary widely in size, from 0.03 km<sup>2</sup> (Piton de la Fournaise – *Reunion Island*, Hirn et al., 1991) to 4712 km<sup>2</sup> (Blacktail – *U.S.A*, Morgan et al., 1984) corresponding to a  $D_{CIR}$  of 0.2 km and 77.46 km respectively.
- The 91.8 % of the samples (i.e. 235 calderas) have a  $D_{CIR} < 25$  km. The remaining calderas included in the *CATEGORIES* “ $D_{CIR} 25 - 50$  km” (5.9%, **CS** = 15) and “ $D_{CIR} > 50$  km” (2.3%, **CS** = 6) comprise a 8.2 % (21 samples).

Evidently, we consider of special interest for the understanding of collapse mechanisms to study the spatial distribution of calderas according to their dimensions. Results obtained are represented in Figure 2.51.

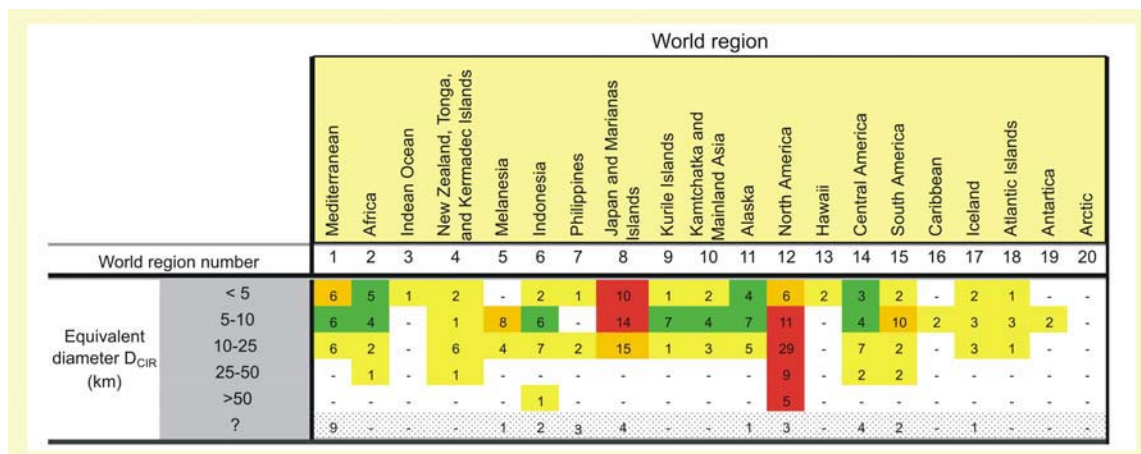


**Fig. 2.51:** Representation of information included in the “*CCDB DATA TABLE*” of figure 2.43 comprising the spatial distribution of calderas in each *CATEGORY* of the *CHARACTERISTIC* “Dimensions”. The colours correspond to the “*MAXIMUM NORMALIZATION*”.

The main results are:

- Calderas with a  $D_{CIR} < 5$  km (**CS** = 50) are worldwide distributed with a moderate maximum at Japan and the Marianas Islands (20%, 10 samples).
- Calderas with a  $D_{CIR}$  included in the *CATEGORY* “5 – 10 ka” (**CS** = 92) are also worldwide distributed but with two moderate maximums at Japan and the Marianas Islands (15.2%, 14 samples) and the region of North America (12%, 11 samples).

- Calderas with a  $D_{CIR}$  between 10 and 25 km (**CS** = 93) are worldwide distributed with a moderate maximum corresponding to the region of North America (31.2%, 29 samples).
- From the calderas with a  $D_{CIR} > 25$ , a 66.7 % (14 samples) is located in North America and the rest is distributed with a 9.5 % along Central and South America and with a 4.8 % in Africa, New Zealand, Tonga and Kermadec Islands, and Indonesia.

### ➤ Collapse type

In Figure 2.52 we represent the distribution of the different collapse types for those calderas with information.

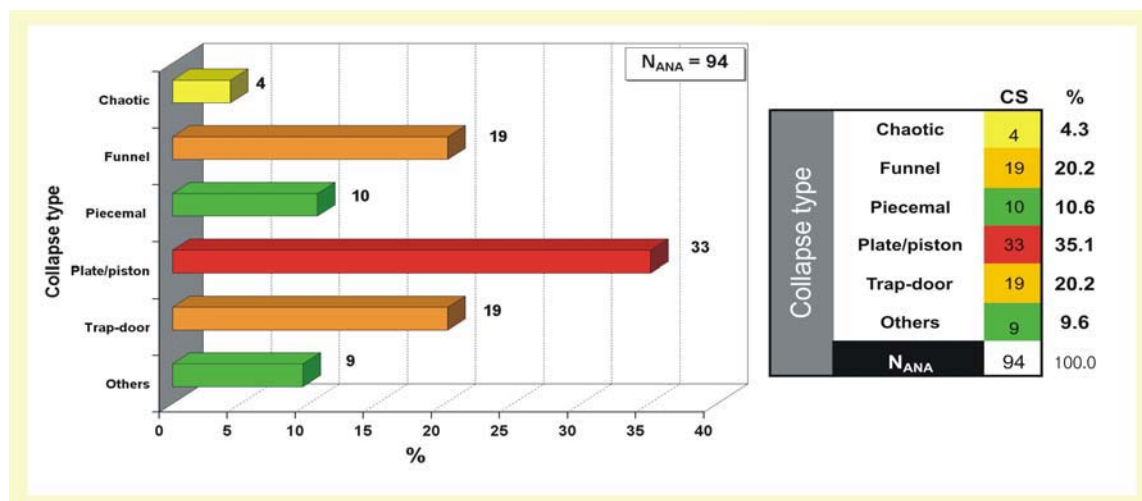


**Fig. 2.52:** Results for the distribution of collapse types of the calderas included in the CCDB. Colours correspond to the "MAXIMUM NORMALIZATION". (Left) Histogram with the percentages of calderas located in the different CATEGORIES of the CHARACTERISTIC "Collapse type". Bold numbers at the right of the bars specify the number of calderas included in this CATEGORY CS.  $N_{ANA}$  at the left top corner indicates total number of calderas with information about the CHARACTERISTIC "Collapse type". (Right) Representation of information included in the "CCDB DATA TABLE" of Figure 2.42. Here are represented the number of calderas included in each CATEGORY CS.

The main results are:

- It exist a maximum at the CATEGORY "Plate/piston" with a 35 %, equivalent to 33 calderas. Furthermore, also funnel and trap-door collapse calderas are also quite frequent (20.2%, **CS** =19 in each CATEGORY "Funnel" and "Trap-door").
- It exist a minimum at the CATEGORY "Chaotic" (4.3%, **CS** = 4)

Now, we are interested in studying the spatial distribution of the calderas according to the *CHARACTERISTIC* “Collapse type”. The most remarkable results are (Fig. 2.53):

- A 68.4 % (13 samples) of the calderas included in the *CATEGORY* “Funnel” are located in Japan and the Marianas Islands.
- In North America are located a 48.5 % (16 samples) and a 52.6 % (10 samples) of the calderas comprised in the *CATEGORIES* “Plate/Piston” or “Trap-door”, respectively.

We will revise the possible reasons for this preferential distribution once finished the CCDB data analysis and when all the results will be available.

		World region																			
		Mediterranean	Africa	Indian Ocean	New Zealand, Tonga, and Kermadec Islands	Melanesia	Indonesia	Philippines	Japan and Marianas Islands	Kurile Islands	Kamchatka and Mainland Asia	Alaska	North America	Hawaii	Central America	South America	Caribbean	Iceland	Atlantic Islands	Antarctica	Arctic
World region number		1	2	3	4	5	6	7	8	9	10	11	12	13	14	15	16	17	18	19	20
Collapse type	Chaotic	4	-	-	-	-	-	-	-	-	-	-	-	-	-	-	-	-	-	-	-
	Funnel	-	-	-	-	-	-	-	13	-	-	-	1	2	1	2	-	-	-	-	-
	Piecemeal	5	1	-	2	-	-	-	1	-	-	-	-	-	-	-	1	-	-	-	-
	Plate/piston	3	4	-	1	2	-	-	4	-	-	-	16	-	3	-	-	-	-	-	-
	Trap-door	2	-	-	-	-	-	-	3	-	-	-	10	-	1	3	-	-	-	-	-
	Others	2	-	-	-	-	-	-	2	-	-	1	2	-	1	1	-	-	-	-	-
?		11	7	1	7	11	18	3	20	9	9	16	34	-	14	11	2	9	5	2	-

**Fig. 2.53:** Representation of information included in the “CCDB DATA TABLE” of figure 2.43 comprising the spatial distribution of calderas in each *CATEGORY* of the *CHARACTERISTIC* “Collapse type”. The colours correspond to the “MAXIMUM NORMALIZATION”.

❖ **DEPOSITS PROPERTIES**

➤ **Volume of extruded deposits and magma**

In this section, we analyse the information provided by the database in connection with the amount of deposits or magma extruded during the caldera-forming event. Results obtained are illustrated in Figures 2.54 and 2.55. In short:

- Both histograms are very similar. The most abundant events are those included in the *CATEGORY* “100 -500 km<sup>3</sup>” and also those involving less than 50 km<sup>3</sup> of magma or deposits.
  
- Caldera-forming events involving more than 2000 km<sup>3</sup> (deposits or magma) are scarce and rare. The database includes only four samples: La Pacana and Yellowstone with a volume of extruded deposits over 2000 km<sup>3</sup> and La Garita and Toba in which more than 2000 km<sup>3</sup> of magma was extruded during the caldera-forming event.

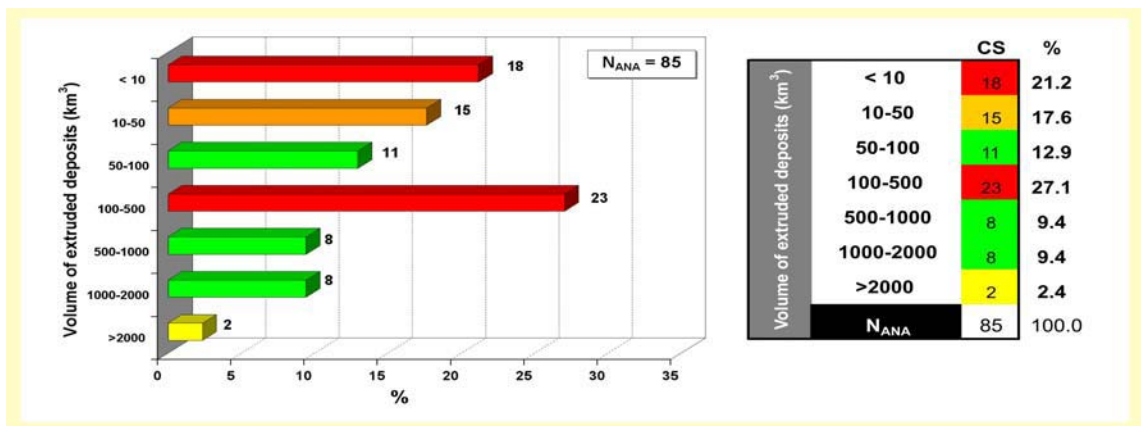


**Fig. 2.54:** Results for the analysis of the volume of extruded deposits of calderas included in the CCDB. Colours correspond to the “*MAXIMUM NORMALIZATION*”. (Left) Histogram with the percentages of calderas located in the *CATEGORIES* of the *CHARACTERISTIC* “Volume of extruded deposits”. Bold numbers at the right of the bars specify the number of calderas included in this volume interval or *CATEGORY CS*. **N<sub>ANA</sub>** at the left top corner indicates total number of calderas with information about the *CHARACTERISTIC* “Volume of extruded deposits”. (Right) Representation of information included in the “*CCDB DATA TABLE*” of Figure 2.42. Here are represented the number of calderas included in each *CATEGORY CS*.

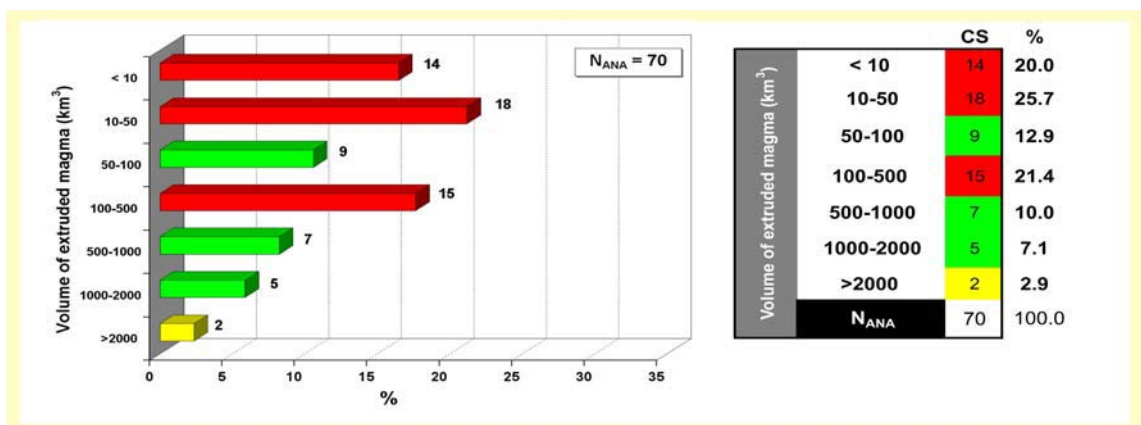


**Fig. 2.55:** Results for the analysis of the volume of extruded magma of calderas included in the CCDB. Colours correspond to the “*MAXIMUM NORMALIZATION*” (Left) Histogram showing the percentages of calderas located in the different *CATEGORIES* of the *CHARACTERISTIC* “Volume of extruded magma”. Bold numbers at the right of the bars specify the number of calderas included in this volume interval or *CATEGORY CS*. **N<sub>ANA</sub>** at the left top corner indicates total number of calderas with information about the *CHARACTERISTIC* “Volume of extruded magma”. (Right) Representation of information included in the “*CCDB DATA TABLE*” of Figure 2.42. Here are represented the number of calderas included in each *CATEGORY CS*.

The *CCDB DATA TABLE* represented in figure 2.56 provides answers to the question as to whether there is any relationship between the volume of the extruded material (both deposits or magma) and the geographical setting.

		World region																			
		Mediterranean	Africa	Indian Ocean	New Zealand, Tonga, and Kermadec Islands	Melanesia	Indonesia	Philippines	Japan and Marianas Islands	Kurile Islands	Kamchatka and Mainland Asia	Alaska	North America	Hawaii	Central America	South America	Caribbean	Iceland	Atlantic Islands	Antarctica	Arctic
World region number		1	2	3	4	5	6	7	8	9	10	11	12	13	14	15	16	17	18	19	20
Volume of extruded deposits (km <sup>3</sup> )	< 10	6	-	1	-	-	-	1	7	-	-	-	1	-	1	1	-	-	-	-	-
	10-50	1	1	-	-	1	1	-	4	-	-	1	4	-	2	-	-	-	-	-	-
	50-100	3	1	-	-	1	-	-	2	-	-	1	3	-	-	-	-	-	-	-	-
	100-500	2	-	-	1	-	1	-	4	-	-	-	14	-	1	-	-	-	-	-	-
	500-1000	-	-	-	-	-	1	-	-	-	-	-	8	-	-	-	-	-	-	-	-
	1000-2000	-	-	-	1	-	-	-	-	-	-	-	6	-	-	-	-	-	-	-	-
>2000	-	-	-	-	-	-	-	-	-	-	-	1	-	-	-	3	-	-	-	-	-
?		25	12	1	8	13	18	2	45	9	9	15	66	2	20	18	2	9	5	2	8
Volume of extruded magma (km <sup>3</sup> )	< 10	1	-	-	-	-	-	-	10	-	-	1	1	-	1	-	-	-	-	-	-
	10-50	3	1	-	-	2	2	-	2	-	-	2	4	-	2	-	-	-	-	-	-
	50-100	2	-	-	2	-	-	-	3	-	-	-	-	-	1	-	-	-	1	-	-
	100-500	-	-	-	1	-	-	-	1	-	-	-	-	-	1	1	-	-	-	-	-
	500-1000	-	-	-	-	-	-	-	-	-	-	-	11	-	-	-	-	-	-	-	-
	1000-2000	-	-	-	-	-	-	-	-	-	-	-	6	-	-	-	-	-	-	-	-
>2000	-	-	-	-	-	3	-	-	-	-	-	4	-	-	1	-	-	-	-	-	-
>2000	-	-	-	-	-	-	-	-	-	-	-	1	-	-	-	-	-	-	-	-	-
?		21	11	1	6	11	15	3	27	9	9	14	36	2	15	16	2	9	4	2	-

Fig. 2.56: Representation of information included in the “CCDB DATA TABLE” of figure 2.43 comprising the spatial distribution of calderas in each *CATEGORY*. The colours correspond to the “MAXIMUM NORMALIZATION”.

Based on the information included in Figure 2.56 we can conclude that:

- Calderas related to extruded volumes (deposits or magma) smaller than 10 km<sup>3</sup> (CS = 32) are found mainly in Japan and the Marianas Islands (53.1%, 17 samples) and the Mediterranean (18.8 % , 6 samples).
- Calderas with an extruded volume between 100 km<sup>3</sup> and 500 km<sup>3</sup> (CS = 38) are mostly located in North America (65.8%, 25 samples).
- Out of 32 samples of voluminous caldera-forming events (more than 500 km<sup>3</sup> of extruded material), 81.25 % (26 samples) are located in North America, and an additional 6.25 % in South America, Indonesia and New Zealand, Tonga, and Kermadec Islands.

Similar to the caldera dimension criterion, the region of North America hosts almost all calderas involving extruded volumes of more than 500 km<sup>3</sup>. I will further focus on this interesting observation at the end of the field data analysis..

## ❖ MAGMA CHAMBER PROPERTIES

### ➤ Composition of extruded magma

Figure 2.57 illustrates all available information regarding the composition of the extruded magma during the caldera-forming event.

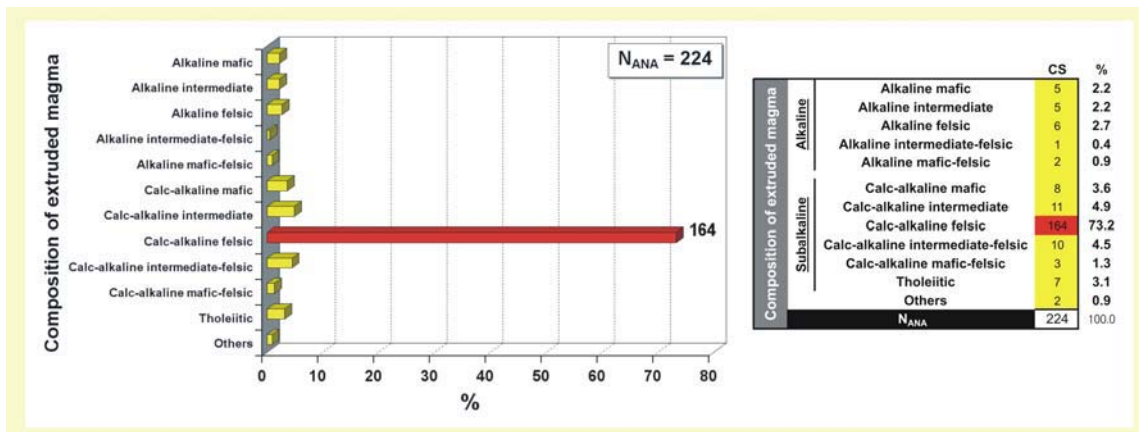


**Fig. 2.57:** Results for the analysis of the composition of the magma extruded during the caldera-forming events included in the CCDB. Colours correspond to the “*MAXIMUM NORMALIZATION*” (Left) Histogram showing the percentages of calderas located in the different *CATEGORIES* of the *CHARACTERISTIC* “Composition of extruded magma”. Bold numbers at the right of the bars specify the number of calderas included in this composition or *CATEGORY CS*.  $N_{ANA}$  at the left top corner indicates total number of calderas with information about the *CHARACTERISTIC* “Composition of extruded magma”. (Right) Representation of information included in the “*CCDB DATA TABLE*” of Figure 2.42. Here are represented the number of calderas included in each *CATEGORY CS*.

The most remarkable observations are:

- At 73.2%, felsic calc-alkaline magmas are among the most abundant compositions (CS =164).
- Each composition different from the former is merely represented by less than 5 %. (CS <11).

Investigating the worldwide distribution of calderas based on their magma composition of the caldera-forming eruption we observe that (Fig. 2.58):

- Calc-alkaline felsic calderas (CS = 164) show a worldwide distribution with a clear cluster at 31 % in the area of North America (51 samples).
- The regions of Japan and the Marianas Islands and Indonesia also host a considerable number of calc-alkaline felsic calderas, 20 (12.2 %) and 17 (8.5%) samples, respectively.

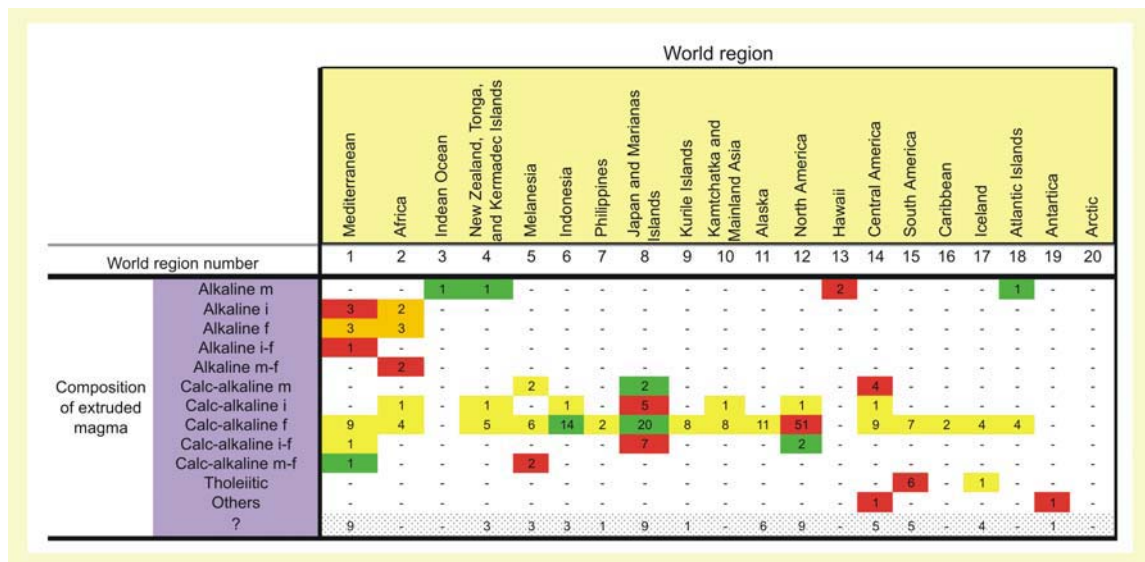


**Fig. 2.58:** Representation of information included in the “CCDB DATA TABLE” of figure 2.43 comprising the spatial distribution of calderas in each *CATEGORY*. The Colours correspond to the “MAXIMUM NORMALIZATION”. f Felsic ; i Intermediate; m Mafic; i-f Intermediate-felsic; m – f Mafic – felsic .

❖ REGIONAL AND PLATE TECTONIC

➤ Crustal type

I now focus on information concerning the *CHARACTERISTIC* “Crustal types”. Results are summarized in figure 2.59.

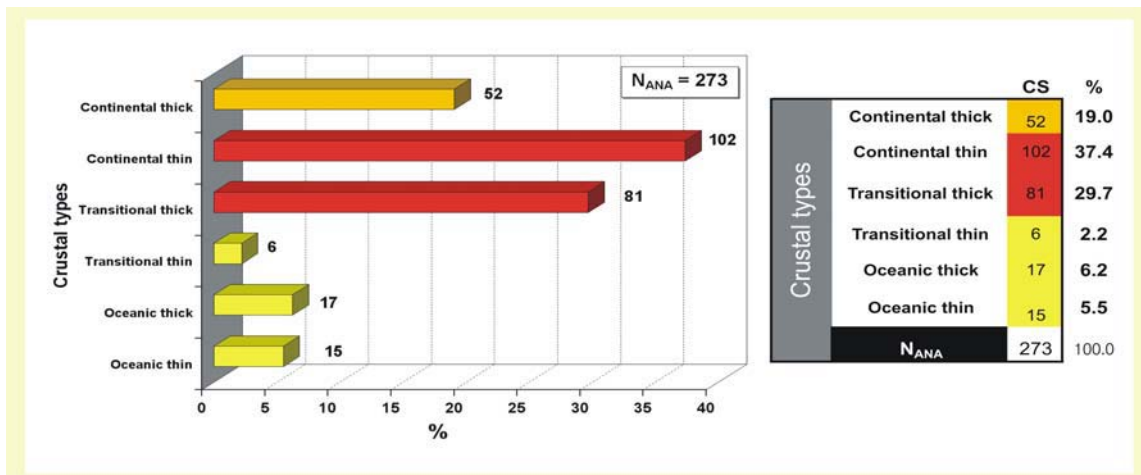


**Fig. 2.59:** Results for the analysis of the crustal type of samples included in the CCDB. Colours correspond to the “*MAXIMUM NORMALIZATION*” (Left) Histogram showing the percentages of calderas located in the different *CATEGORIES* of the *CHARACTERISTIC* “Crustal types”. Bold numbers at the right of the bars specify the number of calderas included in the *CATEGORY*. **N<sub>ANA</sub>** at the left top corner indicates total number of calderas with information about the *CHARACTERISTIC* “Crustal types”. (Right) Representation of information included in the “*CCDB DATA TABLE*” of Figure 2.42. Here are represented the number of calderas included in each *CATEGORY*, **CS**.

We observe that:

- The *CATEGORIES* with an abundance of calderas are “Continental thin” (37.4 %, **CS** = 102), “Transitional thick” (29.7%, **CS** = 81) and “Continental thick” (19%, **CS** = 52).
- The rest of *CATEGORIES* record less than the 6.5% (17 samples) of the total number of calderas (**N<sub>ANA</sub>** = 273) each.

Analysing the spatial distribution of the calderas depending on their crustal type (Fig. 2.60)

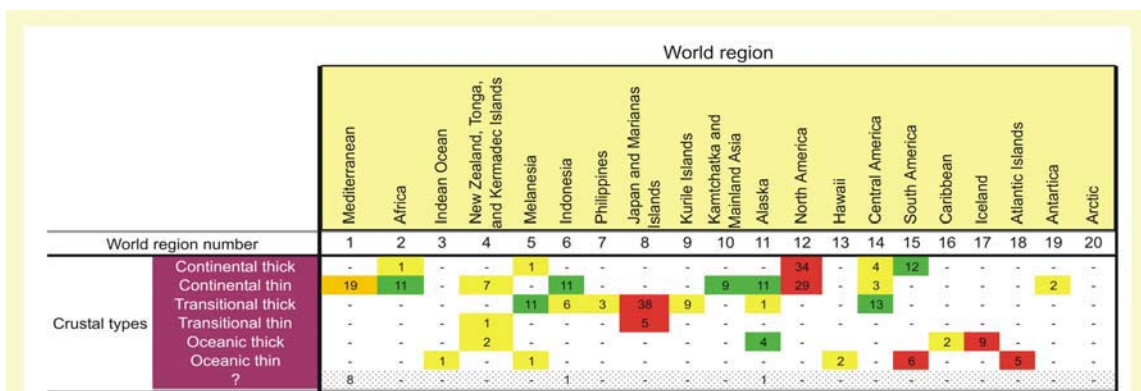


**Fig. 2.60:** Representation of information included in the “*CCDB DATA TABLE*” of figure 2.43 comprising the spatial distribution of calderas in each crustal type. The colours correspond to the “*MAXIMUM NORMALIZATION*”.

- Almost all calderas located in continental thick crust (**CS** = 52) are located in North America (65.4%, 34 samples) and to a lesser degree in South America (23%, 12 samples).
  - Calderas included in the *CATEGORY* “Transitional thick” (**CS** = 81) are mainly located in Japan and the Marianas Islands (46.9%, 38 samples). Also, the regions of Central America and Melanesia host a considerable number of calderas, 13 (16%) and 11 (13.5%), respectively.
  - The distribution of those calderas located in areas of continental thin crust (**CS** = 102) is more uniform. It has a maximum in the region of Japan and the Marianas Islands (28.4%, 29 samples) and shows a second peak in the Mediterranean area (18.6%, 19 samples). The rest of the samples in *CATEGORY* “Continental thin” are distributed mainly in Africa, Indonesia, Kamtchatka and Mainland Asia and Alaska with around a 10% (9-11 samples) in each region.
- **Tectonic setting**

This section deals with the most common tectonic setting of the CCDB calderas (Fig. 2.61).

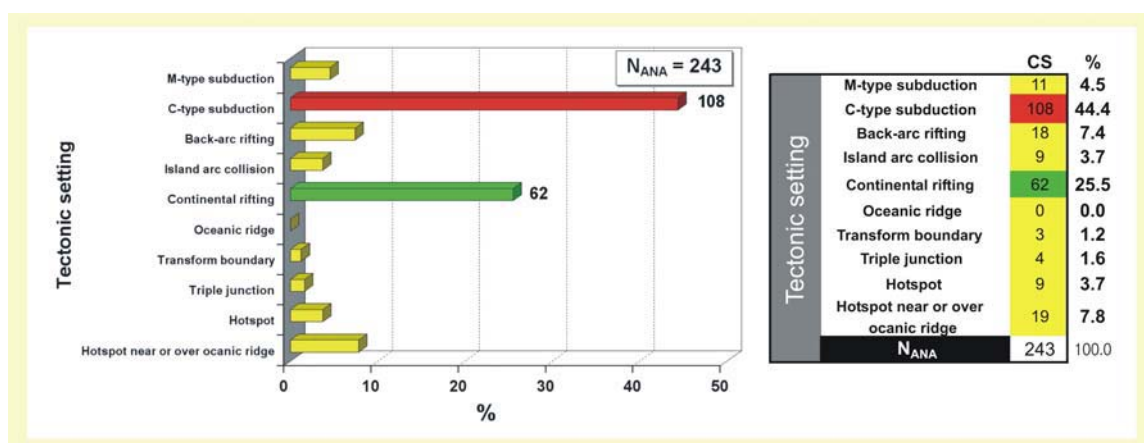


**Fig. 2.61:** Results for the analysis of the tectonic setting of the calderas included in the CCDB. Colours correspond to the “*MAXIMUM NORMALIZATION*” (Left) Histogram with the percentages of calderas located in the different *CATEGORIES* of the *CHARACTERISTIC* “Tectonic setting”. Bold numbers at the right of the bars specify the number of calderas included in the *CATEGORY CS*.  $N_{ANA}$  at the left top corner indicates total number of calderas with information about the *CHARACTERISTIC* “Tectonic setting”. (Right) Representation of information included in the “*CCDB DATA TABLE*” of Figure 2.42. Here are represented the number of calderas included in each *CATEGORY CS*.

The most important results are:

- More than the 40% (**CS** = 108) of the CCDB calderas with information on the tectonic setting (**N<sub>ANA</sub>** = 243) are located in C-type subduction zones.
- In areas of continental rifting, we find 62 calderas (**CS** = 62) corresponding to 25.5% of the analysed calderas.
- The rest of *CATEGORIES* with the *CHARACTERISTIC* “Crustal types” each host less than 20 calderas (**CS** < 20), i.e. less than 8 % of the total number of calderas with information about the tectonic setting.

The spatial distribution of calderas in the different *CATEGORIES* of the *CHARACTERISTIC* “Tectonic setting” gives the following insights (Fig. 2.62):

- The great majority of calderas in C-type subduction zones (**CS** = 108) are located in Japan and the Marianas Islands (31.5%, 34 samples) and the rest is more or less uniformly distributed with a percentage within the interval 14 - 8% (15-9 samples) along Central America, South America, Indonesia, North America, Kurile Islands and Alaska.
- Calderas in a context of continental rifting (**CS** = 62) are mainly located in North America (72.6%, 45 samples).
- Calderas associated with hotspot near or close to oceanic ridges (**CS** = 19) are principally located in Iceland (47.4%, 9 samples) and South America (31.5%, 6 samples).

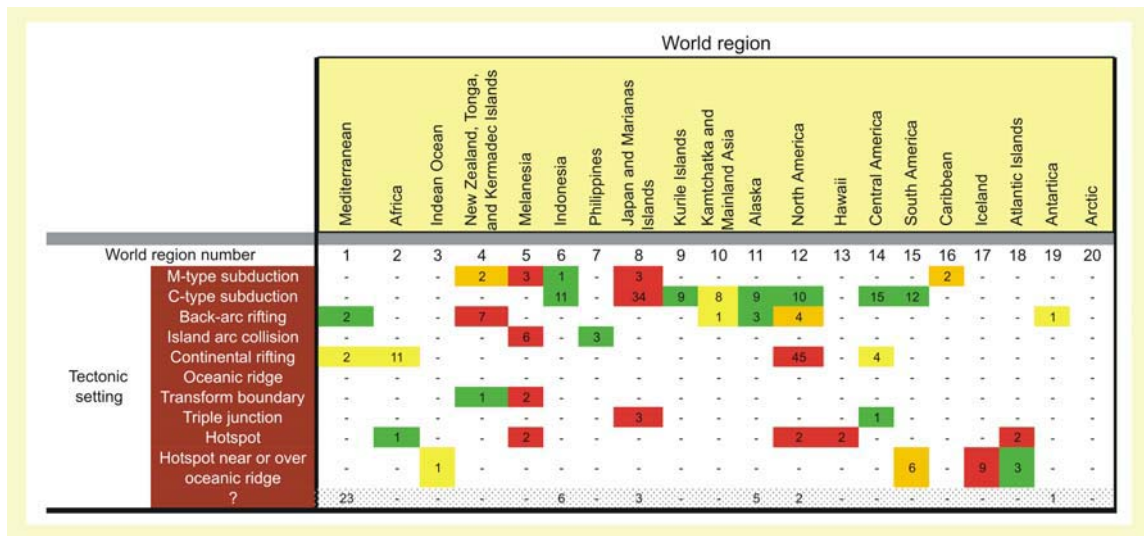


Fig. 2.62: Representation of information included in the “CCDB DATA TABLE” of figure 2.43 comprising the spatial distribution of calderas in each tectonic setting. The colours correspond to the “MAXIMUM NORMALIZATION”.

➤ Existence of relevant regional faults

In connection with the CHARACTERISTIC “Existence of relevant regional faults” it is noteworthy that 43.8% (124 samples) of the calderas are close to or superimposed on relevant regional structures.

However there does not seem to be a spatial clustering of calderas with this CHARACTERISTIC, indicating an independence on the location of the collapse calderas (Fig. 2.63).

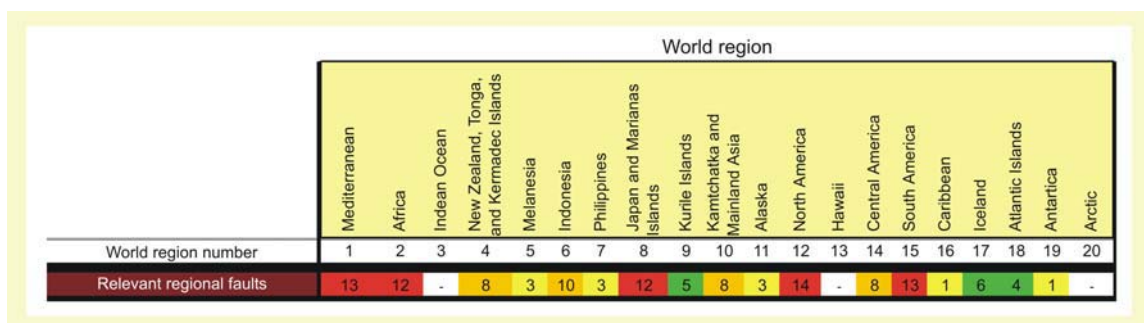
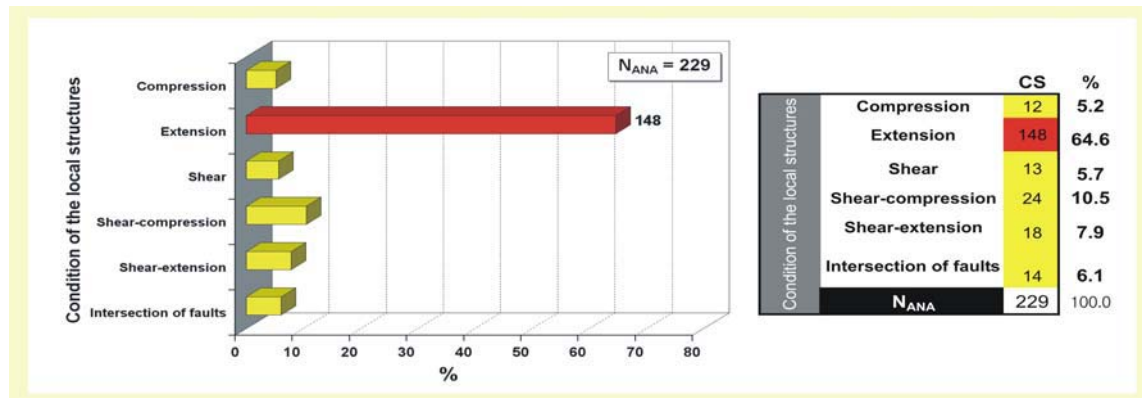


Fig. 2.63: Representation of information included in the “CCDB DATA TABLE” of figure 2.43 comprising the spatial distribution of calderas over or close to relevant regional faults. The colours correspond to the “MAXIMUM NORMALIZATION”.

### ➤ Condition of local structures

Figure 2.64 shows information regarding the *CHARACTERISTIC* “Condition of the local structures”.



**Fig. 2.64:** Results for the analysis of the type pre-caldera edifice of samples included in the CCDB. Colours correspond to the “*MAXIMUM NORMALIZATION*” (Left) Histogram with the percentages of calderas located in the different *CATEGORIES* of the *CHARACTERISTIC* “Condition of the local structures”. Bold numbers at the right of the bars specify the number of calderas included in the *CATEGORY CS*. **N<sub>ANA</sub>** at the left top corner indicates total number of calderas with information about the *CHARACTERISTIC* “Condition of the local structures”. (Right) Representation of information included in the “*CCDB DATA TABLE*” of Figure 2.42. Here are represented the number of calderas included in each *CATEGORY CS*.

The main observations are :

- ❑ Local structures are principally extensional (64%, **CS** = 148 ).
- ❑ The rest of structures are less common, they each represent less than a 11% (**CS** ≤ 24).

When studying the spatial distribution of the calderas according to the condition of the local structures, we find that (Fig. 2.65):

- ❑ Almost all calderas with compressional local structures (**CS** = 12) are located in Japan and the Marianas Islands (91.7%, 11 samples), only one sample is located in the Kurile Islands.
- ❑ Calderas associated with extensional local structures (**CS** = 148) show a worldwide distribution. They appear to be concentrated in North America (39.9%, 59 samples) and to a lesser degree in the Mediterranean region (12.2%, 18 samples) as well as in Japan and the Marianas Islands (9.5%, 14 samples).

- Shear and compressional local structures (CS = 24) are mainly associated with calderas in Japan and the Marianas Islands (33.3%, 8 samples) as well as in Indonesia (29.2%, 7 samples).

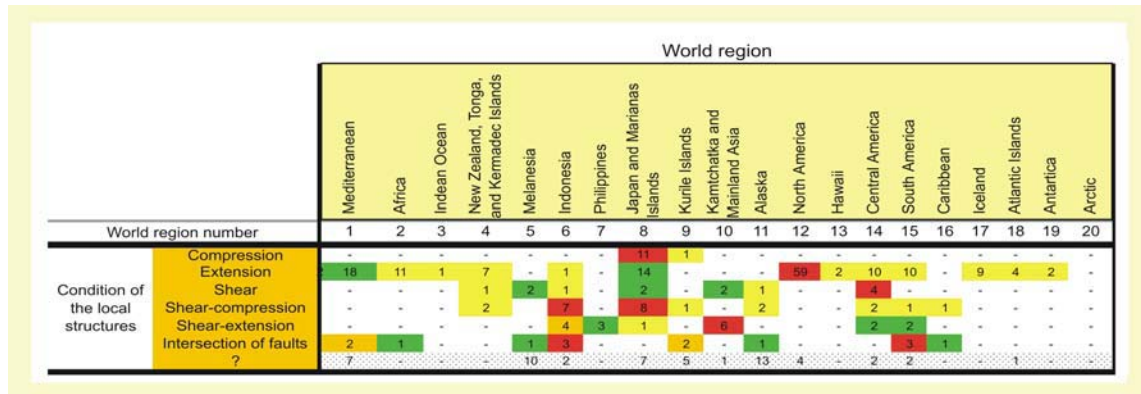


Fig. 2.65: Representation of information included in the “CCDB DATA TABLE” of figure 2.43 comprising the spatial distribution of calderas associated with different types of local structures. The colours correspond to the “MAXIMUM NORMALIZATION”.

❖ PRE-CALDERA ACTIVITY

➤ Type of pre-caldera edifice

Available information in connection with the type of pre-caldera edifice is shown on Figure

2.66.

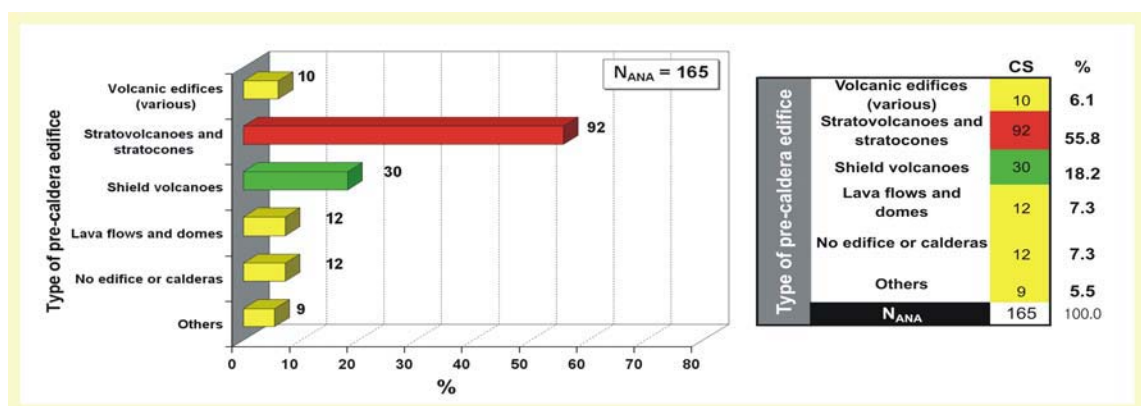
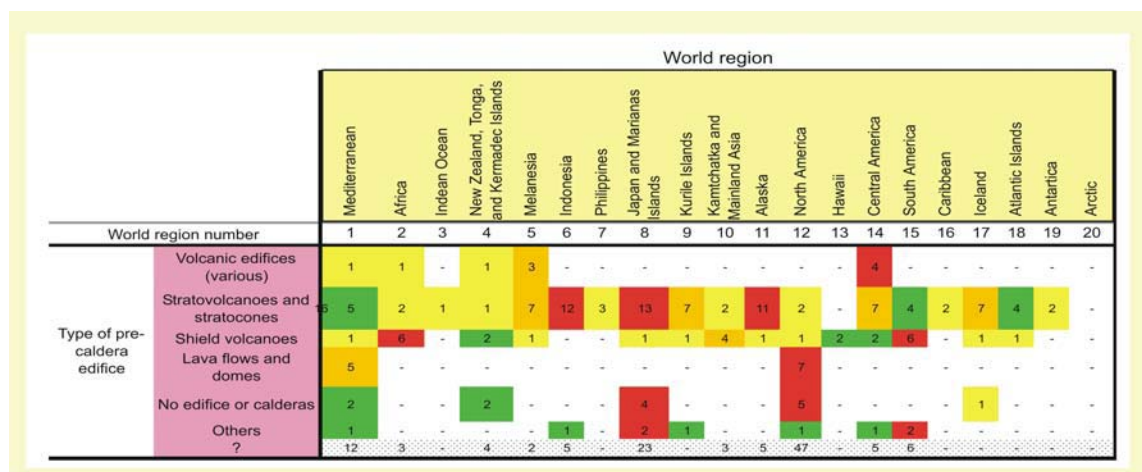


Fig. 2.66: Results for the analysis of the type pre-caldera edifice of samples included in the CCDB. Colours correspond to the “MAXIMUM NORMALIZATION” (Left) Histogram with the percentages of calderas located in the different CATEGORIES of the CHARACTERISTIC “Type of pre-caldera edifice”. Bold numbers at the right of the bars specify the number of calderas included in the CATEGORY CS. N<sub>ANA</sub> at the left top corner indicates total number of calderas with information about the CHARACTERISTIC “Type of pre-caldera edifice”. (Right) Representation of information included in the “CCDB DATA TABLE” of Figure 2.42. Here are represented the number of calderas included in each CATEGORY CS.

Based on information compiled in Figure 2.66, I conclude that:

- Around the 80% (132 samples) of the studied calderas ( $N_{ANA} = 165$ ) show evidence of a volcanic edifice prior to the caldera collapse. Most common are stratovolcanoes and stratocones (53.3% , **CS** = 92). Yet also shield volcanoes contribute a moderate percentage (17.3%, **CS** = 30).
- By contrast, lava flows and domes structures or the absence of a previous edifice are less common.

Similar to the other features, it is interesting to note the spatial distribution of the calderas as a function of the type of pre-caldera edifice (Fig. 2.67).



**Fig. 2.67:** Representation of information included in the “*CCDB DATA TABLE*” of figure 2.43 comprising the spatial distribution of calderas in each *CATEGORY* of the *CHARACTERISTIC* “Type of pre-caldera edifice”. The colours correspond to the “*MAXIMUM NORMALIZATION*”.

I find that (Fig. 2.67):

- Calderas with existing pre-caldera edifices (stratovolcanoes-stratocones (**CS** = 92) and shield volcanoes (**CS** = 30) show an almost worldwide distribution.
- The regions with a higher number of calderas included in the *CATEGORY* “Stratovolcanoes and stratocones” are Japan and the Marianas Islands (14.1 %, 13 calderas), Indonesia

- (13%, 12 calderas) and Alaska (11.9%, 11 calderas). Furthermore, Melanesia, Kurile Islands, Central America and Iceland each show 7.6% (7 samples).
- Two moderate maximums characterize the spatial distribution of those calderas included in the *CATEGORY* “Shield volcanoes” (CS = 30). These correspond to Africa (20%, 6 calderas) (e.g. Silali – *Kenya*, Williams et al., 1984) and South America (20%, 6 calderas) (e.g. Fernandina – *Galapagos*, Munro and Rowland, 1996) .
  - Calderas associated with lava flows and domes (CS = 12) are predominantly located in North America (58.3 %, 7 calderas ) and the Mediterranean region (41.7%, 5 calderas).
  - Calderas included in the *CATEGORY* “No edifice or calderas” (CS = 12) can be found in North America (41.7 %, 5 calderas) and Japan and the Marianas Islands (33.3 %, 4 calderas).
  - The majority of calderas included in the *CATEGORY* “No edifice or calderas” (CS = 12) can be found in North America (41.7 %, 5 caldera samples), as well as Japan and the Marianas Islands (33.3 %, 4 caldera samples).

### ➤ Type of caldera collapse precursor

Figure 2.68 gives the available information on the type of pre-caldera precursors.

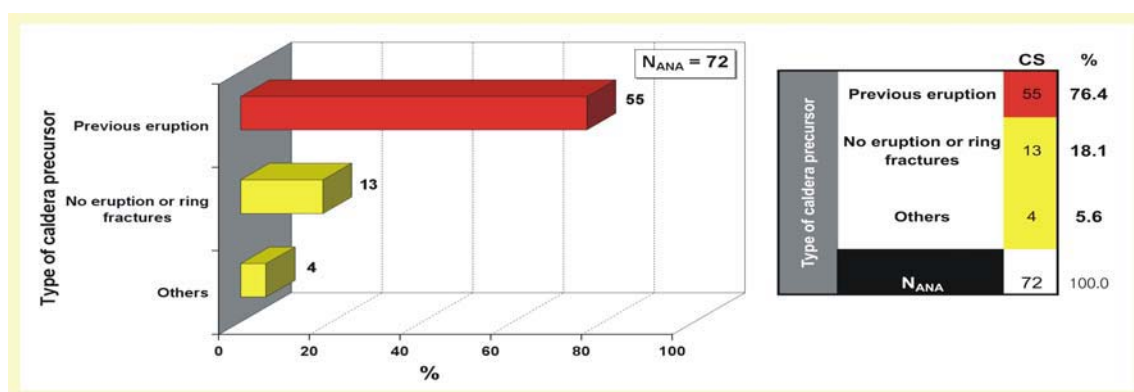


**Fig. 2.68:** Results for the analysis of the type caldera precursor of samples included in the CCDB. Colours correspond to the “*MAXIMUM NORMALIZATION*” (Left) Histogram with the percentages of calderas located in the different *CATEGORIES* of the *CHARACTERISTIC* “Type of caldera precursor”. Bold numbers at the right of the bars specify the number of calderas included in the *CATEGORY CS*. **N<sub>ANA</sub>** at the left top corner indicates total number of calderas with information about the *CHARACTERISTIC* “Type of caldera precursor”. (Right) Reproduction of the information included in the “*CCDB DATA TABLE*” of Figure 2.42. Here are represented the number of calderas included in each *CATEGORY CS*.

Summerizing, I note that:

- The *CATEGORY* showing the highest number of calderas is “Previous eruption” (76.4 % , **CS** = 55), i.e. the existence of an eruptive event prior to the caldera collapse.
- The *CATEGORY* “No eruption or ring fractures” shows 13 calderas (**CS** = 13) corresponding to 18.1%.

Concerning the spatial distribution of calderas and their dependence on the type of collapse precursor, the results are (Fig. 2.69):

- Calderas with an eruption preceding the caldera-forming event (**CS** = 55) show a notably worldwide distribution, with a moderate maximum in the Mediterranean region (20%, 11 samples).
- Calderas included in the *CATEGORY* “No eruption or ring fractures” (**CS** = 13) are concentrated in North America (61.5%, 8 samples)

		World region																			
		Mediterranean	Africa	Indian Ocean	New Zealand, Tonga, and Kermadec Islands	Melanesia	Indonesia	Philippines	Japan and Marianas Islands	Kurile Islands	Kamchatka and Mainland Asia	Alaska	North America	Hawaii	Central America	South America	Caribbean	Iceland	Atlantic Islands	Antarctica	Arctic
World region number		1	2	3	4	5	6	7	8	9	10	11	12	13	14	15	16	17	18	19	20
Type of caldera precursor	Previous eruption	11	7	1	6	6	4	-	8	-	-	2	8	-	3	1	-	-	1	-	-
	No eruption or ring fractures	1	-	-	-	1	-	-	1	-	-	-	8	-	-	2	-	-	-	-	-
	Others	2	-	-	-	1	-	-	1	-	-	-	-	-	-	-	-	-	-	-	-
	?	13	5	-	4	5	14	3	33	9	9	15	47	2	17	15	2	9	4	2	-

**Fig. 2.69:** Representation of information included in the “*CCDB DATA TABLE*” of figure 2.43 comprising the spatial distribution of calderas in each *CATEGORY* of the *CHARACTERISTIC* “Type of caldera precursor”. Furthermore, the colours correspond to the “*MAXIMUM NORMALIZATION*”.

## ❖ POST-CALDERA ACTIVITY

### ➤ Type of post-caldera volcanic activity

This section aims at extending the earlier work of Walker (1984). Here, I try to identify the most common type of post-caldera volcanic activity. Results indicate that (Fig. 2.70):

- The *CATEGORIES* of the *CHARACTERISTIC* “Post-caldera volcanic activity” ( $N_{ANA} = 99$ ) with a higher number of associated calderas are “Type-C” (22.2%, **CS** = 22), “Type-R” (18.2%, **CS** = 18) and “Type-S” (15.2%, **CS** = 15).
- For the rest of analysed calderas the type of post-caldera volcanic activity is uniformly distributed in the *CATEGORIES* “Type-Rs”, “Type-L”, “Type-M”, “Type-CaR” and “Type-CC”. The number of calderas included in each of them range from 11 to 7 samples corresponding to a percentage range from 11.1 % to 7.1%.

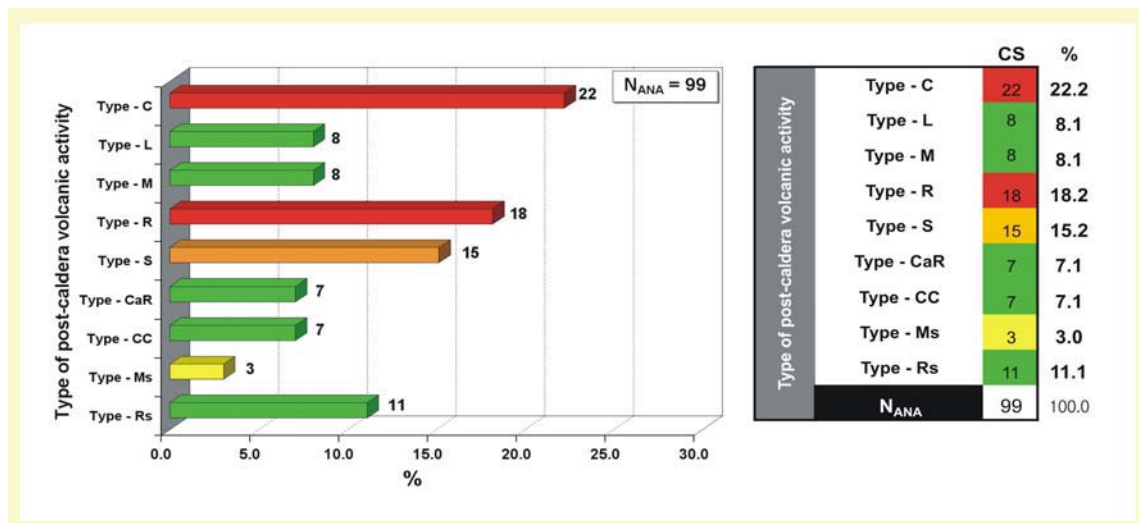


**Fig. 2.70:** Results for the analysis of the type of post-caldera volcanic activity of samples included in the CCDB. Colours correspond to the “*MAXIMUM NORMALIZATION*” (Left) Histogram with the percentages of calderas located in the different *CATEGORIES* of the *CHARACTERISTIC* “Type post-caldera volcanic activity”. Bold numbers at the right of the bars specify the number of calderas included in the *CATEGORY CS*.  $N_{ANA}$  at the left top corner indicates total number of calderas with information about the *CHARACTERISTIC* “Type of post-caldera volcanic activity”. (Right) Representation of information included in the “*CCDB DATA TABLE*” of Figure 2.42. Here are represented the number of calderas included in each *CATEGORY CS*.

The analysis of the spatial distribution of the different *CATEGORIES* included in the *CHARACTERISTIC* “Type of post-caldera volcanic activity” (Fig. 2.71) reveals that there is no preferred geographical location. The highest concentrations differ by a margin of only two samples over the rest of the population.. Obviously, there is not enough representative data for a quantitative analysis.

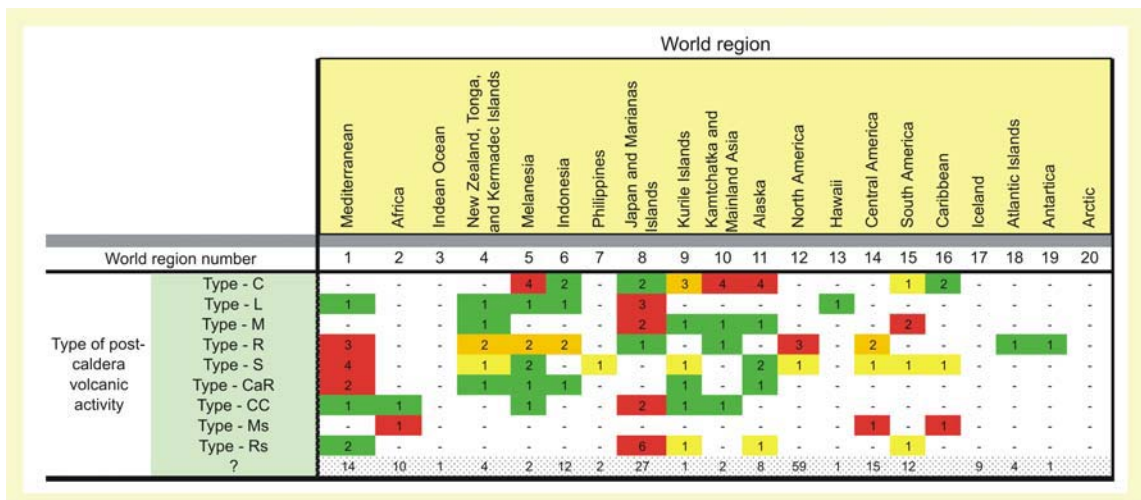


Fig. 2.71: Representation of information included in the “CCDB DATA TABLE” of figure 2.43 comprising the spatial distribution of calderas with the different types of post-caldera volcanic activity. Furthermore, the colours correspond to the “MAXIMUM NORMALIZATION”.

II.5.6.2 Results obtained for the relationship between two *CHARACTERISTICS*

This section reports on the results obtained from the *CCDB DATA TABLE*, considering the relationship between two *CHARACTERISTIC*. (*CHARACTERISTICS* “A” to *CHARACTERISTICS* “B” and vice versa). Similar to the previous section, for those cases in which the number of analysed caldera samples  $N_{ANA}$  is too low, we refrain from a quantitative description, as the result would not be statistically relevant.

❖ **RELATIONSHIP BETWEEN THE *CHARACTERISTICS* “Age” AND “Dimensions”**

- Regardless of their age, most calderas show a diameter  $D_{CIR}$  of less than 25 km (Fig. 2.72 indication A). Out of 164 calderas with information on both *CHARACTERISTICS* “Age” and “Dimensions”, 146 samples (89%) have a  $D_{CIR} < 25$  km.

- 
- The most common dimension for very young calderas ( $< 5$  ka) (33 samples with dimensions information) is a  $D_{\text{CIR}} < 10$  km (90.9%, 30 samples) (Fig. 2.72 indication B).
  - Calderas in the *CATEGORY* “5-50 ka” (38 samples with age information) have a  $D_{\text{CIR}}$  between 5 and 25 km (81.6%, 31 samples) (Fig. 2.72 indication C).
  - For those caldera samples included in the *CATEGORIES* “100 ka - 1 Ma”, “10 – 25 Ma” and “25 – 50 Ma” (21, 15 and 34 samples with dimensions information, respectively) the most frequent dimensions are those corresponding to a  $D_{\text{CIR}}$  between 5 and 25 km (61.9%, 66.7% and 47% equivalent to 13, 10 and 16 samples, respectively) (Fig. 2.72 indication D).
  - The ages of calderas with a  $D_{\text{CIR}}$  between 5 and 25 km are diverse and cover the range from 5ka to 50 Ma) (Fig. 2.72 indication E).
  - Very small calderas ( $D_{\text{CIR}} < 5$  km) (26 samples with age information) are mainly (53.9%, 14 samples) less than 50 ka old (Fig. 2.72 indication F).
  - Calderas in *CATEGORY* “5 – 10 km” (55 samples with age information) are generally younger than 50 ka (58.2%, 32 samples) (Fig. 2.72 indication G).
  - Ages of caldera samples included in the *CATEGORY* “10 – 25 km” (65 samples with age information) are mostly comprised in the *CATEGORIES* “25 – 50 Ma”, “100 ka – 1 Ma” and “5 – 50 ka” (24.6%, 23.1% and 20% equivalent to 16, 15, and 13 samples, respectively) (Fig. 2.72 indication H).

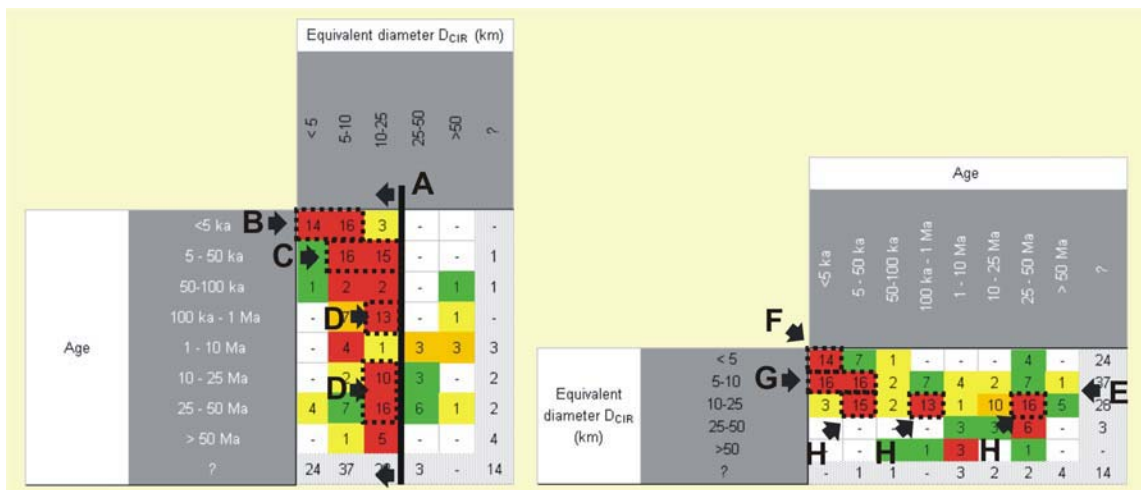


**Fig. 2.72:** Sections of the “CCDB DATA TABLE” represented in Figure 2.42. Here both relationships *CHARACTERISTICS* “Age” to *CHARACTERISTICS* “Dimensions” and vice versa. Squares are coloured according to the “MAXIMUM NORMALIZATION”.

❖ **RELATIONSHIP BETWEEN THE *CHARACTERISTICS* “Age” AND “Volume of extruded deposits”/ “Volume of extruded magma”**

- The volume of extruded magma seems to increase for older calderas (Fig. 2.73 indication A).
- Calderas sample associated with large volumes of extruded deposits/magma are older (Fig. 2.73 indication B).

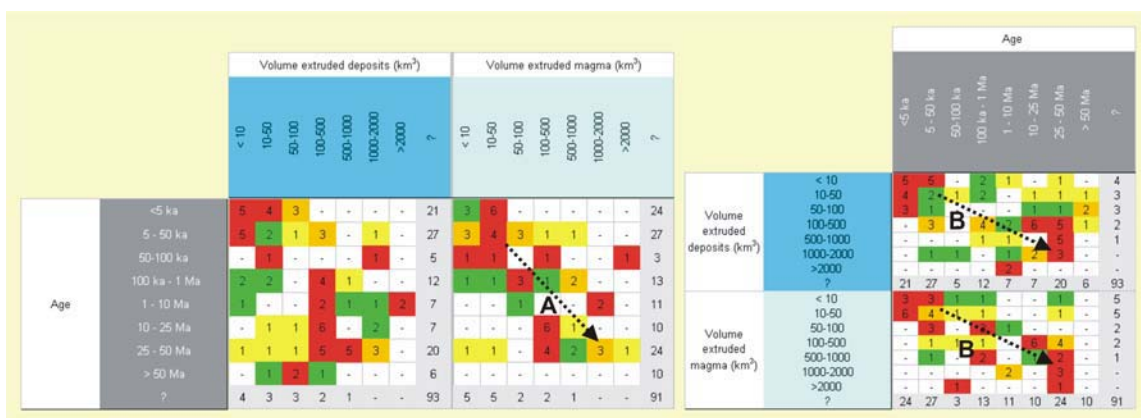


**Fig. 2.73:** Sections of the “CCDB DATA TABLE” represented in Figure 2.42. Here both relationships *CHARACTERISTICS* “Age” to the *CHARACTERISTICS* “Volume of extruded deposits” and “Volume of extruded magma” and vice versa. Squares are coloured according to the “MAXIMUM NORMALIZATION”.

- 
- ❖ **RELATIONSHIP BETWEEN THE *CHARACTERISTICS* “Age” AND “Tectonic setting”**
- Young calderas (< 5 ka) are located in almost all tectonic settings (Fig. 2.74 indication A).
  - Calderas younger than 1 Ma (85 samples with tectonic setting information) are mainly (55.3%, 47 samples) located in C-type subduction zones (Fig. 2.74 indication B).
  - Calderas with an age between 1 and 10 Ma (14 samples with tectonic setting information) are more common in C-type subduction zones (50%, 7 samples) and in areas of continental rifting (35.7%, 5 samples) (Fig. 2.68 indication C).
  - Calderas in the *CATEGORIES* “10 – 25 Ma” and “25 – 50 Ma” (17 and 36 samples with tectonic information, respectively) are mainly distributed in areas of continental rifting (70.6% and 69.4% equivalent to 12 and 25 samples, respectively) (Fig. 2.74 indication D)
  - In C-type subduction zones (67 samples with age information) a considerable percentage (35.8%, 24 samples) has an age assigned in the *CATEGORY* “5 – 50 ka” (Fig. 2.74 indication E).
  - From those calderas located in areas of continental rifting (42 samples with age information) a considerable high percentage (59.2%, 25 samples) has an age assigned in the *CATEGORY* “25 – 50 Ma” (Fig. 2.74 indication F).
  - All calderas included in the database and located in areas of hotspot near or over an oceanic ridge are younger than 50 ka (Fig. 2.74 indication G).

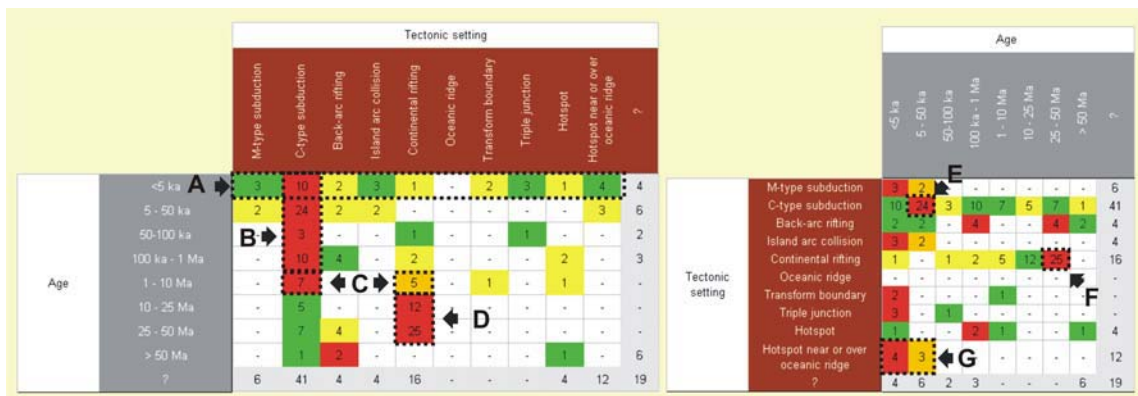


**Fig. 2.74:** Sections of the “CCDB DATA TABLE” represented in Figure 2.42. Here both relationships *CHARACTERISTICS* “Age” to the *CHARACTERISTICS* “Tectonic setting” and vice versa. Squares are coloured according to the “*MAXIMUM NORMALIZATION*”.

❖ ***CHARACTERISTICS* “Age” AND “Crustal types”**

- Independent on the age, the majority of the calderas recorded in the CCDB (172 samples with crustal type information) are located in areas of continental thick (24.4%, 42 samples), continental thin (40.1%, 69 samples) and transitional thick (26.7%, 46 samples) crust (Fig. 2.75 indication A).
- Only few calderas younger than 50 ka (72 samples with crustal type information) are located in areas of transitional thin (4.2%, 3 samples), oceanic thick (5.6%, 4 samples) and oceanic thin crust (8.3%, 6 samples) (Fig. 2.75 indication B). Additionally, two calderas located in the *CATEGORIES* “100 ka – 1 Ma” and “1 – 10 Ma” are also located in oceanic thin and transitional thin crust, respectively (Fig. 2.75 indication C).
- Calderas younger than 50 ka (72 samples with crustal type information) are predominantly located in areas of transitional thick (43.1%, 31 samples) or continental thick crust (37.5%, 27 samples) (Fig. 2.75 indication D).
- Calderas in the *CATEGORIES* “100 ka – 1 Ma” or “10 – 25 Ma” (21 and 17 samples with crustal type information, respectively) are located mainly in areas of continental thin crust (47.6% and 70.6% equivalent to 10 and 12 samples, respectively) (Fig. 2.75 indication E).

- 
- Calderas older than 25 Ma (41 samples with crustal type information) are present only in areas of continental thick crust (73.2%, 30 samples) and in little proportion in continental thin crust (26.8%, 11 samples) (Fig. 2.75 indication F).
  - Calderas in the *CATEGORY* “25 – 50 Ma” (36 samples with crustal type information) are located mainly in areas of continental thick crust (75%, 27 samples) (Fig. 2.75 indication G).
  - The ages of those calderas in areas of continental thick crust (42 samples with age information) correspond mainly (70.6%, 12 samples) to the *CATEGORY* “25 – 50 Ma” (Fig. 2.75 indication H).
  - Calderas included in the database and located in areas of continental thin crust (69 samples with age information) have ages in all the *CATEGORIES* of the *CHARACTERISTIC* “Age” (Fig. 2.75 indication I) with a maximum of samples (23.2%, 16 samples) in the *CATEGORY* “5 – 50 ka” (Fig. 2.75 indication J).
  - From those calderas located in areas of transitional thick crust (46 samples with age information) a considerable high percentage (67.4%, 31 samples) is younger than 50 ka (Fig. 2.75 indication K).
  - Calderas located in areas of transitional thin, oceanic thick and oceanic thin crust are mainly younger than 50 ka (Fig. 2.75 indication L) with two exceptions (Fig. 2.75 indication M).

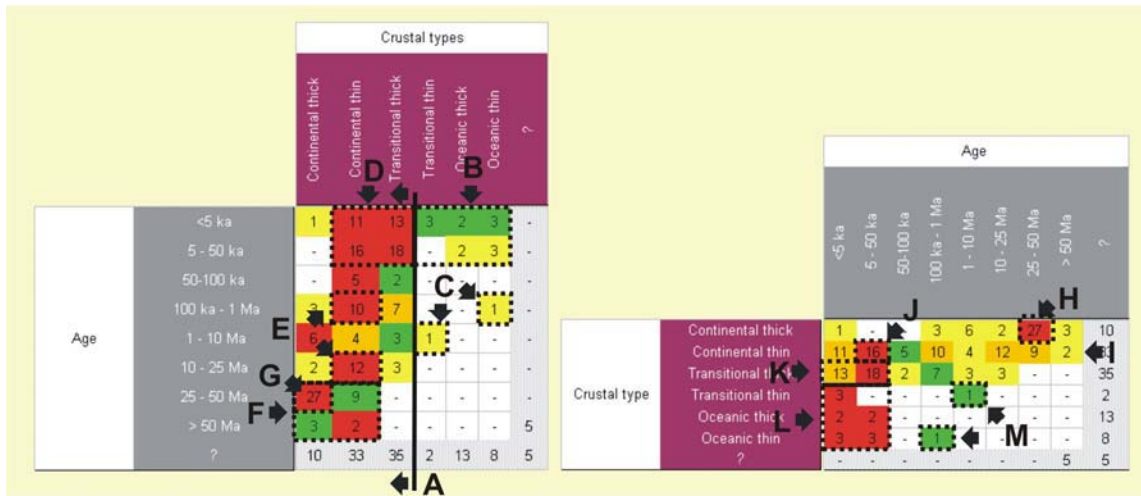


**Fig. 2.75:** Sections of the “CCDB DATA TABLE” represented in Figure 2.42. Here both relationships *CHARACTERISTICS* “Age” to the *CHARACTERISTICS* “Crustal types” and vice versa. Squares are coloured according to the “*MAXIMUM NORMALIZATION*”.

❖ ***CHARACTERISTICS* “Age” AND “Type of pre-caldera edifice”**

- Calderas younger than 1 Ma (69 samples with pre-caldera edifice information) have mainly (66.7%, 46 samples) stratovolcanoes and stratocones as pre-caldera edifice (Fig. 2.706 indication A).
- Calderas in the *CATEGORY* “25 – 50 Ma” Ma (10 samples with pre-caldera edifice information) are characterized for having lava flows and domes as pre-caldera edifice (70 %, 7 samples) (Fig. 2.76 indication B).
- Calderas with stratovolcanoes and stratocones as pre-caldera edifice (48 samples with age information) are mainly younger than 50 ka (70.8%, 34 samples) (Fig. 2.76 indication C).
- The distribution of the calderas included in the *CATEGORY* “Lava flows and domes” (12 samples with age information) according to their age has a moderate maximum at the *CATEGORY* “25 – 50 Ma” (58.3%, 7 samples) (Fig. 2.76 indication D).



**Fig. 2.76:** Sections of the “CCDB DATA TABLE” represented in Figure 2.42. Here both relationships *CHARACTERISTICS* “Age” to the *CHARACTERISTICS* “Type of pre-caldera edifice” and vice versa. Squares are coloured according to the “*MAXIMUM NORMALIZATION*”.

❖ ***CHARACTERISTICS* “Dimensions” AND “Volume of extruded deposits”/ “Volume of extruded magma”**

- Logically, when increasing the value of the equivalent diameter  $D_{CIR}$  calderas are related to larger volumes of erupted deposits and magma (Fig. 2.77 indication A) and vice versa (Fig. 2.77 indication B).
- In some cases, relatively large calderas are associated with small volumes of erupted deposits and magma (Fig. 2.77 indication C) and vice versa (Fig. 2.77 indication D).

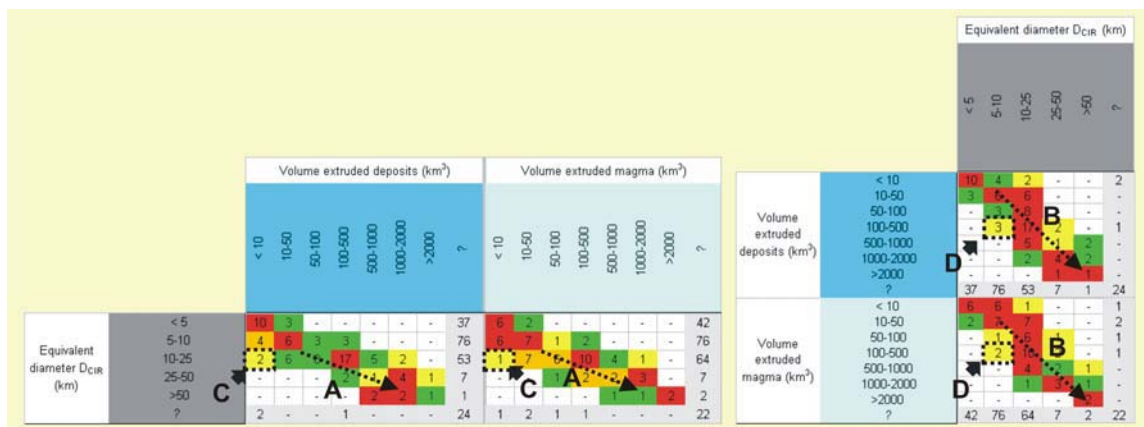


**Fig. 2.77:** Sections of the “CCDB DATA TABLE” represented in Figure 2.42. Here both relationships *CHARACTERISTICS* “Dimensions” to the *CHARACTERISTICS* “Volume of extruded deposits” and “Volume of extruded magma” and vice versa. Squares are coloured according to the “*MAXIMUM NORMALIZATION*”.

❖ ***CHARACTERISTICS* “Dimensions” AND “Collapse type”**

- Calderas with a  $D_{\text{CIR}} < 25$  km (76 samples with collapse type information) may have all the different collapse types considered in this analysis (Fig. 2.78 indication A).
- The distribution of the calderas in the *CATEGORY* “5 – 10 km” Ma (25 samples with collapse type information) according to the collapse type has a moderate maximum at the *CATEGORY* “Plate/piston” (36 %, 9 samples) (Fig. 2.78 indication B).
- Caldera collapses included in the *CATEGORY* “10 - 25 km” (35 samples with collapse type information) are characterized being principally for being mainly plate/piston type (31.4%, 11 samples), trap-door type (25.7 %, 9 samples) or funnel type (22.9 %, 8 samples) (Fig. 2.78 indication C).
- Large calderas ( $D_{\text{CIR}} > 25$  km) included in the CCDB (7 samples with collapse type information) are uniquely associated with plate/piston- and trap-door-type collapses (Fig. 2.78 indication D).
- From the total analysed caldera with information about the *CHARACTERISTICS* “Dimensions” and “Collapse type” (83 samples) those samples with  $D_{\text{CIR}} < 25$  km (91.6%, 76 samples) are the most frequent and may be associated with almost any of the described collapse types (Fig. 2.78 indication E).
- The distribution of funnel type calderas (18 samples with dimensions information) according to their dimensions has a moderate maximum at the interval “10 – 25 km” (44.4%, 8 samples) (Fig. 2.78 indication F).
- The dimensions of plate/piston collapse calderas included in the CCDB (27 samples with dimensions information) correspond principally to a  $D_{\text{CIR}}$  between 5 and 25 km (Fig. 2.78 indication G).

- The distribution of trap-door type calderas (17 samples with dimensions information) according to their dimensions has a moderate maximum at the interval “10 – 25 km” (52.9%, 9 samples) (Fig. 2.78 indication H).

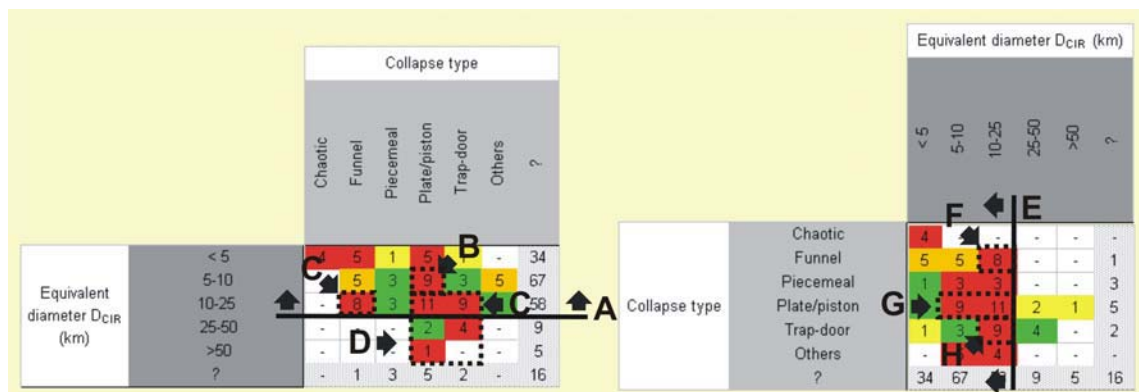


**Fig. 2.78:** Sections of the “CCDB DATA TABLE” represented in Figure 2.42. Here both relationships *CHARACTERISTICS* “Dimensions” to the *CHARACTERISTICS* “Collapse type” and vice versa. Squares are coloured according to the “MAXIMUM NORMALIZATION”.

#### ❖ *CHARACTERISTICS* “Dimensions” AND “Crustal types”

- Regardless of the caldera dimension, the most common crustal types associated with the different calderas included in the CCDB (252 samples with crustal type and dimensions information) are continental thin (37.3%, 94 samples), transitional thick (29.4%, 74 samples) and continental thick (18.7%, 47 samples) crust (Fig. 2.79 indication A).
- From the relatively small calderas ( $D_{CIR} < 10$  km) included in the database (140 samples with crustal type information) a high percentage is mainly located in areas of continental thin (30.7%, 43 samples) and transitional thick (25.7%, 36 samples) crust (Fig. 2.79 indication B).
- Calderas with  $D_{CIR}$  between 10 km and 25 km (91 samples with crustal type information) are distributed with a 45% (41 samples) in areas of continental thin crust and with a 30.8% (28 samples) in areas of transitional thick crust (Fig. 2.79 indication C).

- 
- Large calderas ( $D_{\text{CIR}} > 25$  km) (21 samples with crustal type information) are located uniquely in areas of continental thick (52.4%, 11 samples) and continental thin (47.6%, 10 samples) (Fig. 2.79 indication D).
  - Almost all largest calderas ( $D_{\text{CIR}} > 50$  km) (6 samples with crustal type information) are located in continental thick crust (83.3%, 5 samples) (Fig. 2.79 indication E).
  - Regardless of the crustal types, the most common dimensions for the different calderas included in the CCDB (252 samples with crustal type and dimensions information) are those corresponding to a  $D_{\text{CIR}} < 25$  km (91.7%, 231 samples) (Fig. 2.79 indication F).
  - Areas of continental thick and thin crust are the unique housing calderas of all possible dimensions (Fig. 2.79 indication G).
  - From those calderas located in areas of continental thick crust (47 samples with dimensions information) a relative high percentage of calderas have a  $D_{\text{CIR}}$  between 10 km and 25 km (34%, 16 samples) (Fig. 2.79 indication H).
  - Calderas in areas of continental thin crust (94 samples with dimensions information) are related to a relative high percentage to  $D_{\text{CIR}}$  between 10 km and 25 km (43.6%, 41 samples) and with a medium-high percentage to  $D_{\text{CIR}}$  between 5 and 10 km (29.7%, 27 samples) (Fig. 2.79 indication I).
  - Calderas located in areas of transitional thick crust (74 samples with dimensions information) have mainly a  $D_{\text{CIR}}$  between 5 and 25 km (82.4%, 16 samples) (Fig. 2.79 indication J).
  - The distribution of the calderas located in areas of oceanic thick and thin crust (32 samples with dimensions information) has a maximum at the *CATEGORY* "5 – 10 km" (46.9%, 15 samples) (Fig. 2.79 indication K).

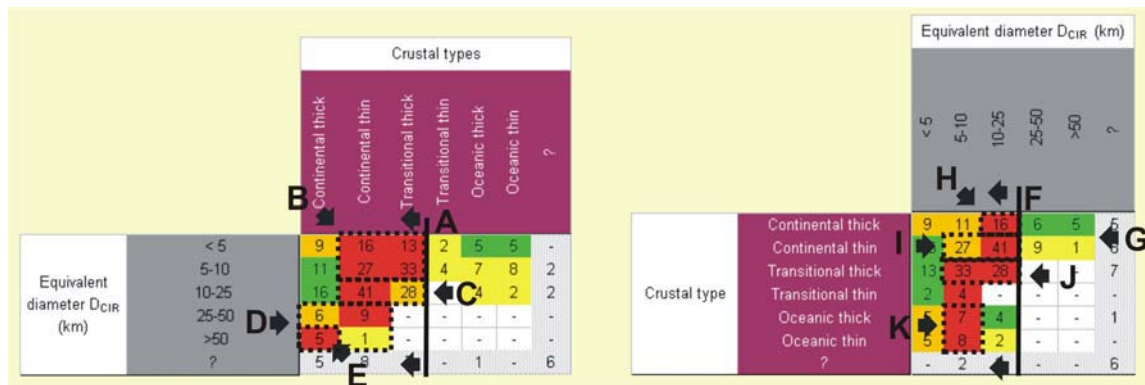


**Fig. 2.79:** Sections of the “CCDB DATA TABLE” represented in Figure 2.42. Here both relationships *CHARACTERISTICS* “Dimensions” to the *CHARACTERISTICS* “Crustal types” and vice versa. Squares are coloured according to the “MAXIMUM NORMALIZATION”.

#### ❖ *CHARACTERISTICS* “Dimensions” AND “Tectonic setting”

- Small calderas ( $D_{CIR} > 10$  km) (122 samples with tectonic setting information) are located mainly in C-type subduction zones (42.3%, 60 samples) (Fig. 2.80 indication A).
- Calderas with a  $D_{CIR}$  between 10 km and 25 km (84 samples with crustal type information) are mainly distributed with a 42.9% (36 samples) in C-type subduction zones and with a 34.5% (29 samples) in areas of continental rifting (Fig. 2.80 indication B).
- Large calderas with a  $D_{CIR}$  in the *CATEGORY* “25 – 50 km” (15 samples with tectonic setting information) are located mainly in areas of continental rifting (80%, 12 samples) (Fig. 2.80 indication C).
- Regardless of the tectonic setting, calderas included in the CCDB (227 samples with tectonic setting and dimensions information) have commonly a  $D_{CIR} < 25$  km (90.7%, 206 samples) (Fig. 2.80 indication D).
- From those calderas located in C-type subduction zones (99 samples with dimensions information) a relative high percentage of calderas have a  $D_{CIR}$  between 5 km and 25 km (79.8%, 79 samples) (Fig. 2.80 indication E).

- In areas of continental rifting (60 samples with dimensions information) a high number of calderas have a  $D_{CIR}$  in the *CATEGORY* “10 – 25” (48.3%, 29 samples) (Fig. 2. 80 indication F).
- Only C-type subduction zones, areas of continental rifting and hotspots have calderas with  $D_{CIR} > 50$  km (Fig. 2. 80 indication G).

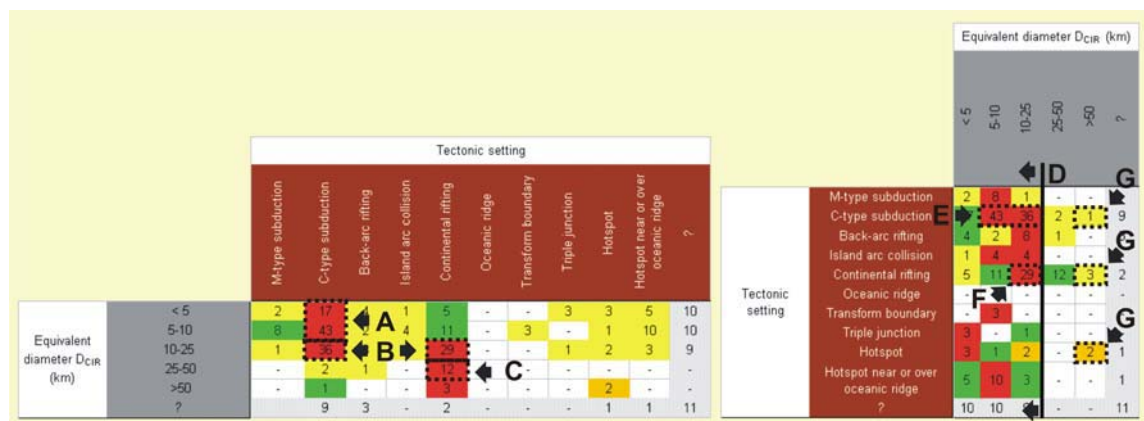


**Fig. 2.80:** Sections of the “CCDB DATA TABLE” represented in Figure 2.42. Here both relationships *CHARACTERISTICS* “Dimensions” to the *CHARACTERISTICS* “Tectonic setting” and vice versa. Squares are coloured according to the “MAXIMUM NORMALIZATION”.

❖ ***CHARACTERISTICS* “Dimensions” AND “Condition of the local structures”**

- Regardless of the caldera dimension, the local structures associated with the different calderas included in the CCDB (213 samples with condition of the local structures and dimensions information) are commonly extensional (64.8%, 138 samples) (Fig. 2.81 indication A).
- Large calderas ( $D_{CIR} > 25$  km) (20 samples with condition of the local structures information) are only related to extensional (90%, 18 samples) or shear-extensional (10%, 2 samples) local structures (Fig. 2.81 indication B).
- Calderas included in the CCDB with a  $D_{CIR} < 25$  km (241 samples with condition of the local structures and dimensions information) may have any type of the local structures (Fig. 2.81 indication C).

- Regardless of the type of local structures of the calderas included in the CCDB (213 samples with condition of the local structures and dimensions information) the most frequent dimensions are those associated with a  $D_{CIR} > 25$  (90.6%, 193 samples) (Fig. 2.81 indication D).
- From those calderas with extensional local structures (138 samples with dimensions information) a high percentage of calderas have a  $D_{CIR}$  between 5 km and 25 km (70.3%, 97 samples) (Fig. 2.81 indication E).
- The distribution of calderas with shear-extensional local structures (18 samples with dimensions information) has a moderate maximum at the *CATEGORY* “10 – 25 km” (61.1%, 11 samples) (Fig. 2.81 indication F).
- The size of those calderas associated with fault intersection (14 samples with dimensions information) is commonly comprised in the interval “5 – 10 km” (71.4%, 10 samples) (Fig. 2.81 indication G).

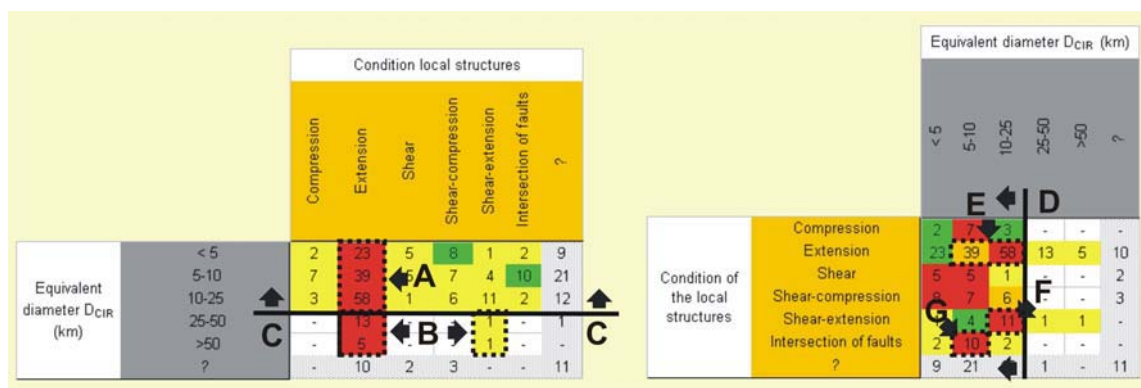


**Fig. 2.81:** Sections of the “CCDB DATA TABLE” represented in Figure 2.42. Here both relationships *CHARACTERISTICS* “Dimensions” to the *CHARACTERISTICS* “Condition of the local structures” and vice versa. Squares are coloured according to the “*MAXIMUM NORMALIZATION*”.

❖ ***CHARACTERISTICS* “Dimensions” AND “Type of pre-caldera edifice”**

- In calderas with a  $D_{CIR} < 25$  km (153 samples with type of pre-caldera edifice information) the most common type of pre-caldera edifice are stratovolcanoes and stratocones (58.2%, 89 samples) (Fig. 2.82 indication A).

- Calderas included in the CCDB with a  $D_{CIR} < 25$  km (153 samples with condition of the local structures and dimensions information) may have any type of pre-caldera edifice (Fig. 2.82 indication B).
- Regardless of the type of pre-caldera edifice, the most common dimensions for the different calderas included in the CCDB (154 samples with condition of the local structures and dimensions information) is those corresponding to a  $D_{CIR} < 25$  km (99.4%, 153 samples) (Fig. 2.82 indication C). For large calderas  $D_{CIR} > 25$  km (21 samples included in the CCDB) we only have information about the type of pre-caldera edifice from one sample (Fig. 2.82 indication D).
- From those calderas with stratovolcanoes and stratocones as pre-caldera edifice (89 samples with dimensions information) a high percentage has a  $D_{CIR}$  between 5 and 10 km (50.6%, 45 samples) and a high-medium percentage between 10 and 25 km (31.5%, 28 samples) (Fig. 2.82 indication E).
- From those calderas with shield volcanoes as pre-caldera edifice (28 samples with dimensions information) the majority of the samples have a  $D_{CIR} < 10$  km (89.9%, 25 samples) (Fig. 2.82 indication F).

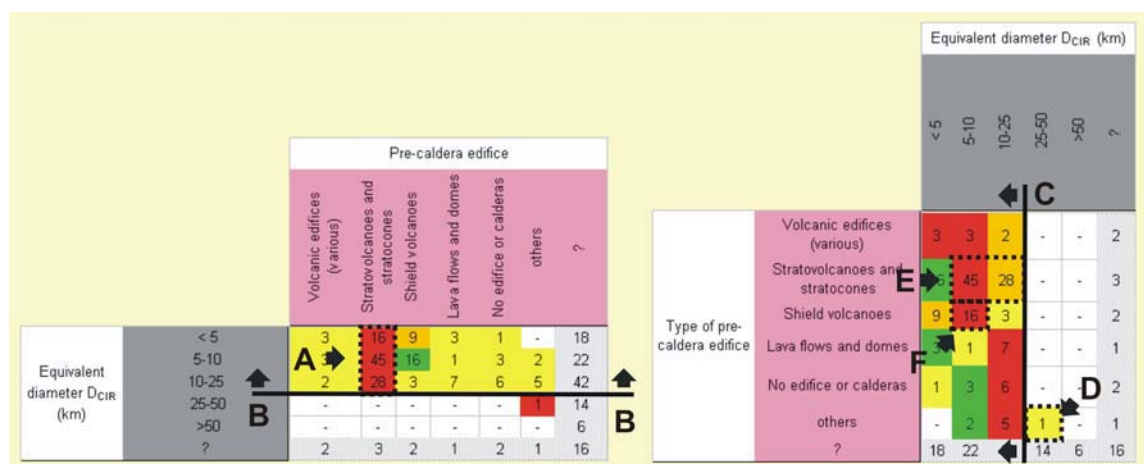


**Fig. 2.82:** Sections of the “CCDB DATA TABLE” represented in Figure 2.42. Here both relationships *CHARACTERISTICS* “Dimensions” to the *CHARACTERISTICS* “Type of pre-caldera edifice” and vice versa. Squares are coloured according to the “*MAXIMUM NORMALIZATION*”.

- ❖ **CHARACTERISTICS “Collapse type” AND “Volume of extruded deposits”/ “Volume of extruded magma”**
- Regardless of the collapse type, the volumes of deposits or magma extruded during the caldera-forming eruptions recorded in the CCDB (76 samples with information about the volume of extruded deposits or magma) are mainly smaller than 500 km<sup>3</sup> (88.2%, 67 samples) (Fig. 2.83 indication A).
- Only calderas with a plate/piston or trap-door collapse (24 and 11 samples with information about the volume of extruded deposits or magma, respectively) may have volumes of extruded deposits or magma over 500 km<sup>3</sup> (33.3%, 7 samples for plate/piston collapses and 18.2%, 2 samples for trap-door collapses) (Fig. 2.83 indication B).
- The caldera-forming eruptions included in the CCDB involving less than 500 km<sup>3</sup> of extruded material (76 samples with collapse type information) may present all the different collapse types considered in this analysis (Fig. 2.83 indication C).
- Those caldera-forming eruptions involving volumes of extruded material larger than 500 km<sup>3</sup> (9 samples with collapse type information) are only plate/piston type (77.8%, 7 samples) or trap-door type (22.2%, 2 samples) (Fig. 2.83 indication D).

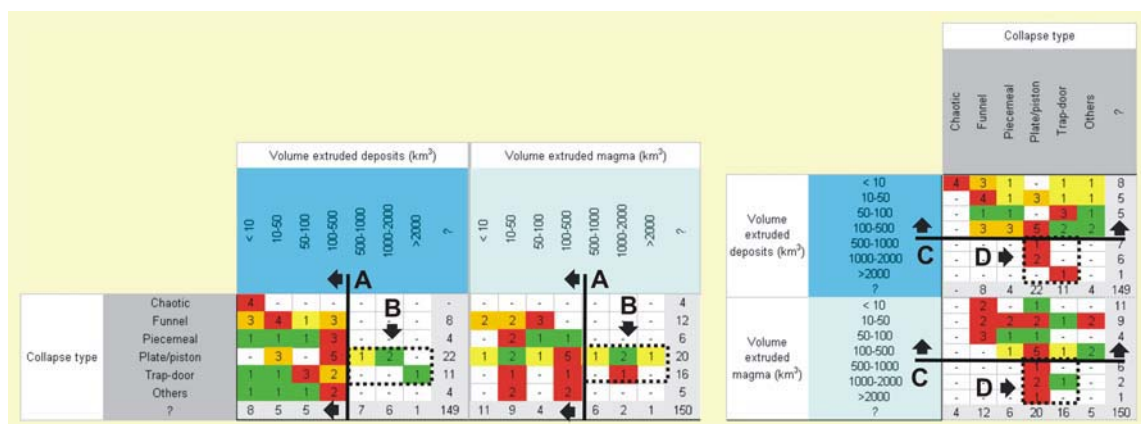


**Fig. 2.83:** Sections of the “CCDB DATA TABLE” represented in Figure 2.42. Here both relationships CHARACTERISTICS “Collapse type” to the CHARACTERISTICS “Volume of extruded deposits” and “Volume of extruded magma” and vice versa. Squares are coloured according to the “MAXIMUM NORMALIZATION”.

❖ **CHARACTERISTICS “Collapse type” AND “Crustal types”**

- Funnel collapse calderas (19 samples with crustal types information) are located mainly in areas of transitional thick crust (73.7%, 14 samples) (Fig. 2.84 indication A).
- From the plate/piston collapse calderas included in the CCDB (31 samples with crustal types information) a high percentage is located in areas of continental thin crust (51.6%, 16 samples) (Fig. 2.84 indication B).
- From the trap-door collapse calderas included in the CCDB (18 samples with crustal types information) a considerable percentage is located in areas of continental thick crust (61.1%, 11 samples) (Fig. 2.84 indication C).
- In areas of continental thick crust (18 samples with collapse type information) collapses are uniquely trap-door (61.1%, 11 samples) or plate/piston (38.9%, 7 samples) type (Fig. 2.84 indication D).
- Only continental thin crust (34 samples with collapse type information) houses calderas with all considered collapse types (Fig. 2.78 indication E) with a considerable maximum at the *CATEGORY* “Plate/piston” (47.1%, 16 samples) (Fig. 2.84 indication F).
- In areas of transitional thick crust (28 samples with collapse type information) collapses are mainly funnel type (50%, 14 samples) (Fig. 2.84 indication G).

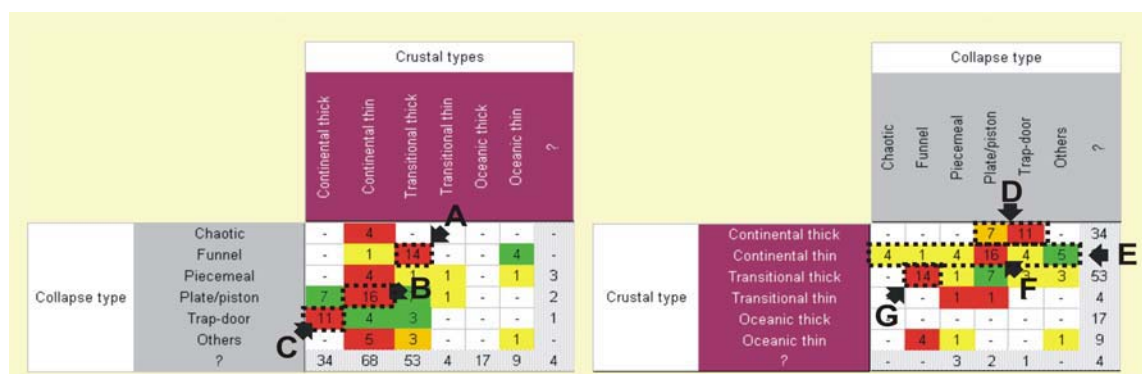


**Fig. 2.84:** Sections of the “CCDB DATA TABLE” represented in Figure 2.42. Here both relationships *CHARACTERISTICS* “Collapse type” to the *CHARACTERISTICS* “Crustal types” and vice versa. Squares are coloured according to the “*MAXIMUM NORMALIZATION*”.

- ❖ **CHARACTERISTICS “Collapse type” AND “Tectonic setting”**
- Funnel collapse calderas (19 samples with tectonic setting information) are located mainly C-type subduction zones (73.7%, 14 samples) (Fig. 2.85 indication A).
- From the plate/piston collapse calderas included in the CCDB (28 samples with tectonic setting information) a high percentage is located in areas of continental rifting (64.3%, 18 samples) (Fig. 2.85 indication B).
- Trap-door collapse calderas included in the CCDB (16 samples with tectonic setting information) are located uniquely in mainly C-type subduction zones (56.3%, 9 samples) and in areas of continental rifting (43.7%, 7 samples) (Fig. 2.85 indication C).
- Calderas located in C-type subduction zones (33 samples with collapse type information) are mainly funnel type (42.4%, 14 samples) or trap-door type (27.3%, 9 samples) (Fig. 2.85 indication D).
- Areas of continental rifting (28 samples with collapse type information) collapses are principally characterized by plate/piston collapse types (64.3%, 18 samples) (Fig. 2.85 indication E).

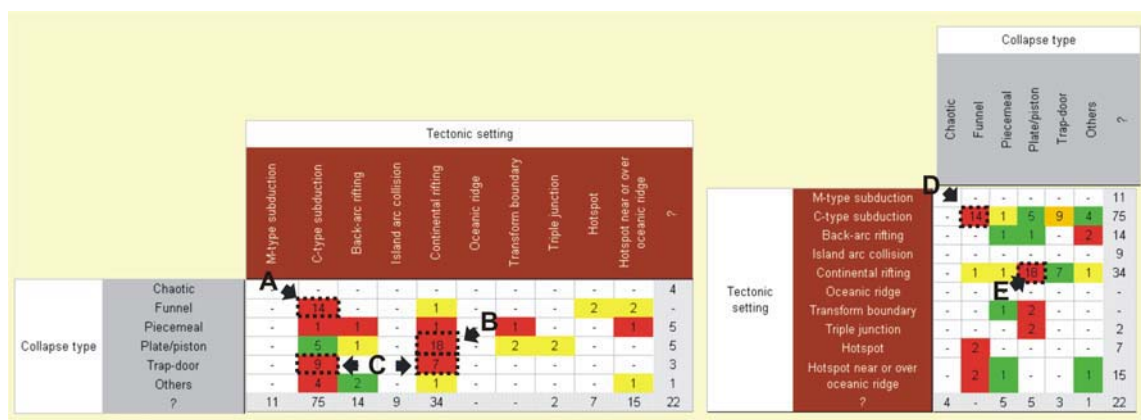


**Fig. 2.85:** Sections of the “CCDB DATA TABLE” represented in Figure 2.42. Here both relationships CHARACTERISTICS “Collapse type” to the CHARACTERISTICS “Tectonic setting” and vice versa. Squares are coloured according to the “MAXIMUM NORMALIZATION”.

❖ **CHARACTERISTICS “Collapse type” AND “Condition of the local structures”**

- Regardless of the collapse type (79 samples with information about the condition of the local structures) the most common structures are the extensional ones (73.4%, 58 samples) (Fig. 2.86 indication A).
- Compressional local structures (6 samples with collapse type information) are only associated with funnel (83.3%, 5 samples) and piecemeal (16.7%, 1 sample) collapse types (Fig. 2.86 indication B).
- Only extensional local structures may be associated with any collapse type (Fig. 2.86 indication C). However, from those samples associated with extensional local structures (58 samples with collapse type information) a considerable high percentage corresponds to plate/piston collapse type calderas (36.2%, 21 samples) and a more moderate one to trap-door-like collapses (20.7%, 12 samples) (Fig. 2.86 indication C).
- Shear-compressional local structures (4 samples with collapse type information) are only associated with trap-door (75%, 3 samples) and piecemeal (25%, 1 sample) collapse types (Fig. 2.86 indication E).

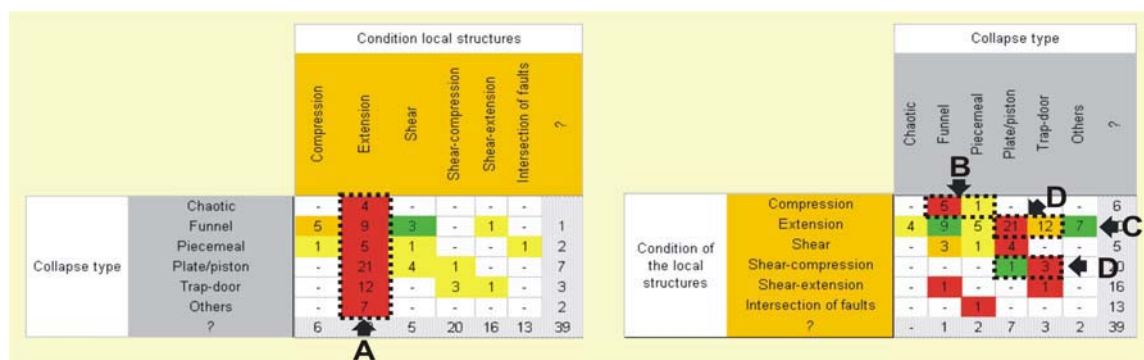


**Fig. 2.86:** Sections of the “CCDB DATA TABLE” represented in Figure 2.42. Here both relationships CHARACTERISTICS “Collapse type” to the CHARACTERISTICS “Condition of the local structures” and vice versa. Squares are coloured according to the “MAXIMUM NORMALIZATION”.

- ❖ **CHARACTERISTICS “Volume of extruded deposits”/ “Volume of extruded magma” AND “Composition of extruded magma”**
- Regardless the volume of deposits or magma extruded during the caldera-forming eruptions recorded in the CCDB (146 samples with information about the composition of the extruded magma), the most frequent composition of the extruded magma is calc-alkaline felsic (69.9%, 102 samples) (Fig. 2.87 indication A).
- Caldera-forming eruptions involving volumes of extruded material > 500 km<sup>3</sup> (32 samples with information about the composition of the extruded magma) may be mainly related to magmas of calc-alkaline felsic composition (96.9%, 31 samples) and one sample to calc-alkaline intermediate magma (Fig. 2.87 indication B).
- Caldera-forming eruptions involving alkaline magmas (10 samples with information about the volumes of the extruded deposits or magma) involve volumes of extruded material < 500 km<sup>3</sup> (Fig. 2.87 indication C).
- Calderas with a calc-alkaline felsic composition of the extruded magmas (146 samples with information about the volumes of the extruded deposits or magma) are the unique covering the whole range of volumes of extruded deposits or magma (Fig. 2.81 indication D). Moreover, a considerable percentage of these calc-alkaline felsic caldera-forming eruptions involve volumes of extruded magma between 100 and 500 km<sup>3</sup> (20.5%, 30 samples) and also significant is the number of samples with volumes included in the *CATEGORY* “10 – 50 km<sup>3</sup>” (16.4%, 24 samples) (Fig. 2.87 indication E).

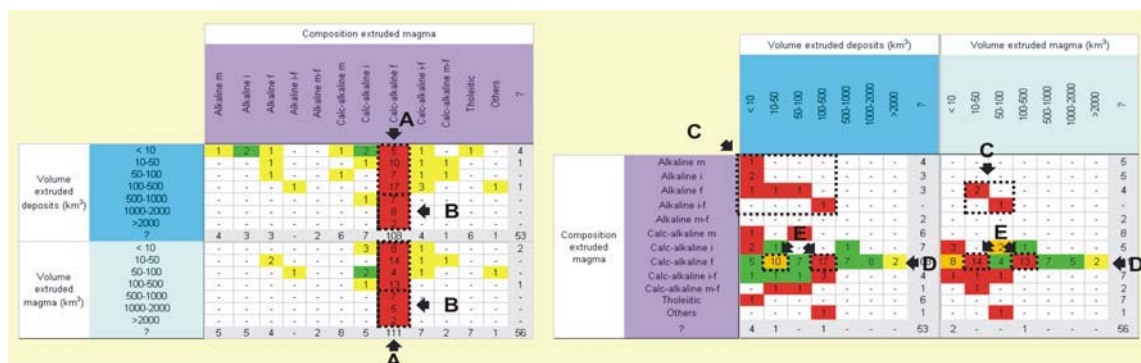


**Fig. 2.87:** Sections of the “CCDB DATA TABLE” represented in Figure 2.42. Here both relationships *CHARACTERISTICS* “Volume of extruded deposits” and “Volume of extruded magma” to the *CHARACTERISTICS* “Composition of extruded magma” and vice versa. Squares are shaded according to the “*MAXIMUM NORMALIZATION*”.

- ❖ **CHARACTERISTICS “Volume of extruded deposits”/ “Volume of extruded magma” AND “Crustal types”**
- Regardless of the volume of deposits or magma extruded during the caldera-forming eruptions recorded in the CCDB (150 samples with information about the volume of extruded material and about the crustal type) the most frequent crustal types are the continental thin (46.7%, 70 samples), transitional thick (26.7%, 40 samples) and continental thick (23.3 %, 35 samples) crust (Fig. 2.88 indication A). In fact, calderas related to caldera-forming eruptions involving less than 500 km<sup>3</sup> of extruded magma may be located in all three crustal types (Fig. 2.88 indication B). However, caldera-forming eruptions involving volumes of deposits or magma larger than 500 km<sup>3</sup> (32 samples with crustal types information a) are located only in areas of continental thin (53.1%, 17 samples) and continental thick (46.9%, 15 samples) crust (Fig. 2.88 indication C).
  - Hardly any caldera sample located in areas of transitional thin, oceanic thick or oceanic thin crust have information about the volume of extruded material during the caldera-forming eruption. Data exist for only three samples (Fig. 2.88 indication D).
  - Only those calderas associated with continental thick and thin crust are associated with any volume of extruded material (Fig. 2.88 indication E).
  - Calderas located in transitional thick crust (40 samples with information about the volume of extruded material) are uniquely associated with caldera-forming eruptions involving volumes of extruded material smaller than 500 km<sup>3</sup> (Fig. 2.88 indication F). Moreover, smaller volumes (< 10 km<sup>3</sup>) appear to be more frequent (42.5%, 17 samples) (Fig. 2.88 indication G).

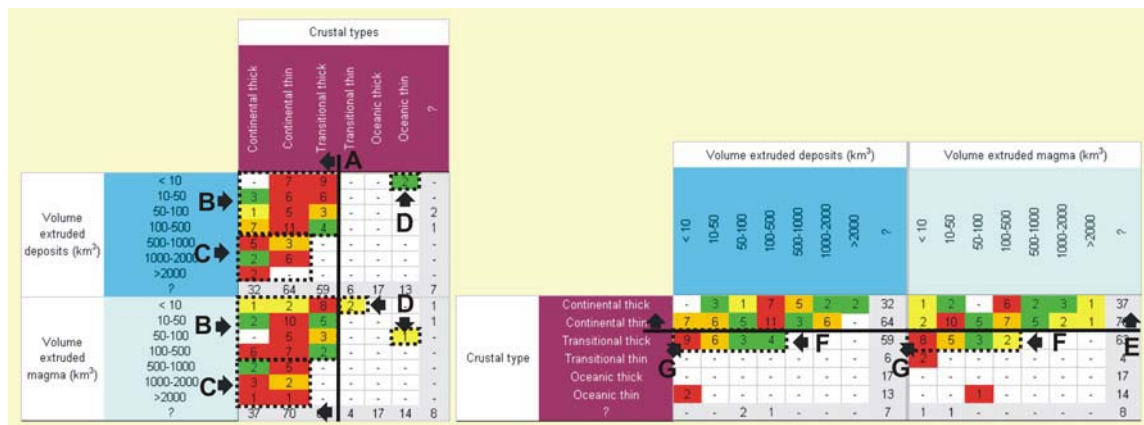


**Fig. 2.88:** Sections of the “CCDB DATA TABLE” represented in Figure 2.42. Here both relationships *CHARACTERISTICS* “Volume of extruded deposits” and “Volume of extruded magma” to the *CHARACTERISTICS* “Crustal types” and vice versa. Squares are coloured according to the “MAXIMUM NORMALIZATION”.

❖ ***CHARACTERISTICS* “Volume of extruded deposits”/ “Volume of extruded magma” AND “Tectonic setting”**

- Caldera-forming eruptions involving volumes of extruded material smaller than 50 km<sup>3</sup> (51 samples with tectonic setting information) are mainly located in C-type subduction zones (56.9%, 29 samples) (Fig. 2.89 indication A).
- From those caldera-samples included in the *CATEGORIES* “100 – 500 km<sup>3</sup>” of both *CHARACTERISTICS* “Volume of extruded deposits” and “Volume of extruded magma” (36 samples with tectonic setting information) a high percentage is located in areas of continental rifting (69.4%, 25 samples) (Fig. 2.89 indication B).
- Caldera-forming eruptions involving volumes of deposits or magma larger than 500 km<sup>3</sup> (32 samples with tectonic setting information) are located in a high proportion in areas of continental rifting (65.6%, 21 samples) and a considerable lower percentage is in C-type subduction zones (15.6%, 5 samples), hotspots (12.5%, 4 samples) and areas of back-arc rifting (6.3%, 2 samples) (Fig. 2.89 indication C).
- Only areas of continental rifting or C-type subduction zones house caldera-forming eruptions involving volumes of extruded material of almost all *CATEGORIES* (Fig. 2.89 indication D).

- From those caldera-forming eruptions located in C-type subduction zones (51 samples with information about the volume of extruded deposits) a relatively high percentage involves volumes smaller than 50 km<sup>3</sup> (60.8%, 31 samples) (Fig. 2.89 indication E).
- Caldera-forming eruptions located in areas of continental rifting (60 samples with tectonic setting information) involve mainly volumes of extruded deposits or magma between 100 and 500 km<sup>3</sup> (41.7%, 25 samples) (Fig. 2.89 indication F).



**Fig. 2.89:** Sections of the “CCDB DATA TABLE” represented in Figure 2.42. Here both relationships *CHARACTERISTICS* “Volume of extruded deposits” and “Volume of extruded magma” to the *CHARACTERISTICS* “Tectonic setting” and vice versa. Squares are coloured according to the “MAXIMUM NORMALIZATION”.

❖ ***CHARACTERISTICS* “Volume of extruded deposits”/ ”Volume of extruded magma” AND “Condition of the local structures”**

- Regardless of the volume of deposits or magma extruded during the caldera-forming eruptions recorded in the CCDB (142 samples with information about the condition of the local structures) the most common associated local structures are the extensional ones (73.2%, 104 samples) (Fig. 2.90 indication A).
- Caldera-forming eruptions involving volumes of deposits or magma larger than 500 km<sup>3</sup> (32 samples with information about the condition of the local structures) are associated only to extensional (87.5%, 28 samples) or shear-extensional structures (12.5%, 4 samples) (Fig. 2.90 indication B).
- Only caldera-forming eruptions involving volumes of deposits or magma smaller than 500 km<sup>3</sup> (123 samples with tectonic setting information) may be associated with all possible condition of local structures (Fig. 2.90 indication C).

- Only extensional local structures may be associated with any volume of extruded material during the caldera-forming eruption (Fig. 2.90 indication D). Furthermore, from those caldera-forming eruptions associated with extensional local structures (104 samples with information about the volume of extruded deposits) a high percentage involves volumes between 100 and 500 km<sup>3</sup> (30.8%, 32 samples) (Fig. 2.90 indication E).

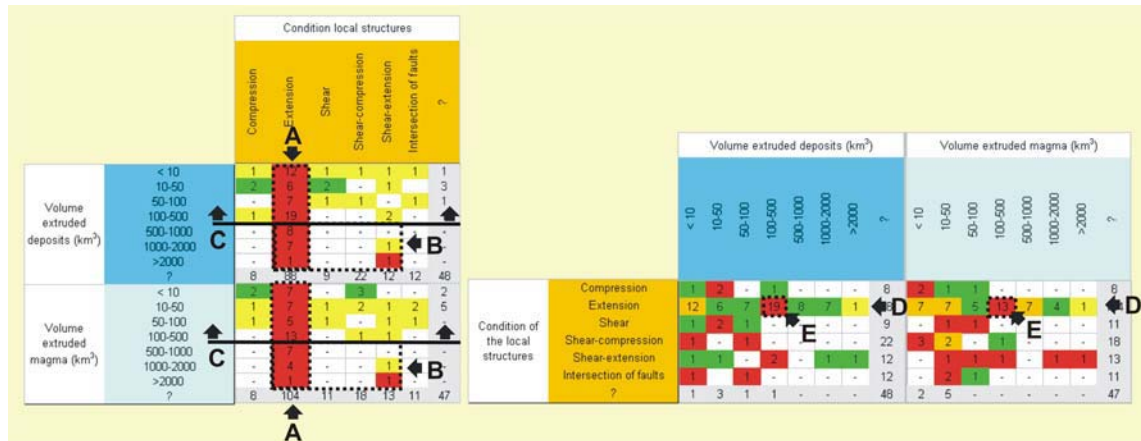


**Fig. 2.90:** Sections of the “CCDB DATA TABLE” represented in Figure 2.42. Here both relationships *CHARACTERISTICS* “Volume of extruded deposits” and “Volume of extruded magma” to the *CHARACTERISTICS* “Condition of the local structures” and vice versa. Squares are coloured according to the “MAXIMUM NORMALIZATION”.

❖ ***CHARACTERISTICS* “Volume of extruded deposits”/ “Volume of extruded magma” AND “Type of pre-caldera edifice”**

- Caldera-forming eruptions involving volumes of deposits or magma larger than 500 km<sup>3</sup> (4 samples with information about the volume of extruded deposits) may be uniquely associated with lava flows, domes or collapse calderas or without previous eruptions (Fig. 2.91 indication A).
- Calderas with a volcanic edifice previous to the caldera-forming eruption (39 samples with information about the volume of extruded deposits) are restricted to volumes of extruded deposits or magma smaller than 500 km<sup>3</sup> (Fig. 2.91 indication B).

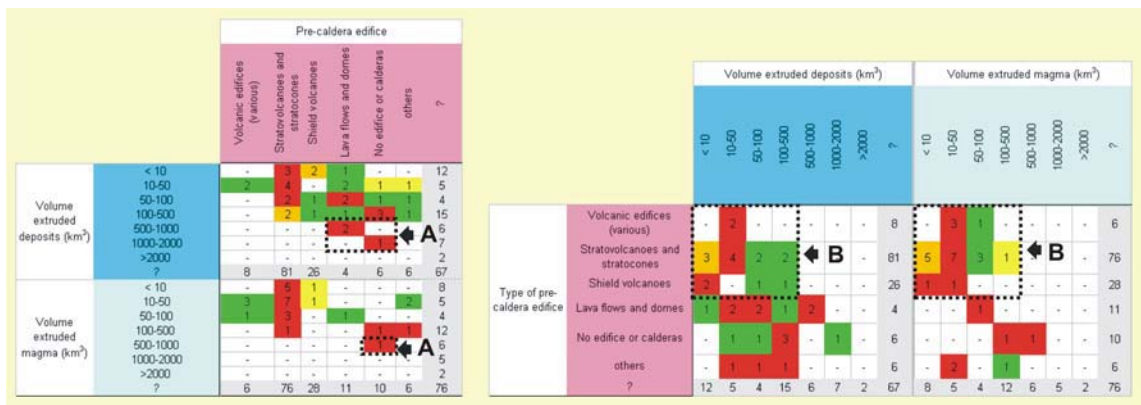


**Fig. 2.91:** Sections of the “CCDB DATA TABLE” represented in Figure 2.42. Here both relationships *CHARACTERISTICS* “Volume of extruded deposits” and “Volume of extruded magma” to the *CHARACTERISTICS* “Type of pre-caldera edifice” and vice versa. Squares are coloured according to the “MAXIMUM NORMALIZATION”.

❖ **CHARACTERISTICS “Composition of extruded magma” AND “Crustal types”**

- Only caldera-forming eruptions involving calc-alkaline felsic magma (157 samples with tectonic setting information) may be associated with all possible crustal types (Fig. 2.92 indication A). However, the most abundant are continental thin (39.5%, 62 samples) and thick (22.3%, 35 samples) and transitional thick crusts (28.7%, 45 samples) (Fig. 2.92 indication B).
- Regardless of the crustal type the most abundant composition (except for thin transitional and oceanic crust) is the calc-alkaline felsic one (Fig. 2.92 indication C).

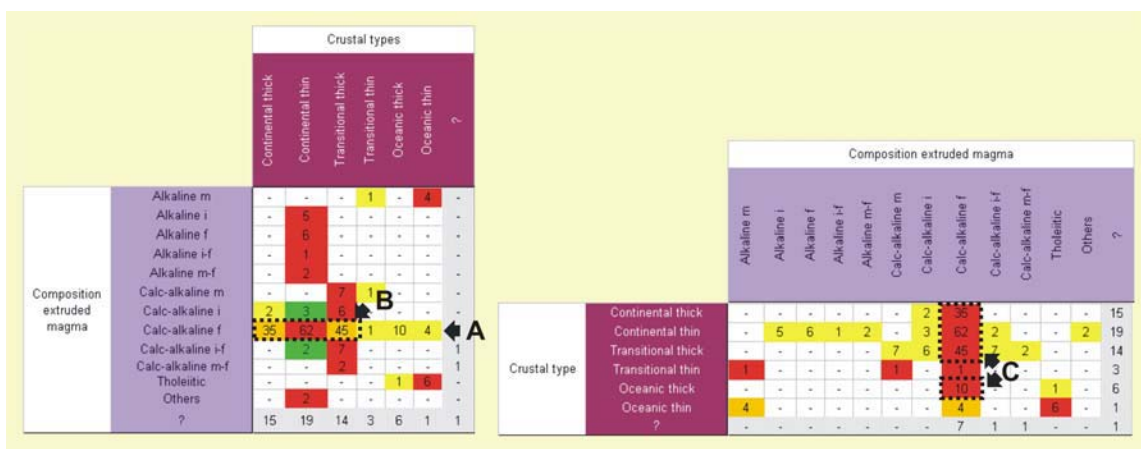


**Fig. 2.92:** Sections of the “CCDB DATA TABLE” represented in Figure 2.42. Here both relationships *CHARACTERISTICS* “Composition of extruded magma” to the *CHARACTERISTICS* “Crustal types” and vice versa. Squares are coloured according to the “MAXIMUM NORMALIZATION”.

❖ **CHARACTERISTICS “Composition of extruded magma” AND “Type of pre-caldera edifice”**

- Regardless of the composition of the magma extruded during the caldera-forming eruptions recorded in the CCDB (200 samples with pre-caldera edifice information) normally the most abundant associated pre-caldera edifices are stratovolcanoes and stratocones (37.5%, 75 samples) and shield volcanoes (13%, 26 samples) (Fig. 2.93 indication A).
- Only caldera-forming eruptions involving calc-alkaline felsic magma (92 samples with pre-caldera edifice information) may be associated with all possible types of pre-caldera edifices (Fig. 2.86 indication B). However, the most abundant are stratovolcanoes and stratocones (66.3%, 61 samples) (Fig. 2.93 indication C).
- Regardless of the type of pre-caldera edifice the most abundant composition is the calc-alkaline felsic one (Fig. 2.93 indication D).

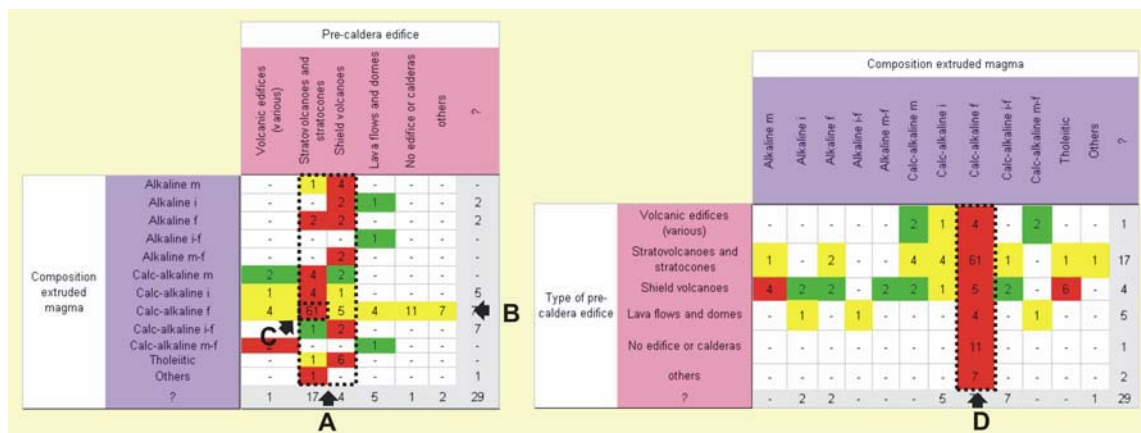


**Fig. 2.93:** Sections of the “CCDB DATA TABLE” represented in Figure 2.42. Here both relationships CHARACTERISTICS “Composition of extruded magma” to the CHARACTERISTICS “Type of pre-caldera edifice” and vice versa. Squares are coloured according to the “MAXIMUM NORMALIZATION”.

❖ **CHARACTERISTICS “Composition of extruded magma” AND “Type of collapse precursor”**

- Regardless of the composition of the magma extruded during the caldera-forming eruptions recorded in the CCDB (62 samples with information about the type of collapse

- precursor) the most common associated collapse precursor is a previous eruption (75.8%, 47 samples) (Fig. 2.94 indication A).
- Only caldera-forming eruptions involving calc-alkaline felsic magma (37 samples with pre-caldera edifice information) may be associated with all possible types of collapse precursors (Fig. 2.94 indication B). However, the most abundant are previous eruptions (59.5%, 22 samples) (Fig. 2.94 indication C).
- Only the *CATEGORY* “Previous eruption” may be related to almost all *CATEGORIES* of the *CHARACTERISTIC* “Composition of extruded magma” (Fig. 2.94 indication D).
- Independent on the type of collapse precursor the most abundant composition is the calc-alkaline felsic one (Fig. 2.94 indication E).

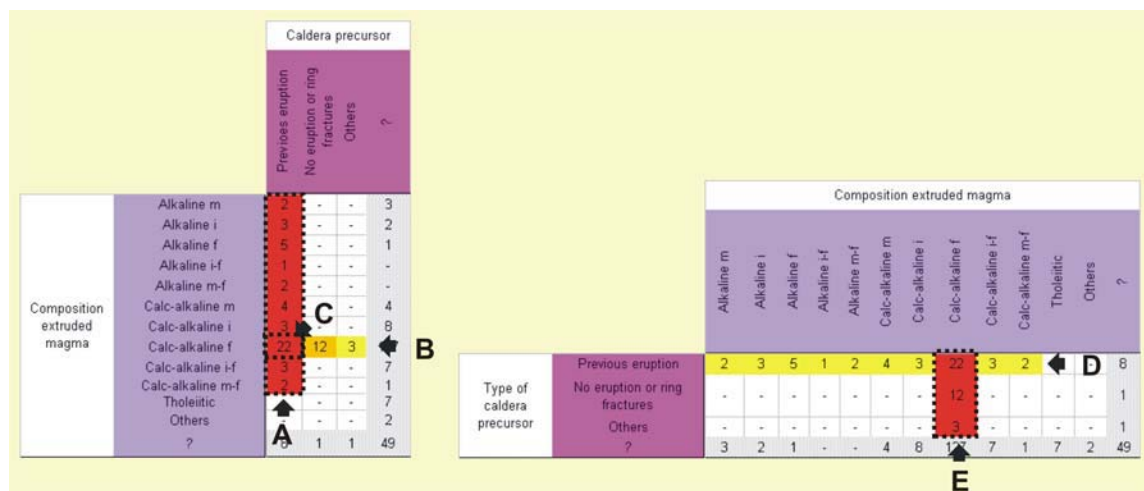


**Fig. 2.94:** Sections of the “CCDB DATA TABLE” represented in Figure 2.42. Here both relationships *CHARACTERISTICS* “Composition of extruded magma” to the *CHARACTERISTICS* “Type of collapse precursor” and vice versa. Squares are coloured according to the “*MAXIMUM NORMALIZATION*”.

❖ ***CHARACTERISTICS* “Composition of extruded magma” AND “Type of post-caldera volcanic activity”**

- Only caldera-forming eruptions involving calc-alkaline felsic magmas (59 samples with post-caldera volcanic activity information) may be associated with all possible types of post-caldera volcanic activity (Fig. 2.95 indication A). However, the most abundant are the

volcanic activities type-C (25.4%, 15 samples), type-R (15.3%, 9 samples) and type-S (15.3%, 9 samples) (Fig. 2.95 indication B).

- Regardless of the type of post-caldera volcanic activity of the calderas recorded in the CCDB (83 samples with information about the composition of the extruded magma) the calc-alkaline felsic composition is the most common one (71.1%, 59 samples) (Fig. 2.95 indication C).

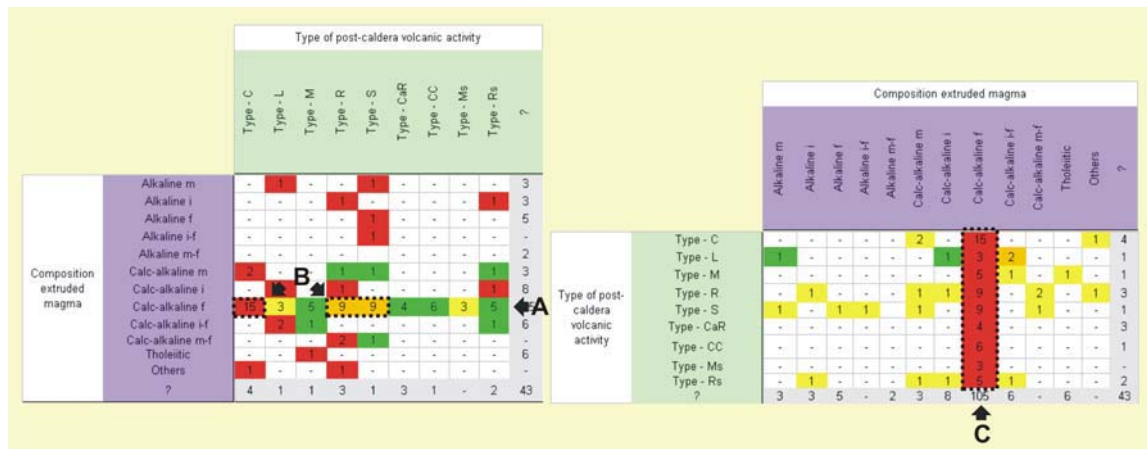
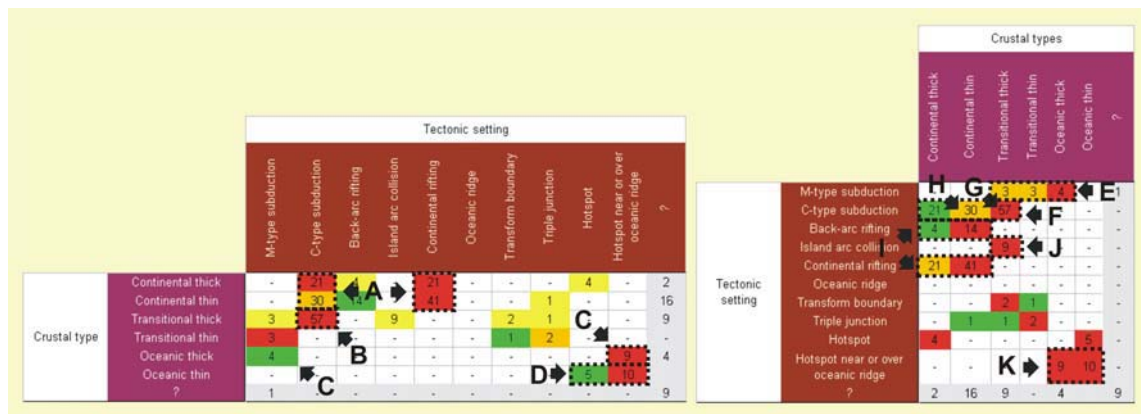


Fig. 2.95: Sections of the “CCDB DATA TABLE” represented in Figure 2.42. Here both relationships CHARACTERISTICS “Composition of extruded magma” to the CHARACTERISTICS “Type of post-caldera volcanic activity” and vice versa. Squares are shaded according to the “MAXIMUM NORMALIZATION”.

❖ CHARACTERISTICS “Crustal types” AND “Tectonic setting”

- Calderas located in continental thick and continental thin crust (50 and 86 samples with tectonic setting information, respectively) are related mainly to C-type subduction zones (42%, 21 samples in continental thick crust and 34.5%, 30 samples in continental thin crust) and areas of continental rifting (42%, 21 samples in continental thick crust and 47.7%, 41 samples in continental thin crust) (Fig. 2.96 indication A).
- Calderas located in transitional thick crust (72 samples with tectonic setting information) are associated basically with C-type subduction zones (79.2%, 57 samples) (Fig. 2.96 indication B).

- 
- Calderas in areas of oceanic thick crust (13 samples with tectonic setting information) are principally related to hotspots close or over oceanic ridges (69.2%, 9 samples) and M-type subduction zones (30.8%, 4 samples) (Fig. 2.96 indication C).
  - Calderas in areas of oceanic thin crust (15 samples with tectonic setting information) are principally related to hotspots close or over oceanic ridges (66.7%, 10 samples) and hotspots (33.3%, 5 samples) (Fig. 2.96 indication D).
  - Calderas associated with M-type subduction zones (10 samples with crustal type information) are related only to transitional thin and thick crust, as well as oceanic thick crust (Fig. 2.96 indication E).
  - Calderas located in C-type subduction zones (117 samples with crustal type information) are associated only with continental thick and thin crust and transitional thick crust (Fig. 2.96 indication F).
  - The distribution of those calderas located in C-type subduction zones according to the crustal type has a maximum at the *CATEGORY* “Transitional thick” (48.7%, 57 samples) (Fig. 2.96 indication G) and a moderate maximum at “Continental thin” (33.3%, 39 samples) (Fig. 2.96 indication H).
  - Calderas located in areas of back-arc rifting or continental rifting (19 and 62 samples with crustal type information, respectively) are associated only with continental thick and thin crust (Fig. 2.96 indication I) with the a higher percentage of samples in the *CATEGORY* “Continental thin” (73.4%, 14 samples in areas of back-arc rifting and 66.1%, 41 samples in areas of continental rifting).
  - Calderas associated with island arc collision are related only to transitional thick crust (Fig. 2.96 indication J).
  - Calderas located in hotspots near or close an oceanic ridge are associated only with oceanic thick and thin crust (Fig. 2.96 indication K).



**Fig. 2.96:** Sections of the “CCDB DATA TABLE” represented in Figure 2.42. Here both relationships CHARACTERISTICS “Crustal types” to the CHARACTERISTICS “Tectonic setting” and vice versa. Squares are coloured according to the “MAXIMUM NORMALIZATION”.

❖ **CHARACTERISTICS “Crustal types” AND “Condition of the local structures”**

- Except for those calderas located in areas of transitional thin crust, the rest of samples (222 samples with information about the crustal types and the condition of the local structures) the most common associated local structures are the extensional ones (63.5%, 145samples) (Fig. 2.97 indication A).
- Calderas with associated compressional local structures (12 samples with crustal type information) are located mainly transitional thick crust (91.7%, 11 samples in continental thick crust and 34.5%, 30 samples in continental thin crust) and only one sample in transitional thin crust (8.3%) (Fig. 2.97 indication B).
- Only extensional local structures (146 samples with crustal type information) may be associated with all the different crustal types considered in the classification (Fig. 2.97 indication C).
- Extensional local structures (146 samples with crustal type information) are mainly associated with in continental thin crust (45.2%, 66 samples) and in a lower proportion with continental thick crust (17.6%, 39 samples) (Fig. 2.97 indication D).

- Shear and shear-compressional local structures (13 and 24 samples with crustal type information, respectively) are more abundant in areas of transitional thick crust (61.5%, 8 samples with shear local structures and 54.2%, 13 samples with shear-compressional local structures) (Fig. 2.97 indication E).
- Shear-extensional local structures and areas with intersecting faults (18 and 14 samples with crustal type information, respectively) are more abundant in areas of continental thin crust (55.6%, 10 samples with shear local structures and 42.9%, 6 samples with shear-compressional local structures) (Fig. 2.97 indication F).

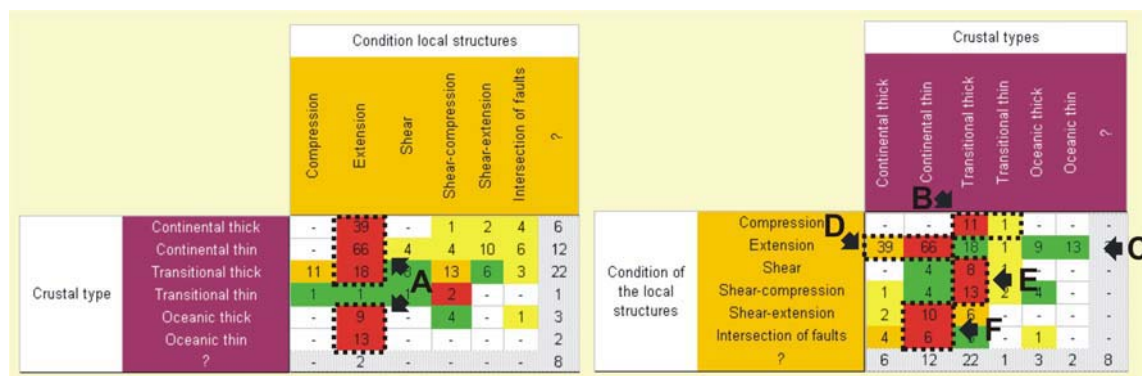


**Fig. 2.97:** Sections of the “CCDB DATA TABLE” represented in Figure 2.42. Here both relationships *CHARACTERISTICS* “Crustal types” to the *CHARACTERISTICS* “Condition of the local structures” and vice versa. Squares are coloured according to the “MAXIMUM NORMALIZATION”.

#### ❖ *CHARACTERISTICS* “Crustal types” AND “Type of pre-caldera edifice”

- Except for those calderas located in areas of oceanic thin crust, the rest of samples (158 samples with information about the crustal types and the type of pre-caldera edifice) the most common of pre-caldera edifices are stratovolcanoes and stratocones (54.4%, 86 samples) (Fig. 2.98 indication A).
- Calderas located transitional thin crust and oceanic thin or thick crust, have uniquely (except for Oskjuvatn caldera in Iceland) stratocones, stratovolcanoes or shield volcanoes as pre-caldera edifices (Fig. 2.98 indication B).

- Only stratovolcanoes or stratocones (91 samples with crustal type information) and shield volcanoes (11 samples with crustal type information) may be associated with all the different crustal types considered in the classification (Fig. 2.98 indication C).
- Collapse calderas with associated pre-caldera stratovolcanoes or stratocones (91 samples with crustal type information) are mainly located in transitional thick (38.5%, 35 samples) and in a lower proportion in continental thin crust (27.7%, 66 samples) (Fig. 2.98 indication D).
- Collapse calderas in the CATEGORIES “Lava flows and domes” (10 samples with crustal type information) and “No edifice or caldera” (9 samples with crustal type information) are uniquely located in continental thick and thin crust and transitional thick crust (Fig. 2.98 indication E).

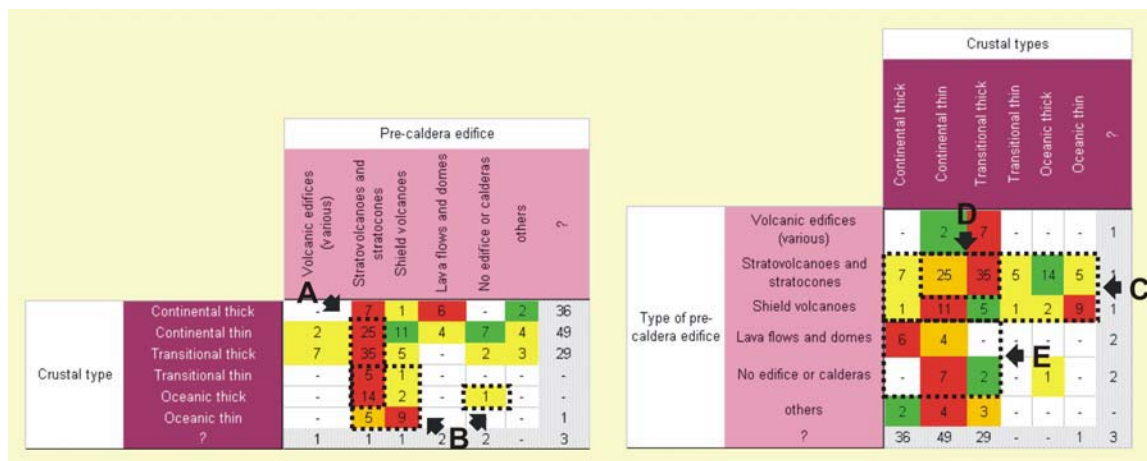


**Fig. 2.98:** Sections of the “CCDB DATA TABLE” represented in Figure 2.42. Here both relationships CHARACTERISTICS “Crustal types” to the CHARACTERISTICS “Type of pre-caldera edifice” and vice versa. Squares are coloured according to the “MAXIMUM NORMALIZATION”.

❖ **CHARACTERISTICS “Tectonic setting” AND “Condition of the local structures”**

- Calderas located in M-type subduction zones (11 samples with information about the nature of the local structures) are mainly associated with shear-compressional local structures (72.7%, 8 samples) (Fig. 2.99 indication A).

- Only calderas located in C-type subduction zones (87 samples with information about the nature of the local structures) may be associated with all different types of local structures (Fig. 2.91 indication B). However, the most abundant are the extensional ones (34.5%, 8 samples) (Fig. 2.99 indication C).
- Calderas associated with areas of back-arc rifting or hotspots (14 and 6 samples with information about the nature of the local structures) are mainly related to extensional local structures (92.9%, 13 samples located in areas of back-arc rifting and 83.3%, 5 samples located in hotspots) (Fig. 2.99 indication D). The rest of samples are associated with local fault intersection.
- Calderas samples in areas of continental rifting or hotspots near or over oceanic ridges (62 and 19 samples with information about the nature of the local structures) are uniquely related to extensional local structures (Fig. 2.99 indication E).
- All types of local structures, except extensional ones, are mainly related to C-type subduction zones (Fig. 2.99 indication F).
- Extensional local structures (131 samples with tectonic setting information) are mainly associated with areas of continental rifting (47.3%, 62 samples) (Fig. 2.99 indication G).

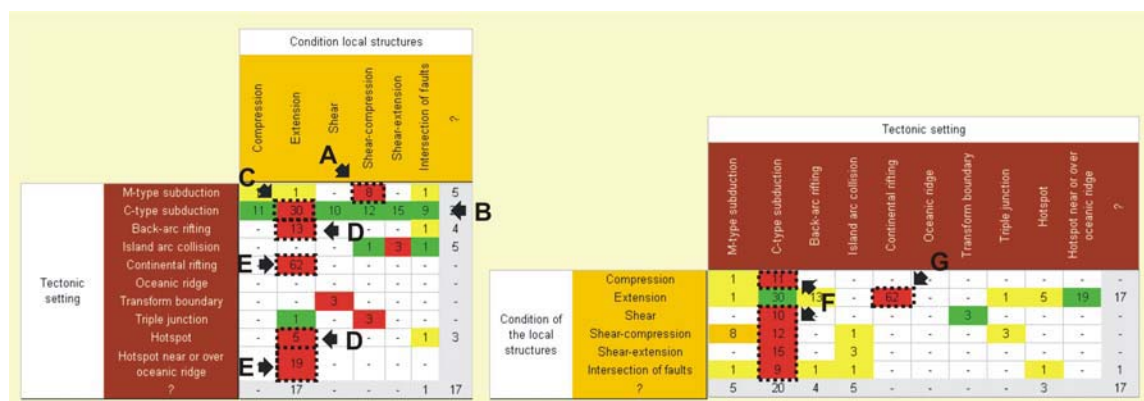


**Fig. 2.99:** Sections of the “CCDB DATA TABLE” represented in Figure 2.42. Here both relationships *CHARACTERISTICS* “Tectonic setting” to the *CHARACTERISTICS* “Condition of the local structures” and vice versa. Squares are coloured according to the “MAXIMUM NORMALIZATION”.

- ❖ **CHARACTERISTICS “Tectonic setting” AND “Type of pre-caldera edifice”**
- Only calderas located in C-type subduction zones and in areas of continental rifting may be associated with all different types of pre-caldera edifice (Fig. 2.100 indication A).
- Calderas located in M-type and C-type (11 and 66 samples with information about the type of pre-caldera edifice, respectively) subduction zones are mainly associated with stratovolcanoes and stratocones (90.9%, 10 samples in M-type subduction zones and 63.4%, 45 samples in C-type subduction zones) (Fig. 2.100 indication B).
- A high percentage of calderas with areas stratovolcanoes or stratocones as pre-caldera edifice (81 samples with information about the tectonic setting) are mainly located in C-type subduction zones (55.6%, 45 samples) (Fig. 2.100 indication C).

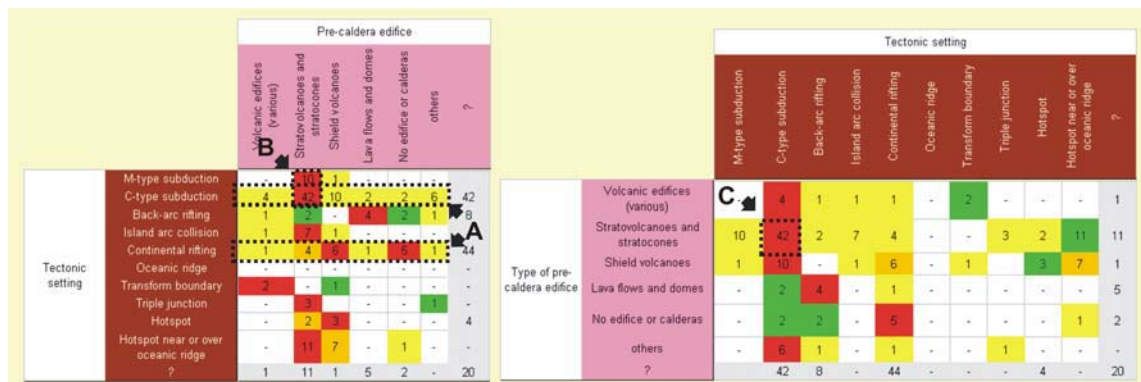


**Fig. 2.100:** Sections of the “CCDB DATA TABLE” represented in Figure 2.42. Here both relationships CHARACTERISTICS “Tectonic setting” to the CHARACTERISTICS “Type of pre-caldera edifice” and vice versa. Squares are coloured according to the “MAXIMUM NORMALIZATION”.

## II.5.7 Discussion

### II.5.7.1 Introduction and general aspects

The main goal of this section is twofold. First, we want to compare our results with those from previous works. This allows us to validate, at least partially, the information contained in the CCDB and to check some previous classification such as the caldera compositional classification (see section II.3.4.4) and the post-caldera

volcanic activity classification (see section II.3.6), also based on literature surveys on calderas. Second, this section is also a discussion of all results presented in sections II.5.6.1 and II.5.6.2.

#### *II.5.7.2 Comparing results obtained with the compositional classification*

We have explained in section II.3.4.4 that Cole et al. (2004) proposed a compositional classification of collapse calderas. These authors admit that there is not a direct relationship between composition and the caldera type and that many calderas may show more than just one composition (see section II.3.4.4 for more details). In this section we want to compare their results with those obtained in our analysis. First of all, we notice that the categories considered in the work of Cole et al., (2004) are conceptually different from our *CATEGORIES*. Whereas they consider four different compositional categories partially independent of the corresponding rock suite (basaltic, andesitic-dacitic, peralkaline and rhyolite calderas), we classify the compositions according to specific rock suites (see section II.5.4). We consider more it logical to assign the composition following the latter criteria, since this reflects the influence of the tectonic setting and the type of crust (Best and Christiansen, 2001), some of the main parameters controlling magma composition (see section I.1.2). In fact, both classifications have discrepancies and similarities. On the one hand, we can correlate the group of “basaltic calderas” proposed by Cole et al. (2004) with our *CATEGORIES* “Calc-alkaline mafic”, “Alkaline mafic” and “Tholeiitic”. However, whereas the classification of Cole et al. (2004) includes andesites and dacites in the same group, we consider the first group as calc-alkaline intermediate and the second as calc-alkaline felsic, jointly with the rhyolites. Consequently, the results of both classifications are not directly comparable.

Anyway, we can analyse the different statements of the work of Cole et al. (2004) with the calderas included in our CCDB. In connection with the group of “basaltic calderas” these authors affirm that these calderas are characteristic of oceanic intraplate hot spot or divergent plates boundaries in a mid-ocean ridge situation (see section II.3.4.4). However, the CCDB contains some samples located in C-type subduction zones (e.g. Santiago – *Nicaragua*, Rymer et al., 1998). Furthermore, we can add that the “basaltic calderas” are all small in size ( $D_{CIR} < 10$  km) and the related

caldera-forming eruptions involve small volumes ( $< 10 \text{ km}^2$ ) of extruded material. However, it is also necessary to mention that there is not a preferential collapse type. “Basaltic calderas” may be funnel (e.g. Kilauea – *Hawaii*, Walker, 1988), piecemeal (e.g. Sierra Negra - *Galapagos*, Munro and Rowland, 1996) or plate/piston (e.g. Nindiri – *Nicaragua*, Rymer et al., 1998).

Regarding the group of “andesitic-dacitic” calderas, Cole et al. (2004) state that these are typical of continental margins and of volcanoes in island arcs located at convergent plate boundaries. However, the CCDB comprises some samples in areas of continental rifting (e.g. Monroe Peak - *U.S.A.*, Lipman, 1984; Steven et al., 1984). Additionally, the authors assert that these calderas typically entail the destruction of stratocones. This can be confirmed with the samples included in the CCDB. Almost all of them (except Monroe Peak caldera) are related to pre-caldera stratovolcanoes or cones, but also to shield volcanoes (e.g. Hakone II – *Japan*, Kuno et al., 1970; Aramaki, 1984). Furthermore, we can add that these calderas may also be funnel (e.g. Mashu – *Japan*, Spera and Crisp, 1981; Aramaki, 1984), piecemeal (e.g. Dorobu – *Japan*, Miura and Tamai, 1998) or plate/piston (e.g. Creed – *U.S.A.*, Ratté and Steven, 1967; Steven and Lipman, 1976; Lipman, 1984). Moreover, their size may vary from  $D_{\text{CIR}} < 5 \text{ km}$  (e.g. Sete Cidades – *Açores*, Newhall and Dzurisin, 1988 and references therein) to 25 – 50 km (e.g. Cerro Galán – *Argentina*, Sparks et al., 1985; Francis et al., 1983, 1989) and the volumes of extruded deposits from  $< 10 \text{ km}^3$  (e.g. Ikeda – *Japan*, Spera and Crisp, 1981) to 500 – 1000  $\text{km}^3$  (e.g. Platoro – *U.S.A.*, Spera and Crisp, 1981; Lipman, 1984).

Comparing the information in the CCDB on peralkaline calderas against the affirmation of Cole et al. (2004) we find that these calderas are located on rifting zones or in areas of unusually high rates of localized extension in convergent margins. Again, these calderas may be of different types (e.g. “Trap-door” Bolsena – *Italy*, Nappi et al., 1991; “Piecemeal” Phlegraean Fields I – *Italy*, Barberi et al., 1991; Scandone et al., 1991; “Plate/piston” Vepe – *Italy*, Nappi et al., 1991). In addition, their size may vary from  $D_{\text{CIR}} < 5 \text{ km}$  (e.g. Vepe – *Italy*) to 10 - 25 km (e.g. Bolsena – *Italy*, Nappi et al., 1991) and the volumes of extruded deposits from  $< 10 \text{ km}^3$  (e.g. Bolsena – *Italy*, Nappi et al., 1991) to 100 - 500  $\text{km}^3$  (e.g. Phlegraean Fields I – *Italy* Barberi et al., 1991; Scandone et al., 1991).

Finally, regarding the group of “rhyolitic calderas”, we do unequivocally support Cole et al. (2004) in their statement that structures are usually  $>10 \text{ km}$  in diameter and that the related caldera-forming eruptions deposited huge volumes of

silicic ignimbrites. Several samples in the CCDB have a  $D_{CIR} < 10\text{km}$  (e.g. On–Take – *Japan*, Newhall and Dzurisin, 1988 and references therein) and involve less than  $10\text{ km}^3$  of extruded deposits (e.g. Kikai – *Ryuku Islands and Kyushu*, Matumoto, 1963; Spera and Crisp, 1981; Aramaki, 1984; Newhall and Dzurisin, 1988 and references therein). Furthermore, the authors state that pre-caldera activity may involve lava flows, low shields, cones, domes and explosion craters, but single large stratovolcanoes are not developed. In contrast, the CCDB records several calderas with associated stratovolcanoes (e.g. Golovnin – *Kurile Islands*, Newhall and Dzurisin, 1988 and references therein). However, it is true that in most cases post-caldera resurgence occurs (e.g. Infiernito – *U.S.A.*, Henry and Price, 1984; Lipman, 1984). We add that these calderas may also be funnel (e.g. Kakuto – *Ryuku Islands and Kyushu*, Aramaki, 1984; Newhall and Dzurisin, 1988 and references therein), piecemeal (e.g. Rotorua – *New Zealand*, Cole, 1990; Milner et al., 2002, 2003), plate/piston (e.g. Long Valley – *U.S.A.*, Steven and Lipman, 1976; Spera and Crisp, 1981 and reference therein) or trap-door (e.g. Infiernito – *U.S.A.*, Henry and Price, 1984; Lipman, 1984). Additionally, “rhyolitic calderas” may be located in areas of continental rifting (e.g. Red Hills – *U.S.A.*, Lipman, 1984; Steven et al., 1984), C-type subduction zones (e.g. Narugo – *Japan*, Newhall and Dzurisin, 1988 and references therein) or island arc collision (e.g. Bulusan – *Philippines*, Newhall and Dzurisin, 1988 and references therein).

In conclusion, we want to point out that the Cole et al. (2004) classification does not provide a satisfactory categorisation of collapse calderas. As these authors state, there is not a direct relationship between magma composition and caldera type and thus in establishing a genetic categorization of collapse calderas their classification may not be appropriate. Although we acknowledge that composition has a certain control on the dynamics of the caldera-forming eruption, since it determines the properties of the erupting magma, we cannot find a direct link to neither the mechanism of collapse nor to the resulting structure(s). However, it must definitively be taken into account in a genetic classification of calderas.

#### *II.5.7.3 Comparing results obtained with the post-caldera volcanic activity classification*

As mentioned in section II.3.6 Walker (1984) intended to investigate and classify the distribution of post-caldera vents as a possible indicator of caldera origin. Remember

that the most remarkable features were the scarcity of examples of type-R (vents occurring along an arcuate line paralleling to the caldera margin), the abundance of caldera types C (A single vent occupies a central or near-central position), L (vents are distributed in a defined straight line or linear zone) and S (Vents are scattered widely within the caldera). Comparing these results with those commented in section II.5.6.1 about the distribution of the calderas in the CCDB, according to the type of post-caldera volcanic activity (Fig. 2.70) we observe that they are very similar. With approximately the same number of analysed samples ( $N_{ANA} = 99$  and Walker's study is performed with 90 calderas) we obtain also a higher percentage of samples in the *CATEGORIES* "Type-C" and "Type-S" (Fig. 2.70). However, we detect two discrepancies. Firstly, whereas Walker's study reveals a low number of type-R samples we obtain also a maximum value in the *CATEGORY* "Type-R". Secondly, we do not observe a high percentage of calderas with type-L post-caldera volcanic activity. The latter discrepancy has a clear and easy explanation. In our classification we include also the *CATEGORY* "Type-Rs" specially defined for those caldera collapses whose posterior volcanic activity occurs unmistakably along regional structures. In our definition we distinguish between those vent located in a straight line or linear zone (*CATEGORY* "Type-L") and those distributed along clear and visible regional structures (*CATEGORY* "Type-Rs"). By contrast, the classification of Walker (1984) does not make this distinction and probably, his classification would consider our type-Rs calderas as type-L. Consequently, looking at Figure 2.70 and add the calderas included in the *CATEGORY* "Type-Rs" into the *CATEGORY* "Type-L" we obtain also a relative high percentage, similar to the *CATEGORIES* "Type-C" and "Type-S".

By contrast, the discrepancy concerning those calderas with type-R post-caldera volcanic activity is not so easy to explain. We consider that one probable reason is that the calderas included in the Walker's survey are different from those comprised in our analysis. However, since the samples considered by Walker (1984) are not included in the corresponding reference, we are not able to check it. Furthermore, we have nine samples more in our analysis, which may also influence the results obtained since we are dealing with considerably low number of samples in each *CATEGORY*. Nevertheless, we consider that the conclusions of Walker's work (1984) asserting that few calderas show positive evidence for possessing a ring fault that has guided subsequent eruptions is, in some measure, wrong. Our database includes several type-R samples and also some

type-CaR (central vent and multiple vents located at the caldera margins) calderas, category not included in Walker's classification. Considering the samples included in the CCDB we consider that, in some cases, ring faults may be areas of weakness for the location of following eruptions. However, we accept and ratify Walker's affirmation. Possibly, regional structures may be a more fundamental line of weakness than any possible ring fault and they are not restrained as a result of caldera formation. This is why it is important to record the type of structures in the caldera area and the existence of regional faults crossing or passing close to the collapse depression.

#### II.5.7.4 Comparing results obtained with other relevant works

We consider also it of special interest to compare our results with the works of Smith (1979) and Spera and Crisp (1984). In their works the authors analyse the relationship between the caldera area  $A_c$  and the volume of extruded deposits  $V_m$  (see section II.3.7). In short,  $\log A_c$  correlates positively with  $\log V_m$ , i.e. there is a positive correlation between the volume of extruded deposits and the area of their associated calderas. If we perform a similar plot for the calderas included in the database (Fig. 2.101) it is evident that we may draw the same conclusion (compare Fig. 2.16 and 2.101). Consequently, we can say that data contained in the CCDB is in agreement with those used by Smith (1979) and Spera and Crisp (1984).

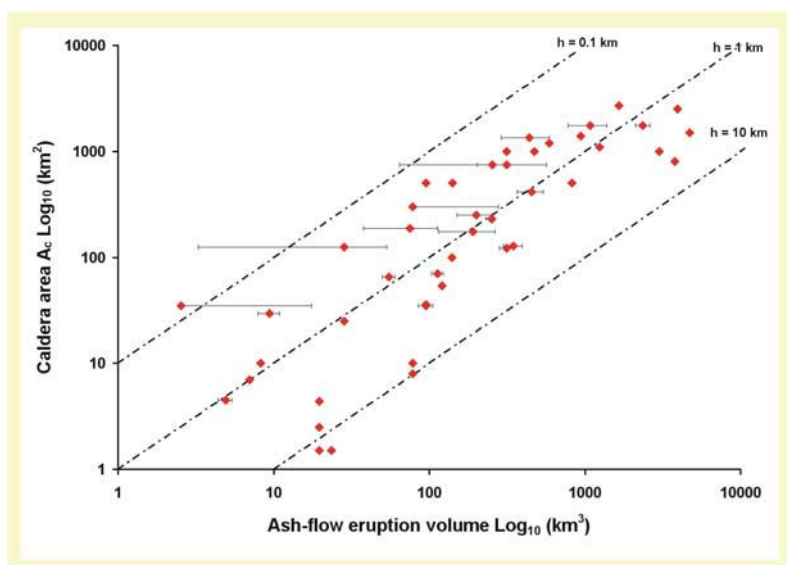


**Fig. 2.101:** Plot of the caldera area  $A_c$  vs. volume of extruded material  $V_m$  during the caldera-forming eruption for the calderas included in the CCDB. Lines are drawn to indicate various depth of drawdown ( $\Delta$  or  $h$ ), assuming the magma chamber has a cylindrical shape ( $\Delta = V_m / A_c$ ). (A) Error bars represent best estimates, not necessarily true error. If area and volume are given in the literature as exact number, they are plotted as points.

### II.5.7.5 Observed general trends

In this section we analyse the results obtained with the CCDB data analysis and discuss the most relevant aspects and remarkable implications.

Regarding the age of the calderas included in the CCDB, results obtained are completely contrary to our expectations. Younger structures are normally more susceptible to detection and observation since they have more probabilities to have been preserved than older ones. Therefore, with increasing age we expect a gradual decrease in the number of calderas. Instead, we observe a maximum at the *CATEGORY* “25 – 50 Ma” (Fig. 2.47). The first attempt is to consider this observation an effect of the selected intervals for the *CHARACTERISTIC* “Age”, i.e. when discretizing the continuous spectrum of age values. Figure 2.102 shows the continuous distribution of the caldera ages. Regardless the *CATEGORIES* defined for the *CHARACTERISTIC* “Age”, the number of calderas with an age between 25 and 50 Ma is very high. Notice that due to the type of graph, flat parts of the line indicate that there are several calderas with the same or approximately the same age. Additionally, calderas with an age in the *CATEGORY* “25 – 50 Ma” are principally located in the region of North America. Taking up again the spatial distribution of the collapse calderas included in the CCDB, a considerably high number of samples (22.3%, 63 samples) are situated in North America. Due to the high number of calderas in this area, the existence of a feature common to almost all or at least a great majority of the calderas distorts the whole CCDB data analysis. Although being only a characteristic of the calderas located in North America, due to the high number of samples in this region, this feature appears as the most common one within all the calderas in the CCDB. From now on, we will refer to this phenomenon as the “North America calderas effect”. Thus, during the results discussion it is necessary to take into account the spatial distribution of the calderas. This effect appears also in the age analysis. A high percentage of the calderas located in North America (51.5%, 34 samples) are between 25 and 50 Ma old, hence when analysing the age of the calderas included in the CCDB we observe a maximum in this interval deforming the age distribution, i.e. the curved of Figure 2.102 becomes flatter than expected. An additional and also interesting question is why almost all calderas in North America are older than 10 Ma and especially between 25 and 50 Ma old. Evidently, it can be simply a question of field data restrictions. It is possible that older calderas are worse preserved in this area

or that this area has a more extensive geological record of this time period than other studied zones. However, it exist the possibility that during this period some particular tectonic and/or magmatic configuration had favoured the formation of collapse calderas. During this section we will take into account these considerations. Also interesting is the fact that old calderas ( $>10\text{Ma}$ ) are mostly located in areas of continental rifting (Fig. 2.74) and consequently, in zones of continental crust (Fig. 2.75). Apparently, both observations are constrained by the “North America calderas effect”, since almost all calderas in North America are older than 10 Ma and are located in continental crust and in a continental rifting tectonic setting. However, it is logical to consider that the best preservation conditions for these structures are intraplate areas, far from the plate boundaries where allegedly deformation rates may be higher.

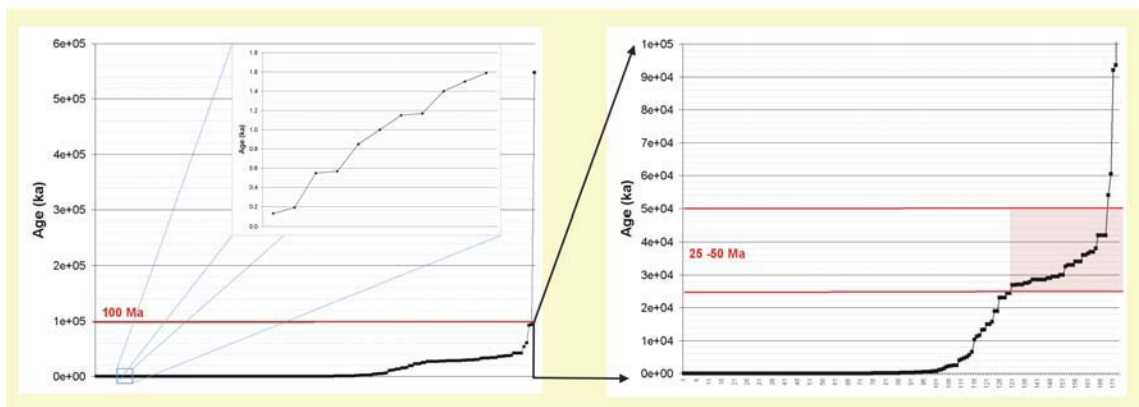


**Fig. 2.102:** Graph showing the continuum spectrum of data regarding the ages of the calderas included in the CCDB. Each black square corresponds to a caldera sample. Notice that due to the type of graph, flat parts of the line indicate that there are several calderas with the same or approximately the same age.

Concerning the dimensions of the collapse calderas included in the CCDB, we observe that almost all samples have an  $D_{\text{CIR}}$  between 5 and 25 km (Fig. 2.50). Possibly, smaller structures ( $D_{\text{CIR}} < 5$  km) are bad preserved and larger ones ( $D_{\text{CIR}} > 25$  km) have a lower probability of occurrence. Probably, a  $D_{\text{CIR}}$  between 5 and 25 km is a compromise between probability of occurrence and capacity of preservation. In fact, in Figure 2.72 we can observe that calderas with dimensions comprised within this interval may be older than 50Ma.

The study of collapse calderas dimensions leads us to consider a possible maximum concerning the size of a collapse caldera. As other geological structures (e.g.

plutons) we suppose that there must be a dimensions threshold for collapse calderas. The largest caldera included in the CCDB is Blacktail (USA) with an area of 4712.4 km<sup>2</sup> (100 × 60 km) and 1500 km<sup>3</sup> of caldera-forming related deposits. Thinking about the factors controlling this threshold we expect to find a certain influence of the maximum volume of storable magma in the crust and the horizontal extension of the associated magma chamber. Probably, crust thickness, regional and local stress fields, composition and time of residence of magma, are some of the most influential factors. Although, a more exhaustive analysis of this point would be very interesting, it is out of the scope of this study. However it is an aspect to consider in future works.

Of especial interest is to analyse why the largest calderas ( $D_{CIR} > 50$  km) included in the CCDB. There are few large calderas in North America (Blacktail, Kilgore, Yellowstone I and II, La Garita) and one in Sumatra (Toba). Concerning the Toba caldera Bellier and Sébrier (1994). assume that its dimension is related to the interaction of the caldera structure with the regional strike-slip fault (Fig. 2.103). The Toba caldera, as other calderas in this region, occurred in the pull-apart basin of the strike-slip fault. In the case of the calderas in North America the tectonic configuration was also suitable for the formation of huge collapse calderas. Additionally, some large calderas ( $D_{CIR} > 25$  km) we have experimented stages of pre-caldera doming (e.g. Kilgore - *U.S.A.*, Morgan et al., 1984) or post-caldera resurgence (e.g. Toba – *Sumatra*, Spera and Crisp, 1981 and references therein). We have also observed that large calderas are commonly associated with large volumes of extruded deposits, although this relationship is not always accomplished. There are also small calderas associated with large volumes of extruded deposits (see sections II.2.2 and II.2.3). In this case, subsidence may be accommodated at depth or the breaking and dilatation of the subsiding material distort the real caldera volume (see sections II.2.2 and II.2.3). There exists also large calderas involving relative small volumes of extruded material, which may indicate a possible outflow of magma throughout a non-controlled zone or most probable, erosion of the caldera-forming eruption related deposits (see sections II.2.2 and II.2.3). Additionally, we observe that the largest calderas are felsic cal-alkaline. All calderas with a  $D_{CIR} > 25$ km are rhyolitic (e.g. Emory - *U.S.A.*, Spera and Crisp, 1981; Elston, 1984; Lipman, 1984) or their composition have not been determined yet (e.g. San Carlos - *U.S.A.*, Henry and Price, 1984, 1989). Cerro Galán caldera is the only dacitic and La Pacana and Bursum are between rhyolitic and dacitic. An additional interesting point is that almost all large calderas  $D_{CIR} > 25$ km are located in areas with

extensional structures. Possibly, the existence of these structures is, as some authors propose, a requisite or a favourable factor for the formation of large calderas. The rest of large calderas are associated with shear-extensional structures but never with a compressive component (at least those calderas included in the CCDB). Apparently, tectonic compression structures work against large caldera collapses.

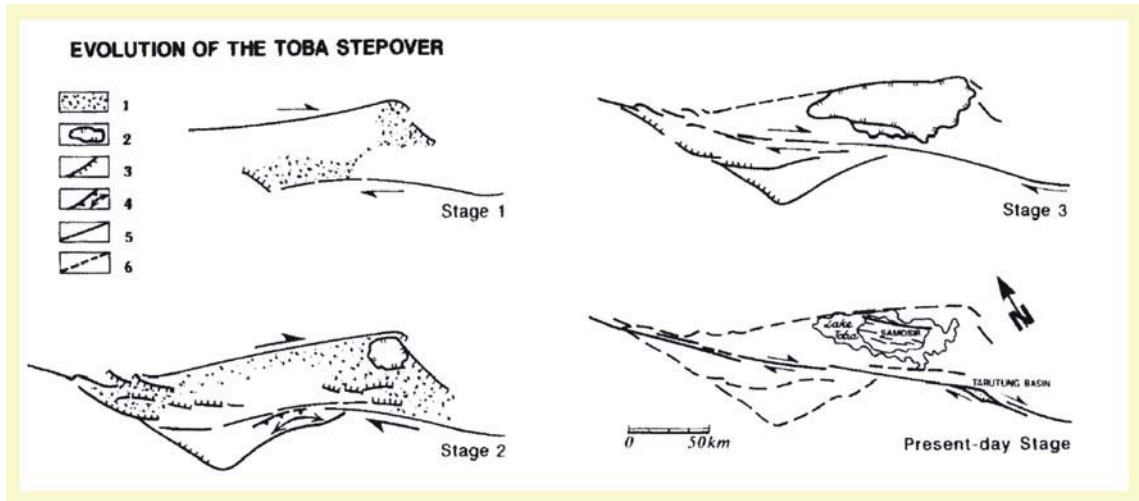


**Fig. 2.103:** Evolutionary sketch of the Toba caldera in four stages deduced from the structural map of the Lake Toba region after interpretation of the SPOT images. The present stage is modified from Detourbet et al. (1993). **1** Subsiding zone; **2** Caldera rims; **3** Active faults with a dominant normal component (ticks on the downthrow side); **4** Active restraining fault zone; **5** Major active strike-slip fault traces; **6** Inactive fault traces. (Modified from Bellier and Sébrier, 1995)

Regarding the type of collapse of the calderas included in the CCDB, the most abundant are plate/piston and secondly trap-door and funnel (Fig. 2.52). The possible reasons for these observations are diverse. First, these collapse types may be the most probable and favourable due to mechanical reasons as shown by analogue modelling (see section II.2.1). Second, these collapse types are the most recognizable or preservable on the field. In fact, according to Lipman's description (Lipman, 1997), the main difference between piecemeal and plate/piston collapses is the coherence of the caldera floor during subsidence. However, the caldera floor is not always exposed and observable. In some cases, it is covered, for example, by post-collapse volcanic activity products such as ignimbrites or lava flows (see section II.2.5). Additionally, it is evident that piecemeal floors are not easy to be recognized. In some cases, it is the distribution of the post-caldera activity, which reveals the disrupted floor. Anyway, regardless the specific collapse type, we can say that the most common observable features on the field

are ring-fractures delimiting a coherent or disrupted subsiding piston (i.e. plate/piston or piecemeal collapses, respectively) or asymmetrical collapses (i.e. trap-door collapses). Looking at the spatial distribution of the different caldera types, we observe a curious phenomenon. Almost all funnel calderas are located in Japan and all piston/plate and trap-door calderas in North America. Probably, this observation is related to the fact that Japan and North America are well-studied areas and consequently, we do not know the type of collapses located in other regions (compare the number of calderas with information about the collapse type in North America or Japan and for example in Indonesia) (Fig. 2.53). However, we can analyse why almost all Japanese caldera are funnel and those located in North America plate/piston or trap-door. Some authors hold (e.g. Sawada, 1984; Yoshida, 1984) that the type of collapse calderas in Japan is directly related to the stress field at the time of the caldera-forming eruption. During compressional periods calderas in this area tend to be funnel type (e.g. Hakone – *Japan*, Kuno, 1970; Aramaki, 1984), whereas during extensional stages calderas are commonly plate/piston like (e.g. Ishizuchi – *Japan*, Yoshida, 1984). If we compare this statement with our results concerning the relationship between the *CHARACTERISTIC* “Collapse type” and “Condition of the local structures” (Fig. 2.86), we can observe that effectively, compressional structures are related to funnel type collapses. Apparently, there is a strong connection between the collapse type and the condition of the local structures. However, we should not forget that in some cases, the number of calderas without information is quite high. Consequently, there is the possibility that large amounts of available may change our observations. Additionally, concerning the relationship *CHARACTERISTIC* “Dimensions” to *CHARACTERISTIC* “Collapse type”, we can say that the largest calderas are uniquely plate/piston or trap-door.

Regarding the volume of extruded magma or deposits we expected to find a regular decrease of calderas when considering larger volumes of erupted material. However, looking at Figures 2.54 and 2.55 for, we observe that although this tendency apparently exists, an strange peak appears at the interval 100-500 km<sup>3</sup>. Evidently, this peak may be an effect of the selected intervals. Therefore, we include here the continuum spectrum of data concerning the volume of extruded deposits (Fig. 2.104). As expected, for high volumes of extruded material number of calderas decreases, i.e. the slope of the curve in Figure 2.104 is exponentially increasing. However, the curve becomes flatter at the interval “100-500 km<sup>3</sup>”, indicating that several calderas are related to the same volume of extruded material. Besides, we have to consider that results

obtained may be possibly distorted due to scarcity of information and due to the “North America calderas effect”. Analysing the spatial distribution of the calderas with volumes of extruded material or magma included in this *CATEGORY* (Fig. 2.56), we observe that almost all of them are located in North America. Nevertheless, we cannot discard the existence of a magmatic and/or tectonic configuration favourable for caldera-forming eruptions involving considerable amounts of magma. However, concerning volume estimations, we have to consider also if available volumes are only an approximation and are far away from the real values. Possibly, the observed peak is an effect of the studies in the area. It is completely feasible, that these calderas have been more accurately studied and therefore more information is available. In some places, there is very few (e.g. Central America) or absolute any (e.g. Iceland) information in the consulted references concerning the amount of extruded material during the caldera-forming eruption.

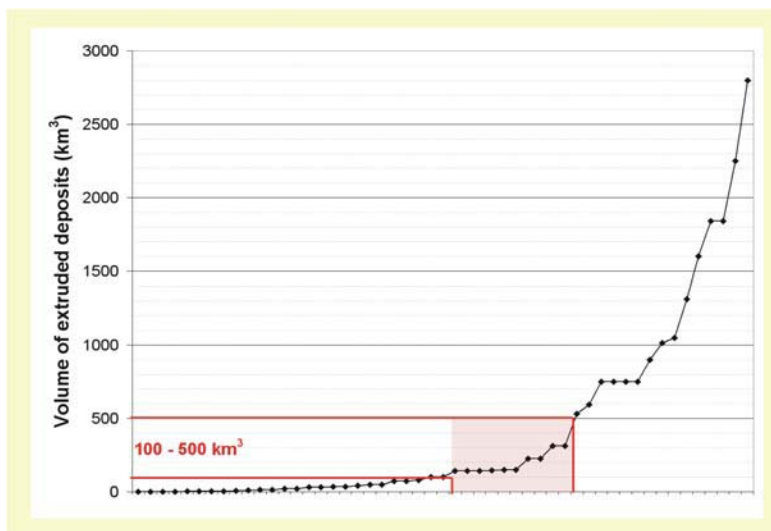


**Fig. 2.104:** Graph showing the continuum spectrum of data regarding the volume of extruded material during the caldera-forming eruptions recorded in the CCDB. Each black square corresponds to a caldera sample. Notice that due to the type of graph, flat parts of the line indicate that there are several calderas with the same of approximately the same volume of extruded material.

Regarding the composition of the magma related to the caldera-forming eruption, the most common composition is the felsic calc-alkaline one (Fig. 2.57). Possibly, due to the tectonic context and the type of crust collapse calderas are located. Principally, felsic cal-alkaline calderas are associated with areas of continental crust (thin or thick) and probably high evolved transitional crust normally, thick transitional crust (Fig. 2.92). However, almost all calderas in North America are felsic calc-alkaline, i.e. the

percentage of calderas related to a felsic calc-alkaline composition increases (“North America calderas effect”). Since the felsic calc-alkaline rock suite includes several individual rock compositions, we consider of special interest to analyse the detailed composition of the calderas included in the *CATEGORY* “Calc-alkaline felsic” (Fig. 2.105). We can observe that the CCDB includes a similar percentage of dacitic and rhyolitic calderas and around a 11% of caldera-forming eruptions associated with rhyodacitic magma or both compositions. Concerning the relationship between the composition of the extruded magma and the type of pre-caldera edifice, calderas with stratovolcanoes, stratocones or shield volcanoes as pre-caldera edifice can have alkaline or calc-alkaline compositions. By contrast, those calderas in the *CATEGORY* “No edifice or calderas” are all felsic cal-alkaline. In the CCDB, only calderas of felsic calc-alkaline composition may present ring-faults as caldera-forming event triggers and may be exempt of an eruptive phase (e.g. energetic Plinian eruption, basaltic eruption, etc.) prior to the formation of ring-faults.

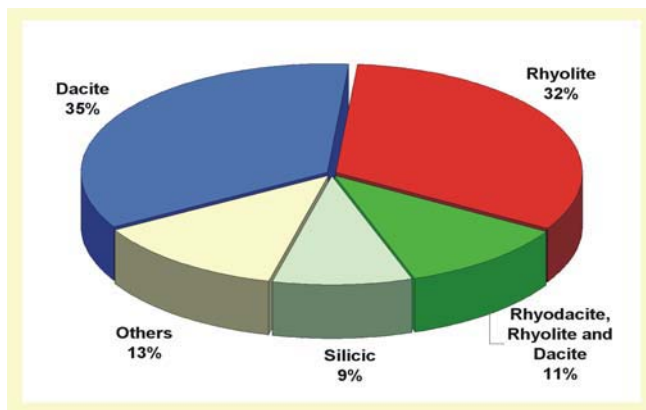


**Fig. 2.105:** Distribution of the individual compositions included in the rock suite felsic calc-alkaline. Observe that the most abundant are the rhyolitic and andesitic compositions or the mixture between them.

Throughout this work, we have insisted in the idea that the type of crust may influence the composition, the magma storage, etc. In our analysis, we have observed that almost all calderas of the CCDB are located in areas of continental crust and on transitional thick crust (Fig. 2.59). Possibly, this distribution is only a reflection of the Earth’s volcanism distribution plus the “North America calderas effect”. In fact, calderas in North America are only associated with continental crust (Fig. 2.60). Since the high number of calderas in Japan and the Marianas Island region is related to transitional thick crust (Fig. 2.60), we can also introduce the “Japan calderas effect.

Additionally, it is possible that the thickness and composition of the crust may favour or work against the formation of collapse calderas. Surprisingly, the number of calderas in areas of continental thick crust is very low, possibly because these areas are old and deeply eroded. Additionally, continental thick crust is related to intraplate tectonic settings and evidently, the percentage of volcanism in this context is much lower than in areas of plate boundary. However, there is the possibility that thick continental crust, due to its mechanical or compositional properties or because the type of associated tectonic setting, is less favourable for the occurrence of caldera-forming eruptions. Finally, all calderas located in continental thick crust are in North America and around ten samples in South America. Is this observation a consequence of the “North America calderas effect”? Additionally, these calderas in areas of continental thick crust are principally associated with areas of continental rifting and C-type subduction zones (Fig. 2.96). By contrast, calderas located in areas of continental thin crust are located in different regions, but the most common associated tectonic settings are also areas of continental rifting and C-type subduction zones (Fig. 2.96). We observe also that there are very few calderas located in areas of transitional thin or oceanic crust. Possibly, collapse calderas associated with oceanic crust may lay under the sea level and are undetectable or the world regions with these two crustal types have been less studied than others. We consider also feasible that the mechanical properties and composition of oceanic crust are not suitable for collapse caldera formation. It is possible that oceanic crust is too thin to house or favour collapse calderas. At least, this could be the explanation for the lack of caldera-forming eruptions involving huge volumes of magma in oceanic crust environments. In fact, calderas with a  $D_{CIR} > 25$  km are all located in continental crust (Fig. 2.79), whereas those located in areas of transitional and oceanic thin or thick crusts have all a  $D_{CIR} < 25$  km (Fig. 2.79). Besides, caldera-forming eruptions associated with volumes of extruded magma or deposits  $>500$  km<sup>3</sup> are uniquely located in areas of continental crust (thick or thin) (Fig. 2.77) and calderas associated with oceanic thick and transitional thin and thick crusts involve volumes of erupted material  $<100$  km<sup>3</sup>. Of course, this last observation can be a question of preservation because most of the latter calderas are located on islands and a considerable percentage of extruded material may be deposited into the sea, thus preventing a correct volume estimate. Additionally, we observe that calderas located in areas of oceanic thick and transitional thin and thick crusts are principally associated with stratovolcanoes and stratocones as pre-caldera edifice. Only one sample Oskjuvatn (Iceland) does not accomplish this general tendency.

Concerning pre-caldera doming periods, it is curious that none of the funnel calderas in Japan do present this characteristic. However, this observation is strongly subjected to the CCDB sampling and restrictions. By contrast, in plate/piston calderas there exist some samples where it is possible to detect pre-caldera doming (e.g. *Kekeya I-Japan*). Something similar happens with post-caldera resurgence episodes, none of the funnel calderas in Japan has experimented resurgence. Contrarily, for some plate/piston calderas there are clear evidences of post-caldera resurgence (e.g. *Job Canyon-U.S.A*).

Also interesting are the results concerning the tectonic setting of collapse calderas. Figure 2.61 indicates that almost all calderas included in the CCDB are located in areas of C-type subduction zone or continental rifting. This distribution is partially a consequence of the distribution of volcanism on Earth's surface (compare Figs. 2.45 and 2.106).

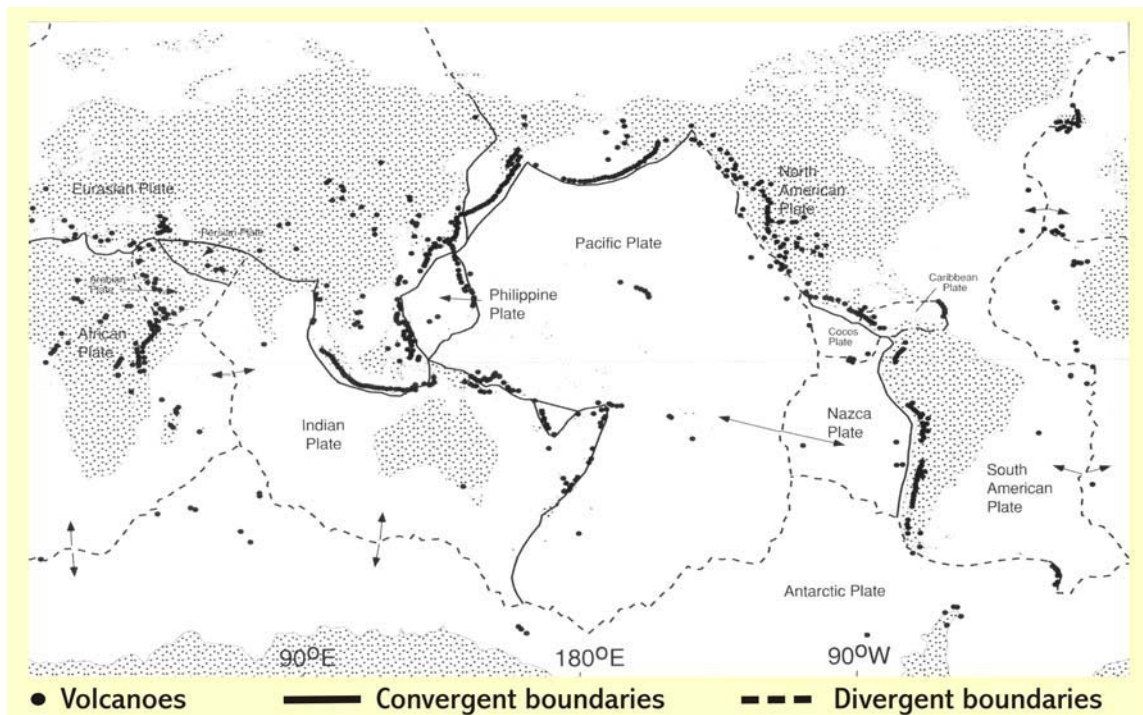


**Fig. 2.106:** World map with the distribution of volcanoes and the plate boundaries. (In Carey, 2005 modified from Sparks et al., 1997)

The fact that calderas are located in subduction zones is a consequence of the global distribution of volcanism, but the fact that C-type subduction zones are more frequent may have other reasons. If we have a look at the spatial distribution of the

calderas associated with C-type subduction zones (Fig. 2.62) we detect that a high percentage (31.5%, 34 calderas) is located in Japan. On the other hand, the abundance of calderas at C-type subduction zones may be a consequence of the “Japan calderas effect”. However, it is also possible that the subduction process itself, which leads to certain structural and magmatic conditions, favours the occurrence of caldera-forming eruptions. Maybe, generation and ascent rate of magma as well as its storage capacity are adequate for the generation of magmatic system susceptible of developing caldera-forming volcanic episodes. Moreover, since almost all calderas in areas of continental rifting are located in North America, it may be then a consequence of the “North America calderas effect”? However, we have to highlight also that a high percentage is located in Africa. If we study any existing connection or relationship between the associated tectonic setting and other caldera features, we observe that calderas with a  $D_{CIR} < 10$  km are associated with C-type subduction zones and those with a  $D_{CIR} > 25$  km to areas of continental rifting. We suspect that from a tectonical and /or compositional point of view, areas of continental rifting are favourable for the formation of larger calderas. On the one hand, we consider that the extensional stress field implicit in these areas may favour the generation of extensional faults, i.e. collapse structures (e.g. typical graben structures). Areas of continental rifting are associated to magmas of rhyolitic composition, which are one of the most common composition associated to caldera-forming eruptions (Fig. 2.105) and to large volumes of erupted material, i.e. magma chambers. Also, notice that these areas of continental rifting are normally associated with thinned continental crust (Condie, 1993; Kearey and Vine, 1996; Strahler, 1997). Given the high number of calderas in this tectonic setting, it is not surprising to find a high proportion of calderas in areas of thin continental crust. Note also, that the number of calderas located at hotspots near an oceanic ridge is higher than those located in isolated hotspots. Apparently, the interaction of the continuous magma supply of hotspots and the extensive structures of the oceanic ridge favour the occurrence of caldera-forming eruptions, i.e. the generation of magma chambers and stress configuration susceptible to caldera-forming eruptions.

In a more reduced scale, we want to take up again the information concerning the condition of the local structures. We have observed that the most abundant type of local structures is the extensional one. In fact, since collapses are controlled by extensional faults, it is not rare to find frequently this type of local structures. Yet, some calderas formed in the presence of compressional structures, which seems surprising. Taking a

detailed look at calderas situated in a compressional setting, we find that these are related to funnel collapses and almost all of them are located in Japan. This observation may be a consequence of the “Japan calderas effect”, but there may also be the possibility of special tectonic or magmatic condition for this phenomenon to occur.

Concerning the pre-caldera edifice, the most common are stratovolcanoes and stratocones. It is interesting to remark that for large calderas there is any information about the type of pre-caldera edifice. Evidently, the existence of volcanic edifices like stratovolcanoes or shield volcanoes prior to a caldera collapse processes is theoretically easy to be observed on the field. In fact, we can assume that in a considerably high percentage, the detection of previous existing volcanic edifice is quite successful. Therefore, it is realistic to consider that those calderas with unknown pre-caldera edifice did not probably have a related pre-collapse volcanic edifice. Otherwise, some kind of information would exist. Consequently, at least we can assume that a part of the largest calderas ( $D_{CIR} > 25$  km) recorded in the CCDB without information about the *CHARACTERISTIC* “Type of pre-caldera edifice” did not have a related pre-collapse volcanic edifice. However, for smaller calderas ( $D_{CIR} < 25$ km) stratocones and stratovolcanoes are the most frequent pre-caldera edifice type. Studying the relationship between the pre-caldera edifice and the tectonic setting, we can observe that those calderas with associated pre-caldera stratocones or stratovolcanoes are predominantly located in C-type subduction zones (Fig. 2.100). Although we have to consider that there exists a high number of calderas with unknown type of pre-caldera edifice.

Also relevant is the fact that most caldera collapse episodes are commonly preceded by a volcanic eruption. Commonly, Plinian phases and occasionally, low energetic mafic eruptions. In other calderas, the caldera eruption is directly originated through the formation of ring-faults. Combining this information with that concerning the type of pre-caldera edifice, we can conclude that those calderas with a pre-caldera volcanic edifice are commonly related to a previous eruption preceding the caldera collapse phase.

### *II.5.7.6 The “North America calderas effect”*

The number of calderas in North America is considerably higher than in other studied regions. We should also remember that this area hosts almost all largest and most voluminous known calderas. Possible explanations are that this area has been more studied during the last decades or that these types of structures may be better preserved and observable there than in other regions. However, there is the possibility that this area is especially prone to the occurrence of caldera-forming eruptions. Hence it is worth analysing the tectonic and magmatic evolution of North America in this context.

Figure 2.107 illustrates the proposed stages of the post-40 Ma tectonic evolution of North America according to Elston and Bornhost (1979). The first tectonic phase was characterized by a subduction of the Farallon plate under the North American plate. During this stage, granodiorite-monzonitic magma formed or equilibrated in the mafic part of the lower crust and lithospheric mantle. At surface occurred eruptions from andesite volcanoes. The subduction process led to an important production of magma, which accumulated in the crust up to 400 km inland from the subduction front. Around 5 Ma later, the East Pacific rise laid near the trench and hot oceanic lithosphere was strained beneath the continental plate. Subduction ceased around 27 Ma ago and the plate was free to extend and crust and lithosphere were thinning as they extended. The associated volcanism together with an associated regional doming covered an area 750 km wide. The last phase is characterized by intraplate block faulting due to plate extension. The affected area was 1 Ma ago 850 km wide.

Whereas Figure 2.107 illustrates the tectonic evolution in cross section, in Figure 2.108 we can observe in plan view, the spatial relation of first-order plate tectonic boundaries to second-order late Cenozoic extensional fractures. Due to the relative plate movement the subduction front has been migrating north-westwards and also the area influenced by the volcanic subduction-related volcanic activity.

Simultaneously to the migration of the trench important extensional areas began to develop inland. In fact, the west of the North America region is characterized by three important extensive areas (Fig. 2.109): the Basin and Range province, the Snake River Plain and the Rio Grande Rift or Graben. Looking at the distribution of calderas in the U.S.A. (Fig. 2.109), we can observe that these are located along the actual volcanic line and at the extensional areas.

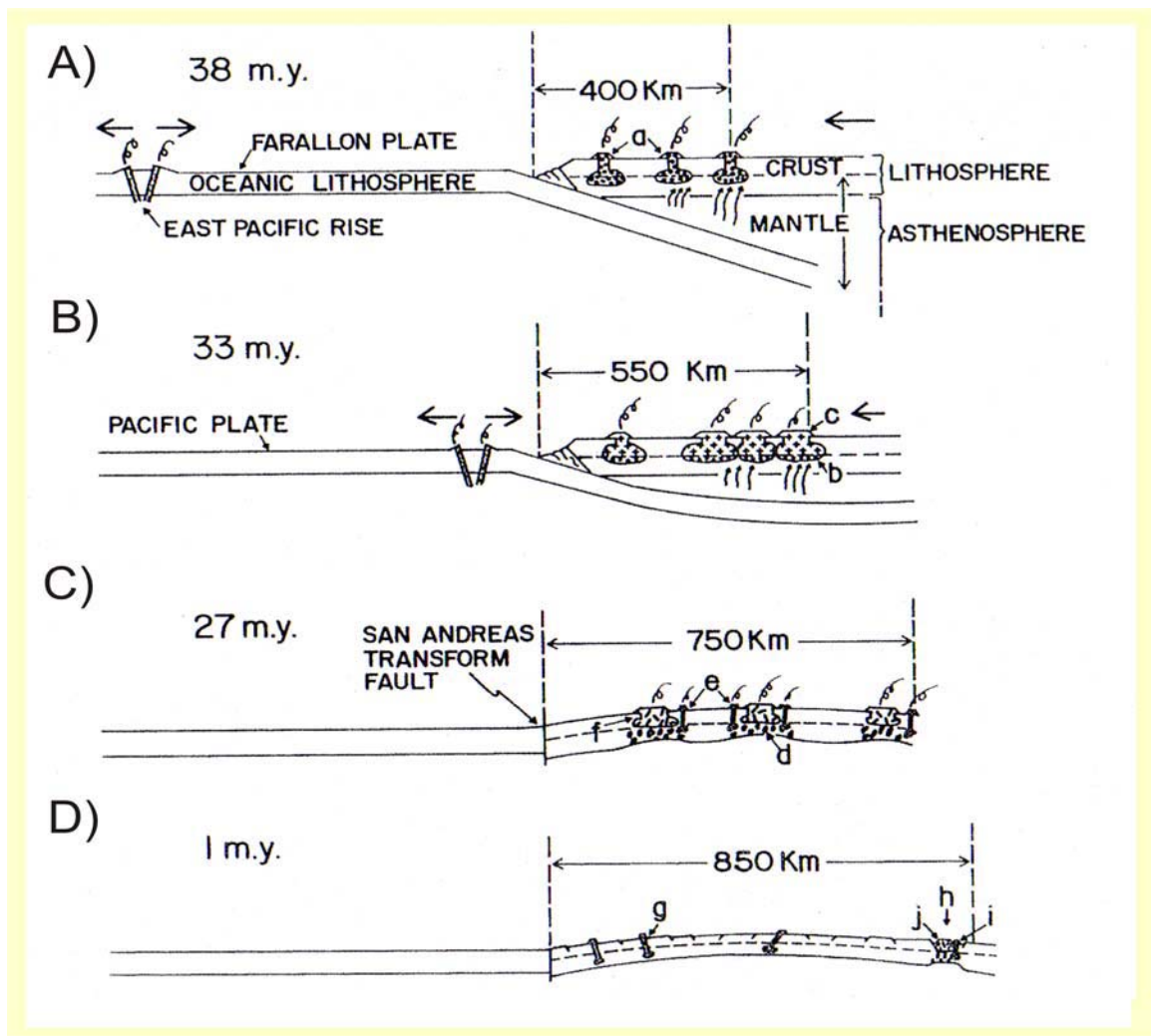


**Fig. 2.107:** Proposed stages of post-40 Ma tectonic evolution. The cartoons represent the sections from the northern end of Baja California to north-central New Mexico. (Modified from Elston and Bornhorst, 1979)

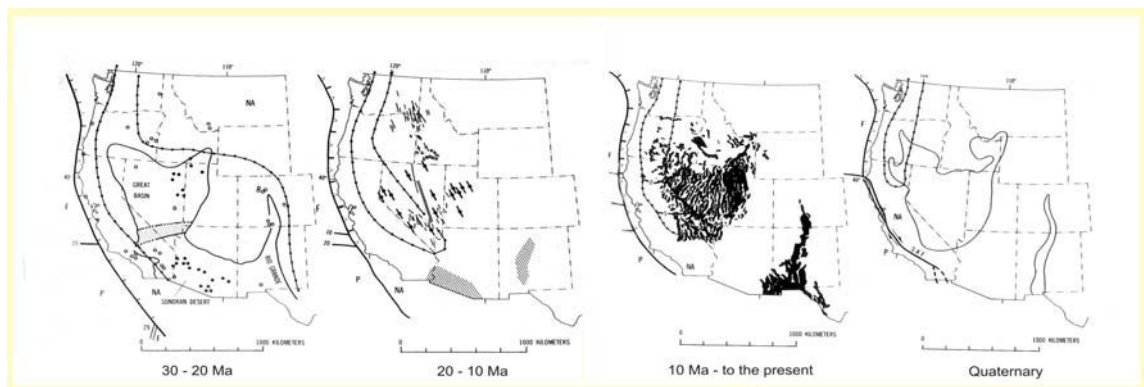


**Fig. 2.108:** Relation of first-order plate tectonic boundaries to second-order late Cenozoic extensional features. (Modified from Eaton, 1979)

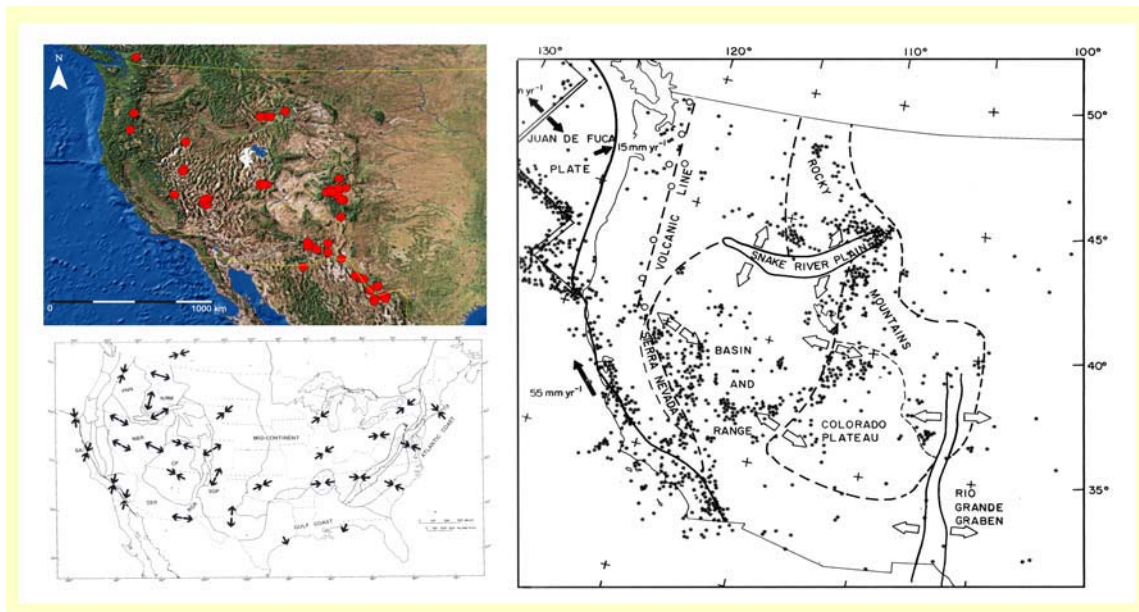


**Fig. 2.109: (Top and left)** Satellite image with the calderas included in the CCDB located in North America (red dots). The dashed yellow lines correspond to the Canada-U.S.A and the U.S.A-Mexico borders. **(Bottom and left)** Map of the U.S.A. with the most important tectonic provinces and the related stress field. Notice that along the plate boundary there is compression but inland dominates extension. (In Condie, 1993 modified from Zoback and Zoback, 1980) **(Right)** Map of the western sector of the U.S.A. On the map are marked the actual volcanic line related to the subduction zone and the extensional areas like the Snake River Plain, the Basin and Range and the Rio Grande Graben. Black dots correspond to the location of seismic events, solid arrows give relative plate velocities and open arrows give stress directions inferred from seismic focal mechanism studies (Modified from Turcotte and Schubert, 1992)

The origin of these extensional zones and their correlation with the evolution of the subduction has been long studied. A detailed explanation of their origin is beyond the scope of this work, but we want to present the most relevant conclusions in order to correlate them with the caldera collapse processes. In this context, the Basin and Range and the Rio Grande graben or rifts are of special interest since they show the highest density of collapse calderas (Fig. 2.109).

Olsen et al. (1987) explained that the Rio Grande rift extends as a well-defined series of asymmetrical grabens from Leadville, Colorado, to Presidio, Texas, and Chihuahua, Mexico, a distance of more than 1000 km. Although at the south the rift is not physiographically distinctive with respect to the adjacent Basin and Range province, yet it can be distinguished from this province by a variety of geologic and geophysical signatures (Seager and Morgan, 1979). Over much of its length the rift is part of a broad region of “rift-like” late Cenozoic extensional deformation, i.e., a region characterized by large crustal blocks separated by steeply dipping normal faults. In central New

Mexico, this region is more than 200 km in width and a broadly linear, northeast-trending array of late Cenozoic volcanic fields, commonly referred to as the Jemez lineament corresponds to a major boundary or zone of weakness in the lithosphere. In southern New Mexico and northern Chihuahua, the rift is physiographically distinguishable from the Basin and Range province extending across southern Arizona and southern New Mexico. Although the style (i.e., extensional deformation) and timing of structural deformation of the entire extended region are similar to that of the main rift grabens, the magnitude of deformation is much less. The formation of the Rio Grande rift and Colorado Plateau transition zone and break-up of the Mogollon-Datil volcanic field all resulted from, and were part of, the very widespread Basin and Range deformational event. Most investigators suggest that the structural development of the rift occurred during two time intervals: (1) an early phase which began just after 30 Ma ago and lasted an estimated 10–12 Ma, and (2) a later phase which began 9 or 10 Ma ago and lasted until about 3 Ma ago (e.g., Chapin and Seegar, 1975; Baldrige et al., 1980). The first event (mid-Oligocene to early Miocene) led to the formation of broad, relatively shallow basins with low-angle normal faults accompanied by large-scale magmatism. The second extensional event (mid-Miocene to Quaternary) involved higher angle faulting and basaltic magmatism, which continue today probably at a slower rate. The formation of the Rio Grande rift may have resulted from the combination of a thermally weakened lithosphere during the subduction phase with a superimposed tensional stress regime (Olsen et al., 1987). Other authors (e.g. Tandon et al., 1999) affirm that the Rio Grande rift is one of the major Cenozoic continental rifts, and consists of a series of north-trending, interconnected, symmetrical graben (Chapin, 1979).

Regarding the Basin and Range province, the earlier extension may have occurred by the plate-motion partitioning mechanism (Henry and Aranda-Gomez, 2000 and references therein). Atwater and Stock (1998) found that motion of the Pacific plate was similarly oblique to the North American plate beginning as early as 33 Ma; the plate boundary was in transtension since inception to about 8 Ma, when Pacific motion became more northerly and more nearly parallel to their boundary. This suggests that east–northeast extension, perpendicular to the boundary, should have begun much earlier than 12 Ma. Additionally, calculated displacements from plate circuit reconstructions agree closely with estimated coast-perpendicular (N60°E) extension in a transect across the Rio Grande rift, Colorado Plateau, and central California from 24 Ma to the present.

Therefore, plate-motion partitioning was probably critical to extension at least as early as 24 Ma. Moreover, the east–northeast extension was also occurring in the latest Oligocene and early Miocene through a large part of the southern Basin and Range (Henry and Aranda-Gomez, 2000 and references therein).

In order to establish the possible time relationship between the occurrence of the caldera collapses and the different tectonic and magmatic events, we have correlated the timing of tectonic and magmatic events in the Rio Grande rift and the major events of western U.S.A. with the age of the collapse caldera located in the U.S.A. (Fig. 2.110). Notice that the age interval with the highest number of caldera samples corresponds to the beginning of the early extension in the Rio Grande rift, to the calc-alkaline volcanism and to the first stages of the Basin and Range deformation. It is evident that there exists a strong correlation between the occurrences of the caldera-forming events and the tectonic evolution of western U.S.A. Apparently, the high amounts of magma generated during the subduction phase and the subsequent extensional phase favoured caldera collapses in North America.

Although North American volcanism (including volcanic calderas) has clearly benefited from a greater amount of dedicated studies over the last decades, the high density of calderas in this part of the world may be due its particular tectonic and magmatic evolution which appears to be exceptionally suitable for the formation of at least a certain type of collapse calderas.

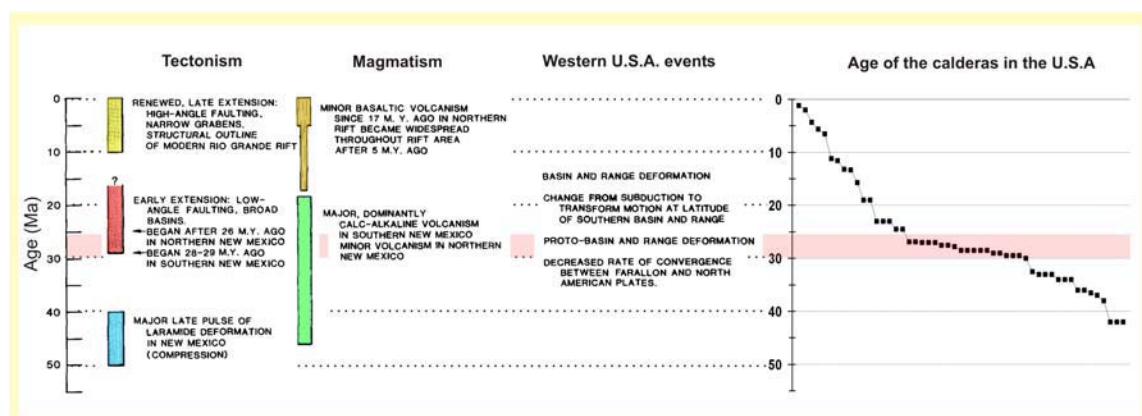


**Fig. 2.110:** Time correlation between the major magmatic and tectonic events and the occurrence of collapse caldera in the U.S.A. **(Left)** Timing of tectonic and magmatic events in the Rio Grande rift area compared to major events of the western United States. (Modified from Olsen et al., 1987) **(Right)** Graph with the age distribution of the collapse caldera located in the U.S.A. Each black square corresponds to a caldera sample. Notice that the red coloured stripe indicates that age interval with the highest number of calderas. It corresponds to the beginning of the early extension in the Rio Grande rift, to the calc-alkaline volcanism and to the first stages of the Basin and Range deformation.

It is also necessary to consider that these especial tectonic and magmatic conditions identified for the North America region may also occur in other world regions like Mexico or Central and Southern Andes. A more detailed study of the last two areas is out of the scope of this work but should be taken into account for future works.

#### *II.5.7.7 Field classification of collapse calderas*

According to the results obtained with the *CCDB DATA ANALYSIS* we can clearly distinguish between two different types of collapse calderas according to the corresponding field observations:

➤ **Type A:**

Calderas included in this group are quite large ( $D_{\text{CIR}} > 25$  km) plate/piston or trap-door structures. Additionally, the associated deposits are primordially felsic calc-alkaline. The caldera-forming eruptions involve normally important volumes of magma ( $>100$  km<sup>3</sup>) and in general, there is no information or evidences about a possible pre-caldera edifice like composite volcanoes. In connection with this observation, these caldera-forming events normally initiate directly with the opening of ring faults at the beginning of the eruption. There is no evidence of eruptive phases preceding the formation of the ring faults. In most cases, these calderas occur in areas of continental thick or thin crust and occasionally, in evolved transitional thick crust. These collapse calderas are uniquely associated with extensional or shear-extensional local structures. The most common tectonic settings are C-type subduction zones and areas of continental rifting.

➤ **Type B:**

Calderas included in this group tend to be smaller than those of type A ( $D_{\text{CIR}} < 25$  km). Although, the most common associated deposits are primordially felsic calc-alkaline, it is also possible to find mafic calc-alkaline or alkaline samples. The caldera-forming events can involve important volumes of magma but in general, they are less voluminous than type A eruptions. In most cases, there is evidence of the existence of pre-caldera edifices, especially composite volcanoes: stratovolcanoes or stratocones. Additionally, most of these caldera-forming events are preceded by a Plinian

eruption. These calderas may occur in any type of crust and tectonic settings and may be associated with any type of local structures (e.g. compressional, extensional, shear, etc.), but the most common are extensional settings.

### II.5.8 Restrictions of the field data analysis

Obviously, field data and the corresponding analysis involve a series of restrictions. In this section we try to summarize at least the most important ones, especially those affecting the interpretations of the *CCDB DATA TABLE* results. Figure 2.111 illustrates the whole process that takes place from the obtaining of field data to the *CCDB DATA ANALYSIS* passing through the revision of previous works and the creation of the *CCDB DATA TABLE*. We have also marked in Figure 2.111 the most important restrictions to consider when passing from a step to the next one.

The first step is the obtaining of field data (Fig. 2.111). As we have already mentioned (see section II.2.5), there are several restrictions directly involved in their acquisition, which may affect the quality and availability of field data. The main phenomena that may affect the preservation of structures and deposited materials related to a caldera-forming eruption are principally: erosion, reworking, subsequent post-caldera volcanic activity that may destroy or bury the materials and structures, and post-caldera deformation processes. Evidently, these processes may affect both the degree of exposure of the geological record and the possibility of field data. As mentioned before (see section II.2.5), the availability and quality of field data may lead for example to miscorrelations between proximal and distal facies or between intra- and extracaldera deposits. For example, this could result in errors when calculating volumes of extruded material useful for estimating the eruption size. Additionally, misinterpretations of the nature of deposits (e.g. mistaking large coherent slide blocks for lithological mixed caldera-collapse breccias) may lead to errors in the inferred stratigraphic sequence and consequently, in the eruptive sequence.

The next step in the *CCDB DATA ANALYSIS* is the revision of previous works referring to collection and interpretation of field data and the introduction of the compiled data in the *CCDB*. In this case, the most important restrictions are the existence of errors in the consulted references (e.g. misinterpretations of studied field data), the possibility that the information in the consulted references is old-fashioned, subjectivity in the interpretations depending on each author and also typographical errors in

consulted references or when introducing the data in the *CCDB*. The main advantage of these last restrictions in comparison with those implicit in field data and their interpretations is that almost all errors committed in this part of the process may be solved with an active updating and upgrading of the *CCDB*.

Once introduced the available information in the *CCDB* we create the *CCDB DATA TABLE*. Although this process is practically automatic, the *CCDB DATA TABLE* should not have further errors than those coming from previous steps. However, we should keep in mind that in some cases, we define the *CATEGORIES* of the *CCDB DATA TABLE* and reclassify the available information according to our own criteria. Consequently, a wrong definition of the *CATEGORIES* and the subsequent reclassification may introduce some errors in the interpretation of the information.

Finally, the last step is the *CCDB DATA ANALYSIS*. Theoretically, since the field data information has been normalized to assign objectively the levels of “high”, “medium-high”, “low-medium” and “low”, the analysis itself should be restrictions free. However, the drawn conclusions and interpretations are strongly dependent on the amount of available information. Obviously, general tendencies supported by a considerably high number of calderas will be more reliable than that supported by a small number of samples. Occasionally, due to the low number of calderas with available information, quantification becomes meaningless. The percentage values are not representative for a strict quantitative classification (see section II.5.6).

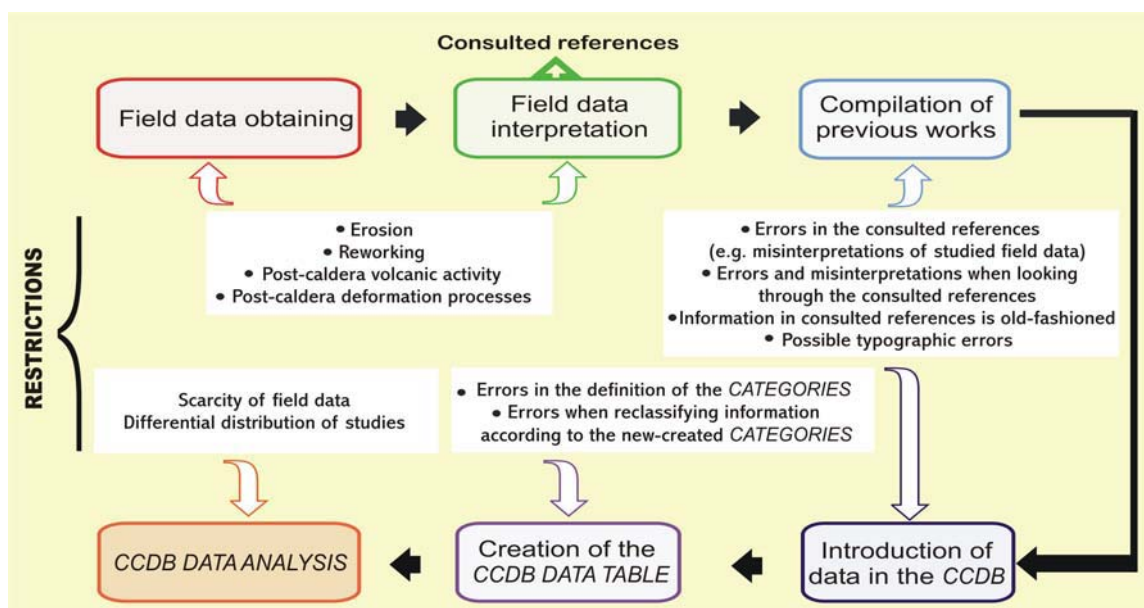


**Fig. 2.111:** Sketch of the different restrictions present in the studied field data and the performed *CCDB DATA ANALYSIS*.

## **II.6 SUMMARY AND CONCLUSIONS**

In this chapter we have introduced and summarised the most important aspects of field evidence on collapse calderas. We have revised the most essential published works and summarized their most relevant findings. We have also created a database recording existing information on collapse calderas. This database is an indispensable tool for studying and understanding these volcanic structures as well as for a statistical evaluation of dependent parameters. The generation, consultation and evaluation of this Collapse Caldera DataBase (CCDB) is not only restricted to this work. The objective is to publish the database on the www in the form of an interactive web page permitting registered users access to the database and sharing of recorded information. The database is coded to implement further extension and upgrading of recorded data.

The analysis of information included in the latest version (CCDB 1.0) has been employed for the analysis reported in this thesis. The scope was to i) find general trends among different parameters and their effect on resultant collapse structures calderas and ii) distinguish between different caldera types or groups for a further determination of common physical prerequisites for their formation. We have identified two families among collapse calderas. Collapse calderas included in the first family are large ( $D_{CIR} > 25$  km) and commonly related to a pre-caldera volcanic edifice. In most cases, the caldera-forming eruption lacks a pre-collapse energetic Plinian phase. These calderas are principally located in areas of continental (thin or thick) or thick transitional crust and are intimately related to extensive tectonic structures. Apparently, they are also located in zones of effective magma generation and accumulation. The second family includes calderas formed by vertical collapse of a pre-existing volcanic edifice, commonly long-lived stratovolcanoes or stratocones. These calderas seem to form after an energetic Plinian phase.

We have shown that there are areas that display a particular tectonic and magmatic evolution both of which may favour the formation of collapse calderas (North America and Northern Mexico). However, we cannot ignore limitations associated with the available field data and their effect on the interpretation of the compiled information. It is therefore imperative to acknowledge that both field data and interpretations are dynamic entities i.e. they are and have to be subject to both revision and updating.

Results obtained in this chapter will be combined with those in chapters III and IV in order to propose a genetic classification of calderas.